TECH LIBRARY KAFB, NM
0060763

NASA CONTRACTOR REPORT

NASA CR-

NASA CR-1646

LOAN COPY: RETURN TO
AFWL (DOGL)
KIRTLAND AFB, N. M.

A DESIGN SUMMARY OF STALL CHARACTERISTICS OF STRAIGHT WING AIRCRAFT

by M. A. McVeigh and E. Kisielowski

Prepared by
DYNASCIENCES CORPORATION
SCIENTIFIC SYSTEMS DIVISION
Blue Bell, Pa.
for Langley Research Center

NATIONAL AERONAUTICS AND SPACE ADMINISTRATION • WASHINGTON, D. C. • JUNE 1971

TECH LIBRARY KAFB, NM
0060763

1. Report No.	2. Government Accession No.	3. Recipient's Catalog No.
NASA CR-1646		

4. Title and Subtitle	5. Report Date
A DESIGN SUMMARY OF STALL CHARACTERISTICS OF STRAIGHT WING AIRCRAFT	June 1971
	6. Performing Organization Code

7. Author(s)	8. Performing Organization Report No.
M. A. McVeigh and E. Kisielowski	DCR-305
	10. Work Unit No.
	126-13-10-06-23

9. Performing Organization Name and Address	11. Contract or Grant No.
Dynasciences Corporation Scientific Systems Division Blue Bell, Pennsylvania	NAS1-8389
	13. Type of Report and Period Covered
	Contractor Report

12. Sponsoring Agency Name and Address	14. Sponsoring Agency Code
NATIONAL AERONAUTICS AND SPACE ADMINISTRATION WASHINGTON, D. C. 20546	

15. Supplementary Notes

16. Abstract

A method of wing design using lifting line theory described in NACA Reports 865 and 1090 has been computerized and used to study the parameters which affect wing stall characteristics. The results of the study and the computer program are described. The effects of airfoil section variations, Reynolds number, aspect ratio, wing twist and taper ratio are presented in design chart form.

17. Key Words (Suggested by Author(s))	18. Distribution Statement
Subsonic Wing Design Strip Theory Computer Program	Unclassified - Unlimited

19. Security Classif. (of this report)	20. Security Classif. (of this page)	21. No. of Pages	22. Price*
Unclassified	Unclassified	226	$3.00

*For sale by the National Technical Information Service, Springfield, Virginia 22151

SUMMARY

Presented in this report is a comprehensive review of the existing technical literature and a design summary of stall characteristics applicable to light straight wing aircraft. These characteristics are obtained with the aid of a digital computer program which utilizes the most up to date analytical methods employing lifting line theory and the available experimental test data for wing section characteristics. The computer results are presented in the form of stall charts suitable for preliminary design purposes. Based on the extensive parametric study covering a total of 331 different aircraft configurations, it can be concluded that in modern airplane design satisfactory stalling characteristics can be readily built in with no appreciable loss in airplane performance or handling qualities. A proper combination of wing taper, twist and type of airfoil sections with minor post-design fixes, if required, can in most cases provide satisfactory wing stall characteristics.

FOREWORD

This report presents a design summary of stall characteristics of straight wing aircraft.

The work was performed by the Scientific Systems Division (SSD) of the Dynasciences Corporation, Blue Bell, Pennsylvania, for the National Aeronautics and Space Administration (NASA), Langley Research Center, Hampton, Virginia, under contract number NAS 1-8389 during the period from July 1968 through September 1969.

The NASA technical representatives were Mr. Robert T. Taylor and Mr. William J. Alford, Jr. The contributions of the NASA technical personnel to this work are gratefully acknowledged. Acknowledgement is also extended to NASA computer personnel, especially Mrs. Belinda Adams, for their support in this program.

Messrs. James C. Sivells and Hartley A. Soulé were special technical consultants on this project and Mr. Ron Anton was computer consultant.

CONTENTS

		Page
	SUMMARY	iii
	FOREWORD	v
	LIST OF ILLUSTRATIONS	viii
	LIST OF TABLES	xi
	LIST OF SYMBOLS	xiii
SECTION 1	INTRODUCTION	1
SECTION 2	BASIC CONSIDERATIONS OF AIRPLANE STALLING	4
SECTION 3	THEORETICAL ANALYSIS	21
SECTION 4	COMPUTER PROGRAM	42
SECTION 5	PARAMETRIC INVESTIGATION	75
SECTION 6	SCALE MODEL WIND TUNNEL TESTING	131
SECTION 7	DESIGN PROCEDURES	136
SECTION 8	CONCLUSIONS AND RECOMMENDATIONS	142
SECTION 9	REFERENCES	144
APPENDIX A	INTERNAL LISTING OF THE COMPUTER PROGRAM	149
APPENDIX B	AVAILABILITY OF THE COMPUTER PROGRAM	189
BIBLIOGRAPHY		190

ILLUSTRATIONS

Figure		Page
1	Representative Lift Curve (Reproduced from Reference 13)	10
2	The Low-Speed Stalling Characteristics of Airfoil Sections Correlated With Reynolds Number and the Upper-Surface Ordinates of the Airfoil Sections at the 0.0125-Chord Station	12
3	Wing Leading Edge Mofifications for Controlling Wing Stall	20
4	Definition of Parameters for Transformation of Wing-Body Combination	26
5	Typical Load Distributions for Obtaining Factors for Altering Two-Dimensional Data	37
6	Illustration of Method for Correcting Two-Dimensional Section Data	39
7	Extrapolations of Lift Curve Slopes at Low Reynolds Number	51
8	Variation of Section Lift-Curve Slope with Thickness-Chord Ratio at Constant Reynolds Number NACA 644 Sections	54
9	Corrected Lift Curves for NACA 64-421 Airfoil at Low Reynolds Numbers	55
10	Method of Tabulation of Section Characteristics	57
11	Schematic Representation of Section Data Storage in the Computer	59
12	Nomenclature for Developing Interpolation Formulae	61
13	Computer Program Block Diagram	62
14	Schematic Representation of the Computer Input Cards	63
15	Experimental and Calculated Characteristics for a Wing of Aspect Ratio 8.04	68

Figure		Page
16	Experimental and Calculated Characteristics for a Wing of Aspect Ratio 10.05	70
17	Experimental and Calculated Characteristics for a Wing of Aspect Ratio 12.06	72
18	Experimental and Calculated Characteristics for Wing with 60% Flap; Aspect Ratio 9.02; Taper Ratio 0.4; Washout 2^{o}	74
19	Typical Lift Distributions Along Wing Span	81
20	Variation of $c_{l\,max}$ with Reynolds Number and Thickness-Chord Ratio	83
21	Variation of $C_{L\,max}$ with Reynolds Number and Taper Ratio	86
22	Effect of Aspect Ratio on Stall Margin Distribution	88
23	Effect of Aspect Ratio on Wing Stall Pattern	91
24	Effect of Aspect Ratio and Taper Ratio on $C_{L\,max}$	94
25	Increment of Induced-Drag Coefficient Due to Washout, 230 Series Airfoil Section	98
26	Effect of Root Thickness-Chord Ratio on Stall Margin Distribution	101
27	Effect of Root Thickness-Chord Ratio on Wing Stall Boundaries	104
28	Effect of Root Thickness-Chord Ratio on $C_{L\,max}$	107
29	Effect of Tip Thickness-Chord Ratio on Stall Margin Distribution	111
30	Effect of Tip Thickness-Chord Ratio on $C_{L\,max}$	114
31	Effect of Reynolds Number on Stall Margin Distribution	117
32	Effect of Reynolds Number on Wing Stall Pattern	120

Figure		Page
33	Effect of Reynolds Number on C_{Lmax}	123
34	Effect of Wing Camber on Stall Margin Distribution	127
35	Effect of Fuselage	128
36	Effect of the Span of a 20% Chord Split Flap on the Wing Stalling Characteristics	130
37	Variation of Wing Maximum Lift Coefficient with Stall Speed	138

TABLES

Tables		Page
I	Airfoil Section Data Available for Use with the Computer Program.....	56
II	Typical Computer Output.....	65
III	Summary of Configurations Studied.....	76

SYMBOLS

A	non-dimensional fuselage semiheight
A'	fuselage semiheight, ft.
AR	wing aspect ratio,
A_n	coefficients in trigonometric series
a	non-dimensional average distance of point on wing from fuselage cross-section focii
a'	average distance of point on wing from fuselage cross-section focii, ft.
a_o	section lift-curve slope, per degree
B	non-dimensional fuselage semiwidth
B'	fuselage semiwidth, ft.
$b, \bar{b}$	wing span, ft.
$b_f, \bar{b}_f$	flap span, ft.
C_D	total wing drag coefficient, $\frac{D}{qS}$
C_{D_o}	wing profile drag coefficient, $\frac{D_o}{qS}$
C_{D_i}	wing induced drag coefficient, $\frac{D_i}{qS}$
C_L	wing lift coefficient, $\frac{L}{qS}$
C_M	wing pitching moment coefficient, $\frac{M}{qSc'}$
C_d	total section drag coefficient
C_{d_i}	section induced drag coefficient
C_{d_o}	section profile drag coefficient
C_l	section lift coefficient, $\frac{l}{qc}$

C_{l_i}	design lift coefficient
C_{l_o}	two-dimensional, uncorrected value of lift coefficient
$C_{l_{max}}$	maximum section lift coefficient
$(C_{l_{max}})_o$	maximum two-dimensional section lift coefficient
C_l^*	section lift coefficient at end of flap
C_{l_1}	section lift coefficient for that part of lift distribution involving no discontinuity in angle of attack
C_{l_2}	section lift coefficient for part of lift distribution due to discontinuity in angle of attack
C_{l_α}	section lift-curve slope, per degree
$C_l\delta$	section lift coefficient with deflected flaps, calculated assuming linear lift curves
C_m	section pitching moment coefficient
$C_{m_{\frac{c}{4}}}$	section pitching moment coefficient about quarter-chord point
c	wing chord at any spanwise station, ft.
c'	wing mean aerodynamic chord, ft.
c_R	wing root chord, ft.
c_T	wing tip chord, ft.
D	total wing drag, lbs.
D_o	wing profile drag, lbs.
D_i	wing induced drag, lbs.
E	edge velocity factor
e	non-dimensional eccentricity of fuselage cross-section

e'	eccentricity of fuselage cross-section, ft.
F	factor used in altering two-dimensional lift curves
FF	value of $\frac{c_{\ell\,max}}{(c_{\ell\,max})_o}$ at $y=y^*$ taken at the flap side of y^*
G_{mk}	coefficient of transpose of matrix G'_{mk}
G'_{mk}	coefficient of a matrix
H	non-dimensional wing height above fuselage centerline
K	section camber level measured in terms of section design lift coefficient
K_{ij}	coefficient of the inverse of matrix G_{mk}
L	wing lift, lbs.
ℓ	section lift, lbs.
M	wing pitching moment, lbs. ft.
q	dynamic pressure, lbs/ft.^{2}
R_e	Reynolds number
R'_e	Reynolds number based on mean aerodynamic chord
S	gross wing area, sq. ft.
T	thickness factor
t	wing section maximum thickness, ft.
tr	maximum wing root thickness, ft.
X	coordinate parallel to fuselage centerline, positive forward, ft.
Y	non-dimensional spanwise distance
Y_o	non-dimensional coordinate of wing-fuselage junction
$y,\bar{y}$	spanwise coordinate, ft.

A DESIGN SUMMARY OF STALL CHARACTERISTICS OF STRAIGHT WING AIRCRAFT

By M. A. McVeigh, E. Kisielowski
DYNASCIENCES CORPORATION

SECTION I

INTRODUCTION

Federal and military aviation regulations require that all aircraft possess stalling characteristics which comply with the established specifications. The final evaluation of an airplane is made in flight tests in which all factors influencing its stalling characteristics are integrated. At this stage, however, it may be too late or very expensive to make any alterations necessary to meet the established requirements.

It is highly desirable therefore, to predict the maximum lift and stalling characteristics of an aircraft at an early design stage and, on the basis of the predicted characteristics, to incorporate such modifications in the design as may give promise of satisfying the FAA or military stall requirements. With this end in mind, extensive research effort directed toward a comprehensive understanding of the aerodynamics of unswept wings has been accomplished in prior years. This research effort was directed along lines of theoretical work, wind tunnel experiments and flight tests.

On the theoretical front substantial progress has been made. Prior to the World War II an adaptation of the lifting line theory in which the wing airfoil sections were assumed to possess a linear variation of lift with angle-of-attack was the only available method for predicting the maximum lift and stalling characteristics of unswept wings. In the region of maximum lift, however, the section lift curves are usually quite nonlinear. Consequently, predictions based on the method were quite unreliable in the maximum lift range. Shortly after the close of World War II Sivells (References 1 and 2) presented a method for calculating unswept wing characteristics by lifting line theory utilizing nonlinear airfoil section lift data. The values of maximum lift and the point of initial stall predicted by this approach agree well with experimental observations, and the method is regarded as a very effective design tool. Other major theoretical contributions were made by Theodorsen (Reference 3) and by Multhopp (Reference 4). These references provide valuable methods for developing improved airfoil sections and for determining wing-fuselage interference effects.

Wind tunnel experiments have provided extensive information in such important areas as: two-dimensional airfoil section

characteristics (References 5 and 6); the aerodynamic characteristics of complete wings at high Reynolds number (Reference 7); the characteristics of a large number of complete airplanes (Reference 8); and compressibility effects on maximum lift (Reference 9). Certain portions of the wind tunnel test data have direct design applications, other portions provide a basis on which to evaluate the applicability of new theories, and still other portions provide information on which to base empirical design guidance.

The flight test results provide a comprehensive evaluation of the integrated effect of all the factors that contribute to the airplane flying qualities. Measurement of the flight characteristics of many airplanes of different types has permitted a definition of those characteristics which provide for good flying qualities. Additionally, the flight test results provide a reference base for the correlation of theoretical prediction and wind tunnel experimental results.

Much of the research effort referenced above was accomplished and the results were published in numerous isolated reports, during and shortly after the end of World War II. Immediately after this period, interest in the problems of straight wing aircraft was diverted to the pressing problems of supersonic military aircraft incorporating swept wing configurations. In general, unswept (straight) wing technology is not applicable to swept wing configurations. Consequently, the wealth of information pertaining to the maximum lift and stalling of unswept wing aircraft has not previously been coordinated and hence has not received adequate attention. Nevertheless, in the general aviation field, interest still centers on subsonic aircraft incorporating unswept wing configurations. A need therefore exists for the application of available unswept wing stall technology to the design of such aircraft.

This report presents a comprehensive bibliography of prior work in the field, and, insofar as practicable, presents the most pertinent information in a form suitable for design application. In the preparation of this report a comprehensive review has been conducted of all pertinent literature although no attempt is made to synopsize each of the reports under one section. Effort has been made, however, to incorporate the information gained from this extensive review into design guidance procedures, recommendations, cautions, etc. Based on this comprehensive review of pertinent literature a mathematical model was formulated and programmed for the CDC 6600 digital computer. The computer which employs available nonlinear wing section characteristics can be utilized to predict maximum lift and the spanwise load distribution of a wing with or without fuselage.

As a result of this study it can be concluded that design for good airplane stalling characteristics is still part art and part science. It appears obvious, however, that application of the available knowledge in early design stage will greatly improve the probability of obtaining satisfactory stalling characteristics or, at least, may yield an airplane design whose characteristics can be made acceptable as the result of minor modifications during early flight test phase.

SECTION 2

BASIC CONSIDERATIONS OF AIRPLANE STALLING

2.1 MINIMUM REQUIREMENTS FOR ACCEPTABLE STALL CHARACTERISTICS

The MINIMUM REGULATORY requirements for the stalling behavior of small aircraft are stated in the Federal Aviation Regulations, Part 23 "Airworthiness Standards: Normal, Utility and Acrobatic Category Airplanes" (Reference 10). With the legalistic qualifications deleted, the regulations require that for specified power, gear and flap settings acceptable stalling characteristics be demonstrated for two flight maneuvers, one in straight flight with the wings level and one in a coordinated turn. In both cases the primary control manipulation is a steady progressive upward movement of the elevator until the airplane is stalled or the elevator reaches its stop.

The demonstration procedures and acceptable stalling characteristics are defined as follows:

For the straight-flight maneuver, the airplane is trimmed at a speed fifty percent greater than the stalling speed before the elevator movement is started. With the usual three control system, it must be possible to produce and correct roll by unreversed use of the rolling control and to produce and correct yaw by unreversed use of the directional control up to the time when stall becomes apparent, i.e. when an uncontrollable downward pitching motion develops or until the elevator reaches its stop.

For the two-control system airplanes, rolling motions must be produced and corrected by unreversed lateral control without excessive yaw. During recovery from the stall, it must be possible to prevent the occurrence of more than 15 degrees of roll or yaw by normal use of the controls.

For the turning-flight maneuver, the airplane is placed in a steady, level, coordinated turn with a 30-degree bank angle before the speed is reduced. When stall occurs, it must be possible to regain normal level flight without excessive loss of altitude or uncontrollable rolling or spinning tendencies.

For both maneuvers as stalls are approached, there must be a clear and distinct stall warning which begins at a speed about 5 to 10 miles per hour higher than the stalling speed and continues until the stall is reached. For airplanes that cannot be stalled for the two maneuvers specified, it must be shown that if they can be stalled in steep climbs, then recovery shall not require excessive speeds and/or accelerations. Multi-engine aircraft have additional single engine-out requirements pertaining to stalls in turning flight.

In summary, the regulations require that for gentle maneuvers the aircraft shall have some stall-approach warning, effective lateral control up to the stall, and sufficiently effective lateral control after the stall to restrict yawing and rolling disturbances to small angles. Furthermore, recovery from the stall shall not involve excessive altitude loss, speed increase, or structural loading.

2.2 DESIRABLE STALL CHARACTERISTICS

For more safety, it would be better if there were no uncontrollable motions during a stall and recovery. A 15-degree change in the angle of bank or heading could have serious consequences if it occurred close to the ground and off the end of the runway following a misjudged landing and the start of the go-around climb.

Since it is generally conceded that there is no such thing as a "good" stall (Reference 11), the safest low-speed characteristics are those that do not change noticeably to the limit of the up-elevator travel. These are, of course, the characteristics sought by "stall-proofing" an airplane, such that the angle of attack for maximum lift can never be attained. This is not easy to accomplish for reasons which will be discussed later.

For airplanes which can be stalled (i.e. aircraft angle of attack exceeds that for maximum lift), there is no unanimity of opinion on the least desirable type of motion that may result. The consensus, however, is that probably the least undesirable stall characteristic would be for the nose of the airplane to drop abruptly by a small but distinguishable amount before the occurrence of excessive rolling and yawing motions requiring the use of either lateral or directional controls. Also, under such conditions, if the elevator control is eased forward the airplane should promptly return to unstalled flight. Slight skidding or yawing motions should have no appreciable effect on these characteristics.

The preceding are the more or less limiting conditions. Anything between the case of mild nose dropping and the stalling characteristics defined by the Federal Aviation Regulations (FAR) is a matter of the degree of violence of the rolling and yawing motions that develop at the stall. It should be noted that aside from the specified angular deviations in yaw and roll, the wording of the regulations is qualitative and open to individual interpretation.

2.3 STALL-PROOFING

Stall-proofing aircraft by limiting the up-elevator travel was suggested at least thirty-five years ago and is a subject on which much research time and effort has since been expended. There are two major reasons why this solution has not been more widely applied.

The first, but not necessarily the more important of these reasons, is the opinion that a stall-proof airplane may not be completely acceptable nor most saleable to the specific segment of the general public most interested in personal flying. This group is considered to be composed largely of more adventurous persons (e.g. the buyers of sports cars, the water skiers) who want more than transportation from an airplane. Therefore, the amount of effort that might be put into designing an airplane to be stall-proof depends on the purpose and the market for which the airplane is intended. It is possible to stall-proof an airplane for certain flight conditions and not for others. Fortunately the landing approach condition is one of the simplest and one for which some effort may be warranted.

The other reason why most aircraft are not completely stall-proofed is the technical difficulty of so doing. The elevator angle for a given angle of attack varies with a large number of interrelated aircraft dimensional and mass parameters. Among the more important not under the control of the designer are the center of gravity location on a given flight, the throttle, flap and trim settings; and the exterior surface condition, particularly the wing and horizontal tail surfaces. Added to these are all those other parameters among which the designer normally has to compromise. The basic longitudinal balance and, hence, the elevator angle for stall, depends on the relative proportions of the wing and the horizontal tail surfaces, the tail length, vertical location of the tail, the orientation of the tail relative to the propeller slipstream, and the proximity of the tail to the ground during takeoff and landing.

2.4 STALL WARNING

It is less difficult to obtain stall warning in the airplane as compared to stall proofing. Although it may not always be possible to provide for adequate stall warning in the design stage, it can in many cases be incorporated after aircraft construction.

There are a number of airplane characteristics which can serve as a means of providing warning to the pilot of his approach to the stall. Some of these characteristics are large increases in the elevator force and in the control stick travel near the stalling speed, initially controllable rolling and pitching motions, and vibrations or "buffeting" of the airplane and the control stick. The variation of control forces which are functions of elevator hinge moments are too dependent on the friction and elasticity in the control system between the elevator and stick to provide the consistency needed for stall warning. On the other hand an appreciable increase in the elevator control travel as stall is approached, airframe buffeting and initially controllable angular motions have each been found to give acceptable stall warning. The difficulty is to provide for the start of these warnings in the required speed range and to assure that the airplane angular

motions do not become too severe in amplitude before the stalling speed is reached.

Although inherent stall-warnings are to be preferred, stall warnings can be synthesized by detecting consistent changes in the airflow about the airplane and using the information to activate a mechanical or electronic device to alert the pilot of his approach to stall. The earliest form of a synthesized stall warning was probably the stall red-line on the airspeed indicator. The stall airspeed, however, is one of the poorer indicators of impending stall because it depends on aircraft weight and consequently varies with passenger load and fuel consumption. Variables which are directly related to the stall such as the airplane angle of attack and surface pressure differences give much more reliable indications of impending stall than does airspeed.

Synthetic stall-warning devices can be designed to alert the pilot of his approach to the stall through his sense of sight, hearing or feel. Neither of the first two have been found very satisfactory. In the case of sight, the pilot's attention during takeoff and landing when unintentional stalling is most probable is required outside of the cockpit. In the case of hearing, there is chance for confusion as horns have long been used as a reminder to lower the landing gear. The most satisfactory stall warning device would therefore be the one that would alert the pilot of his approach to the stall through the sense of feel. A description of the most common stall warning devices and their principle of operation is presented in Reference 12.

2.5 FACTORS AFFECTING WING STALL

The Federal Aviation Regulations define the stall characteristics in terms of movement of the elevator and of the effectiveness of the aileron and rudder controls. The wing, however, is the primary element of the airplane affecting the stalling characteristics. Its size relative to weight sets the stalling speed, and its proportions determine the location of the stall, its rate of propagation, and the violence of the resulting motions when the stalling speed is reached.

In the design of airplanes it is normal to start with the wing and select its dimensions by a series of compromises so as to assure good performance, acceptable stalling characteristics, and low structural weight. While not a technical factor a pleasing appearance must be considered because of the effect of style on the marketability of the design. The airfoil section is fundamental to wing design and should be considered early in the preliminary stages. The aerodynamic data for the selected airfoil sections are then used in analyses to determine the span loading of the three dimensional wing. It is on the basis of computed span-load distributions that a decision is made on the final wing proportions. Sections 4 and 5 of this report

present a summary of the theory and a description of the computer program respectively for determining the wing span load distributions required for preliminary design purposes.

2.6 AIRFOIL SECTIONS

The selection of the optimum airfoil sections for a wing is generally made after consideration is given to the following:

a) Section profile drag coefficient should be as low as possible over a range of lift coefficients near the required cruise lift coefficient.

b) Section maximum lift coefficient should be as large as possible since this has a direct bearing on the maximum value of the overall wing lift coefficient which in turn governs the stalling speed.

c) The chosen sections should have sufficient depth to contain the wing structural members and other items such as landing gear.

d) Stalling characteristics of sections near the wing tip should be gradual so as to avoid the possibility of sharp wing drop.

e) The section critical Mach number should be as high as possible to avoid transonic drag rise, if a high speed aircraft is being considered.

All of these requirements cannot be satisfied by any one airfoil section and some compromise must be made. For example, the need for sufficient structural depth, e.g. large thickness-chord ratios, conflicts with the requirement for high values of maximum lift coefficient. Again, a section chosen for its high value of maximum lift coefficient might have undesirably sharp stalling characteristics.

While section maximum lift coefficient is of particular importance in regard to wing stalling characteristics, the section having the greatest value of maximum lift might be sensitive to small dimensional deviations and hence might not realize its ideal performance.

Wing stall characteristics can also be affected by air turbulence or gustiness. The sideslipping and yawing motions produced by gustiness can induce flow breakdown for certain wing sections thus resulting in large changes in wing lift. Much work has been done to correlate flow patterns at the stall with the geometric properties of wing sections and the shape of the lift curve. There are three representative types of

airfoil section stall generally considered in the technical literature, e.g. Reference 13. These types are:

a) Type 1 - Trailing Edge Stall

b) Type 2 - Leading Edge Stall

c) Type 3 - Thin Airfoil Stall

The lift curves for the three types (reproduced from Reference 13) are compared in Figure 1 and a discussion of each type of stall is presented below.

2.6.1 Type 1 - Trailing Edge Stall

The peak of the lift curve for this type of stall is characteristically rounded with a maximum value of lift coefficient of approximately 1.5. The loss of lift after the stall is gradual which is considered to be the least undesirable type of stall. The flow for this type of stall is characterized by a progressive thickening of the turbulent boundary layer on the upper surface of the airfoil as the angle of attack is increased. This is followed by an eventual flow separation which starts at the trailing edge and gradually moves forward as the airfoil angle of attack is increased from about 10°. Maximum lift is obtained when the point of separation reaches about the 50 percent chord station. Beyond maximum lift the forward progression of the separation point continues at about the same rate as prior to stall. The trailing-edge type of stall is generally associated with wings approximately 15% thick or greater.

2.6.2 Type 2 - Leading Edge Stall

Airfoils with the leading-edge type of stall usually have a slightly greater maximum lift than those with a trailing edge stall. At the stall, however, there is a large sudden drop in lift associated with an abrupt separation of the flow from the upper surface near its leading edge. The separation is attributed to the behavior of the upper surface boundary layer. At an angle of attack well below that for maximum lift the boundary layer, which is laminar at the time, separates from the upper surface quite close to the nose, becomes turbulent and reattaches to the surface. The localized region of separated flow is referred to as a "laminar separation bubble". Up to the angle at which the bubble forms the boundary layer behaves the same as for airfoils having trailing-edge separation. The difference at higher angles is due primarily to the nose radius.

As the angle of attack is further increased, the laminar separation point moves forward where the local curvature is greater. At stall the main flow cannot expand rapidly enough for reattachment and a sudden and complete disruption of the

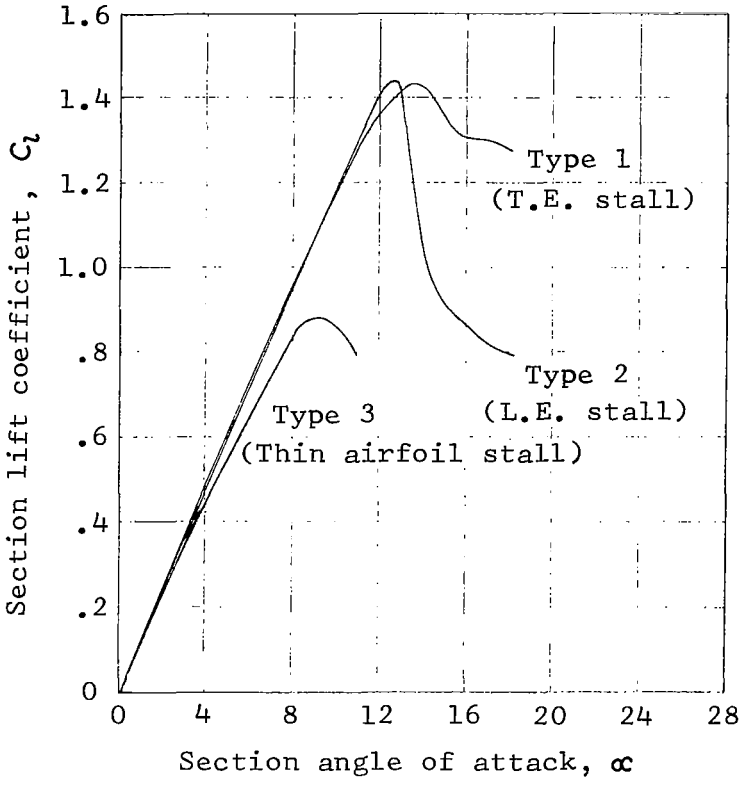

Figure 1. - Representative Lift Curves.
(Reproduced from Reference 13).

flow takes place. As the nose radii of airfoils normally decrease with thickness leading-edge stall is more likely to occur with airfoils with thickness ratios of 12% or less. This type of stall is considered to be the most undesirable.

2.6.3 Type 3 - Thin Airfoil Stall

This type of stall occurs on all sharp leading-edge airfoils (regardless of thickness ratio) and may also be encountered on rounded leading edge airfoils with sufficiently low thickness ratios e.g. $t/c \lesssim 9\%$. As can be noted from Figure 1, the airfoils with Type 3 stall have substantially lower values of maximum lift coefficients than those associated with the airfoil types discussed above.

The type 3 stall is characterized by flow separation from the leading edge with subsequent reattachment further downstream. The exact mechanism of flow reattachment is not clearly understood. Experimental observations have shown that at low angles of attack the flow reattaches to the upper surface of the airfoil at a short distance behind the leading edge and stays attached up to the trailing edge without further separation. With increase in angle of attack, the point of flow reattachment progressively moves toward the trailing edge and the stall is fully developed when the reattachment point occurs approximately at the trailing edge.

Figure 2, reproduced from Reference 14, more clearly delineates the types of stall discussed above and indicates some basis for a correlation between stalling characteristics, Reynolds number and leading edge shape.

2.7 WING PLANFORM EFFECTS

In the design of the wing for stalling characteristics, wing planform is as important as the characteristics of the airfoil sections. Probably the most important planform parameters are the aspect ratio, taper ratio, and the sweep and twist angles if either is used. They have an important influence on airplane performance and wing weight as well as the stalling characteristics. Therefore, effective compromises between these parameters must be made to obtain the required performance, handling qualities and structural integrity of the airplane.

The aspect ratio for a given wing area will directly affect the wing span. Low aspect ratio and short span are conducive to maneuverability for an aircraft intended for aerobatics. High aspect ratios are attractive from the point of view of maximum aerodynamic efficiency or L/D. However, an increase in aspect ratio generally results in an increase of wing root bending moments and probably wing weight. One fact that should

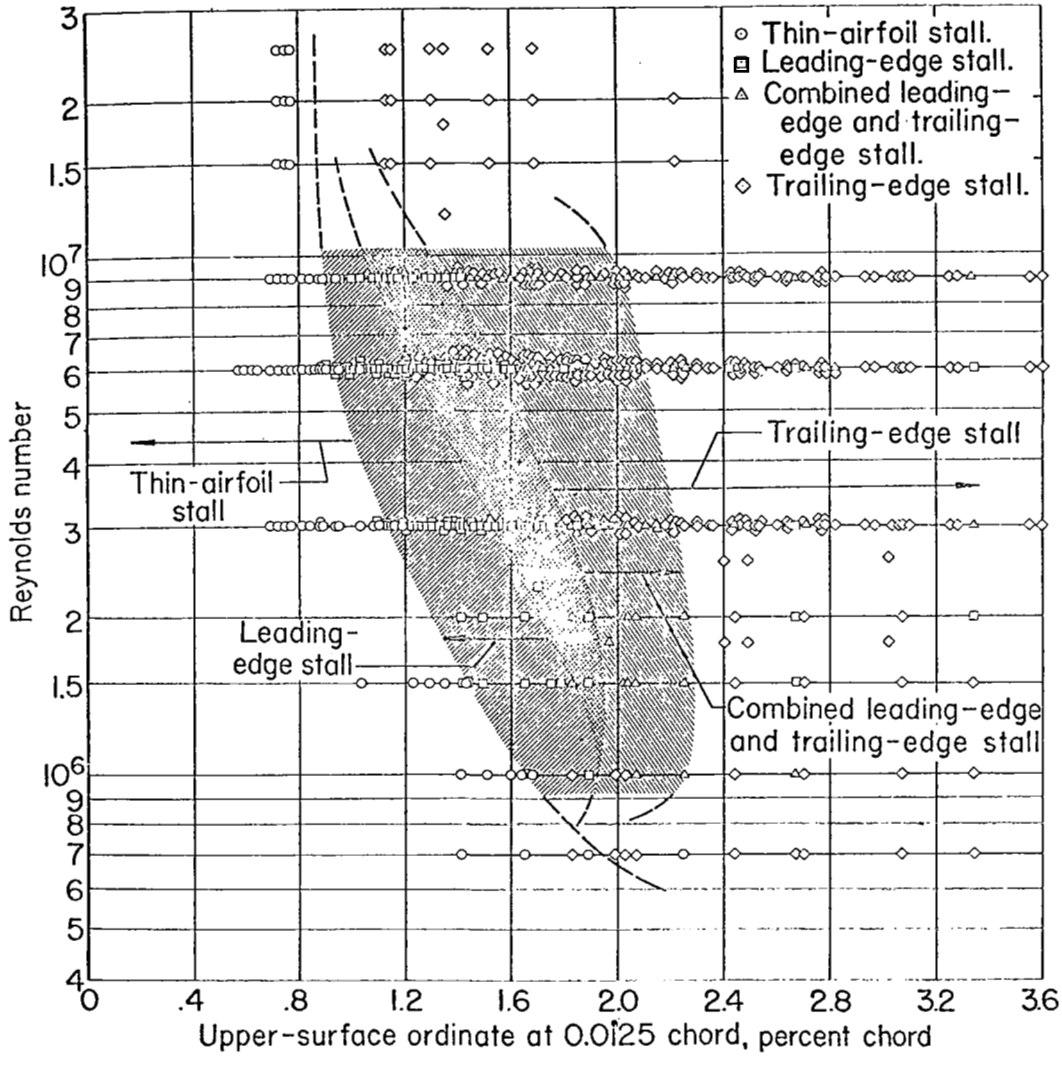

Figure 2. - The Low-Speed Stalling Characteristics of Airfoil Sections Correlated With Reynolds Number and the Upper-Surface Ordinates of the Airfoil Sections at the 0.0125-Chord Station. (Reproduced from Reference 14).

be considered relative to the compromise between maximum L/D and wing root bending moment is that the lift coefficient at which maximum L/D is attained also increases with aspect ratio. The performance characteristic most affected by maximum L/D is the aircraft range. For personal aircraft with relatively light wing loadings operating at altitudes below 10,000 feet, the speed for maximum range may be too slow to make it an attractive cruise speed. The increase in the value of the maximum L/D obtained by increasing the aspect ratio, therefore, may be of little practical use. In fact, if the L/D is much increased for the lift coefficients used in the approach glide, the effect may be to flatten the approach path, make judgment of the landing point more difficult and give the airplane a tendency to "float" after the landing flare. This statement is intended only to imply that increases in aspect ratio do not necessarily lead to improved aerodynamic performance. Improved performance may be better obtained by a reduction of fuselage, engine and landing gear drag.

Taper is normally employed to increase the wing chord and spar depths at the wing root and, hence, offset the adverse weight effects of increasing the aspect ratio. At the same time it increases wing torsional rigidity which is an important structural consideration. Wings can be tapered either in thickness or planform or in any combination of both. When combined taper is incorporated in the wing and straight line surface fairing is used for structural simplicity, airfoil sections between the fairing stations may be slightly distorted.

Sweep shifts the aerodynamic center of the wing fore-and-aft relative to the wing root. Small amounts of it can therefore be used to adjust the longitudinal aerodynamic balance or to improve the position of the aircraft center of gravity relative to the main landing gear.

Wing twist affects the span load distribution by changing the local section angle of attack along the wing span. Negative wing twist or washout may be used effectively to move the stalling point inboard.

High-lift devices such as leading edge slots or trailing edge flaps, if they are installed across the full span, influence the wing stall only through their effect on the section lift characteristics. Rarely, however, are either leading edge slots or trailing edge flaps used over the entire wing span. Leading edge slots over the tip portion of the wing were one of the first means tried for improving the wing stalling characteristics. Such slots increase the angle of stall of the tip sections of the order of ten degrees. Much experimentation with relatively simple fixed slots, as well as with the movable Handley-Page type, led to the early conclusion that neither the complexity

and cost of the automatic slots nor the drag penalty of the fixed slots were warranted for small personal aircraft. There has been a recent revival of interest in movable leading edge devices for the tip portions of the wings of high-speed, swept-wing commercial and military aircraft where their use can be economically justified.

Flaps are usually installed inboard of the ailerons. They depress the angle of attack for zero lift of the airfoils to which they are attached while having only a secondary effect on the stall angle. Inboard flaps, therefore, have the effect of a discontinuous wing twist with wash-in starting at the flap end.

Application of the simple lifting line theory as described in Reference 15 to predict the stalling characteristics of flapped wings will indicate a discontinuity in the spanwise distribution of maximum section lift coefficient and an associated initial stall at the end of the flap. Inasmuch as this discontinuity does not exist in three dimensional flow, early attempts to predict the stalling characteristics of flapped wings (Reference 16 and 17) by the method of Reference 15, did not yield good correlation with experiment. Subsequently, a far more reliable method of applying the lifting line theory was developed (Reference 2). The latter method predicts the point of initial stall quite well and is described in detail in Section 4 of this report.

2.8 CONSTRUCTION TOLERANCES AND SURFACE IRREGULARITIES

In most cases the final wing design represents a compromise among the best dimensions for performance, stall characteristics and structural weight, although occasionally some importance may be given to appearance. Curved leading edges, taper and sweep can add to the attractiveness of a design and give the impression of speed. While such features so used may not necessarily penalize the design, their impact on flight safety and construction costs should be carefully studied.

No adequate method of defining either the permissable deviations of the airfoil ordinates from their specified values or the permissable degree of surface roughness and waviness has been devised. Reference 5 gives some general guide lines concerning the surface conditions and construction tolerances that must be adhered to in order to achieve extensive regions of laminar flow at low values of the lift coefficient. In general, it would appear that if values of $c_{l\,max}$ comparable to those presented in Reference 5 are to be achieved, the surface conditions and construction tolerances over the forward upper surface of the airfoil (approx. 0 to 10% chord) should be at least as good as those indicated in the reference. As shown by the results of Reference 18 "very small errors in airfoil

contour, particularly around the leading edge, could cause large changes in the stalling angle of attack and the resulting value of maximum lift coefficient."

The advisability of applying the stall analysis procedure in the early stages of the airplane design cannot be over-emphasized. This stall analysis procedure relies on the use of published airfoil section data characteristics. The designer is warned, therefore, that unless the aircraft as finally constructed incorporates airfoil sections that are approximately equal in contour and surface condition to those utilized in obtaining the two-dimensional airfoil section data, the calculated stalling characteristics will not necessarily be comparable to those encountered on the flight vehicle.

2.9 WING-FUSELAGE FAIRINGS

One of the more important structural considerations affecting aircraft stall is the fairing between the wing and fuselage. The method of Multhopp used for calculating the effect of the fuselage on the wing lift only accounts for changes in local flow angles of the root sections due to presence of the fuselage. Neither this method nor any other method considered in the course of this study adequately treats the modification of the surface pressures on the wing and fuselage as a result of the mutual interference. Such changes seriously influence the boundary layer at the junction and can cause premature separation of the main flow. The turbulence in the wake behind the separated region may intersect the tail plane where it may induce vibratory loads which if mild, can be used as stall warning. It may, however, result in vibrations severe enough to impair the structural integrity of the aircraft. The violence of the vibrations depends on the extent of the separated region and the location of the horizontal tail relative to wake.

Wing fuselage flow interaction effects largely depend on the position of the wing relative to the fuselage. For the high wing position, where the influence of the fuselage is confined to the lower less critical surface of the wing these effects are quite small. The low wing position with the wing tangent to the fuselage introduces the largest wing-fuselage interaction effects which increase as the angle between the wing-fuselage surfaces becomes more acute.

The wing-fuselage flow interaction can be to some degree controlled by the shape and size of the root fairings associated with each wing position. The high wing position dictates a minimum amount of fairing from aerodynamic considerations, whereas for the low wing position a considerable amount of fairing may be required to ensure proper flow conditions on the upper surface of the wing close to the fuselage. Also, careful consideration should be given to the chord-wise shaping of

the wing root fairing, since it effects the expansion of the flow over the after portion of the junction. The chord-wise shape of the root fairing largely depends on the fore-and-aft position of the wing relative to the fuselage maximum diameter.

Since the geometry of the wing-root fairings critically depends on detail design of the junction there are no established theoretical methods by which the size and shape of the wing-root fairings can be predicted. Some empirical design rules, which can be employed for this purpose are presented in References 19. However, it is generally recommended that the final size and shape of the wing-root fairings be determined by an experiment either in a wind tunnel or in flight.

The fairing problems discussed above are similar to those associated with the nacelles of wing-mounted engines. Location of the nacelles close to the fuselage may result in some additional interaction effects of the nacelle-fuselage flow fields. However, the propeller radius requirements generally ensure sufficient spacing between the nacelles and the fuselage to prevent serious interaction.

2.10 PROPELLER SLIPSTREAM CONSIDERATIONS

Another important consideration of airplane stall is the effect of the propeller slipstream in power-on flight. This effect is introduced through an increase of the local velocity over the wing immersed in the slipstream and the change of wing local angle of attack due to slipstream rotation.

The increased velocity tends to stabilize the flow over the wing immersed in the slipstream. The rotation within the slipstream tends to increase the local angle of attack of the wing sections behind the upgoing propeller blades and decrease the local angle of attack behind the downgoing blades. The overall effect is usually that of promoting an asymmetrical stall. The stall of that portion of the wing behind the upgoing blades is hastened whereas that behind the downgoing blades is delayed. In the case of a single engine airplane the asymmetrical stall can promote serious wing dropping tendencies when the airplane is operating in the vicinity of $C_{L_{max}}$. Reference 8 presents the results of extensive experimental observations of the effect of propeller operation on wing stalling. It is interesting to note, from the results presented therein, that in the case of one of the single engine airplanes investigated, the action of the propeller in promoting an asymmetrical stall is more adverse at the engine idle power condition ($T_c = 0$) than at the power-on condition investigated ($T_c = 0.2$). In the case of another single engine airplane investigated, the effect of power was in the reverse order.

The effects of the asymmetrical stalling in the case of multi-engine aircraft can not be clearly defined primarily due to the fact that these effects are largely dependent on a specific combination of various geometric parameters related to each aircraft.

2.11 STABILITY AND CONTROL CONSIDERATIONS

In the above discussion of airplane stall characteristics, it is assumed that the aircraft is in a steady unyawed trimmed flight, and that the stall is developed through a gradual increase of airplane angle of attack. However, the steadiness of actual flight depends on the longitudinal stability of the aircraft, the control effectiveness, the rate at which the pilot moves the control stick and the atmospheric turbulence.

With reference to atmospheric turbulence, little can be done in design to reduce its effect on the stall. Even assuming that the airplane stability and control are adequate, severe turbulence can upset any aircraft and therefore it should be avoided where possible. In an unavoidable flight in turbulent weather, the Federal Regulations require the pilots of commercial airlines to fly the specific airplane at its designated speed low enough to minimize the structural loads due to the gusts, but high enough to assure that the angle of attack change produced by the probable maximum upward gust will not stall the aircraft. The designer of the private airplane can only suggest that his customers follow a similar practice.

In addition to the angle of attack changes, gustiness will induce rolling and yawing motions that can result in premature unsymmetrical wing stall and sudden roll-off. The danger depends on the stall margin of the wing and on the lateral stability of the aircraft. One of the requirements for good lateral stability is an adequate fin area. The relation between the fin area and the wing dihedral angle determines whether the yawing or rolling component of the lateral oscillation predominates. The occurrence of light oscillations as stall is approached has been suggested as an acceptable stall warning. This phenomenon is usually associated with a reduction of fin effectiveness at large wing angles of attack and is caused by blanketing of the lower portion of the fin by the fuselage or submersion of the fin in a low-energy wing wake.

The longitudinal stability and the elevator effectiveness combine to determine the stick movement required at different parts of the speed range. In general, high-wing positions result in more longitudinal stability at low speeds than at high speeds. Low-wing positions produce the opposite effect. The elevator effectiveness varies with the relative proportions of the elevator and stabilizer, and it decreases after the angle of the

elevator exceeds a critical angle. Hence, for an increasing rate of stick movement as the stall speed is approached, as suggested for stall warning, the high-wing configuration with a small elevator is more desirable.

There are, however, a considerable number of other factors affecting the stability and control characteristics which in turn influence the airplane stall. The subject is too complex for a short comprehensive treatment in this report. Among others, the aircraft stability and control is affected by the size, location and type of flaps; the wing wake and its position relative to the horizontal tail; the orientation of the propeller slipstream relative to both the horizontal and vertical tails and the vertical, as well as the fore-and-aft, position of the center of gravity. These and other factors are adequately treated in the available technical literature, e.g. References 20 and 21.

2.12 FLIGHT VERIFICATION AND CERTIFICATION

The theoretical methods and the design procedures, presented in this report should reasonably well predict the stalling characteristics of unswept wing aircraft, particularly for gliding flight such as in the landing approach. Since these methods and procedures are based upon a number of simplifying assumptions, it is always advisable to verify the theoretical predictions by actual flight tests.

The test procedures to be followed are specified in the Federal Aviation Regulations for Certification Demonstrations cited earlier. If the tests show a need to improve the aircraft stalling characteristics, a flow visualization technique, utilizing tufts is often employed in gaining an understanding of the flow deficiencies. The tufts which are normally short lengths of string attached at intervals on the upper surface of the wing and sometimes on the sides of the fuselage, can be observed and/or photographed from within the test aircraft or the chase plane. The flow patterns indicated by the tufts will define areas of attached and separated flows and can show the spanwise or chordwise location of initial flow breakdown and the rate at which separation increases with small decreases in speed.

The tuft studies, the motions after initial stall and the stall-related vibrations felt in the structure and the control system will generally indicate the design changes required for improving the stalling characteristics after the airplane has been built. No attempt will be made to list or discuss all the possibilities in this report.

One possibility is that a part of the wing will stall suddenly with almost no warning. This type of stall can occur with airfoils exhibiting leading edge stall and with wing proportions

yielding low stall margins at the sections close to the point of initial flow breakdown. Interference between the flows over adjacent sections promotes separation which can spread across the wing very rapidly. The means most used for improving the stalling characteristics in such a case is the installation of a triangular-shaped projection or spoiler, Figure 3 (a), for a short distance along that part of the leading edge over which an earlier stall is desired. Attainment of satisfactory stalling will generally require a trial-and-error procedure, varying the span and spanwise location of the spoiler and its radial location at the leading edge. It may be difficult to obtain a configuration of the spoiler which is effective with full power but not too effective when power is reduced. Spoilers of this type can increase the power-off minimum speed by an objectionable amount and produce large vibrations of the wing, stabilizer or fuselage.

The other extreme possibility is a root stall starting well above the minimum speed. The associated thick turbulent wake, if it impinges on the tail, will produce stall warning, but may also make it impractical to fly the airplane in the speed range required for the landing approach. If the root fillet is properly designed it may be necessary to modify the wing leading edge of the root sections to increase their forward camber and reduce their effective angles of attack. One such leading edge modification is shown in Figure 3(b). It is frequently necessary to tailor the leading edge modification such that a small vibration remains for stall warning. Such modification may be utilized to control the asymmetrical stall that sometimes occurs within the propeller slipstream.

The actual cases are rarely as clearcut as the two just discussed and the reason for poor stalling characteristics is often not clearly understood. During World War II, many aircraft with configurations similar to those of current private owner designs had to undergo post-design stall improvement testing. Many of these cases are in the literature and have been included in the bibliography presented in this report.

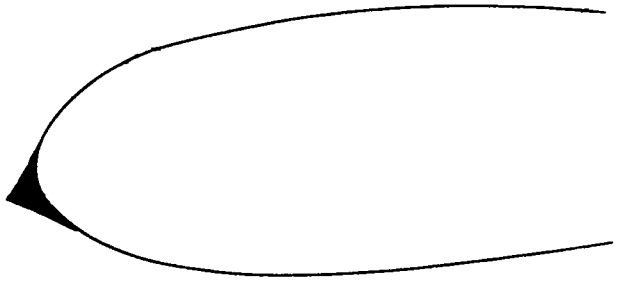

(a) Sharp Leading Edge Strip to Hasten Stall.

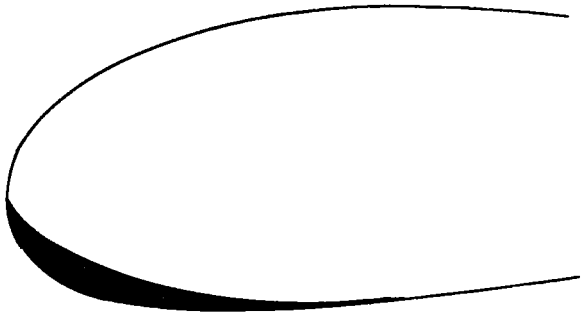

(b) Modified Nose Radius and Camber to Delay Stall

Figure 3. - Wing Leading Edge Modifications for Controlling Wing Stall.

SECTION 3

THEORETICAL ANALYSIS

Presented in this section is a brief review of the available theoretical analysis which formed the basis for developing the mathematical model and the computer program contained in this report. Specifically, in selecting the most suitable theoretical approaches, due consideration was given to the past work in the fields of wing theory and wing-body interference theory. The significant contributions in these areas and their applicability to the present program are discussed in the following pages.

3.1 REVIEW OF THE AVAILABLE THEORIES

3.1.1 Wing Theory

The simplest wing theory involves the concept of the lifting line whereby the wing is replaced by a vortex filament fixed in the wing and a system of trailing vortices. The vortex filament is known as the bound vortex or lifting line. At each point on the span the strength of the vortex is proportional to the local intensity of lift and is related to it through the Kutta-Joukowski law, which is based on the requirement of smooth flow from the wing trailing-edge. In accordance with the Helmholtz theorem of vortex continuity it is assumed that with each elemental change in the spanwise distribution of the strength of the bound vortices there is associated a free vortex which is shed at the wing trailing edge and which passes downstream with the general mass of the fluid. The strength of this vortex is equal to the incremental change in spanwise circulation. This system of free or "trailing" vortices induces velocity components (called downwash) at the wing and thus causes a change in local angles of attack of each wing section.

The problem of evaluating the downwash at each point is difficult because of the interrelation of downwash, lift distribution and wing planform. Using the lifting line theory Prandtl (Reference 22) obtained a solution for the case of a wing with an elliptical lift distribution. Glauert (Reference 23), using Fourier analysis, developed methods for obtaining solutions for wings of any planform and twist. These methods were used by Anderson (Reference 15) to determine the characteristics of wings for a wide range of aspect ratios, taper ratios and linear twist distributions.

All of these approaches discussed above involve the assumption of a linear variation of section lift with angle of attack. This assumption was not utilized in the iterative methods developed by Sherman, Tani, Multhopp, and Boshar (References 24 through 27) which employ nonlinear section lift data in the computations.

Based on these iterative methods Sivells and Neely (Reference 1) developed solutions which yield excellent agreement with the test data up to angles-of-attack close to stall. In a later paper Sivells and Westrick (Reference 2) extended the method of successive approximations to the calculation of the aerodynamic characteristics of wings with deflected flaps or ailerons.

All of the above solutions and methods which are essentially based upon the Prandtl lifting line theory are known to be inadequate for wings of aspect ratio less than about 3. For wings of this class the influence of the chordwise loading can no longer be neglected and resort must be made to the general theory of lifting surfaces to obtain solutions.

Lifting surface theory involves finding a potential flow solution which satisfies the Kutta condition all along the span while at the same time satisfying the boundary condition that there is no flow through the wing surface.

Solutions of varying complexity and accuracy have been advanced by many authors. Early attempts were made by Weissinger, Mutterperl, and Schlichting (References 28, 29 and 30 to use simplifying physical models for the approach to the general problem, e.g. placing a lifting line at the quarter-chord point and satisfying the downwash condition at the three-quarter-chord position. Falkner (Reference 31) proposed a vortex-lattice treatment of the wing thereby approaching a truly continuous lifting surface.

Attempts to use a continuous lifting surface theory without resort to arbitrary physical assumptions or models are exemplified by the work of Garner (Reference 32 and 33) and most notably by that of Multhopp (Reference 34).

When lifting surface theory is used to predict load distributions on high aspect ratio unswept wings at low angles of attack, the results do not differ significantly from those computed using lifting-line theory.

However, to date, lifting surface theory has not been successfully modified to permit the use of nonlinear section lift data and hence cannot be expected to give reliable predictions of load distribution at wing angles-of-attack near the stall. For this reason the lifting-line theory, as modified and presented in Reference 2 has been chosen as the more appropriate method and the one which is better suited to the present task.

3.1.2 Wing-Body Interference Theory

Many methods exist for the calculation of air loads on wing-fuselage combinations and these have been summarized by Schlicting (Reference 35), and by Flax and Lawrence (Reference 36). In view of the foregoing selection of lifting-line theory to calculate essentially wing characteristics, the following discussion will be limited to those wing-body interference methods which have been developed for use with the lifting-line approach.

The spanwise lift distribution over a wing-body combination of minimum induced drag was first treated by Lennertz (Reference 37) for a body consisting of a infinitely long circular cylinder. His solution was generalized by Pepper (Reference 38) to include bodies of any cross-section.

Multhopp (Reference 4), using a conformal mapping technique, obtained a solution for the case of a high aspect ratio wing mounted on an infinitely long cylinder of any shape. This method may be applied if a function can be found which maps the body cross-section conformally onto a circle or a straight line. The advantage of the method is that the transformed cross-section shape automatically becomes a streamline, thus satisfying the fuselage boundary conditions.

An alternative approach is that first used by Lennertz (Reference 37) in which singularities in the form of image vortices are introduced within the fuselage cross-section to satisfy, approximately, the boundary conditions. Zlotnick and Robinson (Reference 39) applied this method to the case of swept wing-body combinations with centrally placed wings.

The use of the image vortex method in combination with the lifting-line method of Reference 1 is restricted to wings which are centrally mounted on circular fuselages. For wings not centrally mounted the equations become extremely complex due to the fact that the image vortices no longer lie on the extended plane of the wing within the fuselage. For other than circular cross-sections, the determination of the number and location of the image vortices is difficult.

Weber, Kirby and Kettle (Reference 40) have modified Multhopp's approach to account for non-zero wing thickness and applied this method to low-aspect-ratio swept wings. In view of this success and because of its simplicity the Multhopp formulation of the wing-body solution (Reference 4) has been adopted herein rather than the more complex method of images of Reference 37.

3.1.3 Propeller Slipstream Effects

As pointed out in Section 2.10, the propeller slipstream exerts an important influence on wing load distribution which in turn affects the aircraft stall characteristics.

A review of the technical literature indicates that there are no adequate theoretical or semi-empirical methods which can properly account for the effects of propeller slipstream on the spanwise load distribution of the entire wing. Most of the available theoretical and experimental investigations, e.g. References 41 through 47 predict wing load distributions solely for that portion of the wing immersed in the propeller slipstream. This approach is considered to be inadequate for predicting stall characteristics of wings spanning the propeller slipstream because the portions of the wing outside the slipstream cylinder are strongly influenced by the slipstream flow. On the other hand, development of a mathematical model for predicting the effects of propeller slipstream on wing load distribution within and outside the slipstream cylinder is rather complex and is considered to be outside of the scope of the present work.

In view of the above difficulties, it was decided to temporarily exclude the power effect from wing stall analysis. However, provisions have been made to include such effects at a later date, when reliable theoretical methods for predicting the effects of propeller slipstream on the load distribution of the entire wing become available. Therefore, in developing the theory presented herein, the method of Multhopp (Reference 4) for wing-body interference effect and the method of Sivells (Reference 2) for the isolated wing have been successfully combined and are presented in the following analysis.

3.2 FORMULATION OF THE ANALYSIS

3.2.1 Conformal Transformation of Wing-Fuselage Combination

A wing in the presence of a lifting fuselage ($\alpha_B > 0$) is subjected to an upwash which decreases towards the wing tips. This upwash has the effect of a variable wing twist, which is a function of fuselage and wing geometries, fuselage angle of attack and aircraft forward speed.

The problem of fuselage-wing flow interaction has been the subject of numerous investigations in the past. As mentioned previously, the approach selected in the present analysis is that based on Multhopp's formulation. In this approach, the wing-fuselage combination is conformally transformed into an equivalent wing with a vertical slit representing the fuselage. The vertical slit is aligned with the cross-flow and is therefore automatically a streamline. The transformation is applicable to fuselage cross-sections which are approximately elliptical or which can be transformed to such by the use of other methods.

If the wing is not centrally mounted on the fuselage it transforms into a slightly curved trace whose curvature increases with an increase in the vertical distance of the wing relative to the center of the fuselage. This introduces an effective dihedral to the transformed wing, but its effect is considered to be small and is therefore not treated in this analysis.

Figure 4 shows the geometry of a wing-fuselage combination in both the real (u) and transformed ($\bar{u}$) planes. The definition of real and transformed parameters is presented in the list of symbols.

The wing load distribution, $c_l(y)$, in the u-plane is a function of the local effective angle of attack $\alpha_e(y)$ of the section under consideration. This effective section angle of attack can be expressed as follows:

$$\alpha_e(y) = \alpha_B + \alpha_R + \epsilon(y) + \Delta\alpha(y) - \alpha_i(y) \qquad (1)$$

Where α_B, α_R, and $\epsilon(y)$ are the body angle of attack, wing-root incidence relative to the body and the wing section geometric twist, respectively.

The angle due to body upwash $\Delta\alpha(y)$ and that induced by the wing trailing vortex system $\alpha_i(y)$ can be determined from the following analysis.

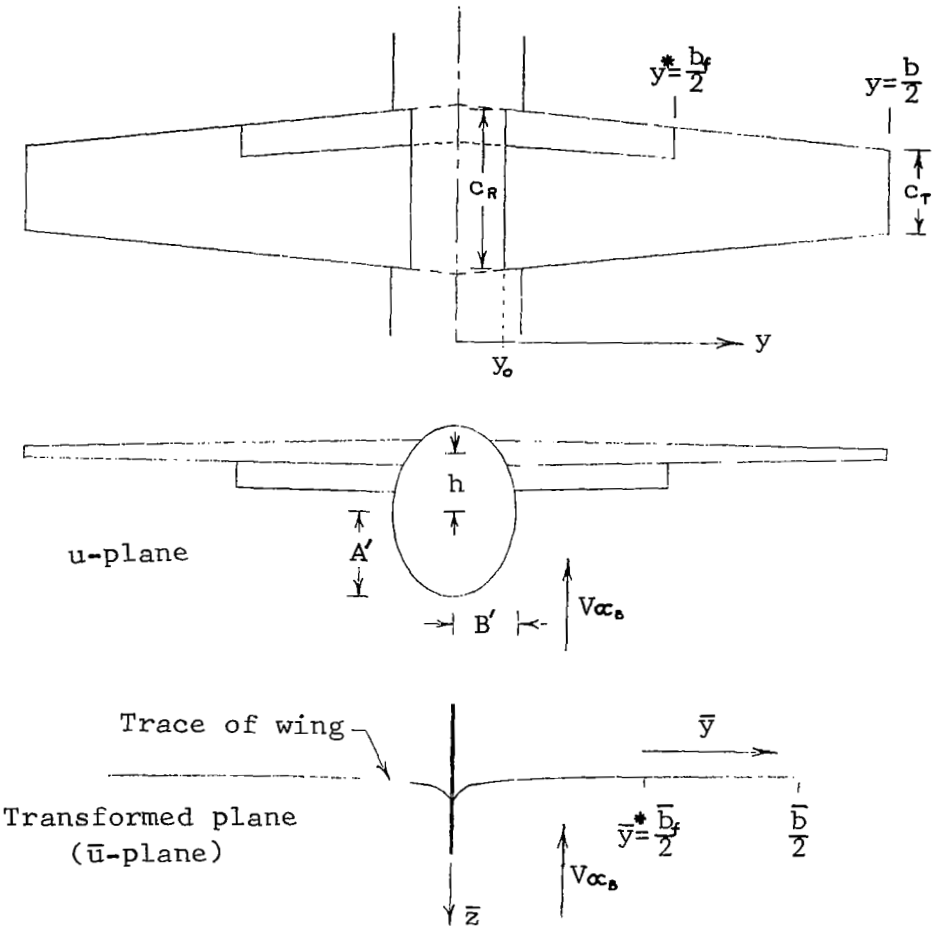

Figure 4. Definition of Parameters for Transformation of Wing-Body Combination

Using Reference 4, the wing angle of attack due to body upwash for zero wing thickness is given by:

$$\Delta \alpha (y) = \alpha_B \left(\underline{R} \frac{d\bar{u}}{du} - 1 \right) \tag{2}$$

where $\underline{R}\, d\bar{u}/du$, is the real part of the derivative of the conformal function $\bar{u}(u)$. For an elliptical fuselage, this derivative can be expressed as follows:

$$\underline{R} \frac{d\bar{u}}{du} = \frac{1}{A'-B'} \left[A' - \frac{B' \frac{a'}{\sqrt{a'^2 - e'^2}}}{1 + \frac{e'^2\, y^2}{(a'^2 - e'^2)}} \right] \tag{3}$$

where,

$$a' = \frac{1}{2} \left(\sqrt{y^2 + (h - e')^2} + \sqrt{y^2 + (h + e')^2} \right) \tag{4}$$

For a circular fuselage equation (3) becomes:

$$\underline{R} \frac{d\bar{u}}{du} = 1 + \frac{A'^2 (y^2 - h^2)}{(y^2 + h^2)^2} \tag{5}$$

For wings of non-zero thickness, Reference 40 suggests that the upwash at the wing is decreased as compared to that for wings of zero thickness. This can be approximately accounted for by reducing the wing angle of attack due to body upwash, $\Delta \alpha (y)$, by a factor T taken as constant across the wing span. The factor can be expressed as the ratio of the body cross-sectional area above and below the wing to the total frontal area of the body. Thus, if the wing is not too thick, there follows:

$$T = 1 - \frac{2\, t_r\, y_o}{\pi\, A'\, B'} \tag{6}$$

Thus, for wings of non-zero thickness, equation (2) can be rewritten as:

$$\Delta \alpha (y) = T\, \alpha_B \left(\underline{R} \frac{d\bar{u}}{du} - 1 \right) \tag{7}$$

If, however, the conformal function for the thick wing, $\left(\underline{R} \frac{d\bar{u}}{du}\right)_T$ could be determined, then equation (7) would be

$$\Delta\alpha(y) = \alpha_B\left[\left(\underline{R}\frac{d\bar{u}}{du}\right)_T - 1\right] \tag{8}$$

Comparing equation (7) and (8) there results:

$$\left(\underline{R}\frac{d\bar{u}}{du}\right)_T = 1 + T\left(\underline{R}\frac{d\bar{u}}{du} - 1\right) \tag{9}$$

Equation (9) represents an approximation to the real part of the derivative of the conformal function applicable to wings of non-zero thickness. This equation is therefore used to relate the induced angle of attack at a point y in the u -plane to that at the corresponding point $\bar{y}$ in the $\bar{u}$ -plane, thus:

$$\alpha_i(y) = \bar{\alpha}_i(\bar{y})\left[\underline{R}\frac{d\bar{u}}{du}\right]_T = \bar{\alpha}_i(\bar{y})\left[1 + T\left(\underline{R}\frac{d\bar{u}}{du} - 1\right)\right] \tag{10}$$

Finally, substituting equations (7) and (10) into equation (1) the effective angle of attack for wings of non-zero thickness is given by

$$\alpha_e(y) = \alpha_R + \epsilon(y) + \left[\alpha_B - \bar{\alpha}_i(\bar{y})\right]\left[1 + T\left(\underline{R}\frac{d\bar{u}}{du} - 1\right)\right] \tag{11}$$

The only unknown which remains to be determined in equation (11) is $\bar{\alpha}_i(\bar{y})$.

The induced angle of attack, in degrees, at a point $\bar{y}$, on the transformed span is given by the familiar relation

$$\bar{\alpha}_i = \frac{180\,\bar{b}}{8\pi^2}\int_{-\bar{b}/2}^{\bar{b}/2}\frac{\dfrac{d\left(\dfrac{\bar{c}_l(\bar{y})\,c}{\bar{b}}\right)}{d\bar{y}}}{\bar{y}_1 - \bar{y}}\,d\bar{y} \tag{12}$$

where $\bar{c}_l(\bar{y})$ is the section lift coefficient in the transformed plane at a point $\bar{y}$. It should be noted that since the transformation is conformal, the circulation $\bar{\Gamma}(\bar{y})$ about any wing section and the associated section lift coefficient $\bar{c}_l(\bar{y})$ in the transformed plane are equal to the corresponding values in the real plane. Since the geometric quantities of chord length (c) and wing twist at each point in the real plane are also the same at the corresponding points in the transformed plane then

$$\bar{c}_l(\bar{y}) = c_l(y) = c_l \tag{13}$$

For wings with undeflected flaps, the spanwise lift distribution in the transformed plane can be expressed as an infinite trigonometric series as follows:

$$\frac{c_l\, c}{\bar{b}} = \sum_{n=1}^{\infty} A_n \sin(n\bar{\theta}) \tag{14}$$

where,

$$\bar{\theta} = \cos^{-1}\left(\frac{2\bar{y}}{\bar{b}}\right) \tag{15}$$

Using equations (12) and (14) there follows, according to Reference 23

$$\bar{\alpha}_l = \frac{180}{4\pi \sin\bar{\theta}} \sum_{n=1}^{\infty} n A_n \sin(n\bar{\theta}) \tag{16}$$

Thus, in order to determine the induced angles of attack the values of the coefficients A_n are required. These are obtained as follows:

The spanwise lift distribution is approximated by a finite trigonometric series of $r-1$ terms corresponding to determining the load at an odd number, $r-1$, of points on the span. That is, the range $0<\bar{\theta}<\pi$ is divided up into r equally spaced intervals where $\bar{\theta}=m\pi/r \quad m=1, 2, \ldots, r-1$.

Thus, equation (14) can be rewritten as:

$$\left(\frac{c_l\, c}{\bar{b}}\right)_m = \sum_{n=1}^{r-1} A_n \sin n\frac{m\pi}{r} \tag{17}$$

Using harmonic analysis, equation (17) yields the coefficients A_n of the trigonometric series, thus

$$A_n = \frac{2}{r} \sum_{m=1}^{r-1} \left(\frac{c_l\, c}{\bar{b}}\right)_m \sin n\frac{m\pi}{r} \tag{18}$$

If equation (18) is now combined with equation (16), an expression is obtained for the induced angle of attack, thus

$$\bar{\alpha}_i = \frac{180}{4\pi \sin\bar{\theta}} \left(\sum_{n=1}^{r-1} n \sin n\bar{\theta} \right) \left[\frac{2}{r} \sum_{m=1}^{r-1} \left(\frac{c_l c}{\bar{b}} \right)_m \sin n \frac{m\pi}{r} \right]$$

$$= \frac{180}{4\pi r \sin\bar{\theta}} \sum_{m=1}^{r-1} \left(\frac{c_l c}{\bar{b}} \right)_m \sum_{n=1}^{r-1} n \left[\cos n \left(\bar{\theta} - \frac{m\pi}{r} \right) - \cos n \left(\bar{\theta} + \frac{m\pi}{r} \right) \right] \qquad (19)$$

Since the induced angle of attack is to be determined at the points $\bar{\theta}$ at which the load distribution is required, i.e. at the points $\bar{\theta} = \frac{k\pi}{r}$ then

$$\bar{\alpha}_{i_k} = \frac{180}{4\pi r \sin\left(\frac{k\pi}{r}\right)} \sum_{m=1}^{r-1} \left(\frac{c_l c}{\bar{b}} \right)_m \sum_{n=1}^{r-1} n \left[\cos n \frac{(k-m)\pi}{r} - \cos n \frac{(k+m)\pi}{r} \right] \qquad (20)$$

or,

$$\bar{\alpha}_{i_k} = \sum_{m=1}^{r-1} \left(\frac{c_l c}{\bar{b}} \right)_m \beta_{mk} \qquad (21)$$

where

$$\beta_{mk} = \frac{180}{4\pi r \sin\frac{k\pi}{r}} \sum_{n=1}^{r-1} n \left[\cos n \frac{(k-m)\pi}{r} - \cos n \frac{(k+m)\pi}{r} \right] \qquad (22)$$

It can be shown that if $k \pm m$ is odd then

$$\beta_{mk} = \frac{180}{4\pi r \sin\frac{k\pi}{r}} \left[\frac{1}{1-\cos\frac{(k+m)\pi}{r}} - \frac{1}{1-\cos\frac{(k-m)\pi}{r}} \right] \qquad (23a)$$

and if $k=m$

$$\beta_{mk} = \frac{180\, r}{8\pi \sin\frac{k\pi}{r}} \qquad (23b)$$

finally, when $k \pm m$ is even and $k \neq m$

$$\beta_{mk} = 0 \qquad (23c)$$

The values of β_{mk} depend only on the number of spanwise stations used and are independent of wing aspect ratio and taper ratio. Knowing the values of β_{mk}, equation (21) can now be utilized to determine the induced angle of attack, $\bar{\alpha}_{i_k}$, at a point on the transformed span, in terms of a known or assumed spanwise lift distribution.

3.2.2 Spanwise Load Distribution for a Wing With No Flap or a Full Span Deflected Flap

The method of determining the lift distribution is one of successive approximations. For a given body angle of attack a distribution of $c_l\, c/\bar{b}$ is assumed and the induced angles of attack are computed using equation (21). Using equation (11) the effective section angles of attack are calculated and the corresponding values of lift coefficient obtained from airfoil data at the appropriate values of the section parameters. This process is repeated until the guessed values agree with the computed values to within the required tolerance.

In order to minimize the number of iterations required to converge on the final distribution of lift coefficient a systematic method is required to generate increasingly better approximations. Such a method is developed in Reference 2 and is herein presented in slightly different notation.

For a wing-body combination with zero thickness wing and no flap deflection, the basic equation to be satisfied during any cycle of the iterative process is the simplified version of equation (11), i.e.

$$\alpha_e(y) = \alpha_g(y) + \epsilon(y) + \alpha_B \left(\underline{R}\frac{d\bar{u}}{du}\right) - \bar{\alpha}_i(\bar{y})\,\underline{R}\frac{d\bar{u}}{du} \qquad (24a)$$

$$= \alpha_g(y) + \epsilon(y) + \alpha_B \left(\underline{R}\frac{d\bar{u}}{du}\right) - \underline{R}\frac{d\bar{u}}{du}\sum_{m=1}^{r-1}\left(\frac{c_l\, c}{\bar{b}}\right)_m \beta_{mk}$$

or

$$\alpha_e(y) = \alpha_k - \underline{R}\frac{d\bar{u}}{du}\sum_{m=1}^{r-1}\left(\frac{c_l\, c}{\bar{b}}\right)_m \beta_{mk} \qquad (24b)$$

where, $$\alpha_k = \alpha_g(y) + \epsilon(y) + \alpha_B \left(\underline{R}\frac{d\bar{u}}{du}\right) \tag{25}$$

Assuming linear section lift-curves the relationship for one cycle of the iteration is

$$\left\{\alpha_k - \underline{R}\frac{d\bar{u}}{du}\sum_{m=1}^{r-1}\left(\frac{c_\ell c}{\bar{b}}\right)_m \beta_{mk}\right\}\left(\frac{a_o c}{\bar{b}}\right)_k = \left(\frac{c_\ell c}{\bar{b}}\right)_k + \Delta_k \tag{26}$$

where Δ_k is the amount to be added to the approximate value $c_\ell\, c/\bar{b}$ to obtain the calculated value.

For the following cycle a value Δ'_k is chosen such that the calculated values are equal to the guessed values thus:

$$\left\{\alpha_k - \underline{R}\frac{d\bar{u}}{du}\sum_{m=1}^{r-1}\left[\left(\frac{c_\ell c}{\bar{b}}\right) + \Delta'\right]_m \beta_{mk}\right\}\left(\frac{a_o c}{\bar{b}}\right)_k = \left(\frac{c_\ell c}{\bar{b}}\right)_k + \Delta'_k \tag{27}$$

Subtracting equation (27) from equation (26) yields

$$\left(\frac{a_o c}{\bar{b}}\right)_k \left(\underline{R}\frac{d\bar{u}}{du}\right)_k \sum_{m=1}^{r-1}\Delta'_m\ \beta_{mk} = \Delta_k - \Delta'_k \tag{28}$$

then with

$$G'_{mk} = \left(\frac{a_o c}{\bar{b}}\right)_k \beta_{mk}\left(\underline{R}\frac{d\bar{u}}{du}\right)_k \qquad m \neq k$$

$$= 1 + \left(\frac{a_o c}{\bar{b}}\right)_k \beta_{mk}\left(\underline{R}\frac{d\bar{u}}{du}\right)_k \qquad m = k$$

there follows

$$\sum_{m=1}^{r-1} G'_{mk}\ \Delta'_m = \Delta_k \tag{29a}$$

or

$$\left[G_{mk}\right]\left\{\Delta'_m\right\} = \left\{\Delta_m\right\} \tag{29b}$$

where G_{mk} is the transpose of G'_{mk} .

Thus, the values to be added to one set of approximate values to obtain a better approximation are given by:

$$\left\{\Delta'_m\right\} = \left[G_{mk}\right]^{-1}\left\{\Delta_m\right\} \tag{30a}$$

or,

$$\left\{\Delta'_j\right\} = \left[K_{ij}\right]\ \left\{\Delta_j\right\} \tag{30b}$$

The matrix of coefficients K_{ij} is easily obtained by the usual methods of matrix algebra.

3.2.3 Spanwise Load Distribution for a Wing With a Deflected Part-Span Flap

The deflection of a part-span flap causes a discontinuity in the distribution of absolute angle of attack at the end of the flap. In order to maintain a continuous spanwise distribution of lift a corresponding discontinuity must exist in the distribution of induced angle of attack.

From Reference 2, the complete lift distribution may be expressed as the sum of two distributions, thus:

$$\frac{c_l c}{\bar{b}} = \frac{c_{l_1} c}{\bar{b}} + \delta\left(\frac{c_{l_2} c}{\bar{b}}\right) \tag{31}$$

where $\delta(c_{l2}c/\bar{b})$ is the distribution due to a unit discontinuity in induced angle of attack and $c_{l_1}c/\bar{b}$ is the remainder of the lift distribution. Since the latter distribution is continuous the multipliers β_{mk} may be used directly to obtain the corresponding induced angles of attack.

$$\alpha_{i_{1k}} = \sum_{m=1}^{r-1}\left(\frac{c_{l_1} c}{\bar{b}}\right)_m \beta_{mk} \tag{32}$$

Since $\bar{\alpha}_{i2k} = \delta$ over the flapped span and $\bar{\alpha}_{i2k} = 0$ over the unflapped span, the total induced angle of attack is

$$\bar{\alpha} i_k = \bar{\alpha} i_{1k} + \bar{\alpha} i_{2k} \tag{33}$$

Now, if the multipliers were used with the total lift distribution

$$\sum_{m=1}^{r-1} \left(\frac{c_l c}{\bar{b}}\right)_m \beta_{mk} = \sum_{m=1}^{r-1} \left(\frac{c_{l_1} c}{\bar{b}}\right)_m \beta_{mk} + \sum_{m=1}^{r-1} \delta \left(\frac{c_{l_2} c}{\bar{b}\delta}\right) \beta_{mk}$$

and $\bar{\alpha} i_{2k}$ were added to both sides, the result would be:

$$\sum_{m=1}^{r-1} \left(\frac{c_l c}{\bar{b}}\right)_m \beta_{mk} + \bar{\alpha} i_{2k} = \sum_{m=1}^{r-1} \left(\frac{c_{l_1} c}{\bar{b}}\right)_m \beta_{mk} + \bar{\alpha} i_{2k} + \sum_{m=1}^{r-1} \delta \left(\frac{c_{l_2} c}{\bar{b}\delta}\right) \beta_{mk} \tag{34}$$

$$= \bar{\alpha} i_k + \sum_{m=1}^{r-1} \delta \left(\frac{c_{l_2} c}{\bar{b}\delta}\right)_m \beta_{mk}$$

Rearranging equation (34) yields:

$$\bar{\alpha} i_k = \sum_{m=1}^{r-1} \left(\frac{c_l c}{\bar{b}}\right)_m \beta_{mk} + \delta \left[\frac{\bar{\alpha} i_{2k}}{\delta} - \sum_{m=1}^{r-1} \left(\frac{c_{l_2} c}{\bar{b}\delta}\right)_m \beta_{mk}\right] \tag{35}$$

A comparison of equation (35) with equation (21) shows that for a wing with a deflected flap an additional term is required which is proportional to the magnitude of the discontinuity. This terms represents a correction factor to account for the inability of a limited trigonometric series to represent adequately the spanwise lift distribution of a wing with deflected flaps.

Equation (35) may be rewritten as:

$$\bar{\alpha} i_k = \bar{\alpha}_{u_k} + \delta \left(\frac{\bar{\alpha} c_k}{\delta}\right) \tag{36}$$

where the uncorrected induced angle of attack is expressed as

$$\bar{\alpha}_{uk} = \sum_{m=1}^{r-1} \left(\frac{c_l c}{\bar{b}}\right)_m \beta_{mk} \tag{37}$$

and the correction factor per unit discontinuity is

$$\frac{\bar{\alpha}_{ck}}{\delta} = \frac{\bar{\alpha}_{i2k}}{\delta} - \sum_{m=1}^{r-1} \left(\frac{c_{l_2} c}{\bar{b}\,\delta}\right)_m \beta_{mk} \tag{38}$$

The distribution of $(c_{l_2} c/\bar{b}\,\delta)$ may be expressed in the form:

$$\frac{c_{l_2} c}{\bar{b}\,\delta} = \frac{1}{90}\left[(\cos\bar{\theta} - \cos\bar{\theta}^*)\log\left\{\frac{1-\cos(\bar{\theta}+\bar{\theta}^*)}{1-\cos(\bar{\theta}-\bar{\theta}^*)}\right\} + \frac{\pi\bar{\theta}^*\sin\bar{\theta}}{90}\right] \tag{39}$$

for $\dfrac{\bar{\alpha}_{i\,2}}{\delta} = 1, \quad 0 < \bar{\theta} < \bar{\theta}^*$;

for $\dfrac{\bar{\alpha}_{i\,2}}{\delta} = 0, \quad \bar{\theta}^* < \bar{\theta} < 180°$;

where $\bar{\theta}^* = \cos^{-1}(2\bar{y}^*/\bar{b})$ and $\bar{\theta}^*$ and δ are in degrees.

The distribution of $c_{l_2} c/\bar{b}\,\delta$ as given by equation (39) depends solely on the spanwise position of the discontinuity at the end of the flap, and applies to outboard flaps which begin at $2\bar{y}/\bar{b} = 1$ and end at $2\bar{y}^*/\bar{b}$. For a wing with symmetrical inboard flaps extending between $2\bar{y}/\bar{b} = 2\bar{y}^*/\bar{b}$ and $2\bar{y}/\bar{b} = -2\bar{y}^*/\bar{b}$ the distribution is obtained by subtracting values of $c_{l_2} c/\bar{b}\,\delta$ for $2\bar{y}^*/\bar{b}$ from those for $-2\bar{y}^*/\bar{b}$. The correction factor per unit discontinuity $\bar{\alpha}_{ck}/\delta$, given by equation (38) is therefore a function of only the spanwise position of the discontinuity and β_{mk}.

It should be noted that two values of $\bar{\alpha}\,c/\delta$ exist at the end of the flap, one corresponding to $2\bar{y}^*/\bar{b} + 0$, (the flap side of $2\bar{y}^*/\bar{b}$) and the other corresponding to $2\bar{y}^*/\bar{b} - 0$, (the unflapped side). The values are related by:

$$\left(\frac{\bar{\alpha}\,c}{\delta}\right)_{\frac{2\bar{y}^*}{\bar{b}}-0} = \left(\frac{\bar{\alpha}\,c}{\delta}\right)_{\frac{2\bar{y}^*}{\bar{b}}+0}^{-1} \tag{40}$$

Either of the two values of $\bar{a}c/\delta$ may be used so long as the value is used with the proper section lift curve.

3.2.4 Modification of the Two-Dimensional Section Lift Data

If the two-dimensional section data were used directly discontinuities would be found in the maximum lift distribution at the ends of the deflected flaps. Since the discontinuities do not actually occur, the two-dimensional data must be adjusted to reflect the fact that sections in the vicinity of the end of the flap exhibit values of $c_{l\,max}$ which lie between those for flapped and unflapped sections. Therefore, following the method of Reference 2 the two-dimensional data is modified to obtain so called three-dimensional section data.

The root section of a wing with a partial-span flaps deflected would act most nearly like that of a wing with full-span flaps. Similarly, the tip section would behave as if it were on a wing with no flap deflection. Now the load distribution for the wing with partial span flaps can be calculated as long as each section is operating in the linear range of its lift curve. A typical distribution, denoted by $c_{l\,\delta}$, is shown in Figure 5.

A lift distribution is now calculated for the same wing with no flap deflection and the ordinates scaled so that the wing has a lift coefficient of unity. Such a distribution, denoted by c_{l_1} is also shown in Figure 5.

This distribution is multiplied by a suitable constant factor k_1 to give the same value at the root as the distribution with the flap deflected and by another factor k_2 to give the same value as the flap distribution at the outermost station used in the computations.

The differences between $c_{l\,\delta}$ and $k_1\,c_{l_1}$ inboard of the flap end and between $c_{l\,\delta}$ and $k_2 c_{l_1}$, outboard of the flap end, are divided by the difference between $k_1\,c_{l_1}$ and $k_2\,c_{l_1}$ taken at the end of the flap. Thus, the resulting values or factors, F can be expressed as follows:

$$F = \frac{c_{l\,\delta} - k_1 c_{l_1}}{c_{l_1}(k_1 - k_2)} \qquad \text{for } \frac{2\bar{y}}{b} < \frac{2\bar{y}^*}{b} \tag{41}$$

and for $\frac{2\bar{y}}{b} > \frac{2\bar{y}^*}{b}$

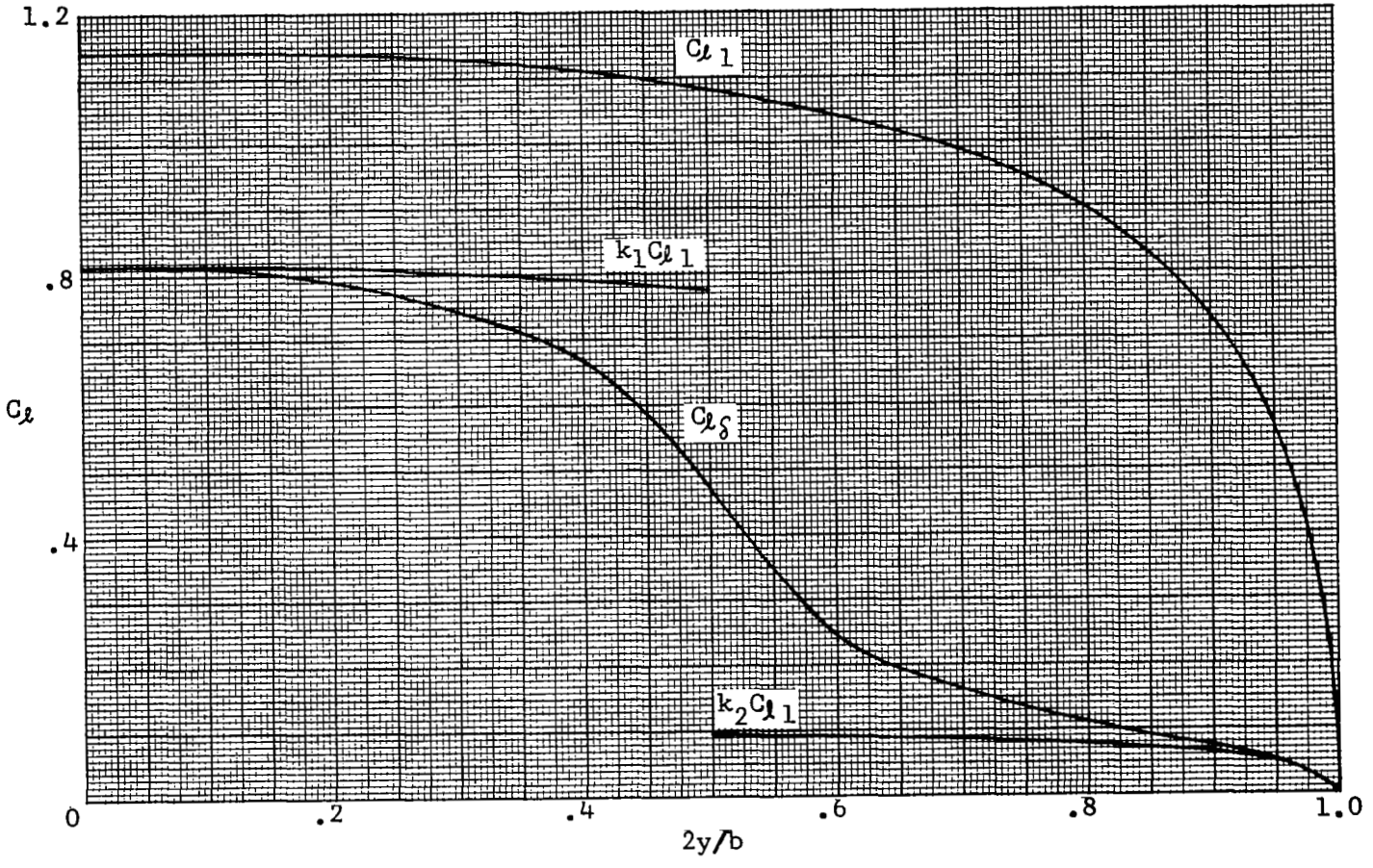

Figure 5. - Typical Load Distributions for Obtaining Factors for Altering Two-dimensional Data.

$$F = \frac{c_l \delta - k_2 c_{l1}}{c_{l_1}(k_1 - k_2)} \tag{42}$$

These factors are relatively insensitive to lift-curve slope and may be used in the non-linear portions of the lift curves.

In calculating the above mentioned distributions, any convenient values of the discontinuity δ and wing angle of attack may be used. Wing twist is omitted in these computations. Having obtained the factors F the values of maximum lift coefficient are then altered according to:

$$c_{l\,max} = (c_{l\,max})_o + F(\Delta c_l^*{}_{max}) \tag{43}$$

where $(c_{l\,max})_o$ is the two-dimensional value of section maximum lift coefficient and $\Delta c_l^*{}_{max}$ is the increment in $c_{l\,max}$ due to flap deflection at the end of the flap.

Figure 6 illustrates the method of obtaining the final corrected lift curves. At each angle of attack (α_o) the two-dimensional uncorrected value of lift coefficient $(c_{l\,o})$, as obtained from the airfoil data, is factored to give the corresponding value of lift coefficient corrected for proximity to the flap end thus,

$$c_{l\,cor} = c_{l\,o} \frac{c_{l\,max}}{(c_{l\,max})_o} \tag{44}$$

This value of lift coefficient would correspond to a value of angle of attack α' on the two-dimensional lift curve. Due to the fact that each wing section is not operating in a true two-dimensional flow, but forms part of a finite-span wing a correction must be made to account for the fact that the air can flow around the wing tips. This extra degree of freedom implies that a section on a finite-span wing must operate at a higher angle of attack than the same section in strictly two-dimensional flow in order to achieve the same value of lift coefficient. This correction was first derived by Jones, Reference 48, in the form of the edge velocity factor given by:

$$E = \frac{\alpha_e - \alpha_{l\,o}}{\alpha_o - \alpha_{l\,o}} \tag{45}$$

Jones originally derived the correction factor for a wing of elliptic planform and expressed it as,

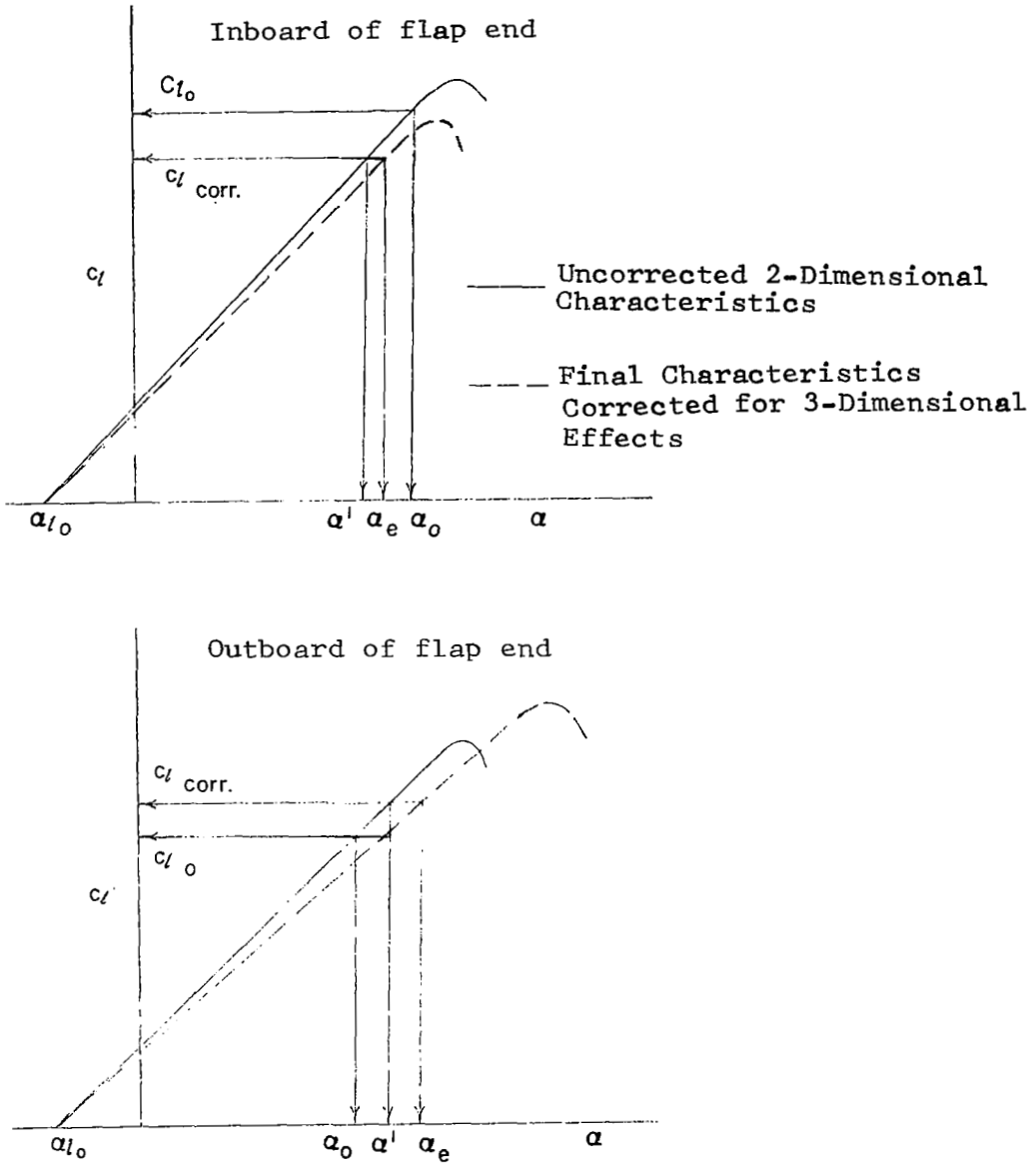

Figure 6. Illustration of Method for Correcting Two-dimensional Section Data.

$$E = \frac{\text{wing semi-perimeter}}{\text{wing span}} \tag{46}$$

Reference 2 gives a more accurate expression, applicable to wings of other than elliptical planform, in the form,

$$E = \sqrt{1 + \frac{4}{AR^2}} \tag{47}$$

Thus, the effective angle of attack, α_e, corresponding to the two-dimensional angle of attack, α', is given by,

$$E = \frac{\alpha_e - \alpha_{l_0}}{\alpha' - \alpha_{l_0}} \tag{48}$$

and since α' is related to the original value α_0 by

$$\frac{\alpha' - \alpha_{l_0}}{\alpha_0 - \alpha_{l_0}} = \frac{c_{l\ max}}{(c_{l\ max})_0} \tag{49}$$

then the correction which must be made to α_0 to account for both edge-velocity and flap proximity is obtained as

$$\frac{\alpha_e - \alpha_{l_0}}{\alpha_0 - \alpha_{l_0}} = E\ \frac{c_{l\ max}}{(c_{l\ max})_0} \tag{50}$$

Figure 6 shows the final corrected lift curves as compared to the original two-dimensional data for two stations, one inboard and the other outboard of the flap end.

The above method of correcting the two dimensional section data to account for flap discontinuity is substantiated experimentally by Reference 2.

It should be noted that the Jones edge velocity correction applies regardless of whether the flap is deflected or not.

3.2.5 Calculation of Overall Wing Characteristics

Once the spanwise lift distribution of a wing has been calculated the determination of drag and pitching moment

coefficients is a simple matter since these quantities depend on the lift distribution.

By the use of Simpson's Rule, the integrated values of lift, induced drag, profile drag and pitching moment coefficients are given by:

$$C_L = \left(\frac{\bar{b}}{b}\right)^2 AR \sum_{m=1}^{r-1} \left(\frac{c\ c}{\bar{b}}\right)_m \eta_m \tag{51}$$

$$C_{D_i} = \frac{\pi}{180} \left(\frac{\bar{b}}{b}\right)^2 AR \sum_{m=1}^{r-1} \left[\left(\frac{c_l\ c}{\bar{b}}\right)\alpha_i\right]_m \eta_m \tag{52}$$

$$C_{D_o} = \left(\frac{\bar{b}}{b}\right)^2 AR \sum_{m=1}^{r-1} \left(\frac{c_{do} c}{\bar{b}}\right)_m \eta_m \tag{53}$$

$$C_M = \frac{AR\ \bar{b}}{b^2 c'} \sum_{m=1}^{r-1} \left(c_m c^2\right)_m \eta_m \tag{54}$$

where

$$c_m = c_{m\ c/4} - \frac{X}{c}\left[c_l \cos(\alpha_B - \alpha_i) + c_{do} \sin(\alpha_B - \alpha_i)\right] \tag{55}$$

$$-\frac{Z}{c}\left[c_l \sin(\alpha_B - \alpha_i) - c_{do} \cos(\alpha_B - \alpha_i)\right]$$

In equation (55) the section lift and drag forces are assumed to act through the quarter-chord points.

The multipliers η_m used in equation (51) through (54) are defined by:

$$\eta_m = \frac{\pi}{6r}\left[3 - (-1)^m\right] \sin\frac{m\pi}{r} \tag{56}$$

Step-by-step computational procedures based on the preceding analysis are presented in the following section.

SECTION 4

COMPUTER PROGRAM

The solution of the mathematical model described in Section 3 was accomplished by means of a specially developed digital computer program. This section presents a detailed description of the computational procedures, the required section data, and the implementation of the computer program. The results of sample calculations are also presented.

4.1 COMPUTATIONAL PROCEDURES

The following is a mathematical description of the individual steps used in the computation of the wing spanwise load distributions. The sequence of the calculations is essentially the same as that set up in the computer program which is described later. The computational procedures cover three separate cases; wings with no flaps, wings with full-span flaps and wings with part-span deflected flaps.

4.1.1 Computation of Basic Parameters

(a) Calculate the following geometric quantities

$$Y_o = B\sqrt{1 - \frac{H^2}{A^2}} \tag{57}$$

$$e = \sqrt{A^2 - B^2} \tag{58}$$

$$T = 1 - \frac{4 Y_o (t/c)_R (c_R/b)}{\pi A B} \tag{59}$$

where Y_o, B, H, A, e are, respectively, $\frac{2y_o}{b}, \frac{2B'}{b}, \frac{2h}{b}, \frac{2A'}{b}, \frac{2e'}{b}$

(b) Calculate a number of points Y' on the exposed wing span for even increments of θ using

$$Y' = Y_o + (1 - Y_o)\cos\theta \tag{60}$$

where

$$\theta = \cos^{-1}\left(\frac{y - y_o}{\frac{b}{2} - y_o}\right) \tag{61}$$

$$= \cos^{-1}\left(\frac{Y - Y_o}{1 - Y_o}\right)$$

(c) Compute the average (non-dimensional) distances of the points Y' from the focii of the elliptic fuselage using

$$a' = \frac{1}{2}\left[\sqrt{Y'^2 + (H-e)^2} + \sqrt{Y'^2 + (H+e)^2}\right] \tag{62}$$

where for the wing tip

$$a' = a_T = \frac{1}{2}\left[\sqrt{1 + (H-e)^2} + \sqrt{1 + (H+e)^2}\right] \tag{63}$$

(d) Transform from the u-plane to the $\bar{u}$-plane using the following relationships for an elliptical fuselage.

$$\frac{\bar{b}}{b} = \frac{1}{A-B}\left\{A - \frac{B\,a_T}{\sqrt{a_T^2 - e^2}}\right\} \tag{64}$$

and

$$\bar{Y}' = \frac{b}{\bar{b}}\,\frac{Y'}{A-B}\left\{A - \frac{B\,a'}{\sqrt{a'^2 - e^2}}\right\} \tag{65}$$

If the fuselage has a circular cross-section compute

$$\frac{\bar{b}}{b} = 1 - \frac{A^2}{1 + H^2} \tag{66}$$

and

$$\bar{Y}' = Y' \left[1 - \frac{A^2}{Y'^2 + H^2} \right] \tag{67}$$

where A is the cross-sectional radius (non-dimensional),

(e) Calculate a new set of points $\bar{Y}$ on the transformed span for even increments in the spanwise variable $\bar{\theta}$ as follows

$$\bar{Y} = \cos \bar{\theta} \tag{68}$$

where

$$\bar{\theta} = \cos^{-1}\left(\frac{2\bar{y}}{\bar{b}}\right)$$

(f) Using the relationship of Y' to $\bar{Y}'$ obtained above, interpolate to find the points on the physical span, Y, corresponding to $\bar{Y}$.

(g) For an elliptical fuselage cross-section obtain values for

$$\underline{R}\,\frac{d\bar{u}}{du} = \frac{1}{A-B}\left[A - \frac{B\sqrt{\frac{a}{a^2 - e^2}}}{1 + \frac{e^2 Y^2}{(a^2 - e^2)^2}} \right] \tag{69}$$

where

$$a = \frac{1}{2}\left(\sqrt{Y^2 + (H-e)^2} + \sqrt{Y^2 + (H+e)^2} \right) \tag{70}$$

or, if the cross-section is circular, use

$$\underline{R}\,\frac{d\bar{u}}{du} = 1 + \frac{A^2 (Y^2 - H^2)}{(Y^2 + H^2)^2} \tag{71}$$

(h) If the wing has a deflected part-span flap calculate the location of the end of the flap in the $\bar{u}$-plane using

$$\bar{Y}^* = \frac{b}{\bar{b}} \frac{Y^*}{(A-B)} \left[A - \frac{B\, a^*}{\sqrt{a^{*2} - e^2}} \right] \tag{72}$$

where

$$a^* = \frac{1}{2} \sqrt{Y^{*2} + (H-e)^2} + \sqrt{Y^{*2} + (H+e)^2} \tag{73}$$

(i) For a wing with linear taper in both chord and thickness from fuselage side to wing tip calculate

$$\frac{c}{c_R} = 1 - (1-\lambda) \left[\frac{|Y| - Y_o}{1 - Y_o} \right] \tag{74}$$

$$\frac{(t/c)}{(t/c)_R} = \frac{1 - \left(1 - \lambda \frac{(t/c)_T}{(t/c)_R}\right) \left[\frac{|Y| - Y_o}{1 - Y_o} \right]}{\frac{c}{c_R}} \tag{75}$$

$$K = K_R + (K_T - K_R) \left[\frac{|Y| - Y_o}{1 - Y_o} \right] \tag{76}$$

$$\epsilon = \frac{\epsilon_T \lambda}{c/c_R} \left[\frac{|Y| - Y}{1 - Y} \right] \tag{77}$$

and

$$R_e = \frac{R_e'(c/c_R)}{c'/c_R} \tag{78}$$

where R_e' is the flight Reynolds number based on the exposed wing mean aerodynamic chord c' which is given by

$$\frac{c'}{c_R} = \frac{2}{3}\left[\frac{1+\lambda+\lambda^2}{1+\lambda}\right] \tag{79}$$

Note that the geometric wing twist, ϵ, is non-linear and that the spanwise distribution of wing section camber level is taken to be linear.

For a wing planform which is not trapezoidal the foregoing quantities may be determined from a drawing or from a special calculation.

(j) Finally, calculate the multipliers β_{mk}, η_m, and the matrix of coefficients K_{ij} using equations (23) (56) and (30) respectively. Also, for part-span deflected flaps obtain $c_{l_2}c/\bar{b}\delta$ and α_{ck}/δ from equations (38) and (39).

4.1.2 Wings With No Flaps or With Full-Span Deflected Flaps

If the wing has deflected or undeflected full-span flaps the computations are simplified since no corrections are required for spanwise discontinuities in induced angle of attack. In this case the computational procedure is as follows:

(a) For the desired body angle of attack calculate the distribution of geometric angle of attack using

$$\alpha_g = \alpha_R + \epsilon + \alpha_B \quad T\left[\underline{R}\frac{d\bar{u}}{du} - 1\right] + \alpha_B \tag{80}$$

(b) Obtain the corresponding c_l and α_o values by interpolation in the two-dimensional section data at the proper Reynolds number, thickness-chord ratio and camber level.

(c) Calculate an initial approximation to the distribution of the loading on the transformed wing using:

$$\frac{c_l c}{\bar{b}} = c_l\left(\frac{AR}{AR+1.8}\right)\left(\frac{c}{c_R}\right)\left(\frac{c_R}{b}\right)\left(\frac{b}{\bar{b}}\right)\left[\frac{1}{2}+(1+\lambda)\sqrt{1-\bar{Y}^2}\right] \tag{81}$$

(d) Calculate the corresponding values of induced angle of attack $\bar{\alpha}_i$ using equation (21) and determine the effective wing angles of attack in the real plane from equation (11).

(e) Now compute the equivalent angles of attack, α_0, for use with the two-dimensional section data thus

$$\alpha_0 = \left[\alpha_e - \alpha_{l0}(1-E)\right] / E \qquad (82)$$

where E is given by equation (47).

(f) Using the section data obtain the values of lift coefficient corresponding to α_0 and then calculate new values of $c_l\, c/\bar{b}$.

(g) Compare these values to the guessed values of $c_l\, c/\bar{b}$ and if agreement is not sufficiently close obtain a set of values of Δj by applying the matrix Kij to the differences between the calculated and guessed values as shown in equation (30b). Add the results to the original guessed values of $c_l\, c/\bar{b}$ and obtain a new and better set of approximate values. Repeat steps (d) through (g) until satisfactory agreement is reached.

(h) Having determined the lift distribution obtain section values of profile-drag coefficient, induced-drag coefficient and pitching moment coefficient.

(i) Finally, using equations (51) through (56), calculate the values of C_L, C_{D_0}, C_{D_i}, and C_M.

4.1.3 Wings With Part-Span Deflected Flaps

(a) Determine the lift distribution for the plain untwisted, unflapped wing-body combination at an angle of attack which is within the linear range of the section lift curves. Scale the resulting lift distribution to give a value of wing lift coefficient equal to unity. Denote this distribution by c_{l_1}.

(b) For the untwisted, flapped wing body combination, select a body angle of attack within the linear range of both the flapped and unflapped section lift-curves. Obtain the value of section lift coefficient, c_{l_R}, for the root section from the airfoil data.

(c) Calculate the initial approximation to the lift distribution in the transformed plane using

$$\frac{c_l\, c}{\bar{b}} = \frac{1}{2} c_{l_R} \left(\frac{c}{c_R}\right)\left(\frac{c_R}{b}\right)\left(\frac{b}{\bar{b}}\right)\left\{1+\sqrt{1-\left(\frac{\bar{Y}}{\bar{Y}^*}\right)^2}\right\} \quad 0 \leq \bar{Y} \leq \bar{Y}^* \qquad (83)$$

and

$$\frac{c_l c}{\bar{b}} = \frac{1}{2} c_{l_R} \left(\frac{c}{c_R}\right) \left(\frac{c_R}{b}\right) \left(\frac{b}{\bar{b}}\right) \left\{ 1 - \sqrt{1-\left(\frac{1-\bar{Y}}{1-\bar{Y}^*}\right)^2} \right\} \quad \bar{Y}^* \leqslant \bar{Y} \leqslant 1 \tag{84}$$

(d) Taking the value of δ as the difference between the flapped and unflapped zero lift angles of the section at the end of the flap, determine the resultant angles of attack, α_e, at the real wing using equations (11), (36), (37), (38), (39). Correct these angles for edge velocity and then use the section data to obtain new values for the lift distribution. Repeat this iterative cycle until a convergence is obtained in the lift distribution. Denote this distribution by $c_{l\,\delta}$.

(e) Calculate the correction factors F from equations (41) and (42).

(f) Using equation (81) obtain the first approximation of the final lift distribution and compute the value of section lift coefficient at the flap end, c_l^*, thus

$$c_l^* = \left(\frac{c_l c}{\bar{b}}\right) \left(\frac{c_R}{c}\right) \left(\frac{\bar{b}}{b}\right) \left(\frac{b}{c_R}\right) \tag{85}$$

(g) Determine the uncorrected value of lift coefficient at the end of the flap using

$$c_{l\,u} = \frac{c_l^*}{FF} \tag{86}$$

where FF is the value of $1 + F\,\Delta c_l^*{}_{max} / (c_{l\,max})_o$ taken at the flap side of $\bar{Y}^*$.

(h) Obtain the angle of attack value, α_o, which corresponds to $c_{l\,u}$, from the flapped section data and correct it to obtain the equivalent angle of attack, $\alpha_{e\,\delta}$ thus

$$\alpha_{e_\delta} = E \times FF\,(\alpha_o - \alpha_{l_o}) + \alpha_{l_o} \tag{87}$$

(i) In the same way find the equivalent angle of attack, $\alpha_{l\,\delta=o}$ for the unflapped side of $\bar{Y}^*$.

(j) The first approximate value of the discontinuity in angle of attack δ is then given by

$$\delta = \alpha_{e_{\delta=0}} - \alpha_e \delta \tag{88}$$

(k) Again, use equations (11), (36), (37), (38), and (39) together with equation (88) to obtain values of the resultant angles of attack, α_e, at each station on the real wing.

(l) The corresponding uncorrected angles of attack are then found using

$$\alpha_o = \frac{\alpha_e - \alpha_{l_o} \left(1 - E \frac{c_{l\,max}}{(c_{l\,max})_o}\right)}{E \frac{c_{l\,max}}{(c_{l\,max})_o}} \tag{89}$$

(m) Use the two-dimensional section lift data to obtain values of c_{l_o} at these angles of attack and factor them to give the correct values of lift coefficient, thus

$$c_l = c_{l_o} \frac{c_{l\,max}}{(c_{l\,max})_o} \tag{90}$$

(n) Compare this calculated lift distribution to the approximate distribution and repeat the iterative process until the convergence is achieved within the specified limits.

(o) Finally, obtain the overall wing-body characteristics using equation (51) through (56).

4.2 SECTION DATA CHARACTERISTICS

The accuracy of wing spanwise load distributions computed by this program largely depends on the quantity and quality of the available section data characteristics. The section characteristics required in the computations are: The two-dimensional section lift-coefficient versus section angle of attack, the section profile-drag and the quarter-chord pitching-moment coefficients versus section lift coefficient. Ideally, the data should be available for as broad a range of Reynolds numbers and thickness-chord ratios as is required to cover the range of these parameters expected in actual flight. Otherwise, linear interpolation and extrapolation of the existing section data are required to perform the computations at the values of Reynolds number and/or thickness-chord ratio outside the available range.

The most reliable airfoil section data which are now available are summarized in References 5 and 6. Reference 5 presents the data obtained for Reynolds numbers between 3×10^6 to 9×10^6 while Reference 6 extends these measurements to values of Reynolds numbers down to 0.7×10^6.

4.2.1 Correction of the Section Data

The senior author of Reference 6 has indicated that errors exist in the values of lift curve slope for all airfoils tested at Reynolds numbers of less than 3.0×10^6. These errors are attributed to an angle of attack change associated with air leakage at the intersection of the test airfoil and the wind tunnel walls. The evidence of the inconsistencies at low Reynolds numbers can be noted by examining the behavior of the values of section lift-curve slope as a function of Reynolds number, shown in Figure 17 of Reference 6. Since the values of lift coefficients obtained from force measurements are known to be correct the irregularities in the trends of c_l/α versus Reynolds number can only be associated with the errors in airfoil angle of attack.

Therefore, a correction procedure based on extrapolation of the high Reynolds number lift-curve slope data was employed to generate approximate section data for low Reynolds numbers. This procedure which was approved by the senior author of Reference 6 is described below.

For each airfoil section the variation of lift-curve slope with Reynolds number was plotted as shown in Figure 7. A straight-line extrapolation of the best fit to the data for Reynolds numbers of 3×10^6 and greater was used to obtain values of lift-curve slope at low Reynolds numbers. These values were then used to correct the quoted angles of attack at constant values of lift coefficient. In making the extrapolations, account was taken of the variation of lift-curve slope with thickness-to-chord ratio at constant Reynolds number as shown in Figure 8. Furthermore, an effort was made to ensure that the extrapolation trends were compatible with the trends of the high Reynolds number data. The magnitude of the correction for a typical section is illustrated in Figure 9. Table I indicates which airfoil section data required this correction.

4.2.2 Preparation of the Section Data for Computer

The airfoil section data, corrected as required using the previously discussed procedures, are prepared in the form of special tables, which are used in the computer. For a given airfoil these data represent the relationships of c_l vs. α, c_{do} vs. c_l, and $c_{mc/4}$ vs. c_l for constant values of Reynolds number. Typical tabulation of these section characteristics suitable for the use in the computer are shown in Figure 10.

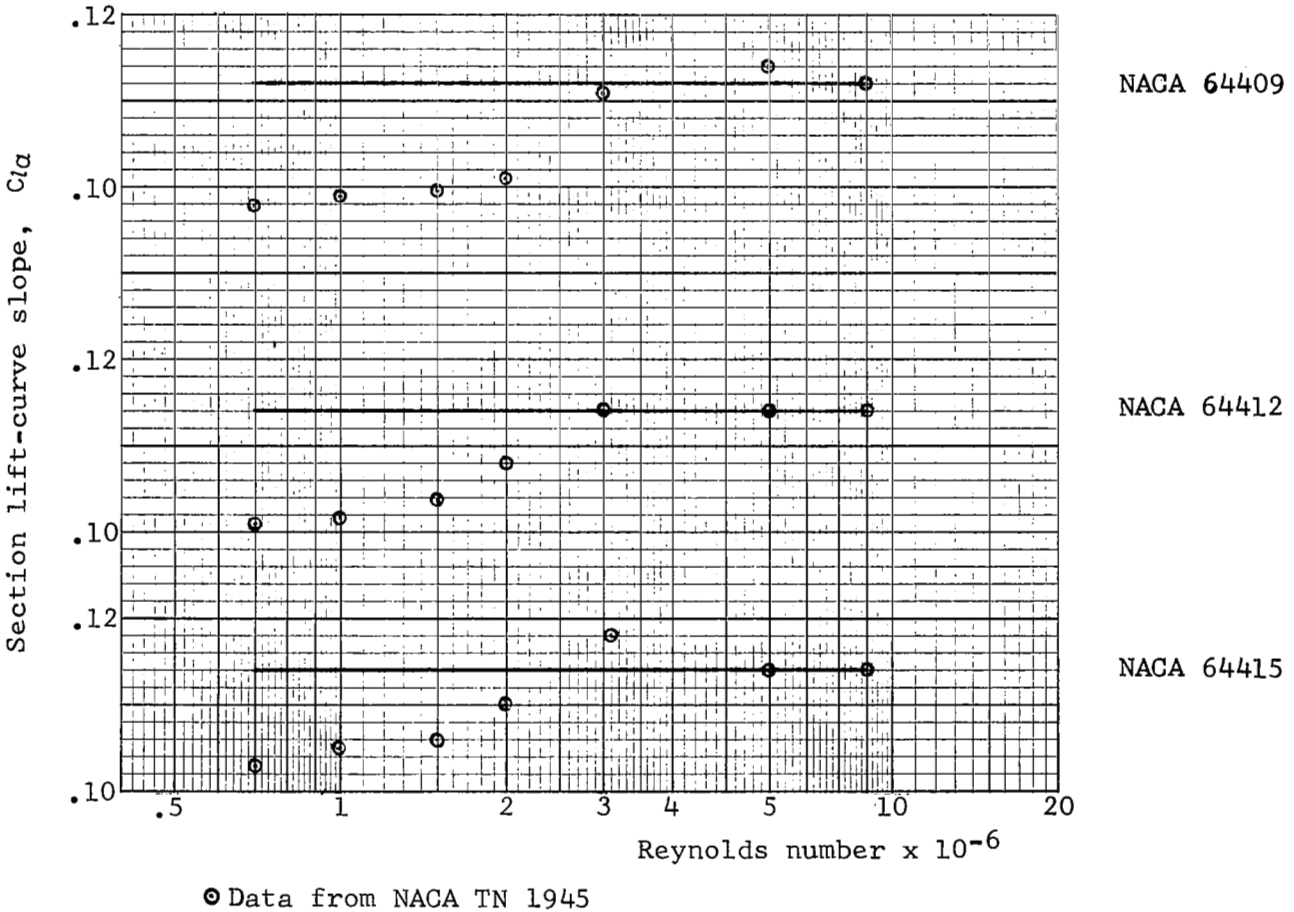

Figure 7. Extrapolations of Lift Curve Slopes at Low Reynolds Number

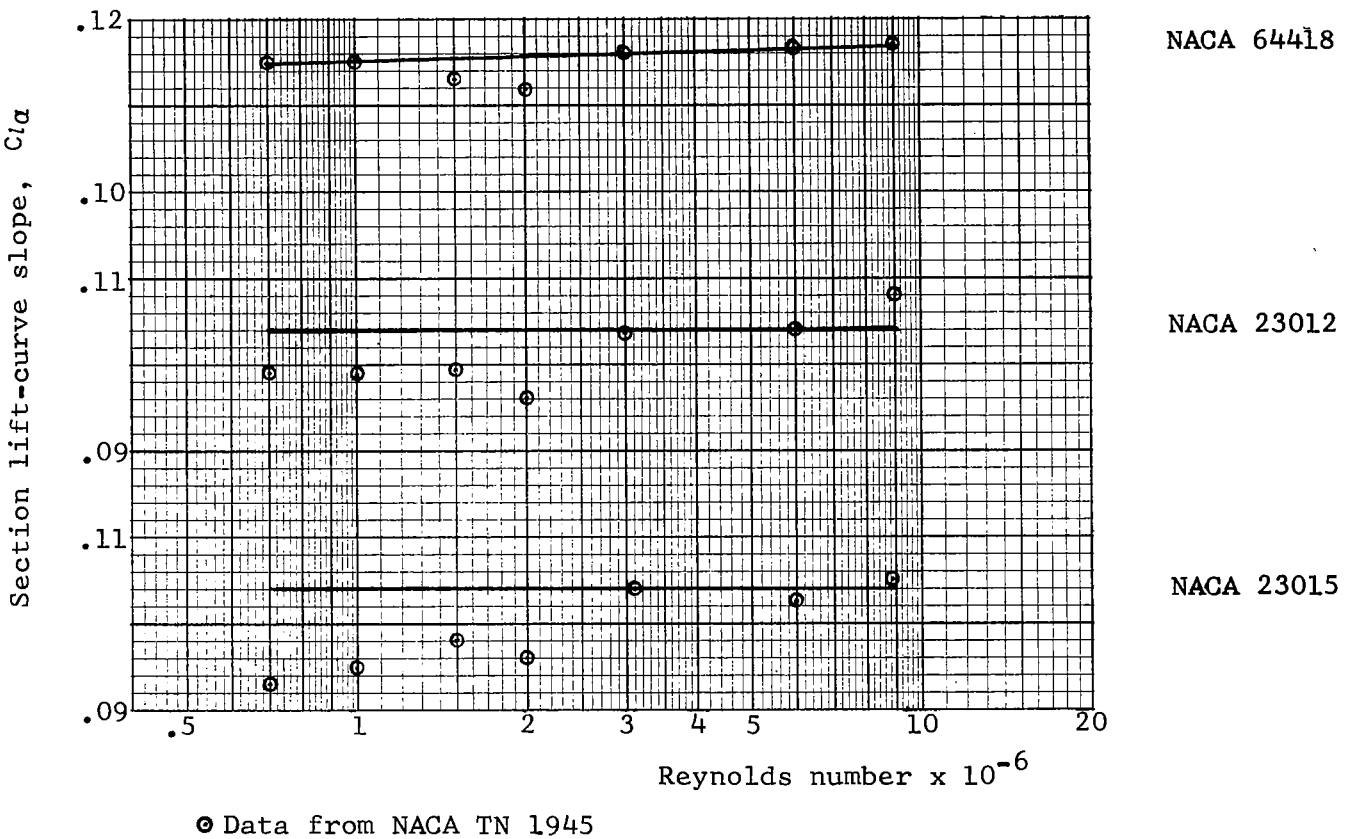

Figure 7. Continued

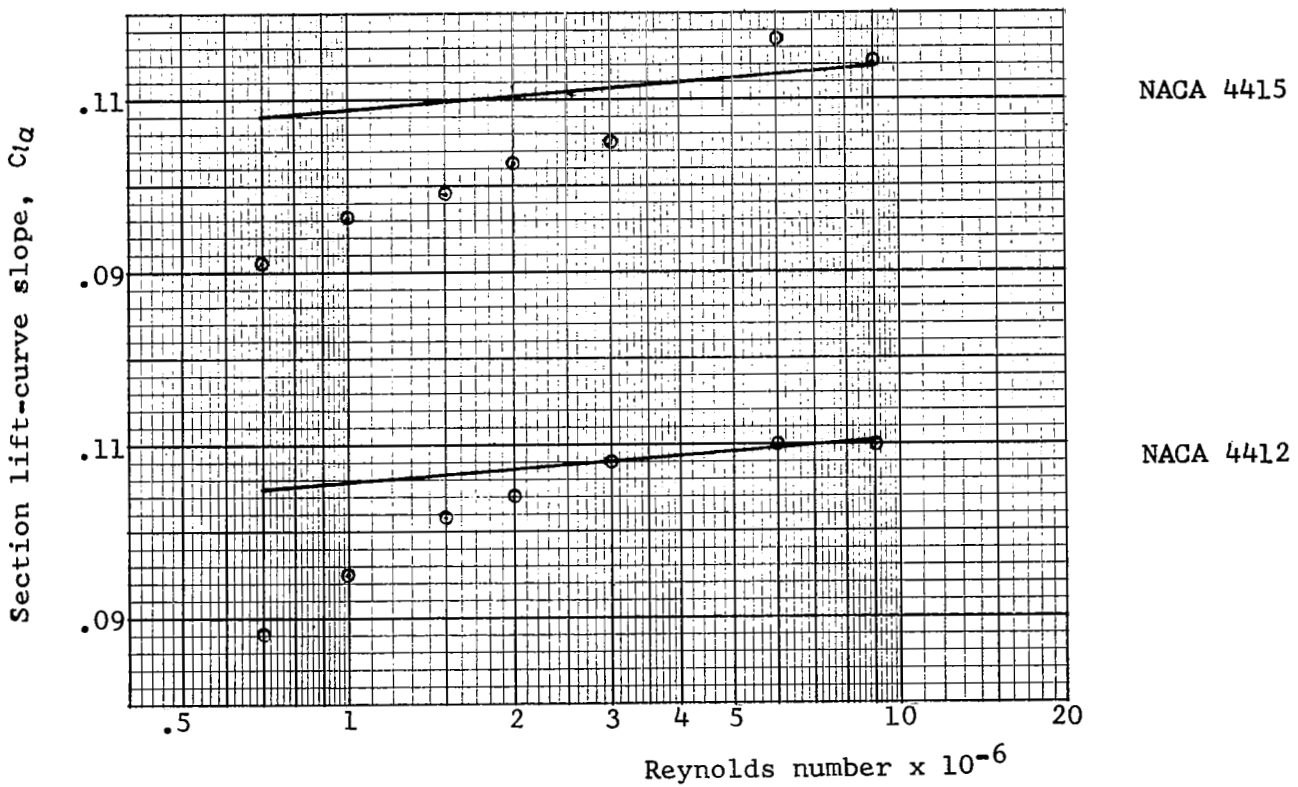

Figure 7. Concluded

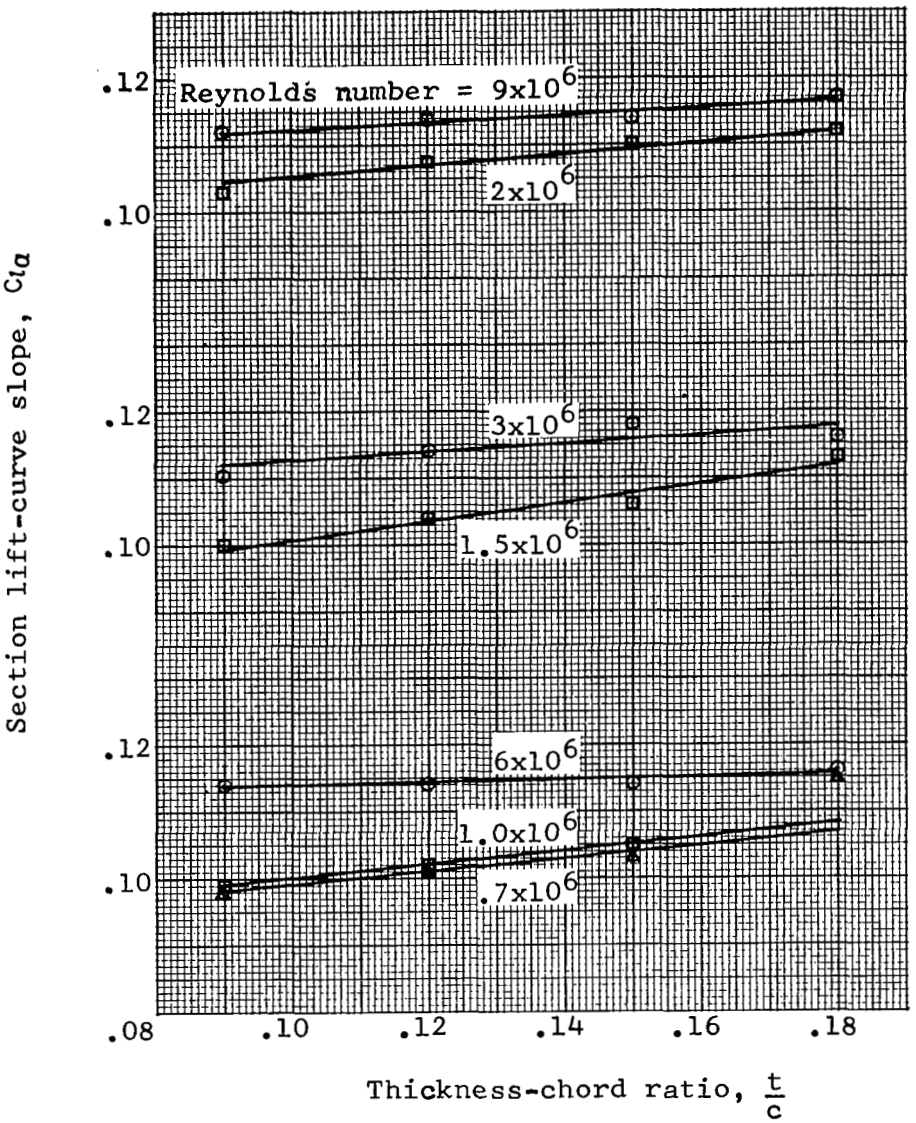

Figure 8. Variation of Section Lift-Curve Slope with Thickness-Chord Ratio at Constant Reynolds number NACA 644 Sections

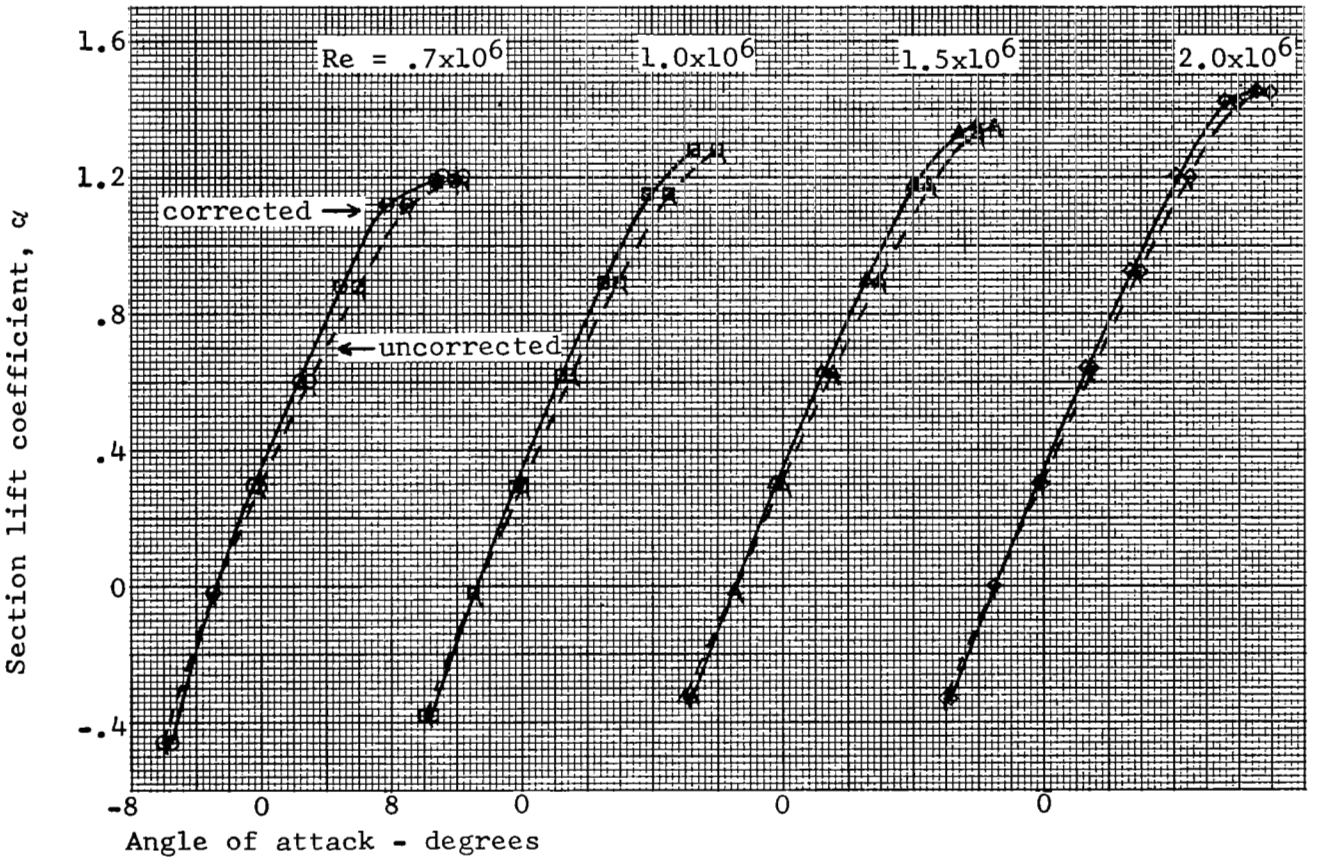

Figure 9 - Corrected Lift Curves for NACA 64-421 Airfoil at Low Reynolds Numbers

TABLE I. - AIRFOIL SECTION DATA AVAILABLE FOR USE WITH THE COMPUTER PROGRAM

Airfoil Series	Thickness Chord Ratios								
	.06	.08	.09	.10	.12	.15	.18	.21	.24
63-2XX	X		X	X	X	X	X	X	
63-4XX					X	X	X	X	
64-2XX	X	X	X	X	X	X	X	X	
64-4XX			X(a)		X(a)	X(a)	X(a)	X	
230XX					X(a)	X(a)	X(b)	X(b)	X(b)
44XX					X(a)	X(a)	X	X	X
24XX					X(b)	X(b)	X(b)	X(b)	X(b)

a Data corrected at Reynolds numbers below 3×10^6.

b No data available for section with 60° split flap.

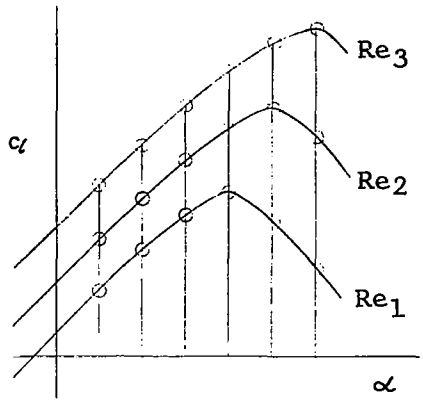

Table of c_l Values

$\alpha°$	Reynolds Number x10^{-6} 0.7	1.0	1.5	2.0	3.0
-90.0*	0	0	0	0	0
-14.0	-0.34	-0.36	-0.40	-0.50	-0.60
:	:	:	:	:	:
12.6	1.37	1.39	1.42	1.48	1.47
:	:	:	:	:	:
20.0	1.22	1.26	1.28	1.30	1.26
90.0*	10.0	10.0	10.0	10.0	10.0
$c_{l_{max}}$	1.37	1.39	1.44	1.49	1.51
α_{max}	12.6	12.6	13.4	13.4	13.4

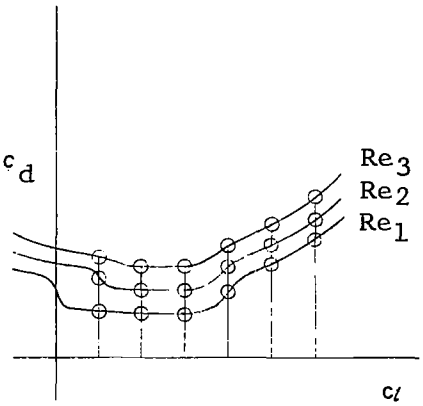

Table of c_d Values

c_l	Reynolds Number x10^{-6} 0.7	1.0	1.5	2.0	3.0
-10.0*	2.000	2.000	2.000	2.000	2.000
-0.2	0.013	0.011	0.009	0.009	0.007
:	:	:	:	:	:
0.9	0.010	0.008	0.008	0.007	0.007
:	:	:	:	:	:
1.4	0.060	0.50	0.040	0.020	0.019
10.0*	2.000	2.000	2.000	2.000	2.000
	0.	0.	0.	0.	0.
	0.	0.	0.	0.	0.

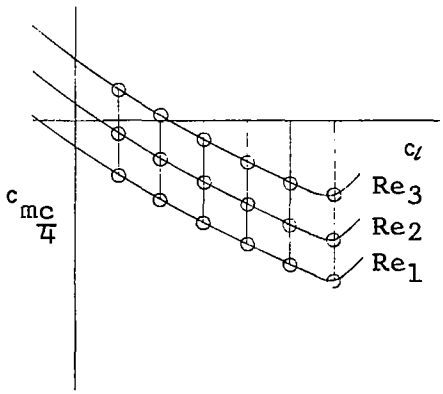

Table of c_m Values

c_l	Reynolds Number x10^{-6} 0.7	1.0	1.5	2.0	3.0
-10.0*	0.	0.	0.	0.	0.
-0.68	-0.09	-0.09	-0.09	-0.09	-0.09
:	:	:	:	:	:
0.99	-0.09	-0.08	-0.09	-0.09	-0.09
:	:	:	:	:	:
1.64	-0.06	-0.06	-0.06	-0.06	-0.06
10.0*	0.	0.	0.	0.	0.
	0.	0.	0.	0.	0.
	0.	0.	0.	0.	0.

* For computer continuity only.

Figure 10. - Method of Tabulation of Section Characteristics.

The tabulation of section lift data is considered to be most critical as compared to the two sets of data cited above. For a given airfoil thickness-chord ratio, values of lift coefficient are carefully read at selected angles of attack for each Reynolds number so as to best define the lift-curves especially in the vicinity of $c_{l\ max}$. Large scale plots of c_l vs. α (e.g. NACA originals) are recommended for this purpose for improved accuracy.

The values of lift coefficient thus obtained are entered in an array as shown in Figure 10 with the first and last entries of angle of attack being -90^o and $+90^o$ corresponding to lift coefficient values of zero and 10.0 respectively. The latter value of section lift coefficient is entered only for the purpose of the computer in order to avoid computational discontinuity in the case of wings with part-span fully deflected flaps. The bottom two rows of the array contain the values of maximum lift coefficient ($c_{l\ max}$) and the corresponding angles of attack at which these first occur (α_{max}). This procedure is repeated for each value of airfoil thickness-chord ratio for which data is available.

Similarly, using the plots of c_{do} vs. c_l and $c_{mc/4}$ vs. c_l the drag and pitching moment tables are prepared and tabulated as shown in Figure 10. In these arrays of data the last two rows are entered as zeros.

Thus, a library of section characteristics tables is prepared. The data is key-punched and stored ready for use in the computer. The families of airfoils for which data has been prepared are summarized in Table I.

4.2.3 Airfoil Data Table Look-up Procedures

The basic airfoil data are read into the computer row-wise and stored on tape. During execution of the program the data is read from tape into core in the form of files. The arrangement and designation of the files is shown diagrammatically in Figure 11. Each file must contain at least two, but not more than five, levels or values of thickness-chord ratio. Each level, or each table of data, is limited to 25 rows and 12 columns. This file size is adequate for most purposes, but may be increased if desired by changing the specifications relating to file size in the program.

Linear interpolation is used throughout and is performed first for the required value of Reynolds number then thickness-chord ratio and finally for the given value of camber. When the required angle of attack is outside the range of the maximum angles of attack listed in the table for the two bracketing

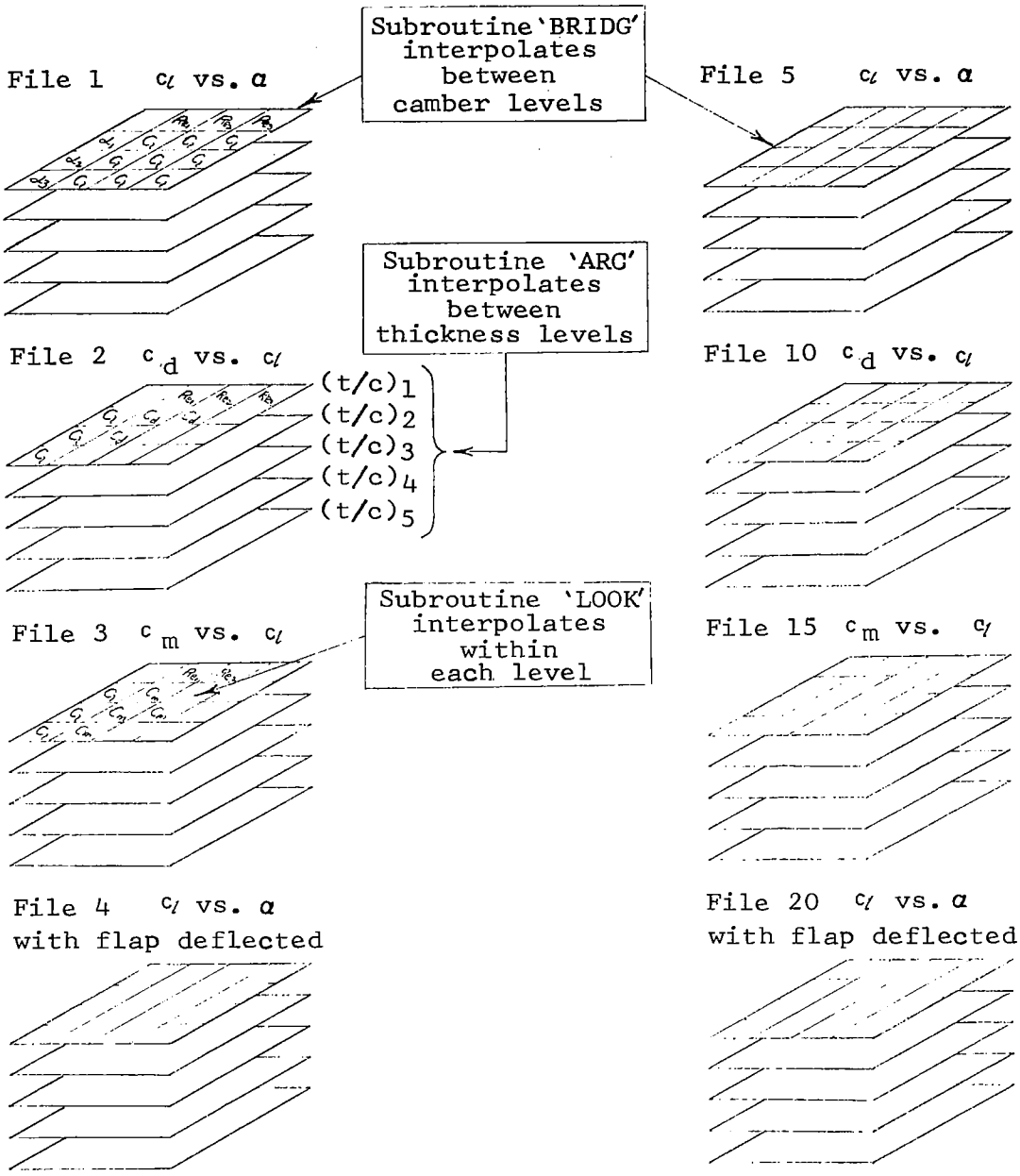

Figure 11. - Schematic Representation of Section Data Storage in the Computer.

values of the parameters under consideration, simple linear interpolation formulae are utilized with no special order of interpolation. A special computational procedure is required to obtain values of lift coefficient when the angle of attack falls between the tabulated values of α_{max}. This procedure is briefly described in the following paragraphs as an aid to understanding the program listing.

Using Figures 12(a) and 12(b), the values of α_{max} and $c_{l\,max}$ at the required value of Reynolds number, Re, are determined for each of the bounding values of thickness-chord ratio, $(t/c)_1$ and $(t/c)_2$. This yields values of lift coefficients at the points m_1, and m_2, respectively. Depending on whether the given value of angle of attack, α, is greater or less than the values of α_{max}, appropriate values of c_l (denoted by X_1, X_2) are obtained for each bracketing value of thickness-chord ratio.

Knowing the values at points m_1 and m_2, new values of $c_{l\,max}$ and α_{max} are calculated corresponding to the required value of thickness-chord ratio and are denoted by the point m_3. Using the previously computed values at points X_1 (or X_2) together with the values at m_3, the above interpolation cycle is repeated to obtain the value of c_l at the required thickness ratio.

This value of c_l now corresponds to the required values of Reynolds number and thickness-chord ratio, but applies only to the camber level associated with the tip airfoil series. The aerodynamic data for the root airfoil series is then called into core and the process is repeated. The final interpolation shown in Figure 12(d) is performed for the correct value of camber level in the same way as that used for thickness-chord ratio.

4.3 DESCRIPTION OF THE COMPUTER PROGRAM

The computational procedures described in Section 4.1 have been programmed for use on the NASA CDC 6600 series computer located at Langley Research Center. The program is written in the Fortran IV machine language. An internal listing of the program is presented in Appendix A and a block diagram illustrating the major logic features is presented in Figure 13.

The program is initiated by reading in the basic configuration parameters punched on cards as indicated in Figure 14. The values of either aerodynamic or geometric twist may be input. Whichever twist is specified the column reserved for the other twist must contain 100. Columns 1 to 11 on card #2 contain the maximum allowable difference between the calculated and approximate values of $c_l\ c/b$ at the end of each iteration. A value of .001 was used in the computations presented later in this report.

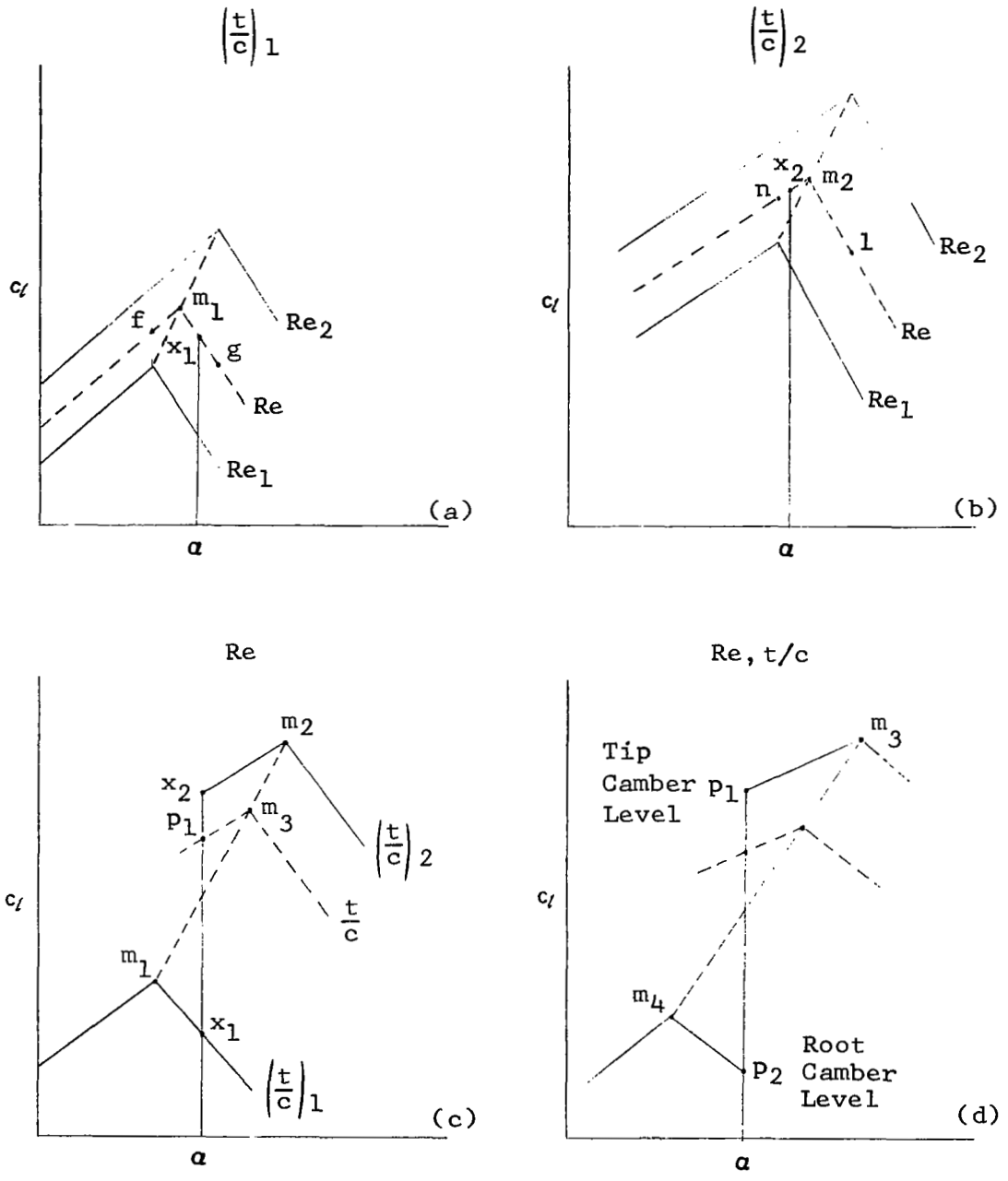

Figure 12. Nomenclature for Developing Interpolation Formulae.

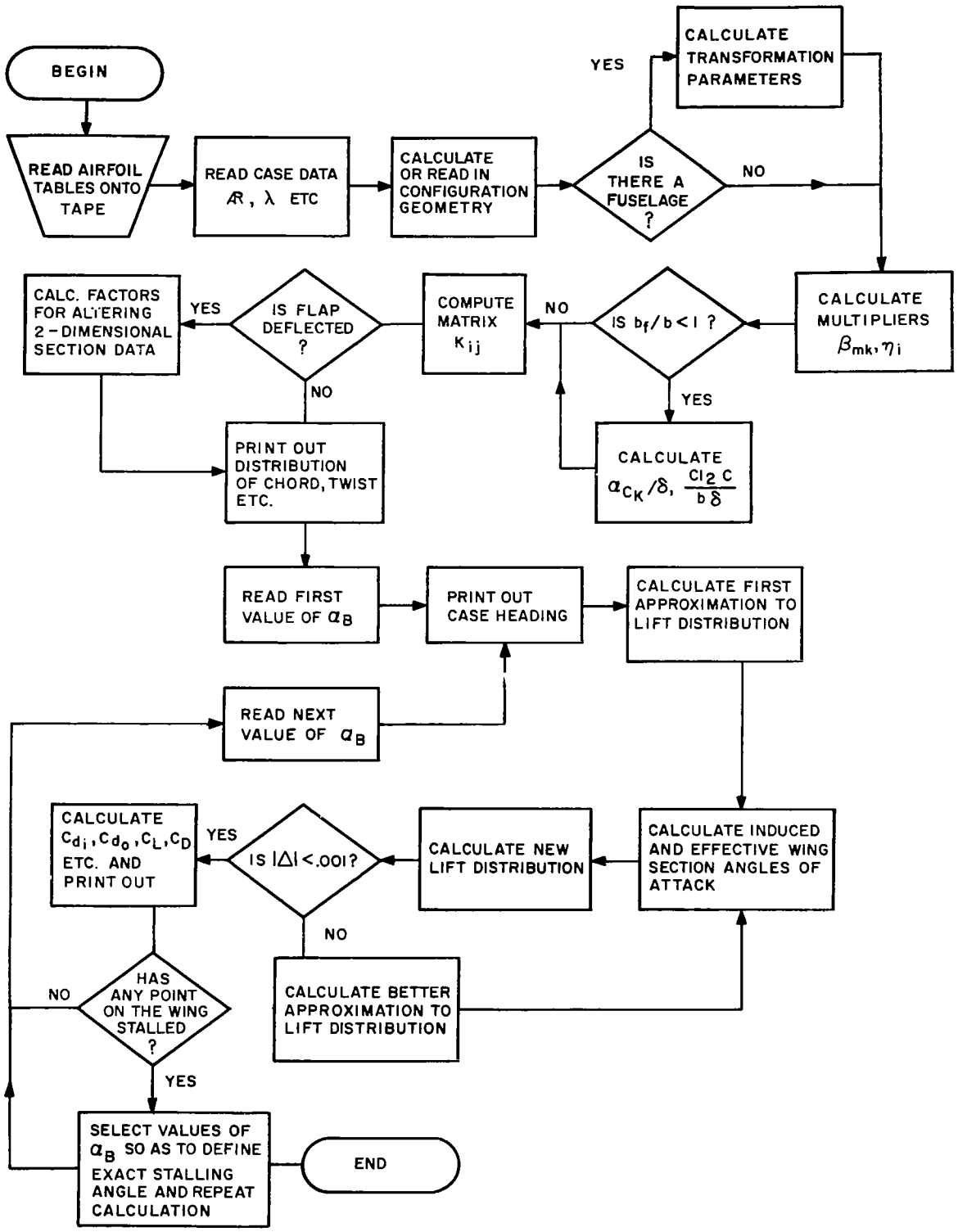

FIGURE 13 COMPUTER PROGRAM BLOCK DIAGRAM

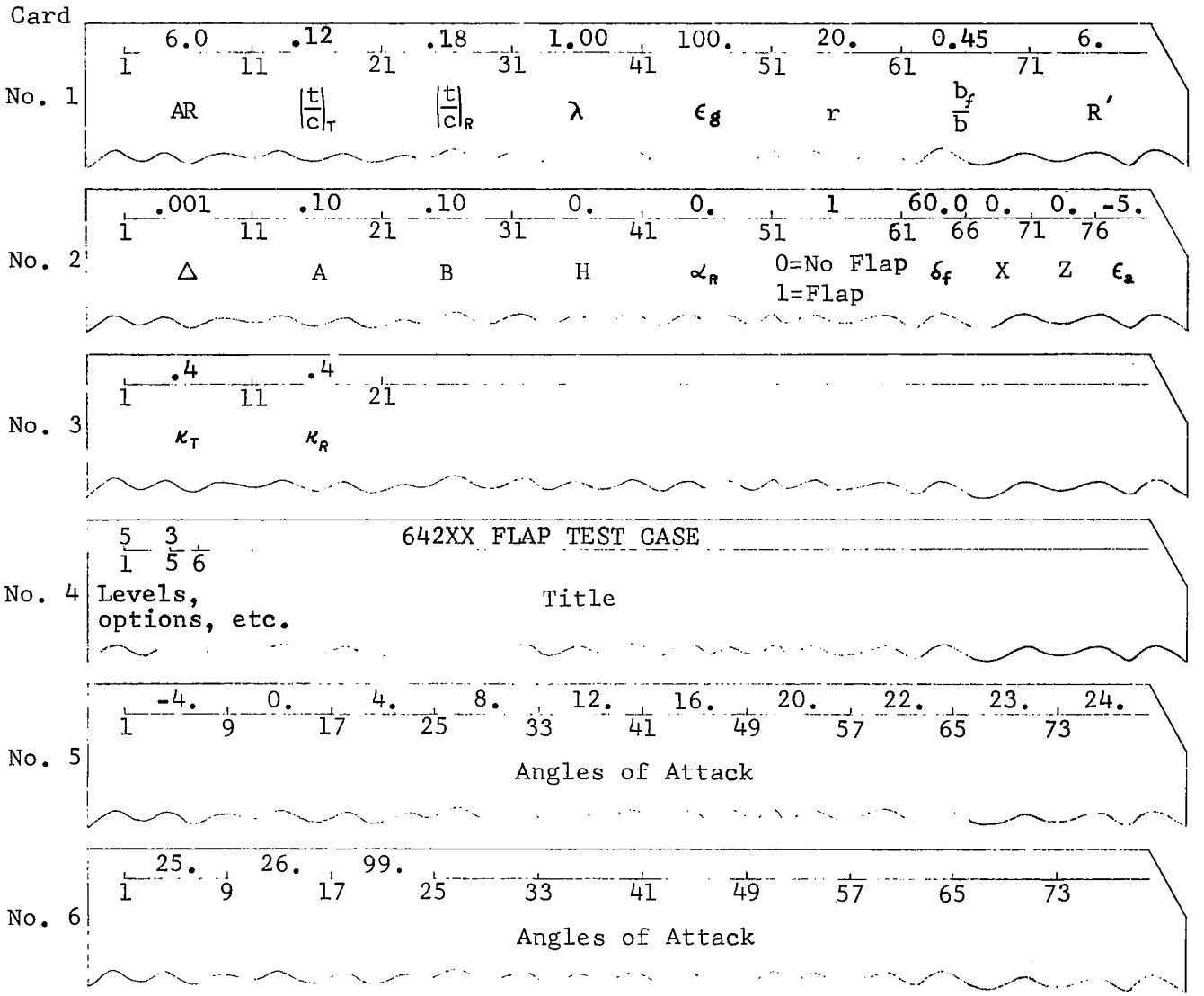

Figure 14. - Schematic Representation of the Computer Input Cards.

Normally the distribution of such planform parameters as chord, twist, local Reynolds number, etc. are calculated but provision is made to read these in if the planform is not trapezoidal. The program performs the computations using 10 control points per wing semi-span. This number of stations is usually adequate for most purposes, however, if it is desired to increase (or decrease) the number of points the program can easily be modified.

Having calculated, or read, the geometric parameters and computed the parameters governing fuselage transformation (if a fuselage is present), the values of the multipliers β_{mk} and η_i are computed and stored. If the calculation is for a wing with a deflected part-span flap the values of the parameters associated with a spanwise discontinuity in angle of attack are computed. The coefficients of the matrix K_{ij} , given by equation (30b), are now computed using a matrix inversion subroutine to obtain successive approximations to the lift distribution. If the calculation is for a flapped wing the program branches to compute the two load distributions required to obtain the factors used in altering the two-dimensional section lift data. Having obtained these factors the basic program iterative loop is entered and executed until a lift distribution is calculated which agrees with the guessed distribution to within the required tolerance. The computed distributions of section lift coefficient, etc., and the corresponding integrated values are immediately printed out for each case run.

If, at any point on the wing, the stall is detected, i.e. the computed value of effective section angle of attack exceeds that for maximum lift, the computations are then repeated for a value of angle of attack half-way between the last two values. If at this intermediate value the wing unstalls the program increases the angle of attack by 0.2 degrees until stall again occurs or until the increments total 1^{o}. Similarly, if stall is still detected at the intermediate value, the angle of attack is decreased until the wing is unstalled or until the total decrease equals 1^{o}.

Alternatively, if, for a given body angle of attack wing stall is not obtained, the computations are performed for the next inputed value of body incidence until the value of $\alpha_B = 99$ is encountered whereupon the calculations are stopped. A typical print out of the final results is presented in Table II.

The computer program described herein can be used to predict the distributions and the integrated values of lift, drag and pitching moment coefficients for wings of trapezoidal planform with zero sweep in the presence of a fuselage at all angles of attack up to and including stall. In addition, these computations

642 SERIES FLAP CASE

SPANWISE STATIONS

(1)	9.97711503E-01	(2)	9.61459121E-01	(3)	9.02092175E-01	(4)	8.21185699E-01	(5)	7.20940345E-01
(6)	6.04219115E-01	(7)	4.74712490E-01	(8)	3.37573147E-01	(9)	2.02203541E-01	(10)	1.00000444E-01
(11)	-2.02203541E-01	(12)	-3.37573147E-01	(13)	-4.74712490E-01	(14)	-6.04219115E-01	(15)	-7.20940345E-01
(16)	-8.21185699E-01	(17)	-9.02092175E-01	(18)	-9.61459121E-01	(19)	-9.97711503E-01	(	

ALPHA MAX

(1)	1.60889831E+01	(2)	1.61635207E+01	(3)	1.63227454E+01	(4)	1.66417263E+01	(5)	1.72603411E+01
(6)	1.85084020E+01	(7)	2.37034870E+01	(8)	1.25746196E+01	(9)	1.39745350E+01	(10)	1.43900028E+01
(11)	1.39745350E+01	(12)	1.25746196E+01	(13)	2.37034870E+01	(14)	1.85084020E+01	(15)	1.72603411E+01
(16)	1.66417263E+01	(17)	1.63227454E+01	(18)	1.61635207E+01	(19)	1.60889831E+01	(	

CL MAX

(1)	1.55000003E+00	(2)	1.55650944E+00	(3)	1.57042592E+00	(4)	1.59829929E+00	(5)	1.65222564E+00
(6)	1.76061569E+00	(7)	2.12708990E+00	(8)	2.55834961E+00	(9)	2.69584410E+00	(10)	2.73499988E+00
(11)	2.69584410E+00	(12)	2.55834961E+00	(13)	2.12708990E+00	(14)	1.76061569E+00	(15)	1.65222564E+00
(16)	1.59829929E+00	(17)	1.57042592E+00	(18)	1.55650944E+00	(19)	1.55000003E+00	(	

THICKNESS / CHORD DISTRIBUTION

(1)	1.20152566E-01	(2)	1.22569392E-01	(3)	1.26527188E-01	(4)	1.31920953E-01	(5)	1.38603977E-01
(6)	1.46385392E-01	(7)	1.55019167E-01	(8)	1.64161790E-01	(9)	1.73186431E-01	(10)	1.79999970E-01
(11)	1.73186431E-01	(12)	1.64161790E-01	(13)	1.55019167E-01	(14)	1.46385392E-01	(15)	1.38603977E-01
(16)	1.31920953E-01	(17)	1.26527188E-01	(18)	1.22569392E-01	(19)	1.20152566E-01	(	

SECTION REYNOLDS NUMBER

(1)	6.00060006E+00	(2)	6.00060006E+00	(3)	6.00060006E+00	(4)	6.00600C6E+00	(5)	6.00060006E+00
(6)	6.00060006E+00	(7)	6.00060006E+00	(8)	6.00060006E+00	(9)	6.000600C6E+00	(10)	6.00060006E+00
(11)	6.00060006E+00	(12)	6.00060006E+00	(13)	6.00060006E+00	(14)	6.0006C006E+00	(15)	6.00060006E+00
(16)	6.00060006E+00	(17)	6.00060006E+00	(18)	6.00060006E+00	(19)	6.00060006E+00	(	

CHORD DISTRIBUTION

(1)	1.00000000E+00	(2)	1.00000000E+00	(3)	1.00000000E+00	(4)	1.00000000E+00	(5)	1.00000000E+00
(6)	1.00000000E+00	(7)	1.00000000E+00	(8)	1.00000000E+00	(9)	1.00000000E+00	(10)	1.00000000E+00
(11)	1.00000000E+00	(12)	1.00000000E+00	(13)	1.00000000E+00	(14)	1.00000000E+00	(15)	1.00000000E+00
(16)	1.00000000E+00	(17)	1.00000000E+00	(18)	1.00000000E+00	(19)	1.00000000E+00	(	

GEOMETRIC TWIST

(1)	-4.92881352E+00	(2)	-4.72977270E+00	(3)	-4.40382321E+00	(4)	-3.95961265E+00	(5)	-3.40922351E+00
(6)	-2.76837490E+00	(7)	-2.05732909E+00	(8)	-1.30437645E+00	(9)	-5.61140405E-01	(10)	-2.43856132E-06
(11)	-5.61140405E-01	(12)	-1.30437645E+00	(13)	-2.05732909E+00	(14)	-2.76837490E+00	(15)	-3.40922351E+00
(16)	-3.95961265E+00	(17)	-4.40382321E+00	(18)	-4.72977270E+00	(19)	-4.92881352E+00	(	

TABLE II. Typical Computer Output

642 SERIES FLAP CASE

BODY ANGLE OF ATTACK, DEG. . =	16.00	VALUE OF DISCRIMINANT. . . . =	.001000
BODY HEIGHT /SPAN. . . . . =	.10	BODY WIDTH / SPAN. . . . . =	.10
ASPECT RATIO . . . . . =	6.00	WING HEIGHT /SPAN. . . . . =	0.00
WING BODY INCIDENCE, DEG . . =	0.00	TIP THICKNESS CHORD. . . . . =	.12
ROOT THICKNESS CHORD . . . . =	.18	GEOMETRIC TWIST, DEG . . . . =	-4.94
NUMBER OF SPANWISE STATIONS. =	20.00	AERODYNAMIC TWIST, DEG . . . =	-5.00
FLAP SPAN / WING SPAN. . . . =	.45	TAPER RATIO. . . . . =	1.00
FLAP SETTING, DEG. . . . . =	60.00	REYNOLDS NUMBER. . . . . =	6.00
COORDINATES OF MOMENT REFERENCE POINT		X= 0.00 Z= 0.00	

DISTRIBUTION OF SECTION LIFT COEFFICIENT

(1)	3.42250509E-01	(2)	6.30955940E-01	(3)	8.65952551E-01	(4)	1.06170561E+00	(5)	1.24114608E+00
(6)	1.43723537E+00	(7)	1.82981852E+00	(8)	2.23042330E+00	(9)	2.42268737E+00	(10)	2.54358422E+00
(11)	2.42268686E+00	(12)	2.23042074E+00	(13)	1.82985557E+00	(14)	1.43723226E+00	(15)	1.24114578E+00
(16)	1.06170626E+00	(17)	8.65954479E-01	(18)	6.30959085E-01	(19)	3.42254744E-01	(	

STALL MARGIN DISTRIBUTION

(1)	1.20774952E+00	(2)	9.25553498E-01	(3)	7.04473366E-01	(4)	5.36593679E-01	(5)	4.11079557E-01
(6)	3.23380322E-01	(7)	2.97271378E-01	(8)	3.27926310E-01	(9)	2.73156732E-01	(10)	1.91415661E-01
(11)	2.73157242E-01	(12)	3.27928873E-01	(13)	2.97234334E-01	(14)	3.23383436E-01	(15)	4.11079859E-01
(16)	5.36593023E-01	(17)	7.04471438E-01	(18)	9.25550353E-01	(19)	1.20774529E+00	(	

BODY ANGLE OF ATTACK, DEG. . = 16.00 LIFT COEFFICIENT . . . . . = 1.666010

TABLE II. Concluded

incorporate the effects of linear spanwise variation in section camber for unflapped wings. The effect of a deflected part-span flap on the lift distributions is included. However, drag and pitching moment results are not included for these cases because of the lack of section drag and pitching moment characteristics for flapped airfoils.

The computer program described above constitutes a part of this report and is therefore available for public use through Computer Software Management and Information Center (COSMIC), as stated in Appendix B.

4.4 RESULTS OF SAMPLE CALCULATIONS

The computer program was used to calculate the characteristics of three unflapped wings and one wing having a 60% span split flap. These computer results were correlated with the corresponding theoretical predictions of References 1 and 2 and the available experimental data. Figures 15, 16, and 17 present computed lift, drag and pitching moment characteristics for unflapped wings of aspect ratio 8.04, 10.05 and 12.06, and Figure 18, shows the variation of lift coefficient with angle of attack for a flapped wing of aspect ratio 9.02, having a 60% span, 20% chord split flap. Included in these figures are typical spanwise distributions of section lift, drag and pitching moment coefficients.

The correlation of the computer results versus theoretical characteristics of References 1 and 2 and the available experimental data are performed, where possible on the basis of the integrated values as well as the spanwise distributions of wing characteristics. Unfortunately, measurements of wing characteristics in the presence of a fuselage, especially of the span loading, are extremely difficult to obtain for the class of wing-fuselage combinations considered herein. As a result, there is a lack of suitable experimental data of the type required for the present comparisons. Some experimental data exists for swept wing body combinations but such data is not applicable for correlations with the straight wing results.

Examining Figures 15 through 18, it can be noted that the computer results are in good agreement with the available experimental data. The slight differences between the present computations and those of References 1 and 2 are attributed to hand versus machine fairing of the section characteristics.

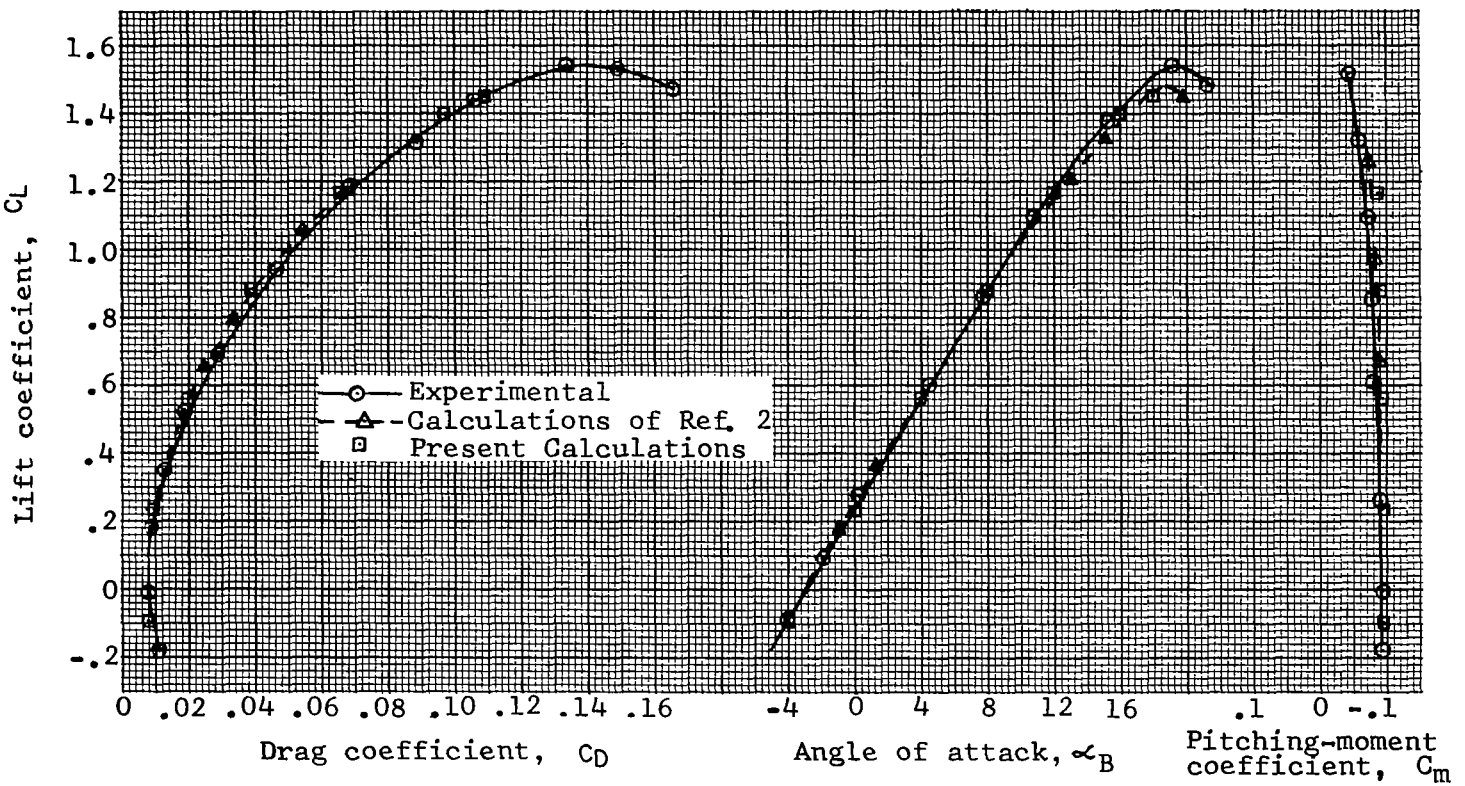

Figure 15. Experimental and Calculated Characteristics for a Wing of Aspect Ratio 8.04.

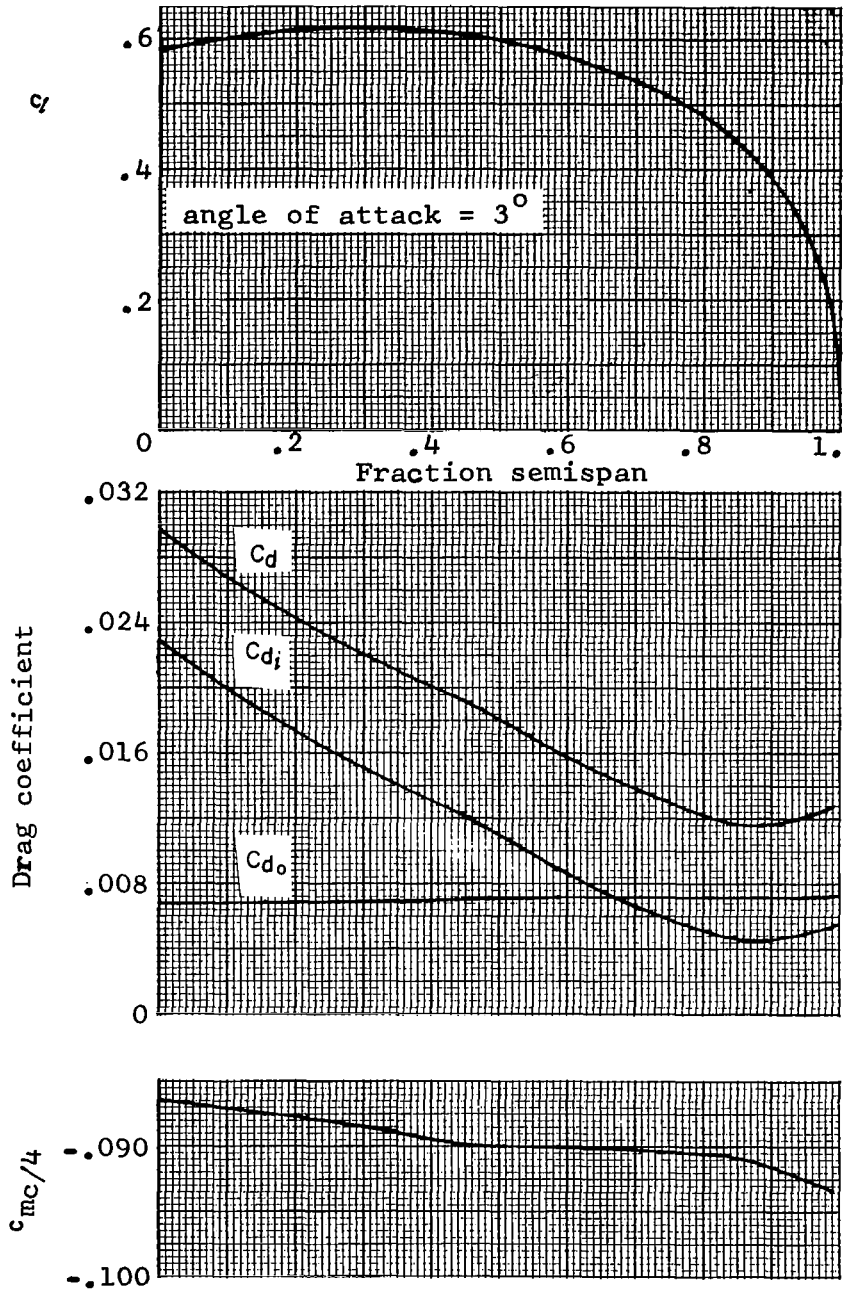

Figure 15. Concluded

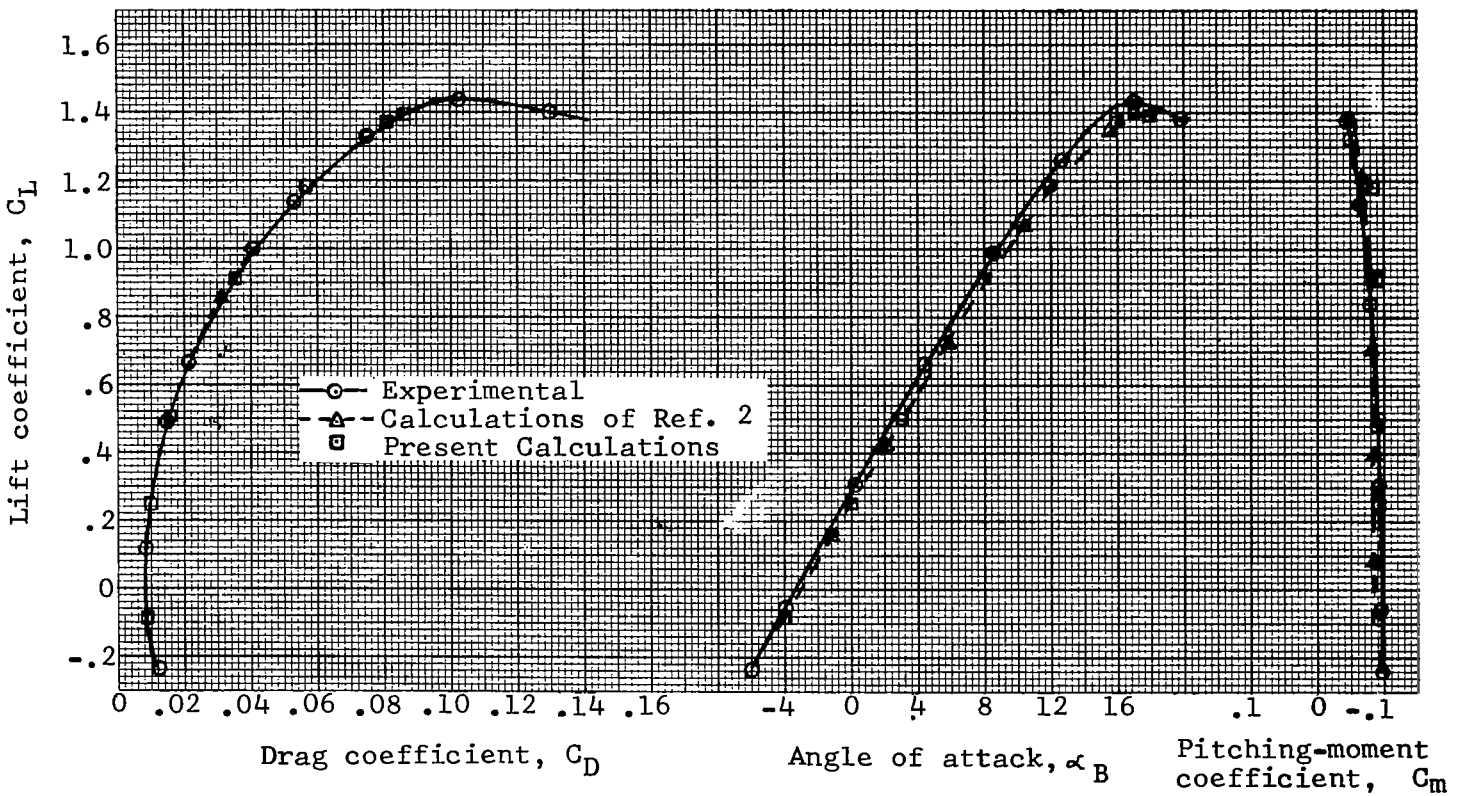

Figure 16. Experimental and Calculated Characteristics for a Wing of Aspect Ratio 10.05

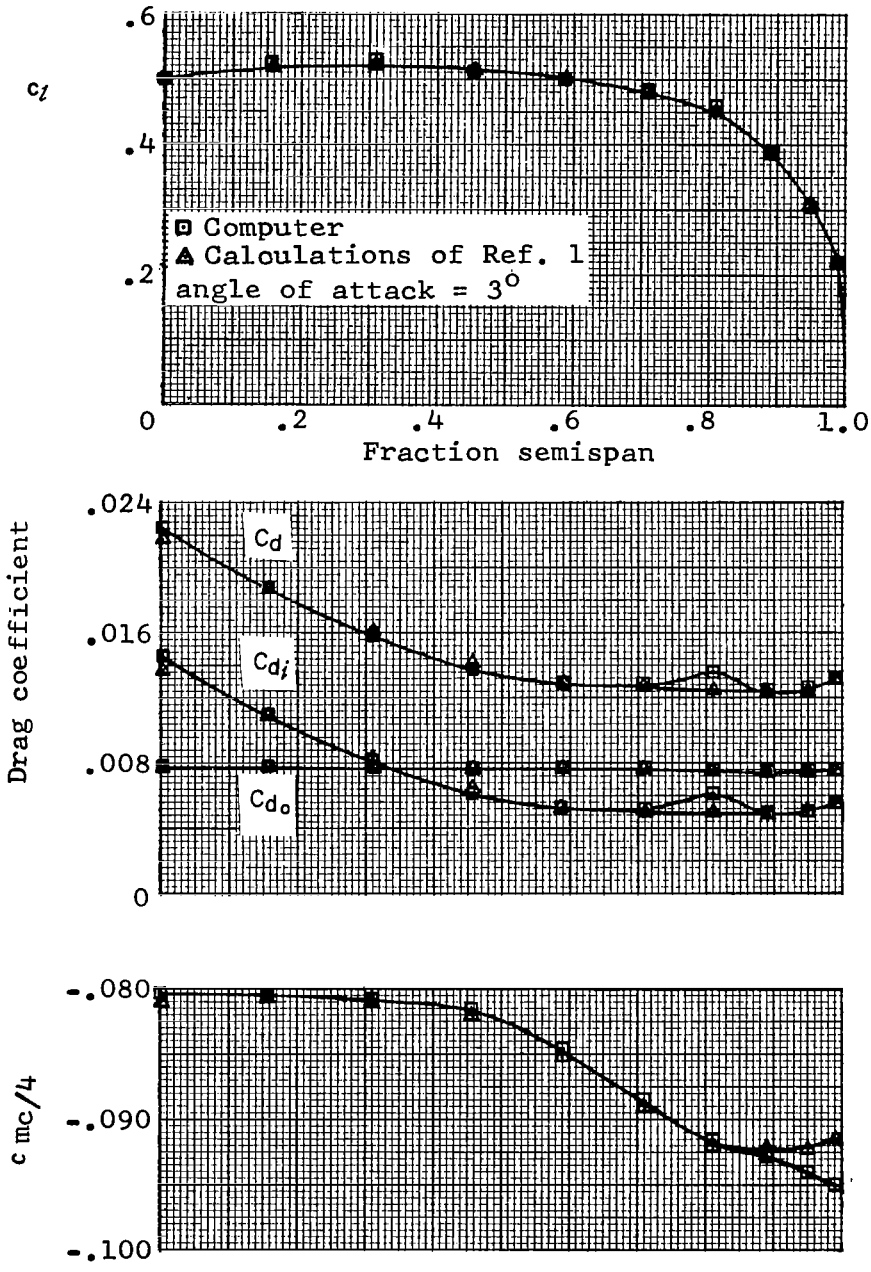

Figure 16. - Concluded

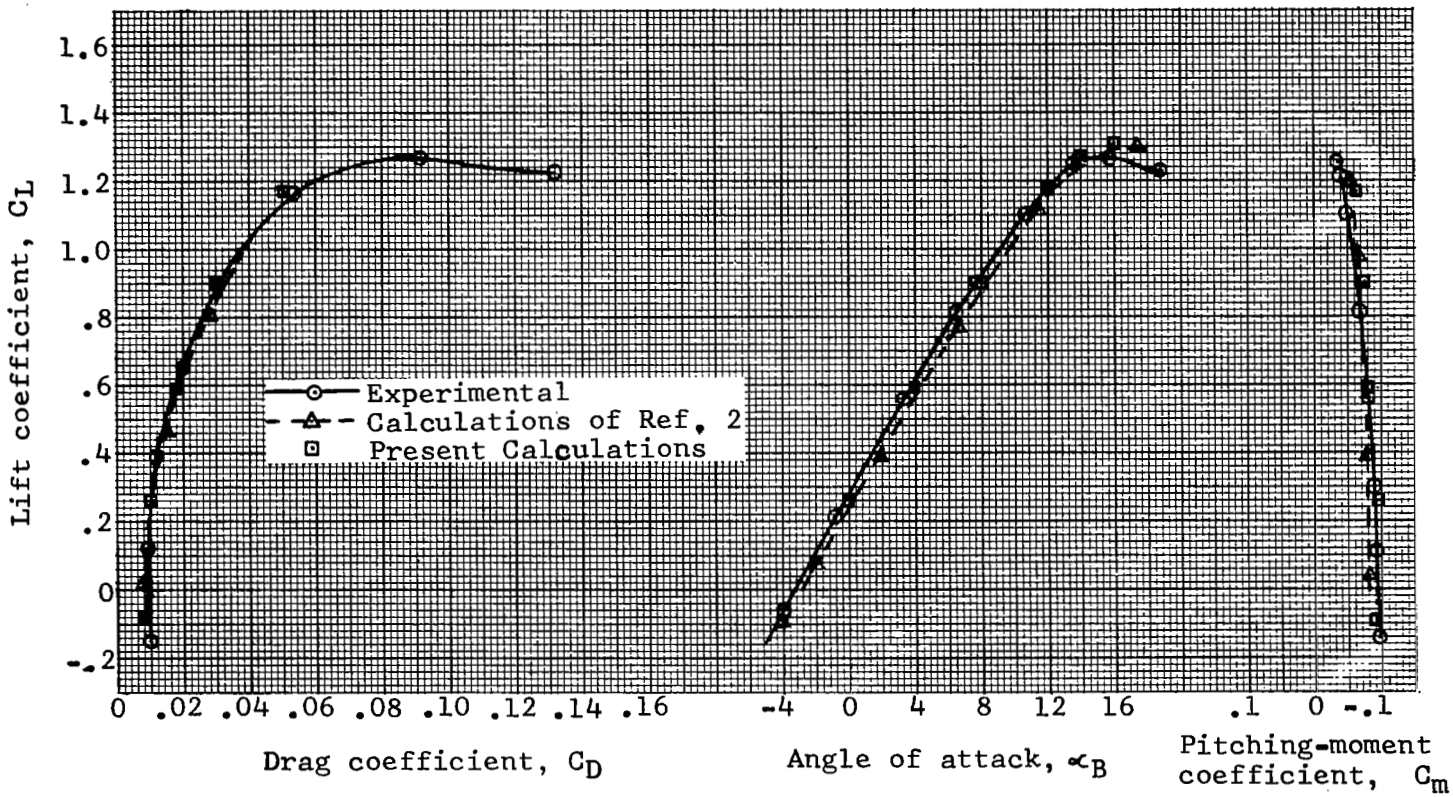

Geometric Washout = 3.0°
Aspect Ratio = 12.06
Reynolds Number = 2.87×10^6

Root Section 4424
Tip Section 4412
Taper Ratio = .4

Figure 17. - Experimental and Calculated Characteristics for a Wing of Aspect Ratio 12.06.

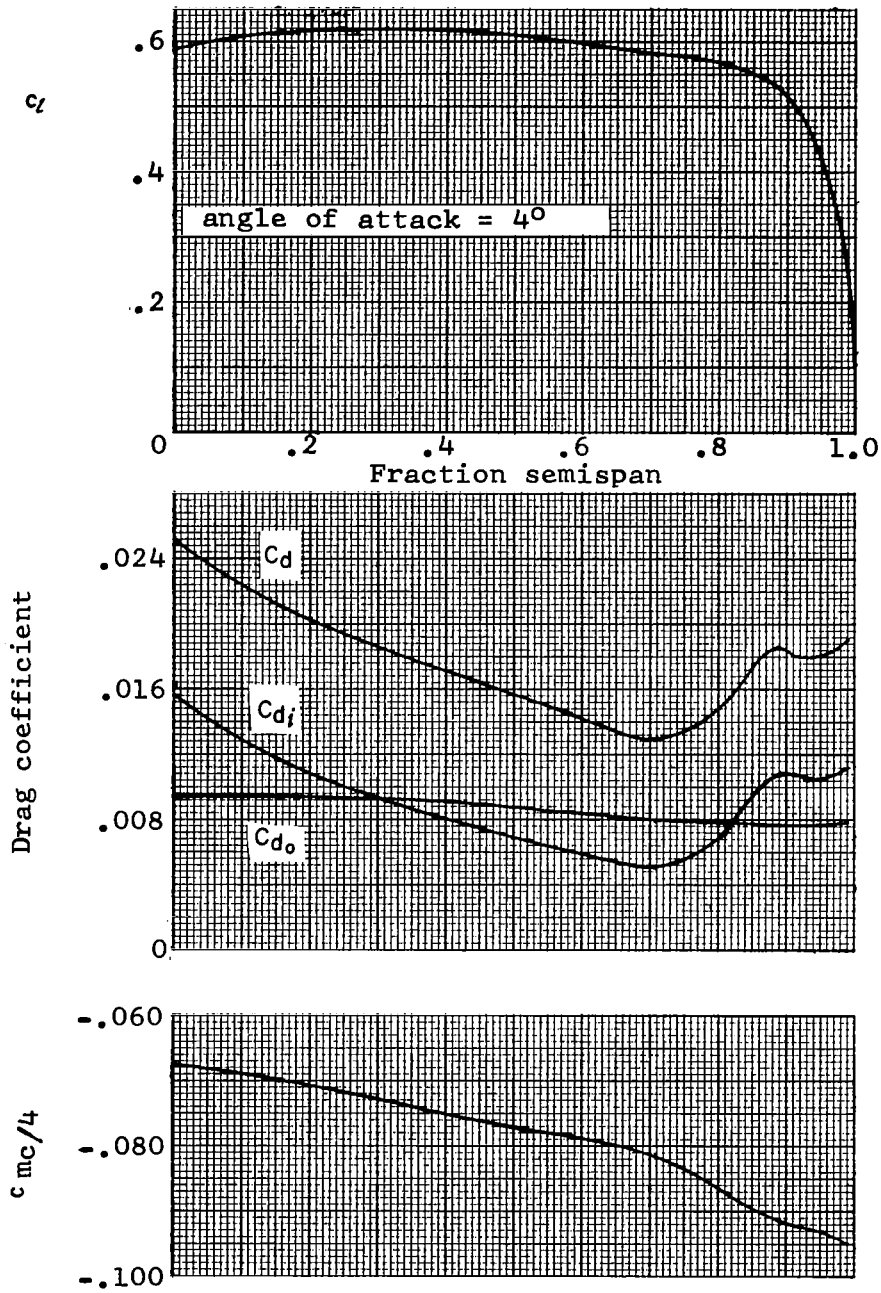

Figure 17. Concluded

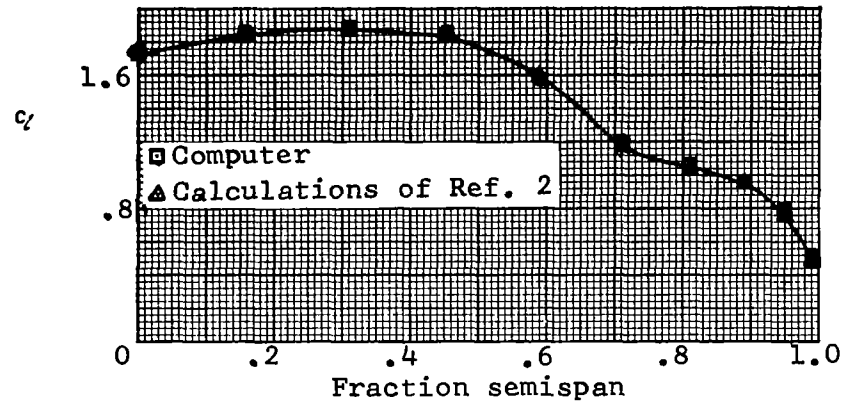

(a) Calculated span load distribution for 10° angle of attack.

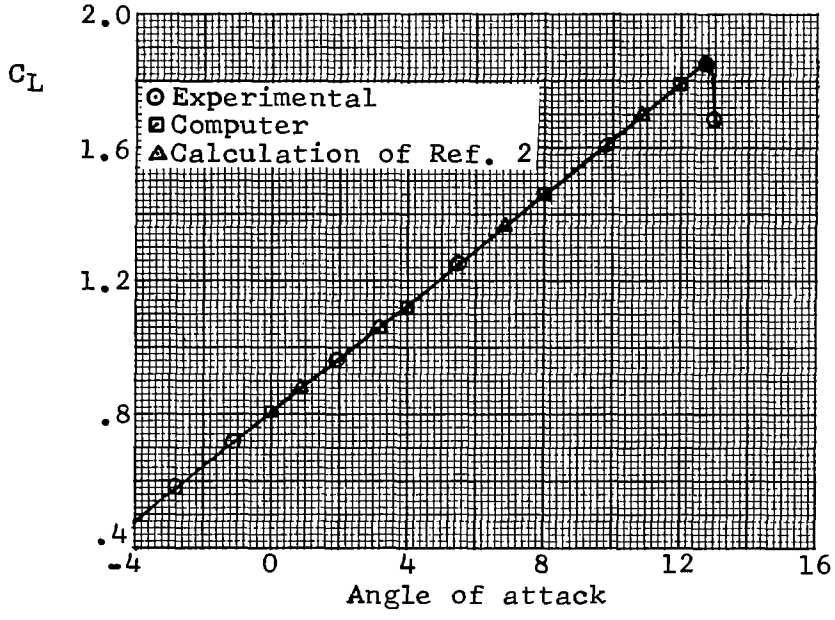

(b) Comparison of experimental and calculated lift curve.

Figure 18. Experimental and Calculated Characteristics for Wing with 60% Flap; Aspect Ratio 9.02; Taper Ratio 0.4; Washout 2°.

SECTION 5

PARAMETRIC INVESTIGATION

The computer program was used to determine the effect of wing geometry on the spanwise lift distribution, the location of the initial stalling point and the corresponding value of the effective maximum wing lift coefficient, $C_{L\,max}$. A similar investigation based on a linearized formulation of the lifting-line theory is reported in Reference 49. The present results may be considered as an extension of this work in that a broader range of parameters was investigated and the more accurate non-linear theory was employed.

5.1 RANGE OF PARAMETERS

The range of parameters selected for this study is representative of that applicable to present-day light aircraft. Computations were performed for wings utilizing the three basic airfoil series commonly encountered, NACA 64 series, 44 series and 230 series. These calculations were selected to show the effect of the three major geometric parameters, aspect ratio, taper ratio and section thickness, together with the influence of washout and linear camber variation from root to tip. Variations in flight Reynolds number, based on the wing mean aerodynamic chord, were also investigated as were the influences of a part-span deflected flap and the presence of a fuselage.

The variation of wing thickness and chord length was linear in all cases but the distribution of washout was non-linear in contrast to that used in Reference 49. The non-linear washout distribution chosen ensures straight-line leading and trailing edges. Washout was aerodynamic which is defined as the angle between the zero-lift lines of the root and tip sections. All wings were of trapezoidal planform without rounded tips, and zero sweep.

The investigation encompassed 331 different configurations which are summarized in Table III. The configuration defined by an aspect ratio of 6, a Reynolds number of 6×10^6 and a root and tip thickness chord ratio of 0.18 and 0.12 respectively was selected as a standard case for systematic variation of the parameters. These variations included the values of aspect ratios of 6, 8, and 10, aerodynamic washout of 0^o, $2\frac{1}{2}^o$, 5^o, and $7\frac{1}{2}^o$, taper ratios of 0.5, 0.75 and 1.0; root thickness ratios of 0.21, 0.18, 0.15, and 0.12; and tip thickness ratios of 0.12 and 0.15.

The complete range of calculations were not performed for untapered wings having $7\frac{1}{2}^o$ washout since this amount of twist would not normally be used on wings of this planform. However, to assist in establishing trends, a few computations were obtained for this washout.

TABLE III - SUMMARY OF CONFIGURATIONS STUDIED

(a) Wings of NACA 44XX Airfoil Section

Taper Ratio			Aspect Ratio			Root t/c				Tip t/c			Aerodynamic Washout-Deg.				Re. No. x 10^{-6}			Comments
1.	.75	.5	6	8	10	.12	.15	.18	.21	.12	.15	.18	0	2.5	5.0	7.5	3	6	9	
x	x	x	x					x		x			x	x	x			x		Aspect Ratio Variation
x	x	x		x				x		x			x	x	x			x		
x	x	x			x			x		x			x	x	x			x		
	x	x	x					x		x						x		x		
	x	x		x				x		x						x		x		
	x	x			x			x		x						x		x		
x	x	x	x						x	x			x	x	x			x		Root (t/c) Variation
x	x	x	x				x			x			x	x	x			x		
x	x	x	x			x				x			x	x	x			x		
	x	x	x						x	x						x		x		
	x	x	x				x			x						x		x		
	x	x	x			x				x						x		x		
x	x	x	x					x			x		x	x	x			x		Tip (t/c) Variation
x	x	x	x					x				x	x					x		
		x	x					x				x		x				x		
x			x					x		x						x		x		
		x	x					x				x				x		x		
x	x	x	x					x		x			x	x	x		x			Reynolds No. Variation
x	x	x	x					x		x			x	x	x			x		
x	x	x	x					x		x						x	x			
x	x	x	x					x		x						x		x		

Total number of configurations = 106

TABLE III - SUMMARY OF CONFIGURATIONS STUDIED - Continued

(b) Wings of NACA 230XX Airfoil Section

Taper Ratio			Aspect Ratio			Root t/c				Tip t/c			Aerodynamic Washout-Deg.				Re. No. x 10^{-6}			Comments
1.	.75	.5	6	8	10	.12	.15	.18	.21	.12	.15	.18	0	2.5	5.0	7.5	3	6	9	
x	x	x	x					x		x			x	x	x			x		
x	x	x		x				x		x			x	x	x			x		Aspect Ratio Variation
x	x	x			x			x		x			x	x	x			x		
	x	x	x					x		x						x		x		
	x	x		x				x		x						x		x		
	x	x			x			x		x						x		x		
x	x	x	x						x	x			x	x	x			x		
x	x	x	x				x			x			x	x	x			x		Root (t/c) Variation
x	x	x	x			x				x			x	x	x			x		
	x	x	x						x	x						x		x		
	x	x	x				x			x						x		x		
	x	x	x			x				x						x		x		
x	x	x	x					x			x		x	x	x			x		Tip (t/c) Variation
	x	x	x					x			x					x		x		
x	x	x	x					x		x			x	x	x		x			Reynolds No. Variation
x	x	x	x					x		x			x	x	x			x		
x	x	x	x					x		x						x	x			
x	x	x	x					x		x						x		x		

Total number of configurations = 99

TABLE III - SUMMARY OF CONFIGURATIONS STUDIED - Continued

(c) Wings of NACA 642XX Airfoil Section

Taper Ratio			Aspect Ratio			Root t/c				Tip t/c			Aerodynamic Washout-Deg.				Re. No. x 10^{-6}			Comments
1.	.75	.5	6	8	10	.12	.15	.18	.21	.12	.15	.18	0	2.5	5.0	7.5	3	6	9	
x	x	x	x					x		x			x	x	x			x		Aspect Ratio Variation
x	x	x		x				x		x			x	x	x			x		
x	x	x			x			x		x			x	x	x			x		
	x	x	x					x		x						x		x		
	x	x		x				x		x						x		x		
	x	x			x			x		x						x		x		
x	x	x	x						x	x			x	x	x			x		Root (t/c) Variation
x	x	x	x				x			x			x	x	x			x		
x	x	x	x			x				x			x	x	x			x		
	x	x	x						x	x						x		x		
	x	x	x				x			x						x		x		
	x	x	x			x				x						x		x		
x	x	x	x					x			x		x	x	x			x		Tip (t/c) Variation
	x	x	x					x			x					x		x		
x	x	x	x					x		x			x	x	x		x			Reynolds No. Variation
x	x	x	x					x		x			x	x	x				x	
x	x	x	x					x		x						x	x			
x	x	x	x					x		x						x			x	

Total number of configurations = 99

TABLE III - SUMMARY OF CONFIGURATIONS STUDIED - Concluded

(d) Effects of Camber, Fuselage and Flaps on Wings of Various NACA Airfoil Sections.

Taper Ratio			Aspect Ratio	Root t/c	Tip t/c	Aerodynamic Washout-Deg.			Re.No. x 10^{-6}			Wing/Body Incidence			Flap Span Wing-Span			Comments
1.	.75	.5	6	.18	.12	0.	2.5	5.0	3	6	9	0^{o}	2^{o}	4^{o}	.45	.60	.75	
x	x	x	x	x	x	x			x									Effect of 0.2 Camber Increase
x	x	x	x	x	x	x				x								
x	x	x	x	x	x	x					x							
x	x	x	x	x	x	x				x		x						Fuselage Effect, High Wing A=1/10 Span
x	x	x	x	x	x	x				x			x					
x	x	x	x	x	x	x				x				x				
x			x	x	x	x				x					x			Flap Effect
x			x	x	x		x			x					x			
x			x	x	x			x		x					x			
x			x	x	x	x				x						x		
x			x	x	x		x			x						x		
x			x	x	x			x		x						x		
x			x	x	x	x				x							x	
x			x	x	x		x			x							x	
x			x	x	x			x		x							x	

Total number of configurations = 27

Grand total of configurations studied = 331

5.2 METHOD OF PRESENTATION OF RESULTS

The effects of various design parameters on the stalling characteristics of unswept wing aircraft are herein presented in the form of plots showing the stall margin distributions, location and movement of stall boundaries and the maximum values of integrated wing lift coefficient.

5.2.1 Stall Margin Distributions

The stall margin, ΔC_l, is defined as the difference between the maximum section lift coefficient and the section lift coefficient when the stall first occurs on the wing. Figure 19 shows typical distributions of C_l, $C_{l\,max}$ and ΔC_l computed for the conditions indicated. The spanwise location of zero stall margin corresponds to the point of onset of stall and the rate of separation of the ΔC_l curve from the horizontal axis indicates the rate of stall propagation across the span. A wing is usually assumed to have sufficient stall margin if a value of $\Delta C_l = 0.1$ is indicated at the 70% semispan station.

Since it would be impractical to present all three distributions (i.e. C_l, $C_{l\,max}$, and ΔC_l) for each of the 331 cases computed, in the manner presented in Figure 19, only the distributions of stall margin are given.

5.2.2 Stall Boundaries

In general, the curve representing the spanwise lift distribution at the onset of wing stall is tangent to the section $C_{l\,max}$ curve at more than one point. This implies that a few adjacent wing sections (i.e. a portion of the wing span) can be stalled simultaneously at a given operating condition. The limiting values of spanwise locations encompassing these stalled sections are defined as the stall boundaries. Using stall margin distributions, such as shown in Figure 19, the inner and outer boundaries of the stalled wing area can be estimated as the spanwise locations where $\Delta C_l = 0.01$. Furthermore, the movement of these stall boundaries affecting the growth and the propagation of wing stall areas can be expressed as a function of the basic design parameters. For example, using Figures 19(a) and 19(b) the stall areas for the unflapped and the flapped wing configurations considered are defined by the stall boundaries 50% to 68% and 10% to 40% of the wing span, respectively.

5.2.3 Maximum Lift Coefficient

Maximum lift coefficient is an important criterion in assessing wing stall characteristics as affected by the variation of basic design parameters. This lift coefficient is defined as the integrated value obtained from the spanwise lift distributions when any one of the wing sections is stalled. Such stall

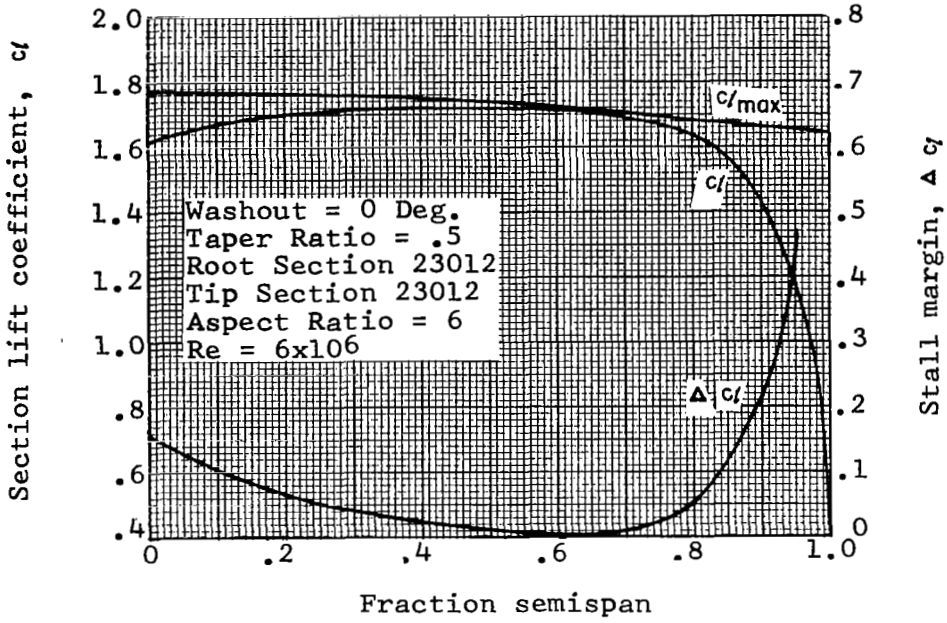

(a) Unflapped wing - 230 series sections.

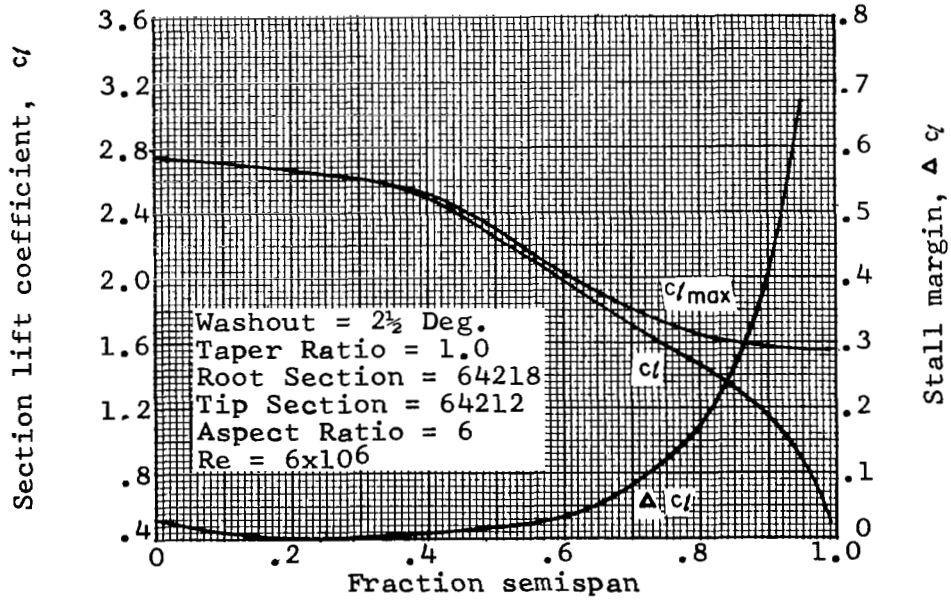

(b) Flapped wing - 60% span flap - 642 series sections.

Figure 19. - Typical Lift Distributions Along Wing Span

is obtained when the local section lift coefficient C_l equals the maximum value ($C_{l\,max}$) of that section. This value depends primarily on section thickness-chord ratio, Reynolds number and the airfoil type. Typical variations of the maximum section lift coefficient ($C_{l\,max}$) with these parameters is shown in Figure 20. The effects of various design parameters on integrated maximum wing lift coefficient are herein presented in the form of carpet plots. These plots facilitate linear readings of non-linear relationships between three variables and thus permit more accurate interpolation (or extrapolation) for intermediate values of the parameters. However, since this method of data presentation is not as commonly used as the familiar X-Y plot, an explanation of the use of carpet plots is presented in the following sub-section.

5.2.4 Carpet Plots

The procedure for constructing and reading carpet plots can be best illustrated by the following example: The carpet plot shown in Figure 21 represents the variation of $C_{L\,max}$ with Reynolds number and taper ratio for a wing employing 230 series sections and a constant value of washout of $7\frac{1}{2}^{o}$. Curve (abc) on this carpet is a conventional (x-y) plot of $C_{L\,max}$ v Reynolds number for a constant value of taper ratio of 0.5. The indicated horizontal unit distance corresponds to a change in Reynolds number of $1x10^6$. Thus, point (a) corresponds to Reynolds number of $3x10^6$ and point (b) which is 3 horizontal units from (a), corresponds to $6x10^6$ and point (c) to $9x10^6$. The curve (def) presents a similar plot for a taper ratio of 0.75.

However, instead of plotting data for $\lambda = .75$ on the same horizontal scale as that for curve (abc) a new scale is chosen whose origin is $2\frac{1}{2}$ horizontal units to the right of the point (a), reflecting the change in taper ratio from 0.5 to 0.75. Thus, as regards changes in taper ratio, each horizontal unit corresponds to a change in λ equal to 0.1. Similarly curve (ghi) for $\lambda = 1.0$ is plotted 5 units to the right of point (a) or $2\frac{1}{2}$ units to the right from point (b). After a new origin is selected for each taper ratio (i.e. point (a) for $\lambda = 0.5$, point (d) for $\lambda = 0.75$ and point (g) for $\lambda = 1.0$), the plotting of the $C_{L\,max}$ vs. Re curves for each taper ratio is accomplished in the conventional way. If all points corresponding to the same value of $C_{L\,max}$ Reynolds number are now joined, e.g. curves (adg) (beh) and (cfi), the resulting curves show the variation of $C_{L\,max}$ with taper ratio for constant values of Reynolds number.

Reading the carpet is as simple as constructing it. If the value of $C_{L\,max}$ is required, say, for $\lambda = 0.62$ and $Re = 5.3x10^6$ it can be obtained as follows: For all three values of taper ratio locate and join points (j), (k) and (l) corresponding to $Re = 5.3x10^6$. This is accomplished by moving 2.3

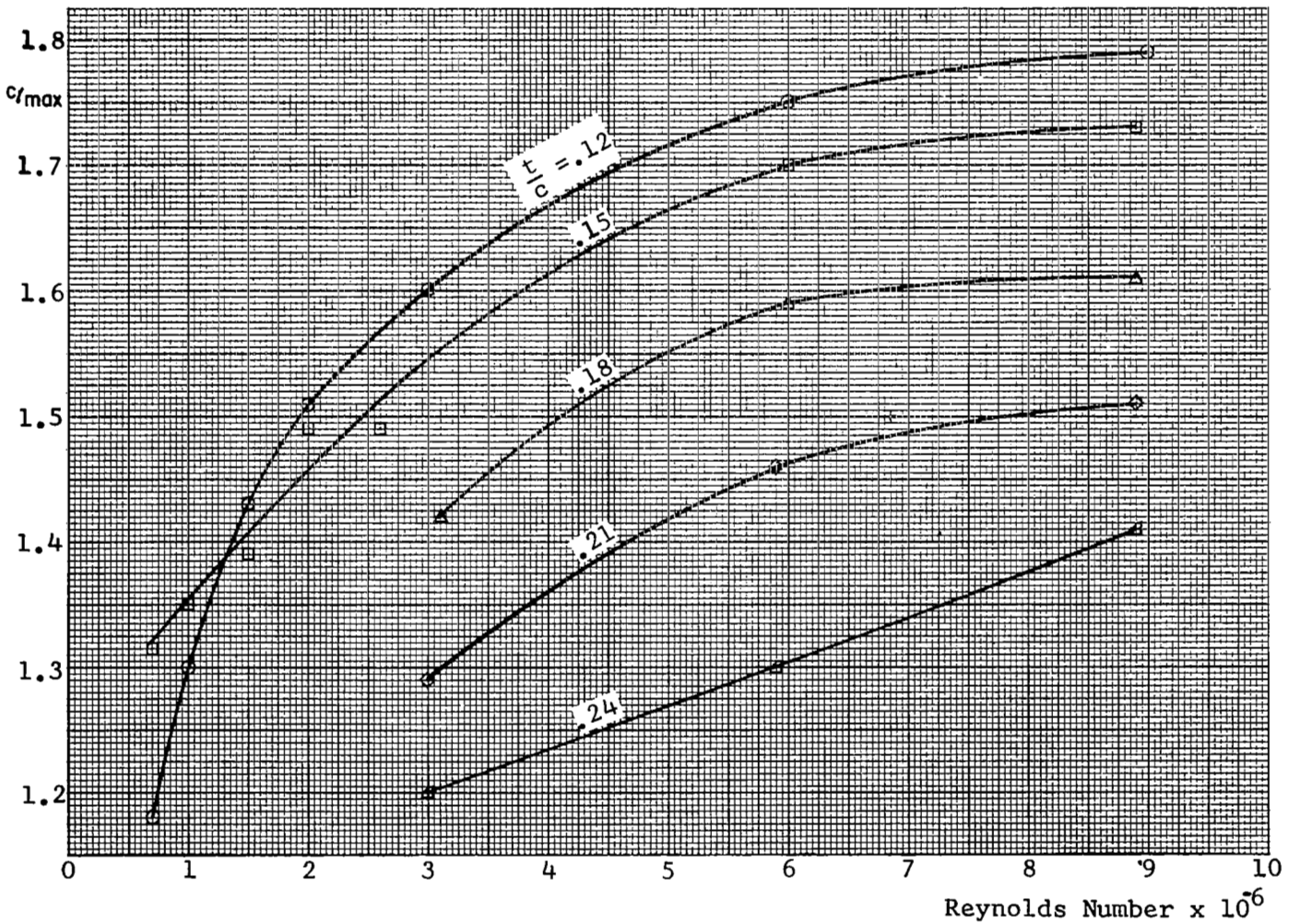

Figure 20. Variation of $c_{l_{max}}$ with Reynolds Number and Thickness-Chord ratio - 230 series sections.

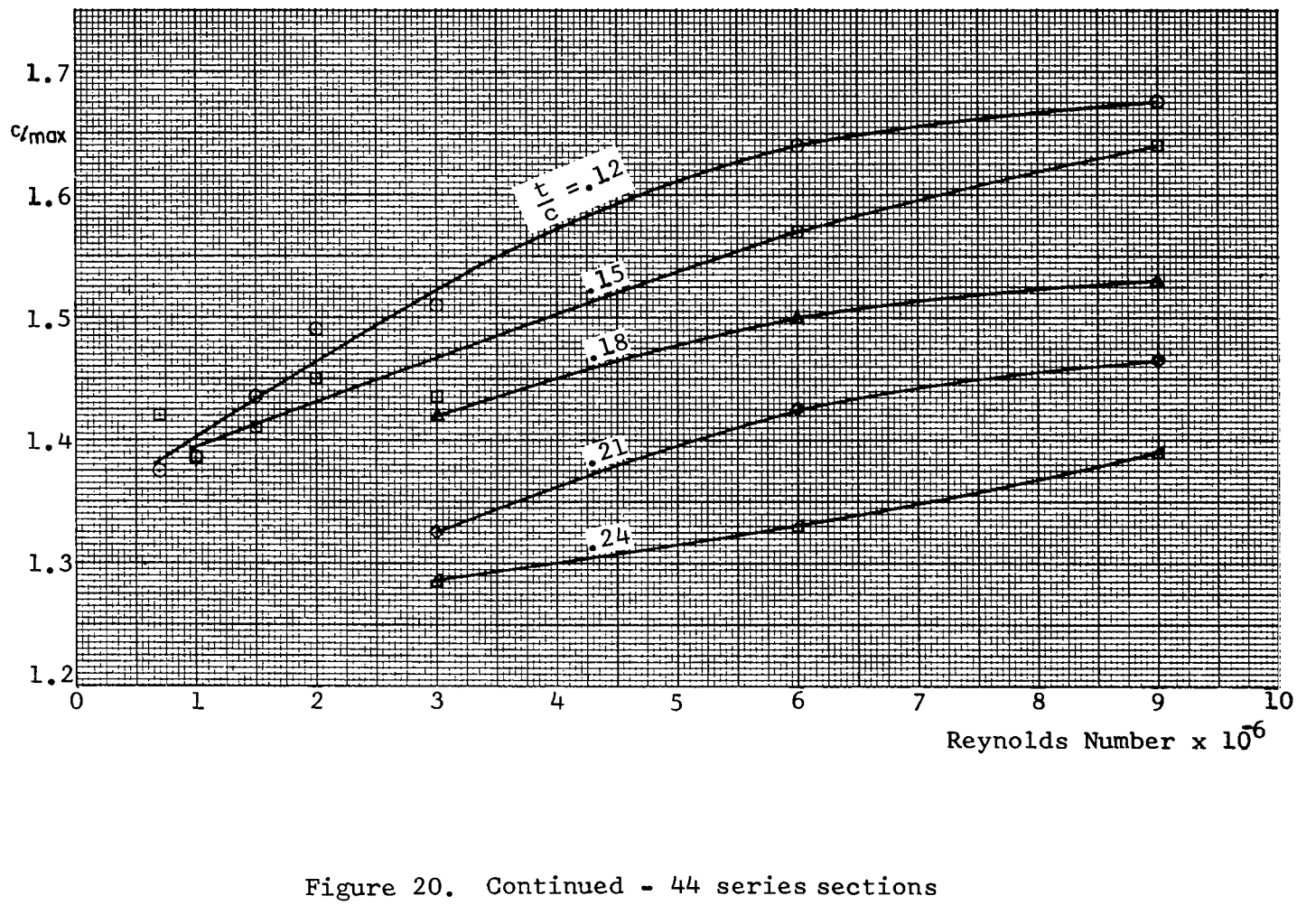

Figure 20. Continued - 44 series sections

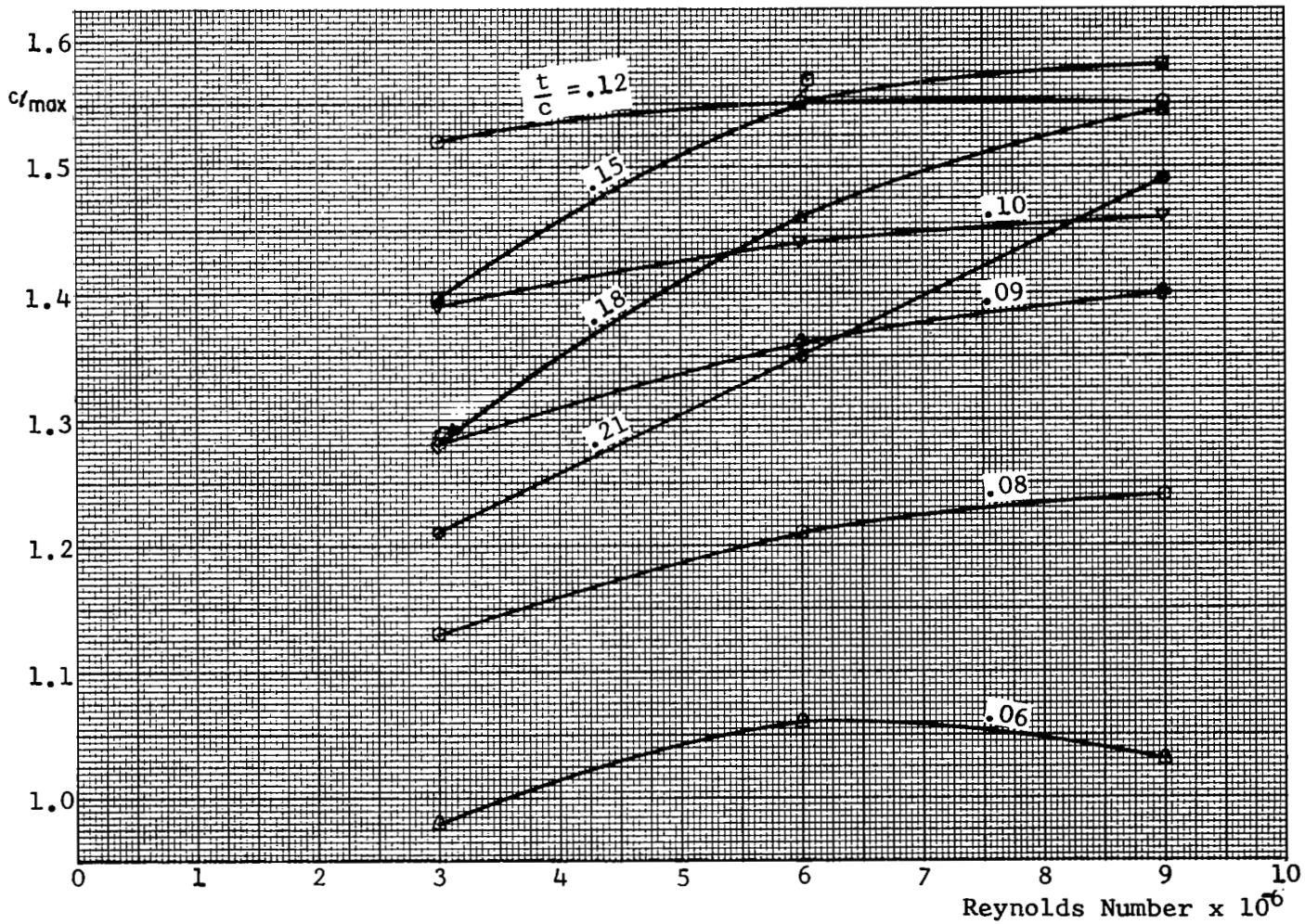

Figure 20. Concluded - 642 series sections

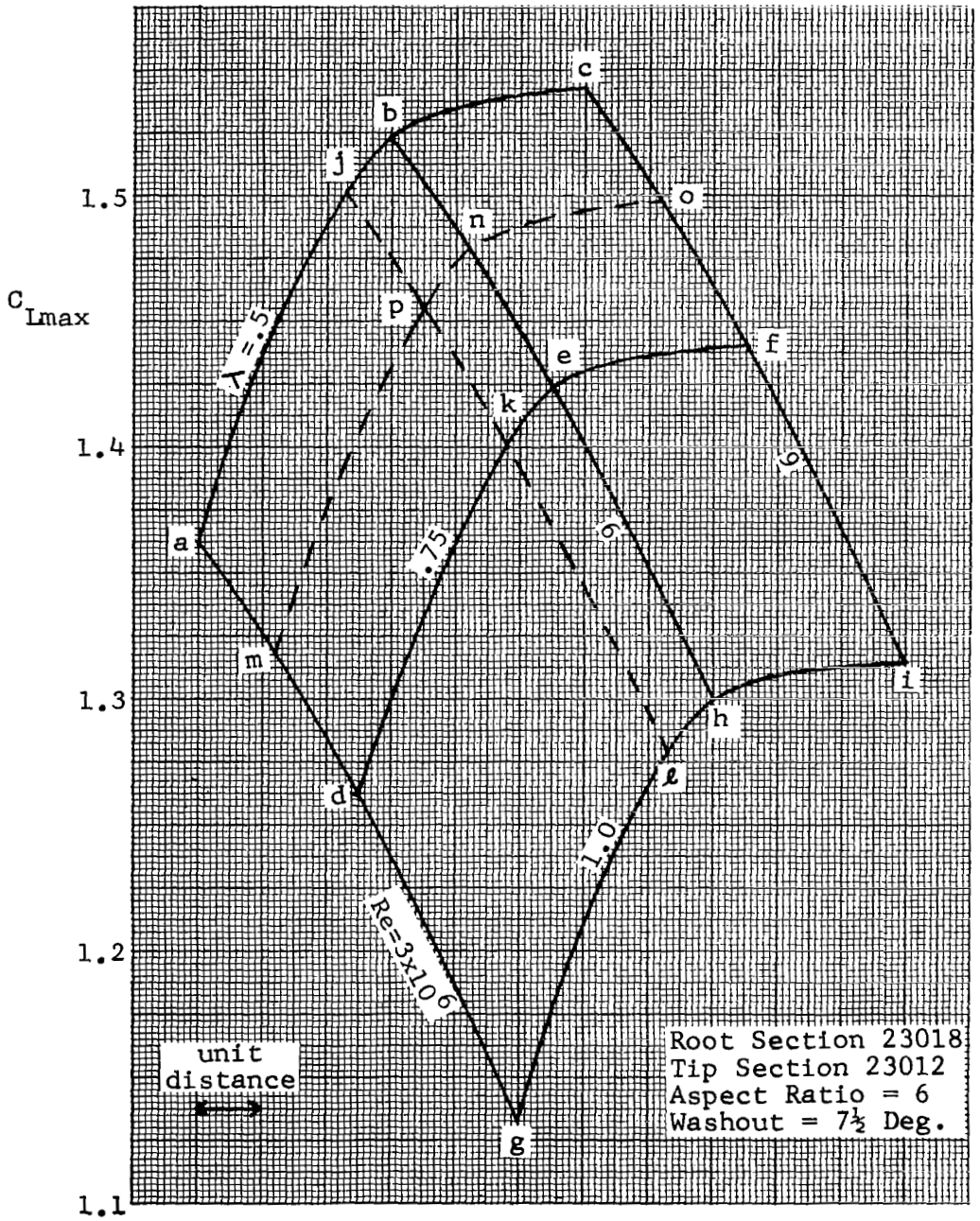

Figure 21. - Variation of C_{Lmax} with Reynolds Number and Taper Ratio.

horizontal units towards the right from point (a) to locate point (j) on the $\lambda = 0.5$ curve, 2.3 horizontal units from point (d) to locate point (k) on the $\lambda = 0.75$ curve and the same number of units from point (g) to locate point (l) on the $\lambda = 1.0$ curve. Similarly, locate and join point (m) (n) and (o) moving 1.2 horizontal units from points (a), (b) and (c) on the corresponding Reynolds number curves, respectively. The point of intersection (p) of the curves (ihl) and (mno) yields the required value of $C_{L_{max}} = 1.445$ for $\lambda = 0.62$ and $Re = 5.3 \times 10^6$.

5.3 COMPUTER RESULTS

Presented in this section is a compilation of wing stall design charts obtained from the computer program. These charts can be used in preliminary design of unswept wing aircraft for determining optimum geometric parameters of a wing to yield good stalling characteristics. The effects of these geometric parameters on stalling behavior of straight wing aircraft are discussed in the following pages.

5.3.1 Effect of Aspect Ratio

Figures 22, 23, and 24 show the effect of aspect ratio on wing stall margins, stall boundaries and the values of maximum wing lift coefficient, respectively. Each of these figures is presented for three different families of airfoil sections, i. e. 230, 44 and 642 series, and for a range of wing taper ratios between 0.5 and 1.0 and wing washout between 0^o and $7\frac{1}{2}^o$.

Examining Figure 22 it can be noted that an increase in aspect ratio results in a reduction of the stall margins at outboard wing stations. This effect is minimized at high values of washout and wing taper ratios. Furthermore, as can be seen from Figures 23 and 24, an increase in aspect ratio appears to have little effect on the spanwise location of stall boundaries and yields only a small increase in wing maximum lift coefficient.

It can therefore be concluded that although wing aspect ratio is important from aircraft performance considerations, its effect on the stalling characteristics is very small. For this reason the remaining stall results which are presented in this section for aspect ratio of 6 only are considered to be typical and representative for the range of aspect ratios associated with present day light aircraft.

5.3.2 Effect of Taper Ratio

Figures 22 through 24 also show that taper ratio is one of the most dominant design parameters affecting wing stall characteristics. For any fixed aspect ratio and wing washout an increase in taper ratio from $\lambda = 0.5$ to $\lambda = 1.0$ (rectangular

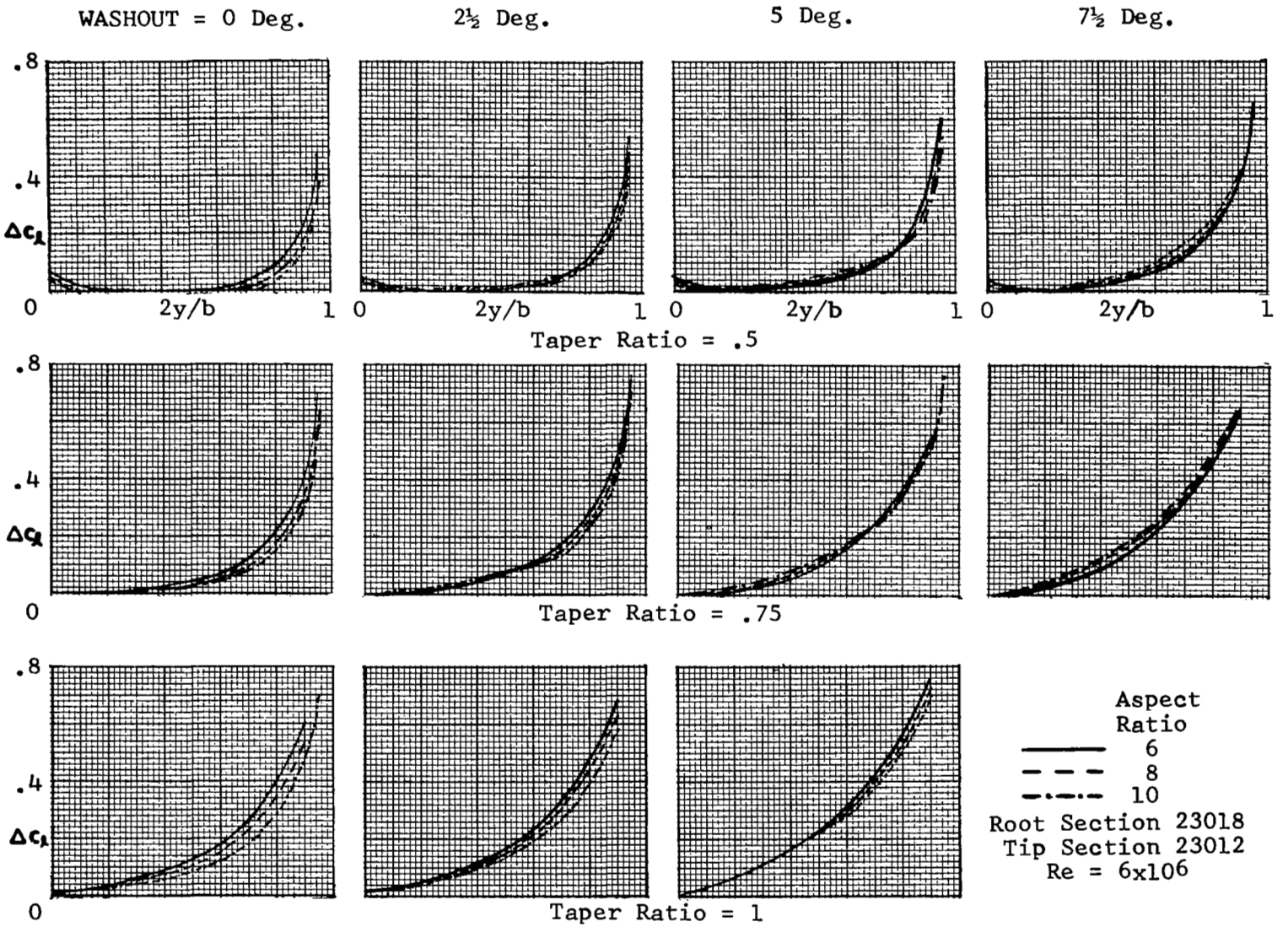

Figure 22. Effect of Aspect Ratio on Stall Margin Distribution

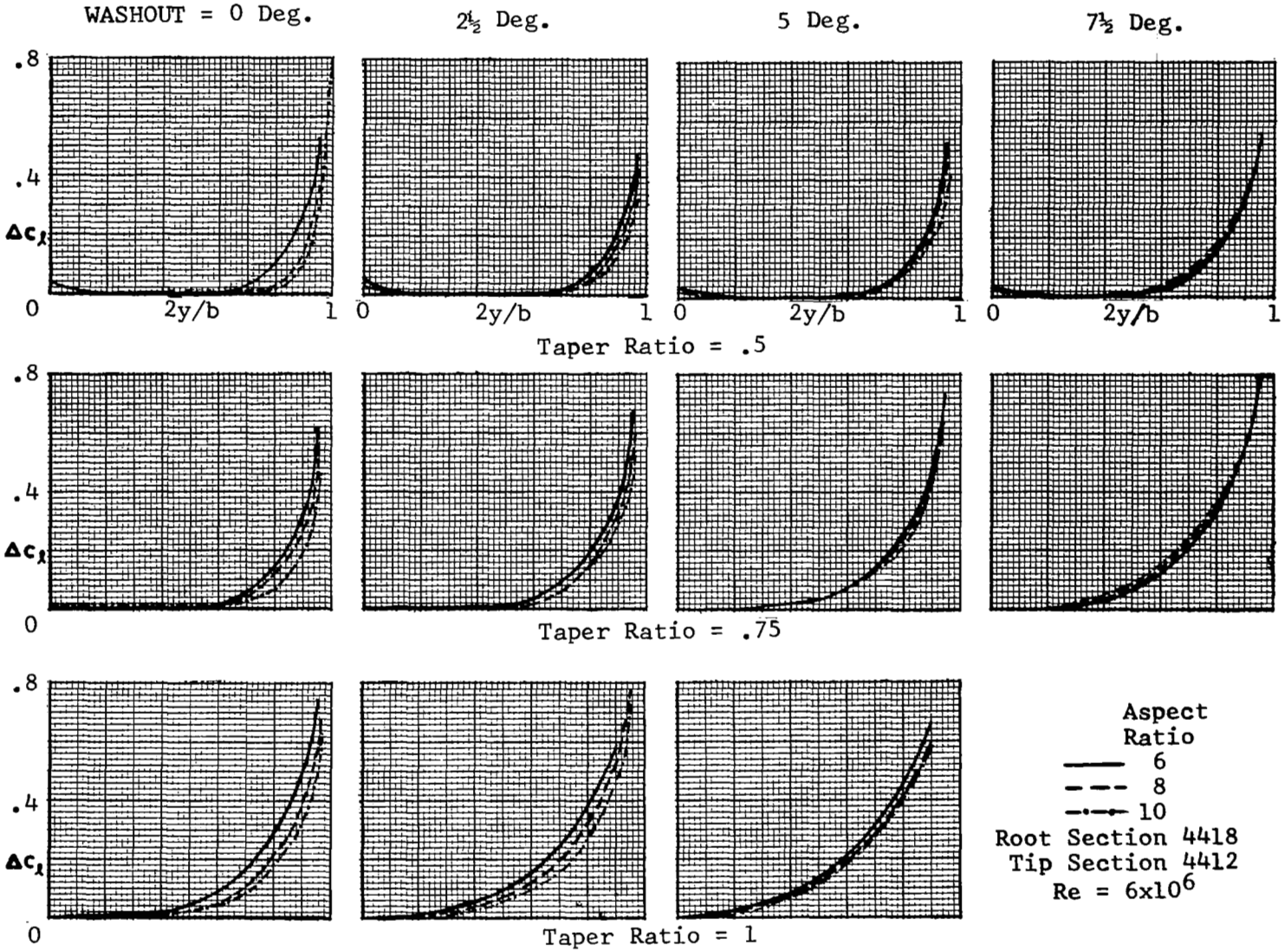

Figure 22. Continued

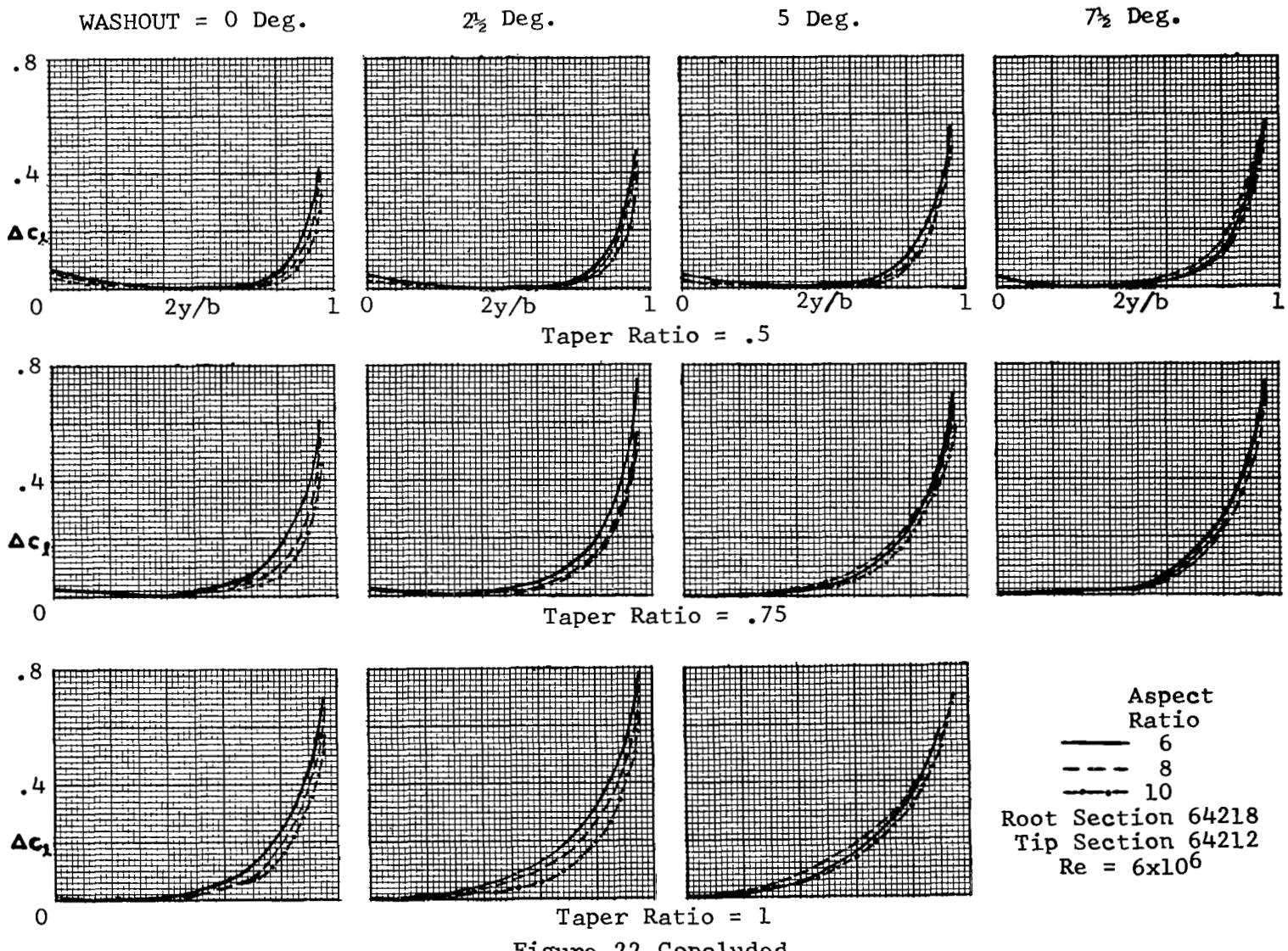

Figure 22.Concluded

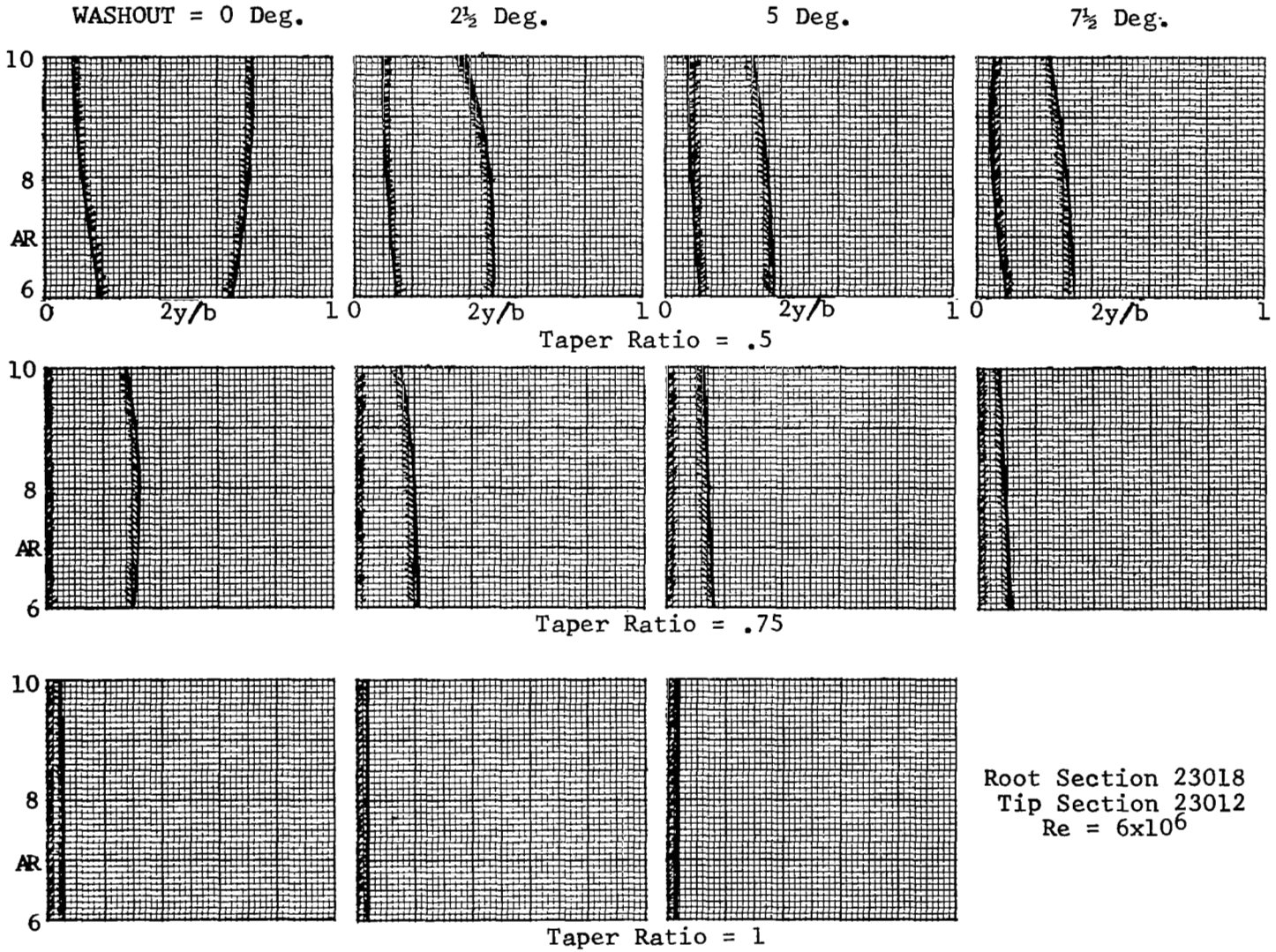

Figure 23. Effect of Aspect Ratio on Wing Stall Pattern.

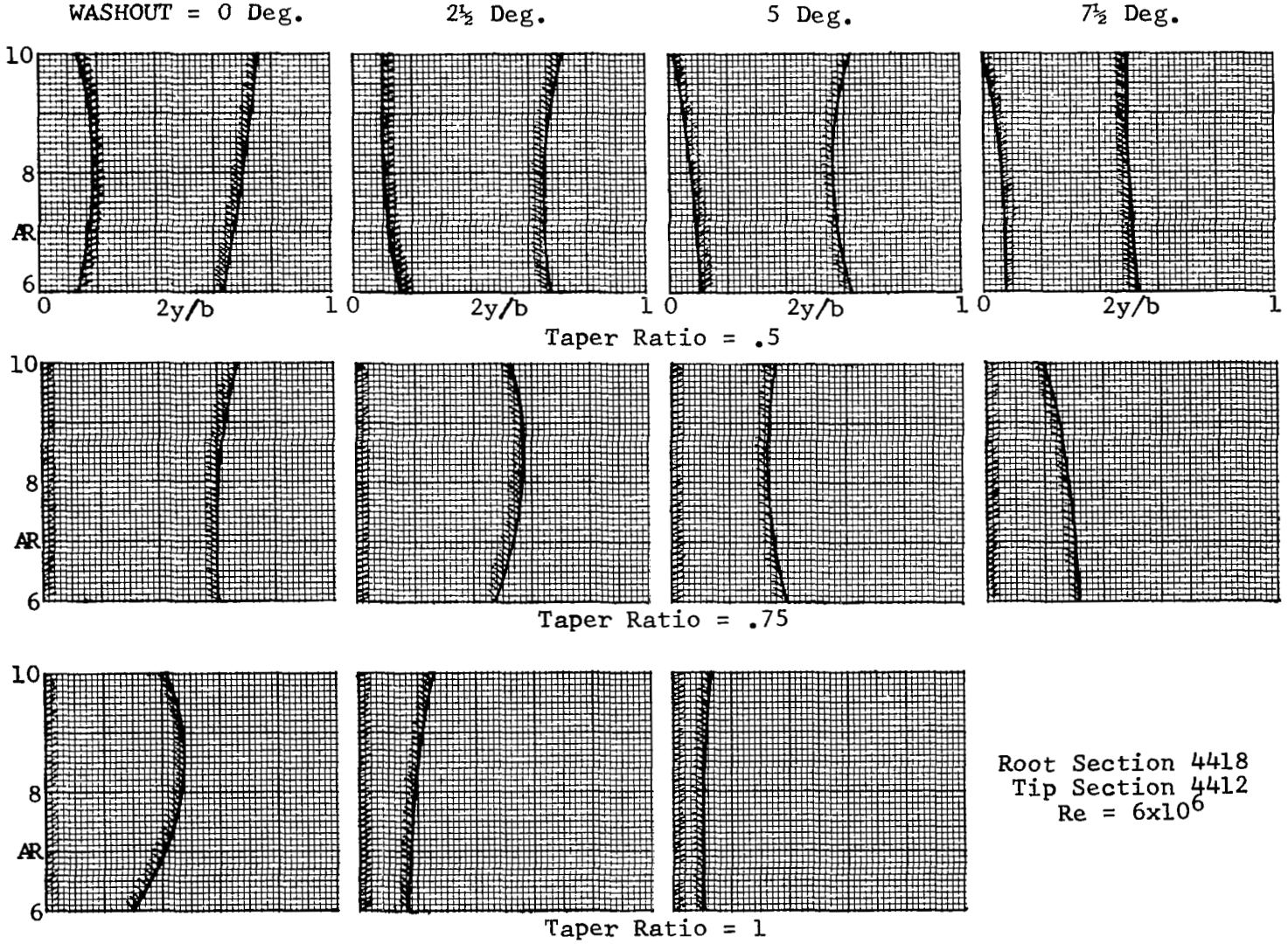

Figure 23. Continued

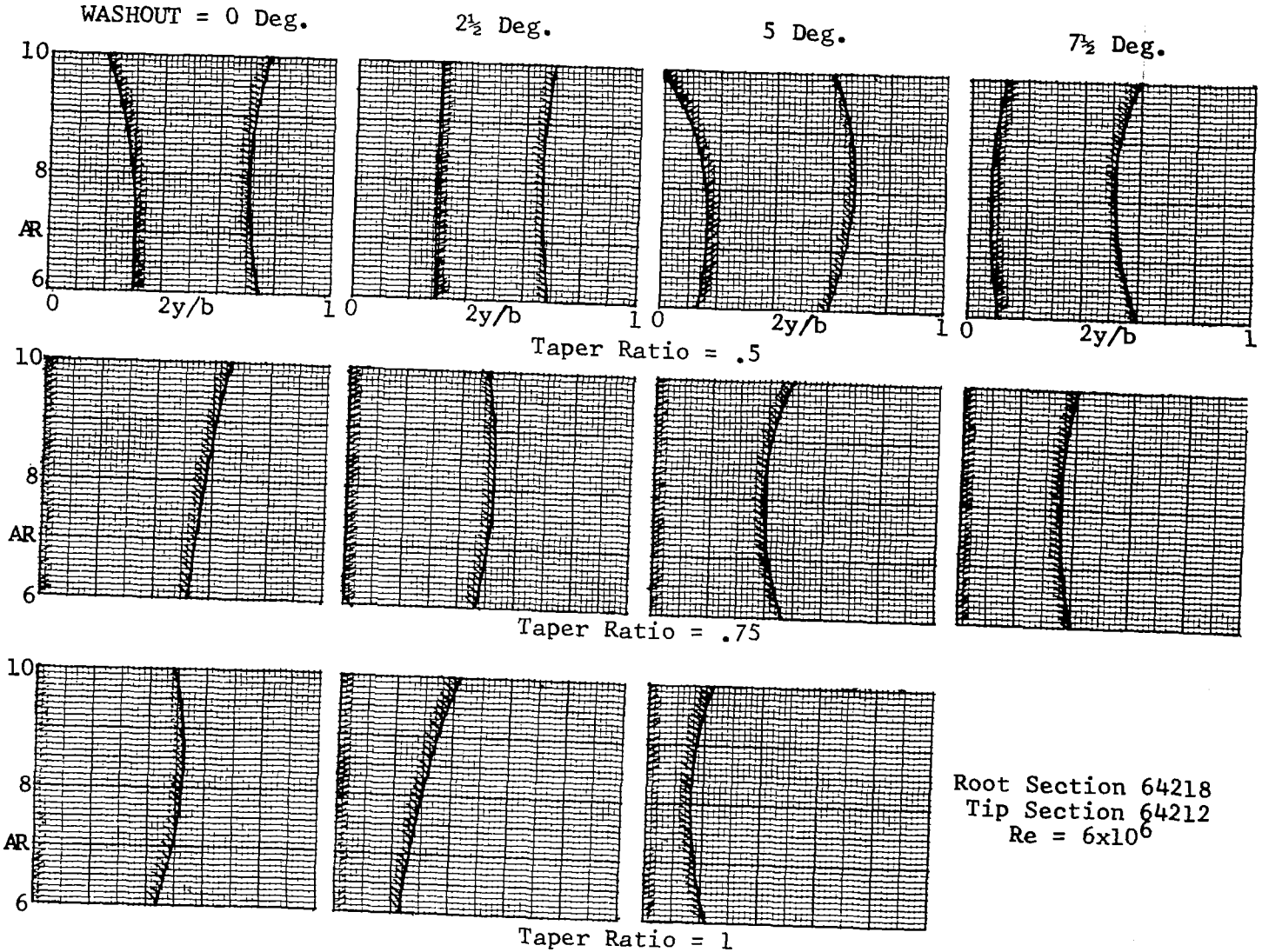

Figure 23. Concluded

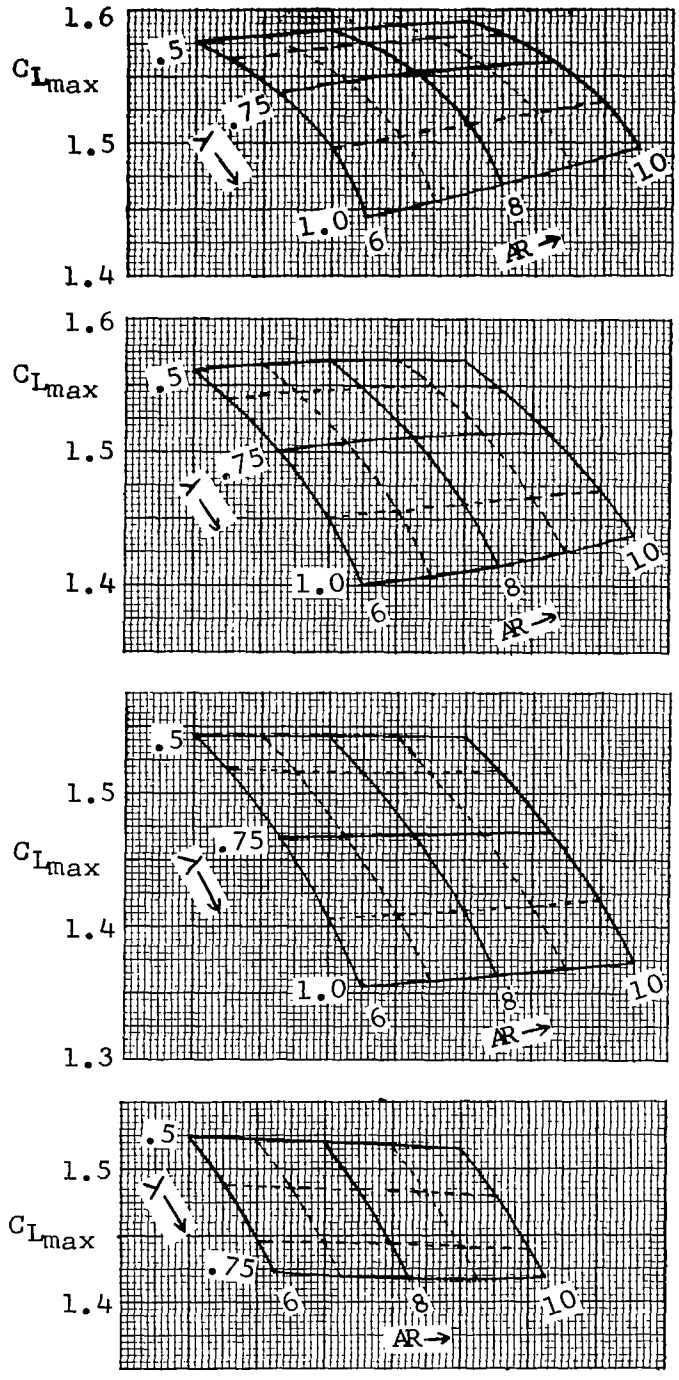

Figure 24. Effect of Aspect Ratio and Taper Ratio on $C_{L_{max}}$.

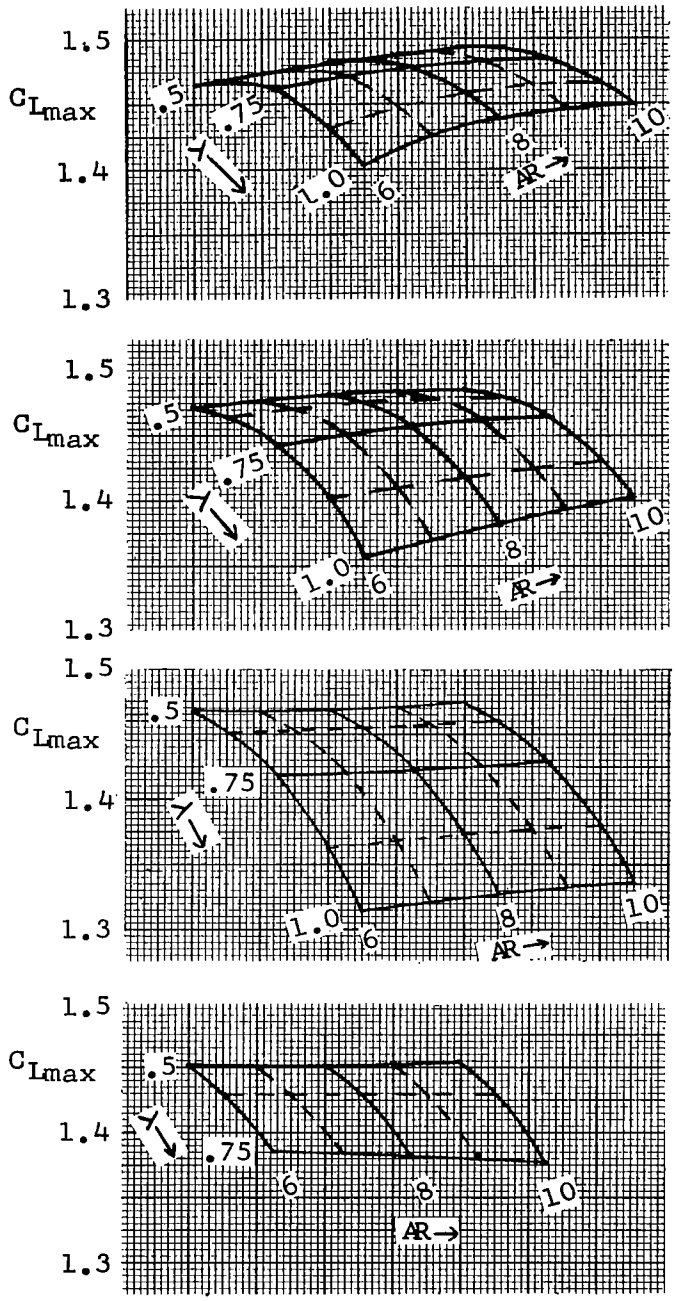

WASHOUT = 0 Deg.

WASHOUT = 2½ Deg.

WASHOUT = 5 Deg.

WASHOUT = 7½ Deg.
Root Section 4418
Tip Section 4412
Re = 6×10^6

Figure 24. Continued

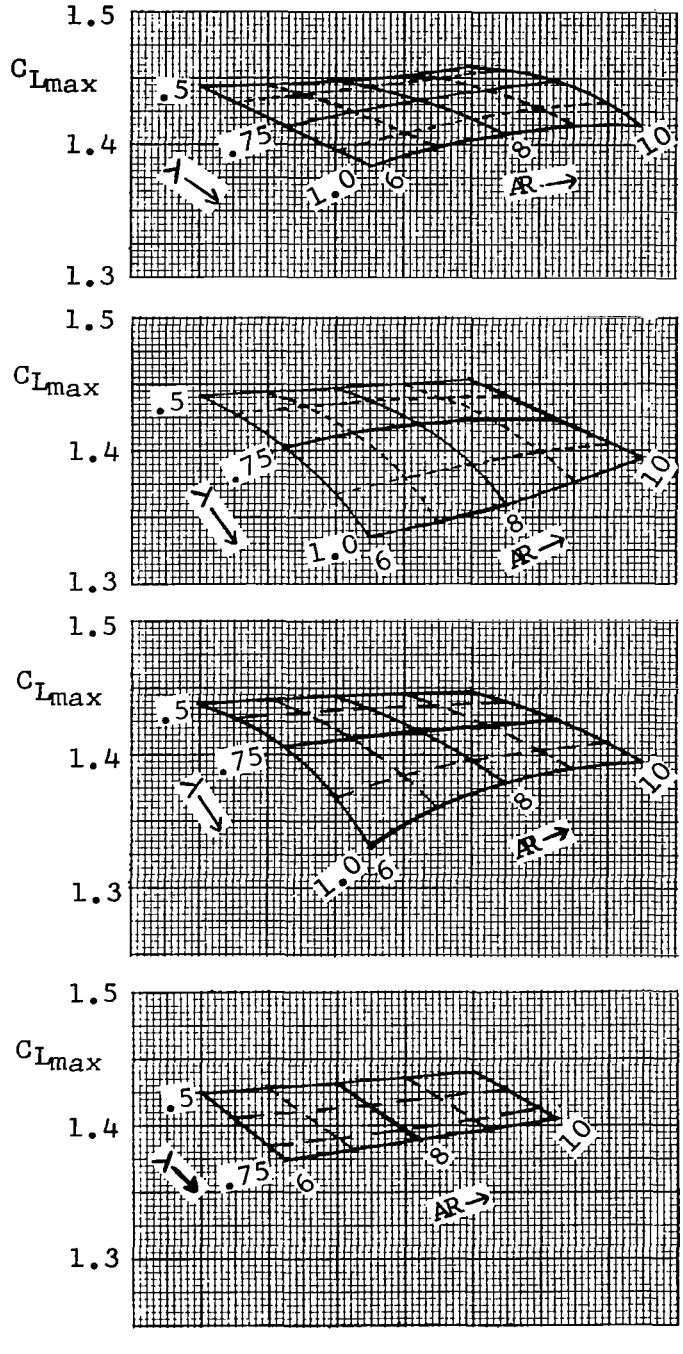

Figure 24. Concluded

wing) results in a substantial increase in stall margin on the outer portion of the wing. This increase in stall margin is associated with a shift of stall boundaries toward the inner portion of the wing.

The advantage of the favorable stalling characteristics obtainable by increasing wing taper ratio is somewhat offset by a reduction of wing $C_{L\,max}$ and hence, for a given wing loading, an increase in stalling speed. This reduction, which can be as high as 12% based on the $C_{L\,max}$ values for a rectangular wing, depends on the airfoil sections and wing washout.

5.3.3 Effect of Wing Washout

Washout is often used to promote desirable stalling characteristics. For a given value of wing lift coefficient, twisting the tip section relative to the root section reduces the values of section lift coefficient in the tip regions and increases section lift coefficient at inboard stations. Since the distribution of section maximum lift coefficient is unaffected by twist, the net result is to increase the stall margins in the tip region and to shift the stall boundaries inboard of the wing. These effects can be seen from Figures 22 and 23.

Examining these figures it can be noted that for a taper ratio of 0.5 washout exerts relatively small influence on the stall margins at 70% semispan. As taper ratio increases, however, the effectiveness of washout becomes greater and is most effective for a rectangular wing ($\lambda = 1$). However, a rectangular wing is unlikely to require washout since, as discussed previously, wings of this planform normally exhibit good stalling characteristics. The beneficial effect of washout appears to be offset by the adverse effect of the linearly diminishing Reynolds number. Therefore, the use of washout seems most justified for moderate values of wing taper ratio.

Furthermore, Figure 24 indicates that for fixed values of aspect ratio and taper ratio, wing washout tends to reduce the value of $C_{L\,max}$. The amount of this reduction depends on the wing sections and the value of washout used.

In addition to the effects discussed above, washout may affect wing performance through changes in both wing profile and induced drag. The increase in induced drag coefficient due to washout above that for an untwisted wing is presented in Figure 25 for two values of aspect ratio 6 and 10. The data is for a wing having 230 series sections with root and tip thickness-chord ratios of .18 and .12, respectively.

As can be seen, at low values of lift coefficient the use of washout causes an increase in induced drag while at high values of C_L washout reduces induced drag. Increased induced drag levels

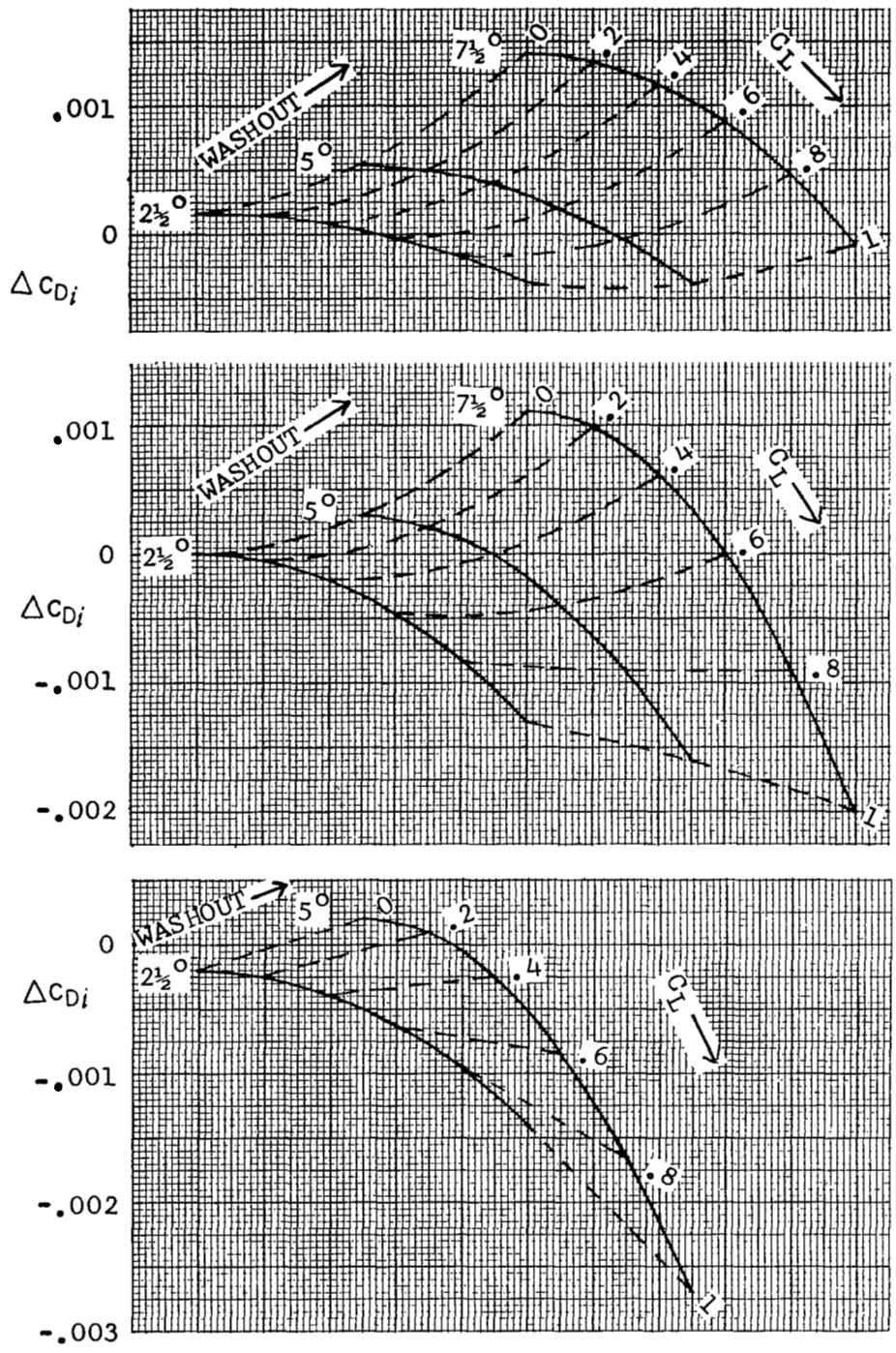

Figure 25. - Increment of Induced-Drag Coefficient Due to Washout, 230 series airfoil section - aspect ratio = 6 , Re = 6×10^6

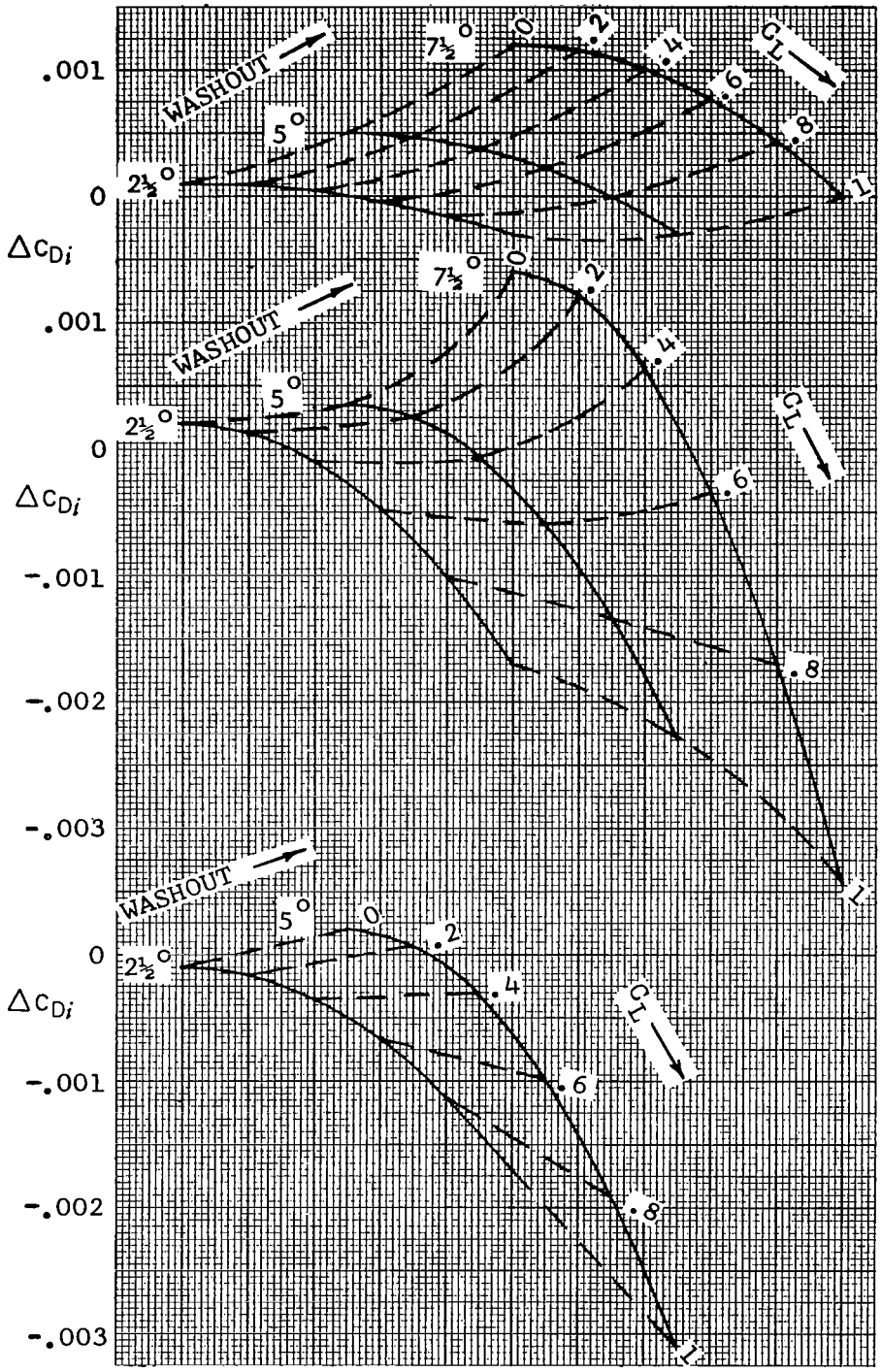

Taper Ratio
.5

.75

1

Figure 25. - Concluded - aspect ratio = 10

at low lift coefficients may impair cruise performance depending on the amount of the increase relative to the overall drag coefficient of the airplane. Changes in profile drag due to washout were found to be sufficiently small that their effects on wing performance can be neglected.

5.3.4 Effect of Root Thickness-Chord Ratio

The effect of root thickness-chord ratio on wing stalling characteristics can be depicted from Figures 26, 27 and 28. These figures are presented for an aspect ratio of 6 wing having the tip thickness fixed at a constant value of 12% and the root thickness varying between 12% and 21%. Three families of airfoil sections are considered; 230 series, 44 series and 642 series.

These figures show that for the wing employing 230 series airfoils increasing root thickness-chord ratio results in an increase in stall margins for outboard wing sections, a general inboard movement of the stall boundaries and a decrease in wing maximum lift coefficient.

Similar effects of the root thickness-ratio can be noted for the wing employing 44-series airfoils, however, in this case the variation in the stalling characteristics is less pronounced.

For the wing employing 642 series airfoil sections, an increase in root thickness-chord ratio causes a reduction in the stall margins on the outboard portion of the wing and tends to move the stall boundaries outboard in contrast to the trends indicated by the results for the other series. This effect is primarily due to the variation of $c_{l\,max}$ with thickness-chord ratio for this particular airfoil series. As can be seen from Figure 20 the amount by which $c_{l\,max}$ decreases with increases in section thickness-chord ratios above 12% is greatest for the 230 series airfoils, less for the 44 series and least for the 642 series sections. In fact, for Reynolds numbers greater than 6×10^6 the 642 series shows a small rise in $c_{l\,max}$ when the section thickness chord ratio increases from .12 to .15.

Furthermore, for a given spanwise distribution of section Reynolds number and thickness-chord ratio the curve of $c_{l\,max}$ versus spanwise distance will be flattest for the wing employing 642 series sections. This has the effect of promoting stall further outboard than would be the case for the wings composed of either 44 or 230 series sections.

The fact that the dependence of $c_{l\,max}$ on (t/c) is least for the 642 series airfoils is again reflected in the results for wing maximum lift coefficient as shown in Figure 28. For this case increasing root thickness-chord ratio results in the

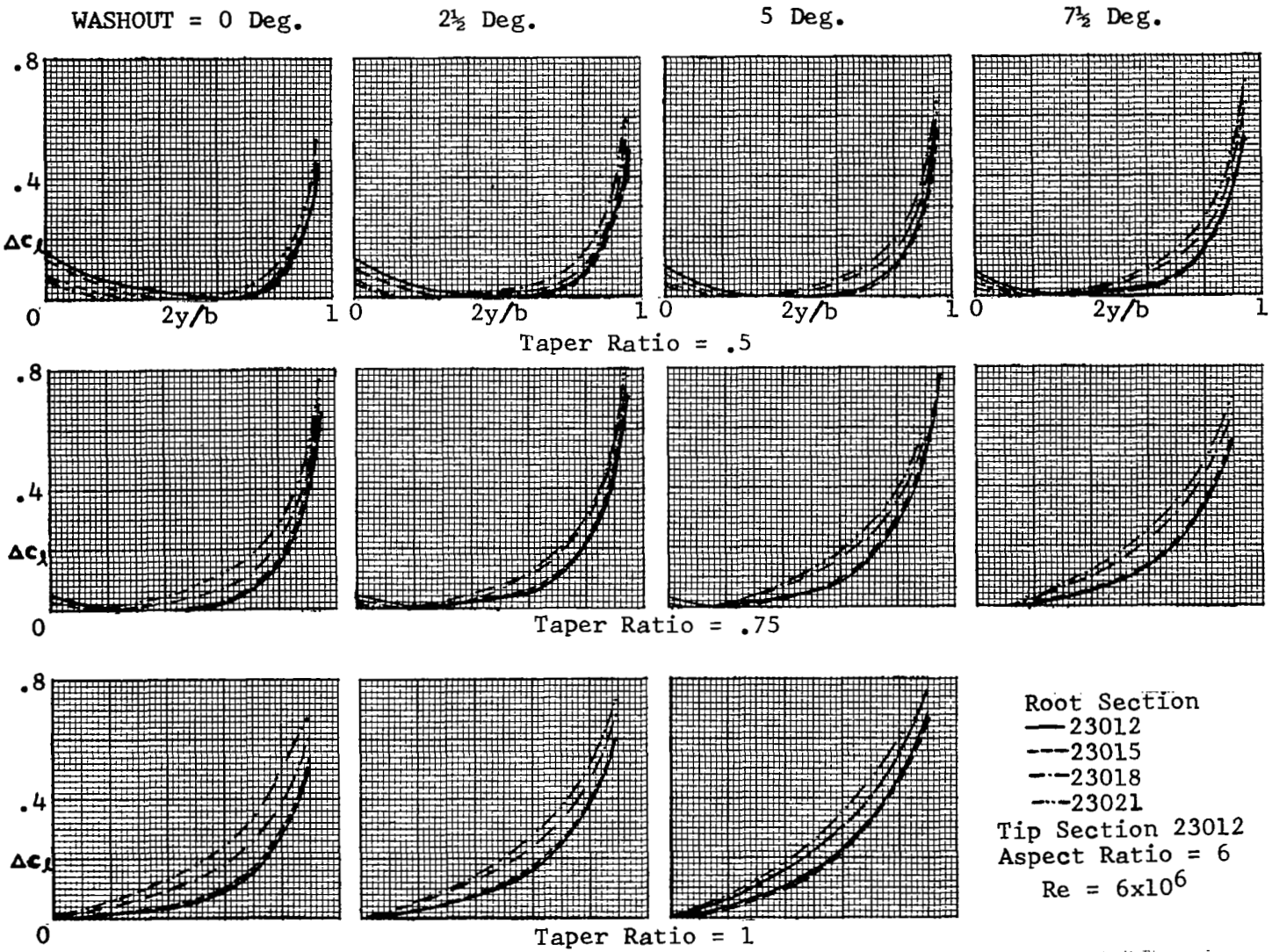

Figure 26. - Effect of Root Thickness-Chord Ratio on Stall Margin Distribution.

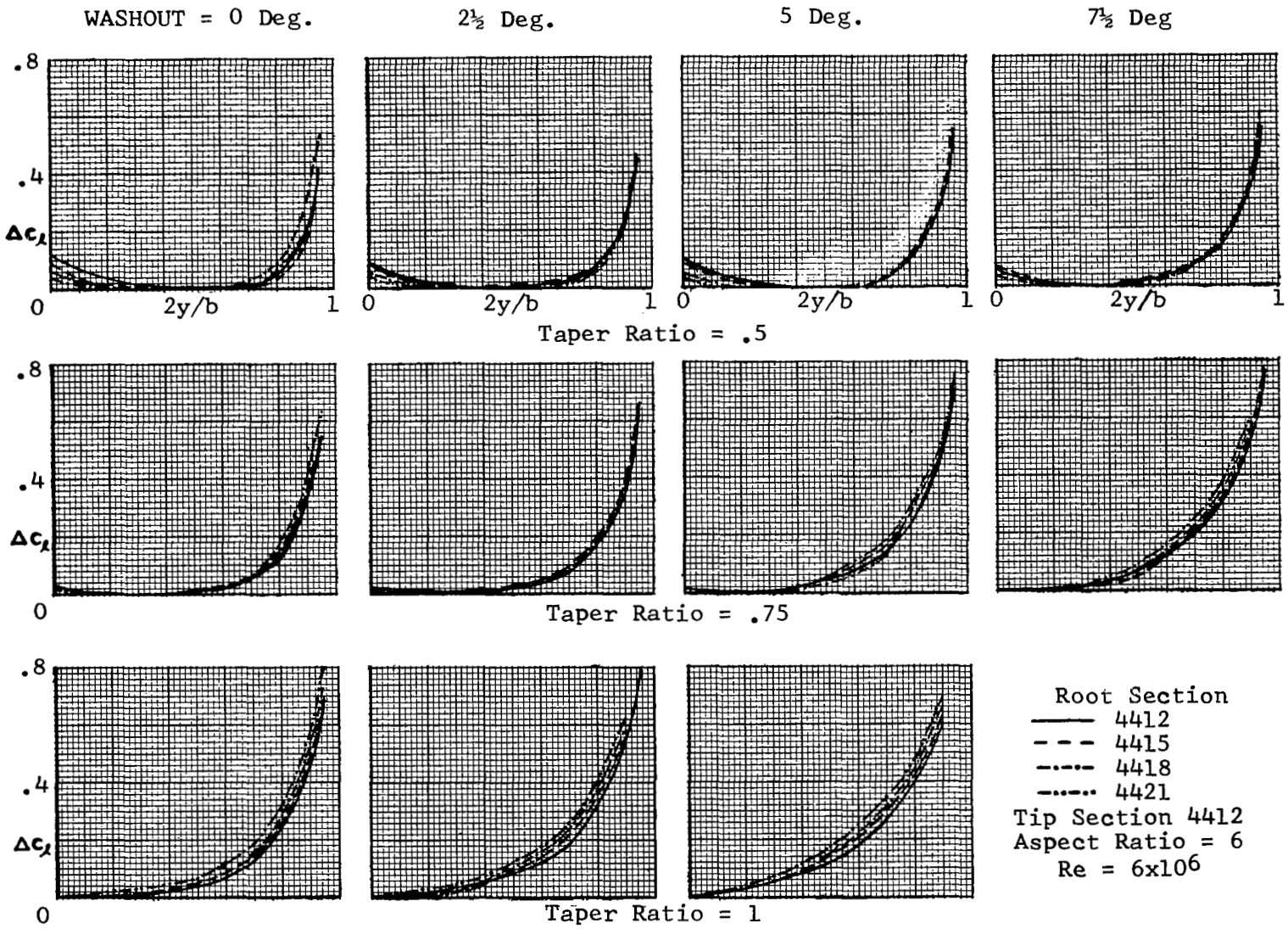

Figure 26. Continued

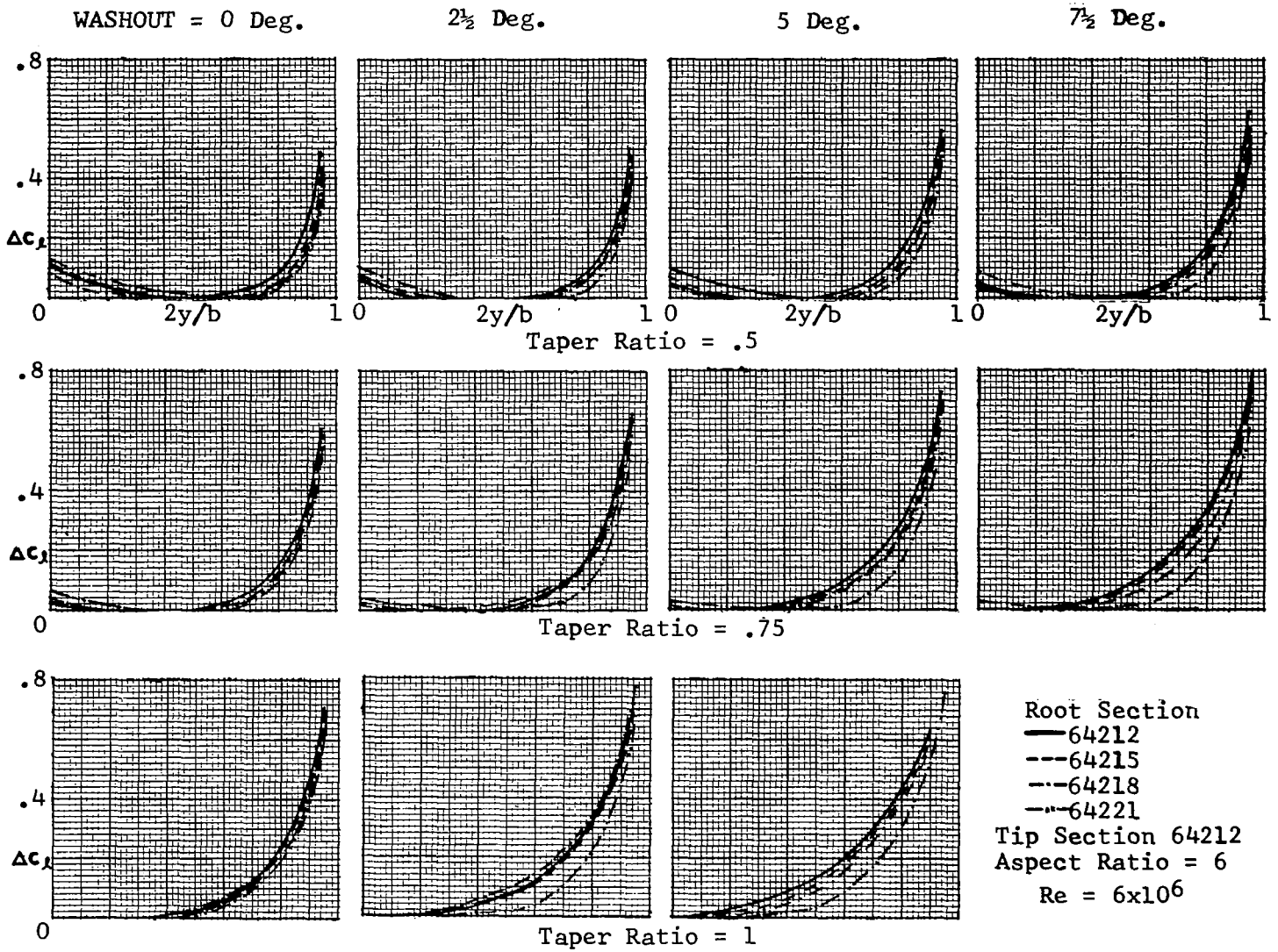

Figure 26. - Concluded

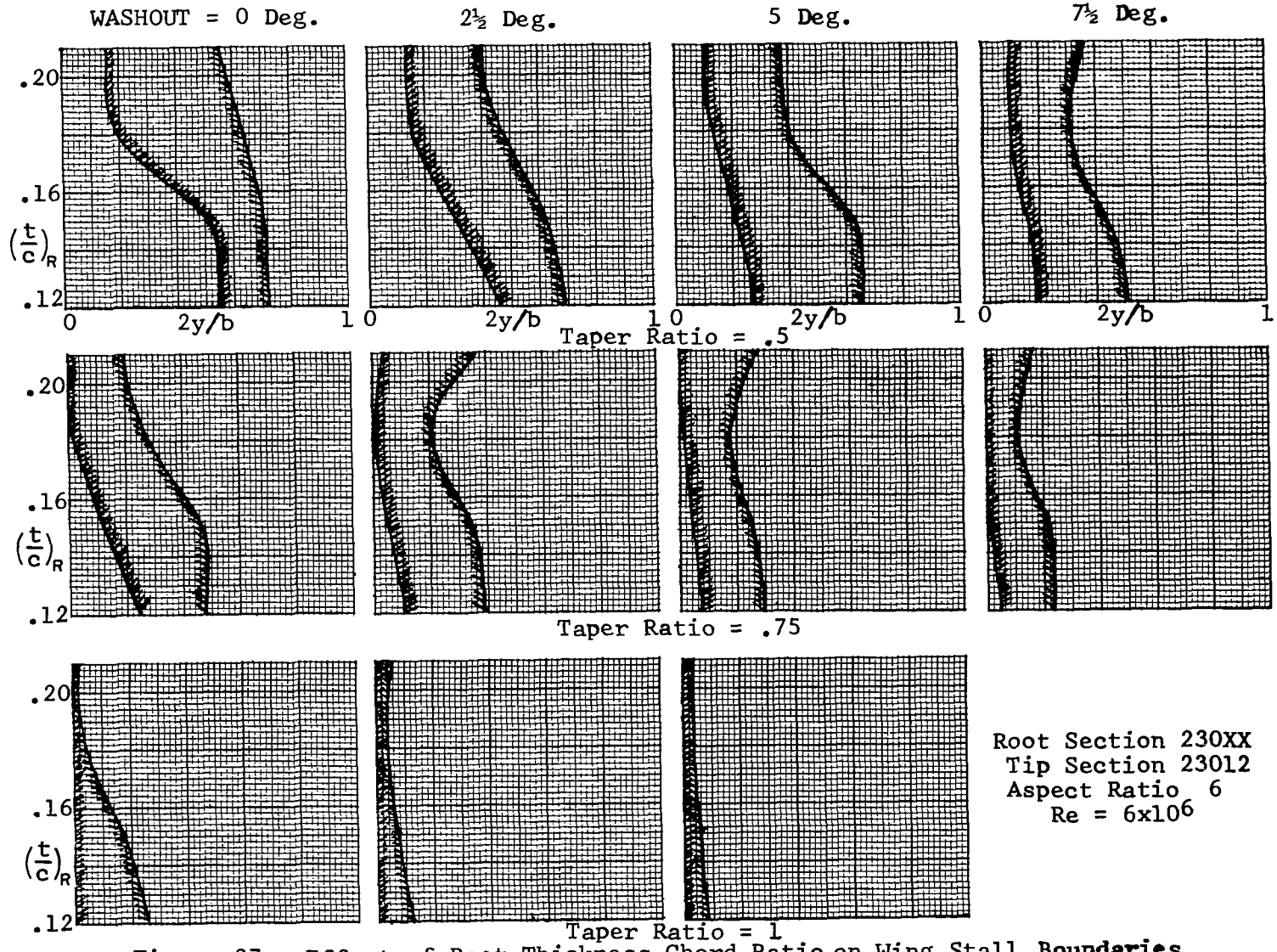

Figure 27. -Effect of Root Thickness-Chord Ratio on Wing Stall Boundaries

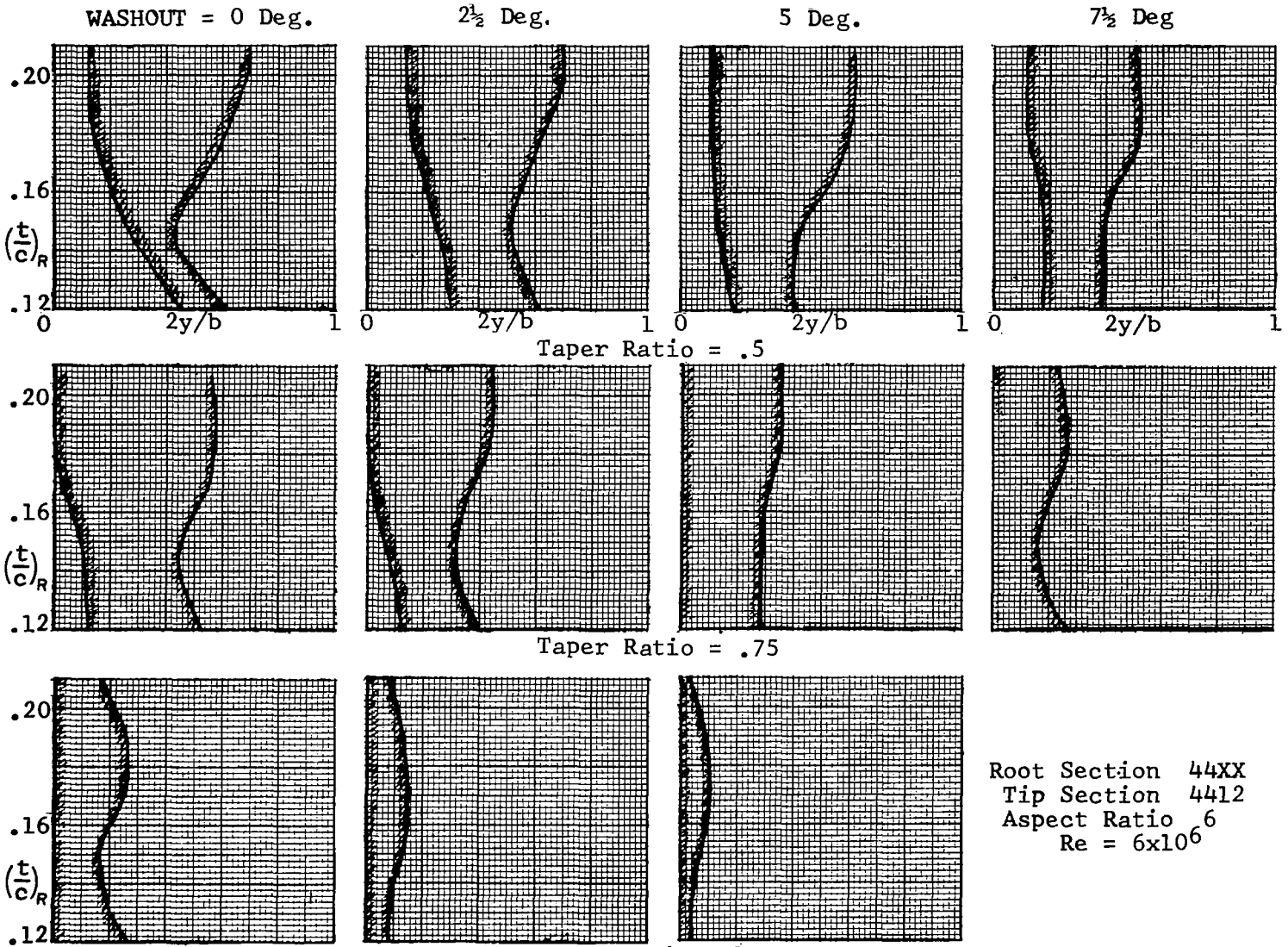

Figure 27. Continued

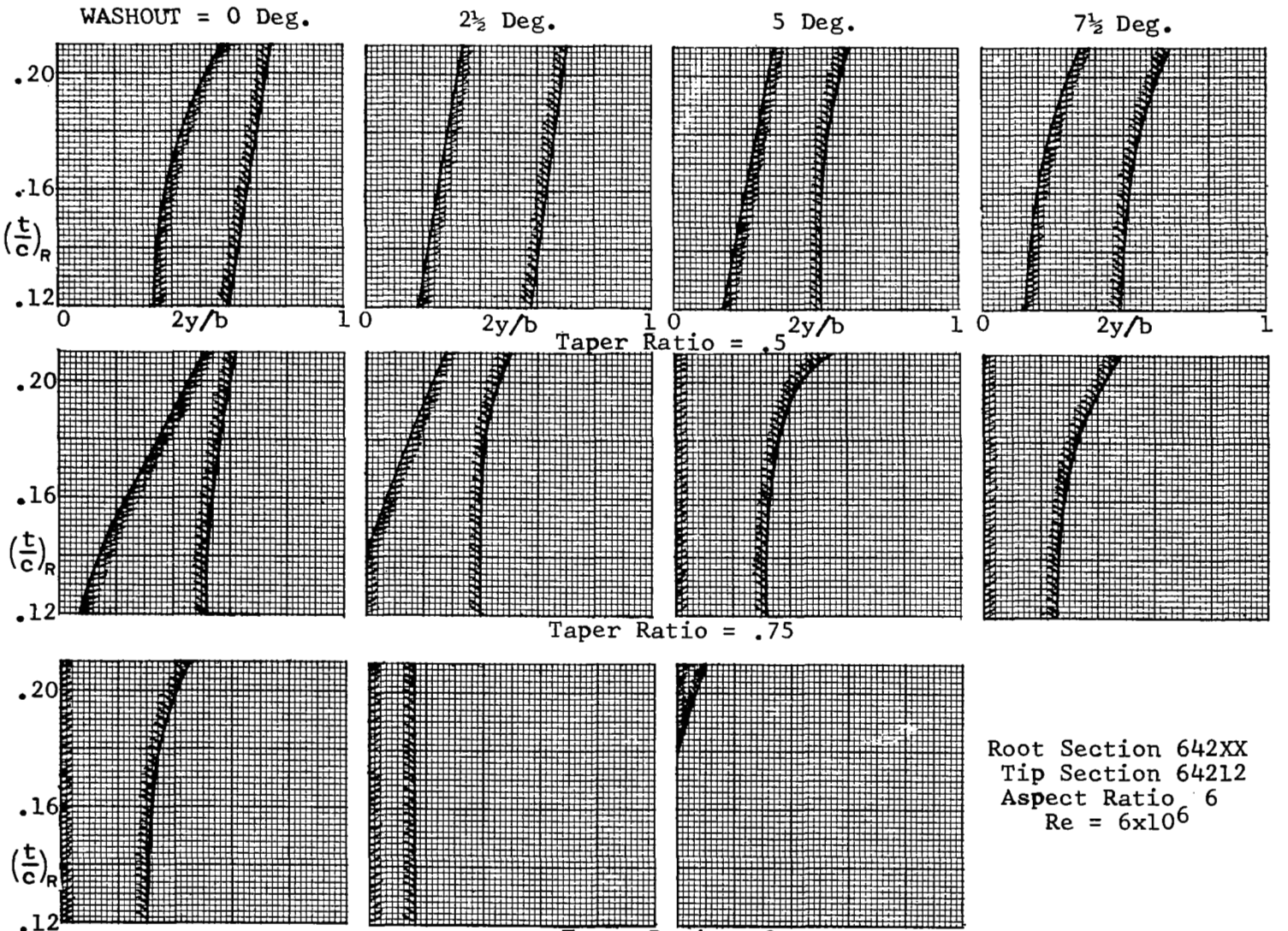

Figure 27. Concluded

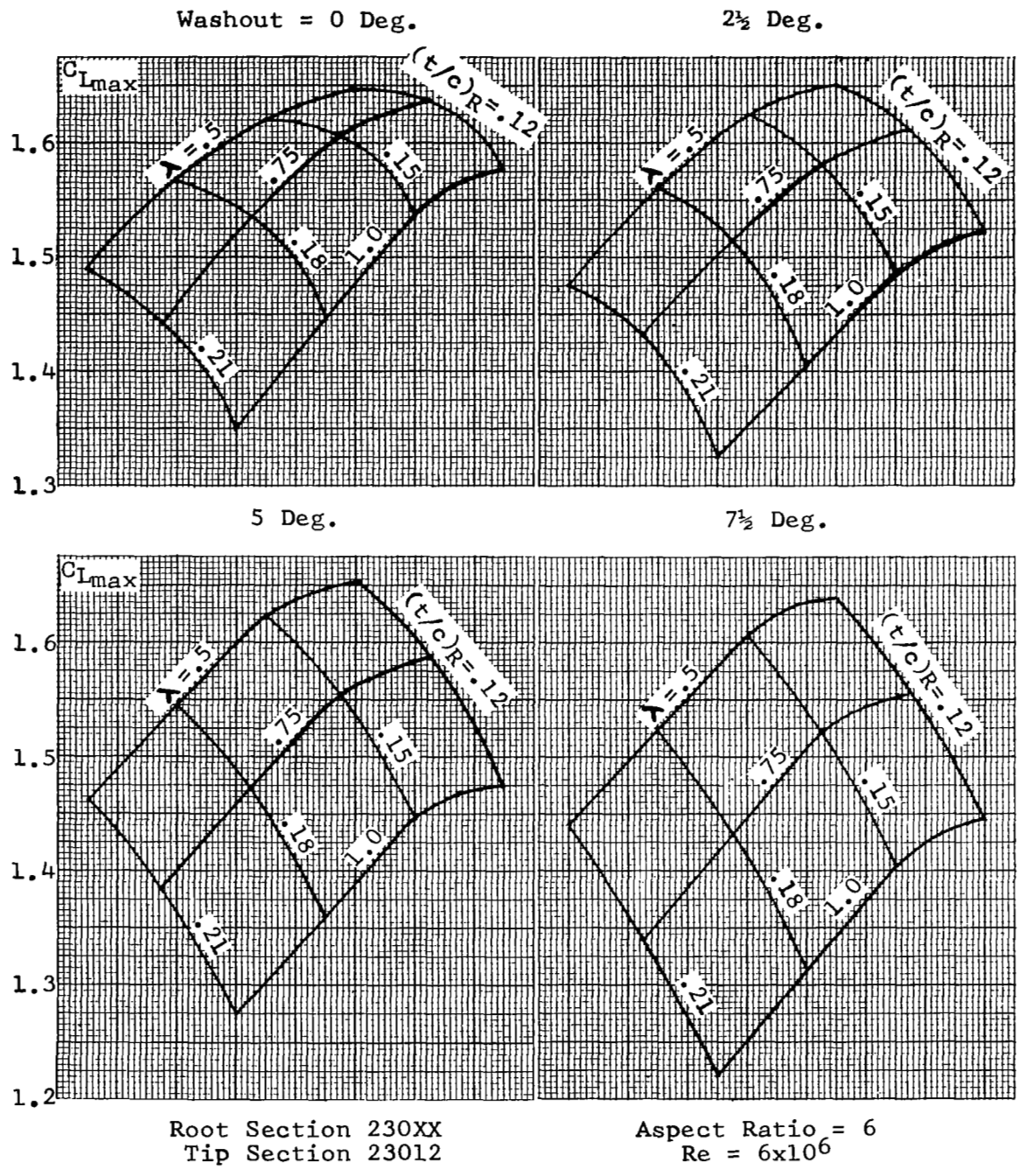

Figure 28. Effect of Root Thickness-Chord Ratio on $C_{L_{max}}$

Washout = 0 Deg.

2½ Deg.

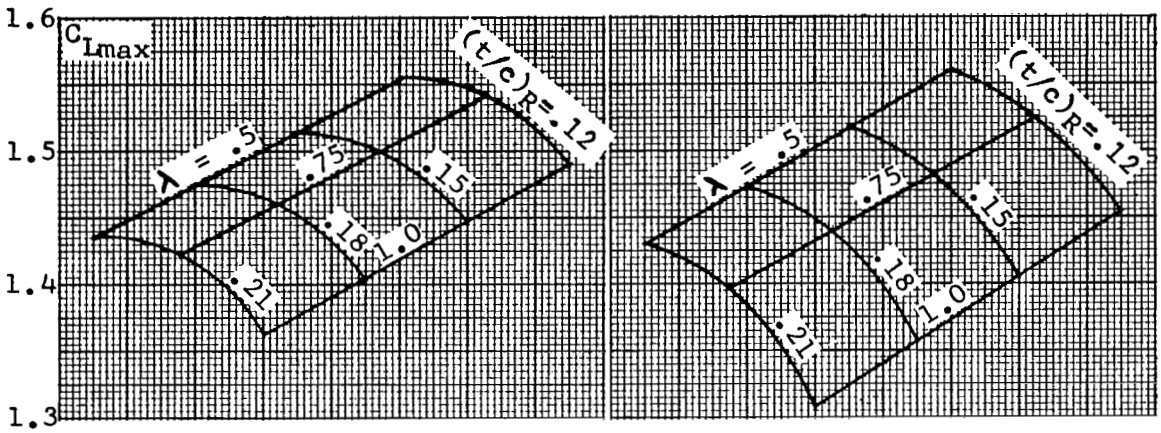

5 Deg.

7½ Deg.

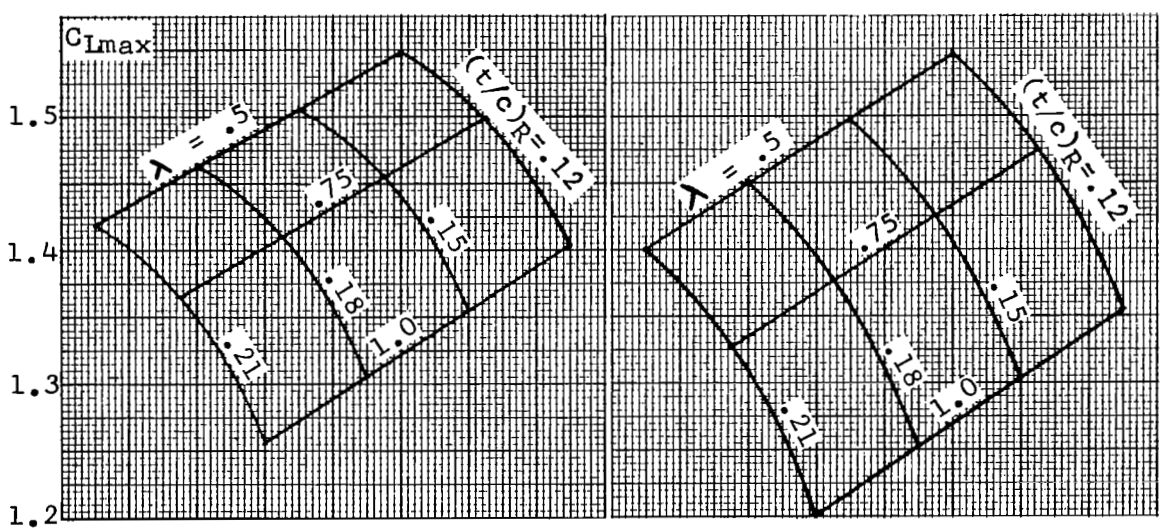

Root Section 44XX
Tip Section 4412

Aspect Ratio = 6
Re = 6×10^6

Figure 28. Continued

Washout = 0 Deg. $2\frac{1}{2}$ Deg.

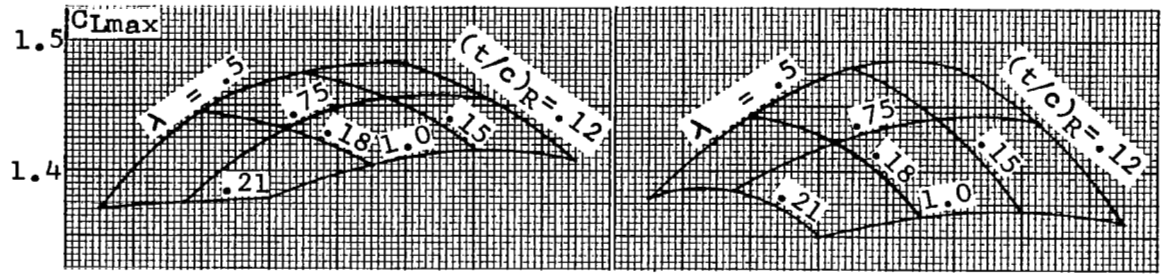

5 Deg. $7\frac{1}{2}$ Deg.

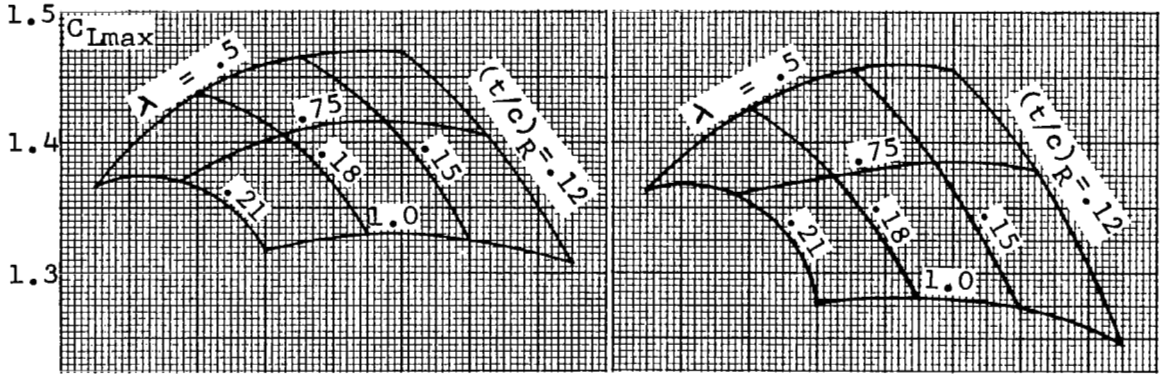

Root Section 642XX
Tip Section 64212

Aspect Ratio = 6
Re = 6×10^6

Figure 28. Concluded

smallest reduction in the value of maximum wing lift coefficient.

5.3.5 Effect of Tip Thickness-Chord Ratio

Figures 29 and 30 show the effects of tip thickness-chord ratio on wing stalling characteristics. The results are presented for a wing having a root thickness-chord ratio fixed at a constant value of 0.18 and tip thickness-chord ratios of 0.12 and 0.15. Limited computations were performed for tip thickness-chord ratio of 0.18 primarily for the purpose of establishing extrapolation trends for the variation of wing maximum lift coefficient.

Figures 29 and 30 indicate that the effect of increasing the tip thickness-chord ratio is to reduce the stall margins and the value of maximum wing lift coefficient. This is due to the fact that an increase in tip thickness-chord ratio results in reduced values of section maximum lift coefficient in the vicinity of the wing tip, thus yielding lower stall margins. Also, the reduction in the values of maximum wing lift coefficient is smaller than that due to increasing root thickness-chord ratio. This is because the major effect of changes in tip thickness is confined to the tip regions where the wing loading is least.

Although the effect of tip thickness-chord ratio on stall boundaries is not presented, it is expected to be similar to that of the root thickness-chord ratio discussed in the previous sub-section.

5.3.6 Effect of Flight Reynolds Number

Since the maximum lift characteristics of most airfoil sections are influenced by Reynolds number (see Figure 20) this parameter potentially represents an effective means of controlling overall wing stall behavior.

The effect of flight Reynolds number on stall margin distributions, stall boundaries and wing maximum lift coefficient is shown in Figures 31, 32 and 33, respectively. These figures indicate that for wings employing 230 and 44 series sections an increase in flight Reynolds number results in increased stall margins over the outboard wing station and a shift of stall boundaries towards the wing root. However, exactly opposite trends are indicated for wings employing 642 airfoil sections. An explanation of this behavior can again be obtained using the results of Figure 20.

It can be noted from this figure that for the 230 and 44 series airfoils the rate of increase of maximum lift coefficient with Reynolds number is larger for the tip sections ($t/c = 0.12$) than that for the root sections ($t/c = 0.18$). This produces larger stall margins at the outboard (thinner) wing sections with increase in flight Reynolds number.

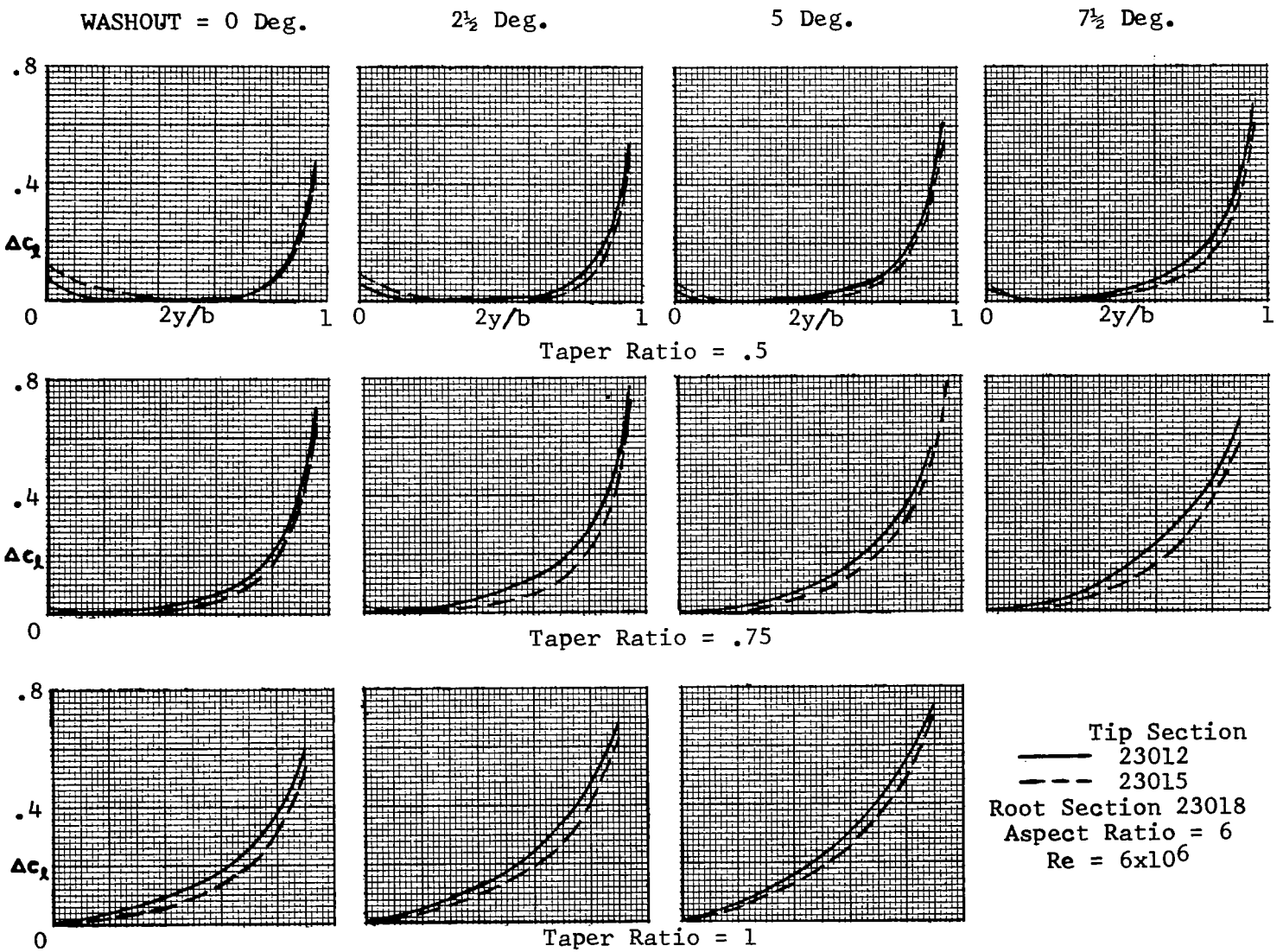

Figure 29. Effect of Tip Thickness-Chord Ratio on Stall Margin Distribution.

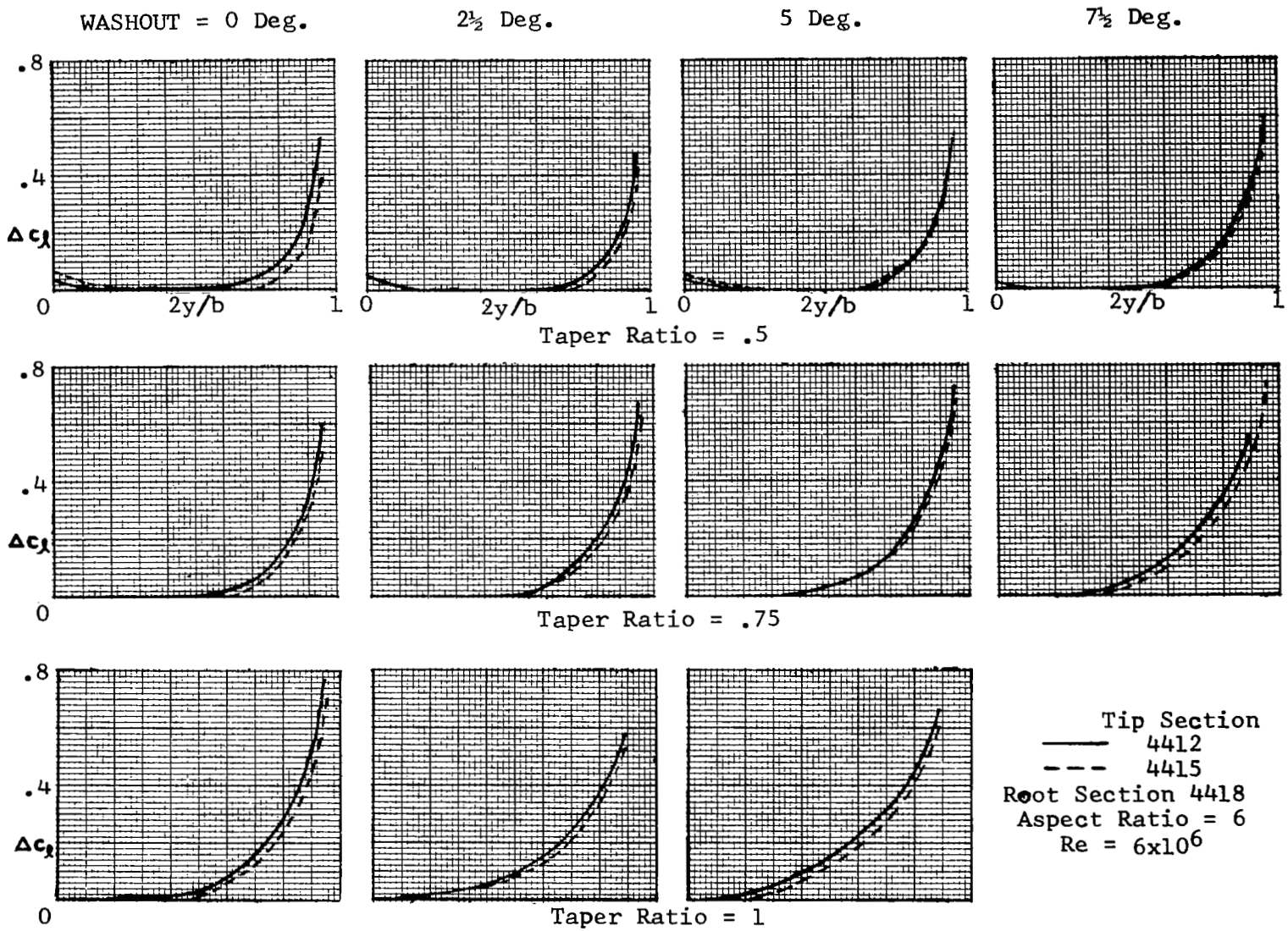

Figure 29. Continued

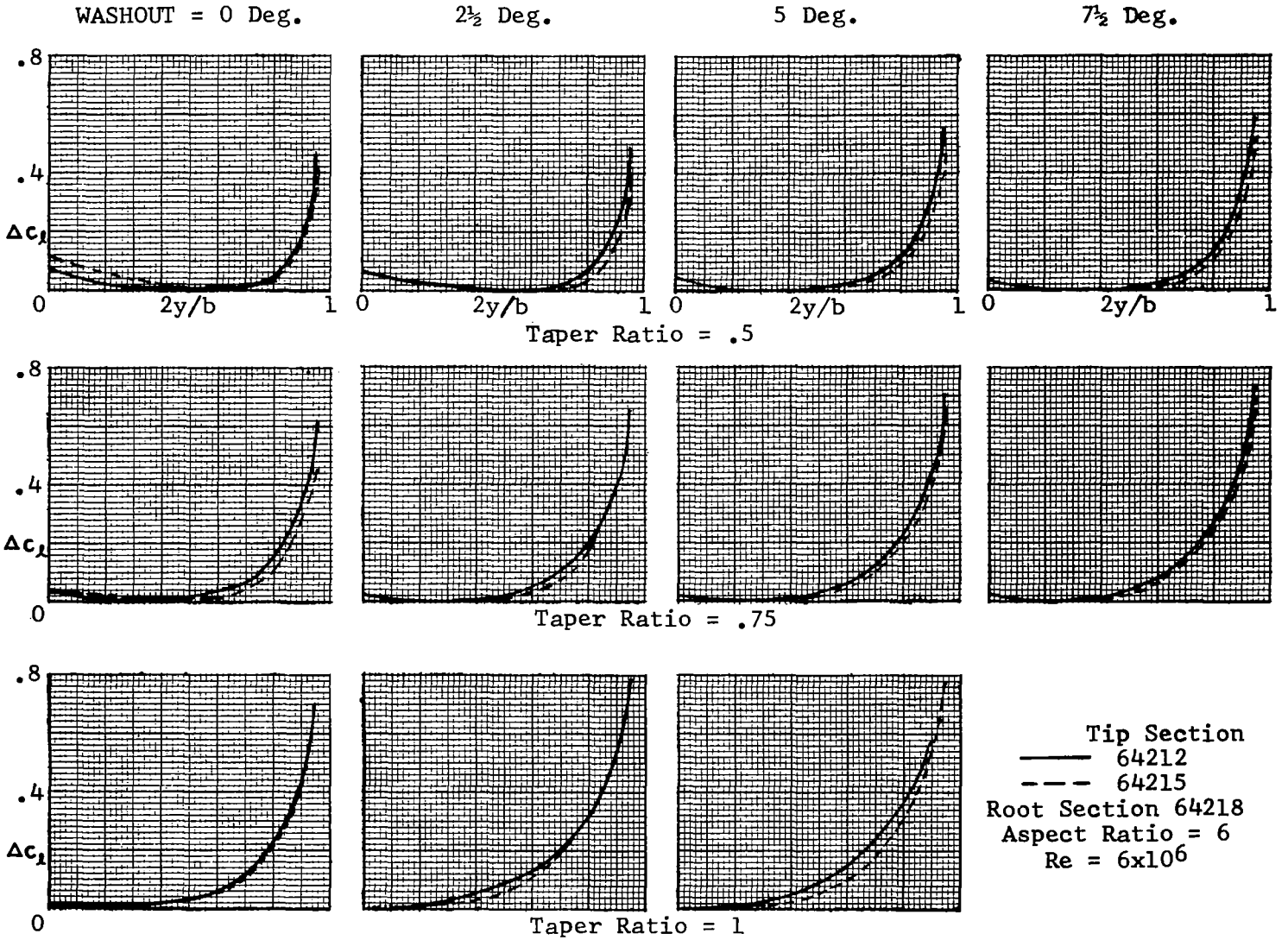

Figure 29. Concluded

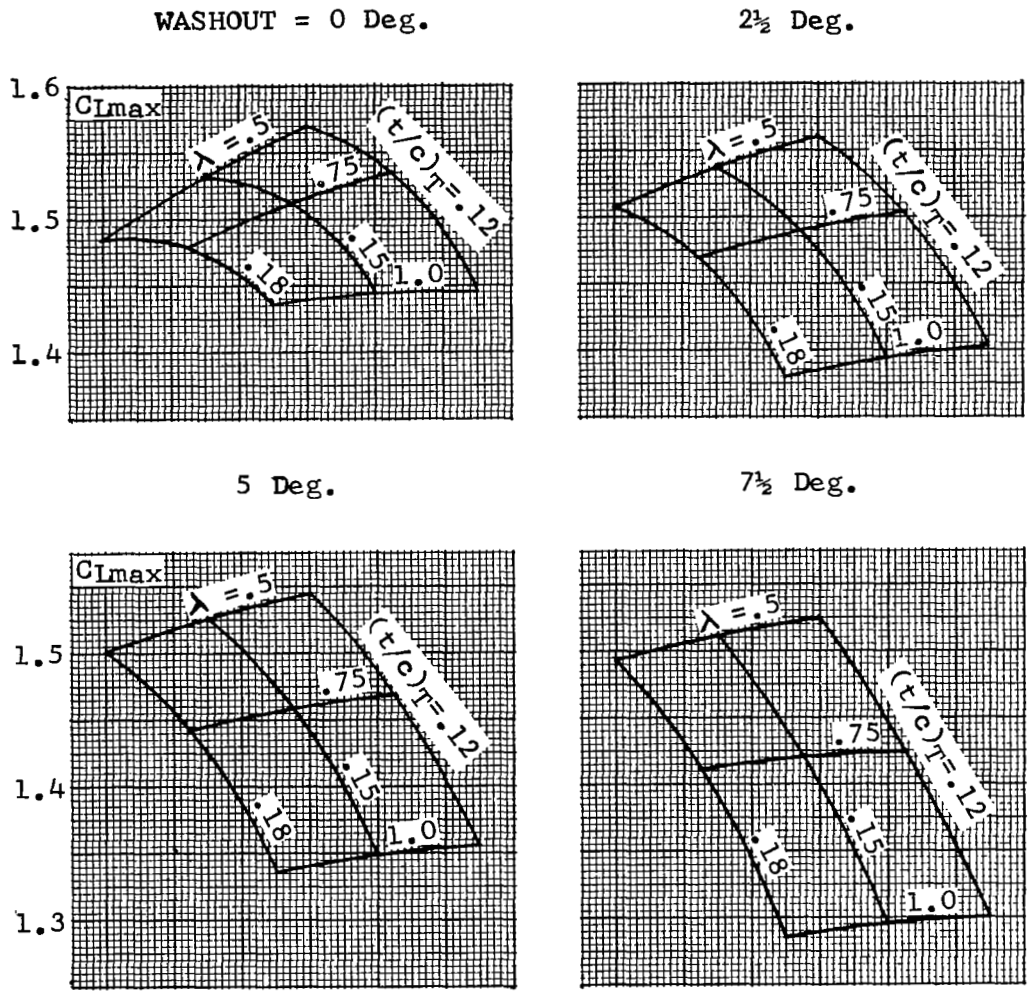

Figure 30. - Effect of Tip Thickness-Chord Ratio on $C_{L_{max}}$

WASHOUT = 0 Deg.

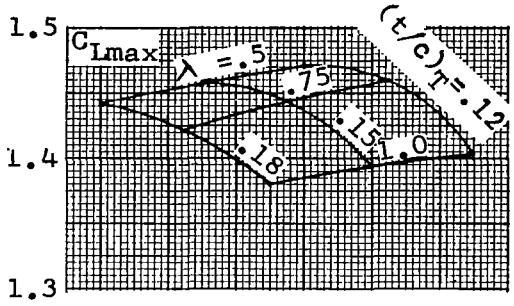

2½ Deg.

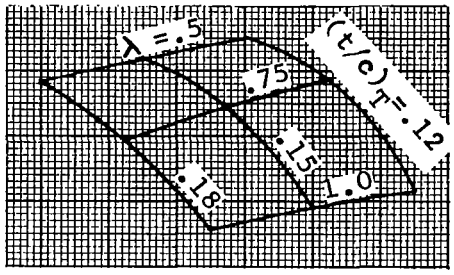

5 Deg.

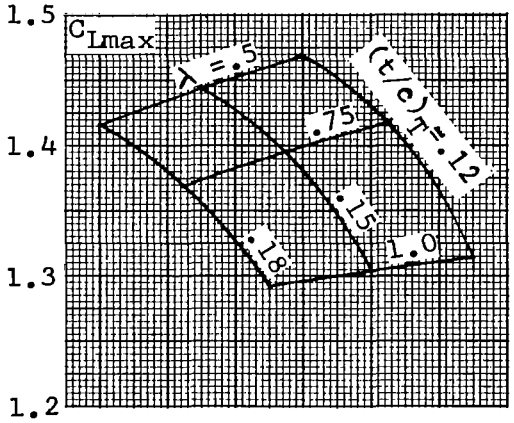

7½ Deg.

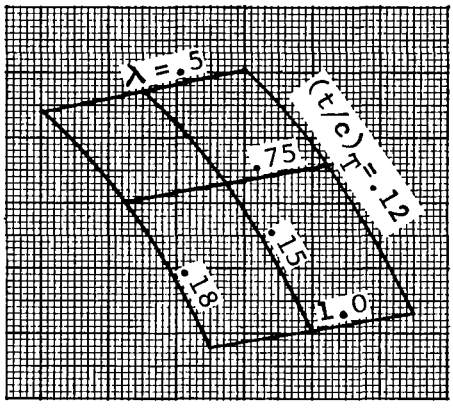

Root Section 4418
Tip Section 44XX

Aspect Ratio = 6
Re = $6X10^6$

Figure 30. Continued

WASHOUT = 0 Deg.

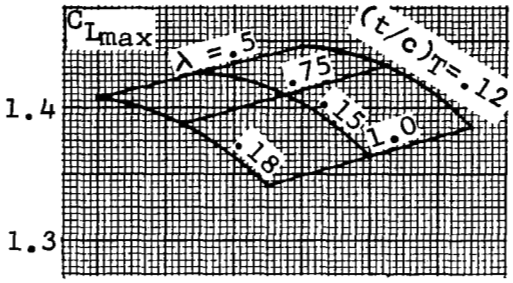

2½ Deg.

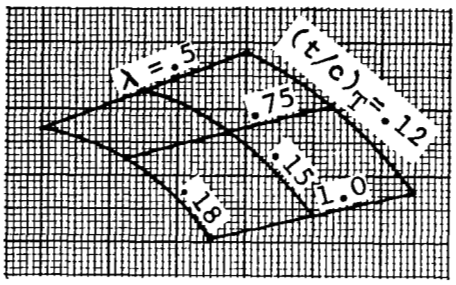

5 Deg.

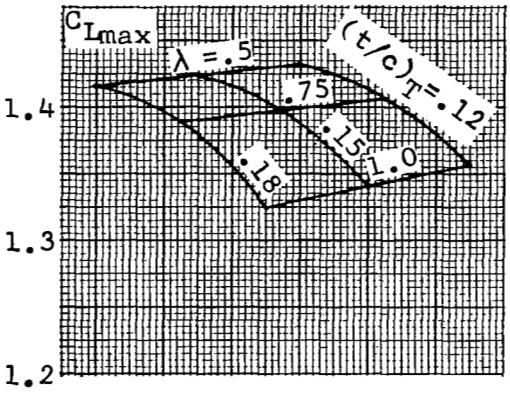

7½ Deg.

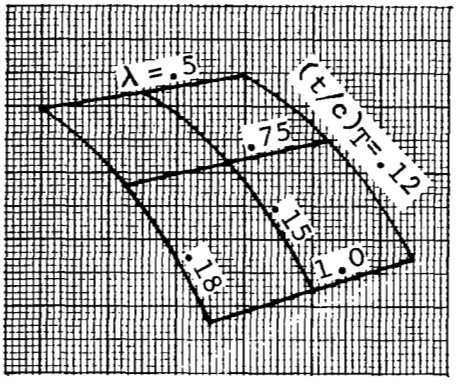

Root Section 64218
Tip Section 642XX

Aspect Ratio = 6
Re = 6×10^6

Figure 30. Concluded

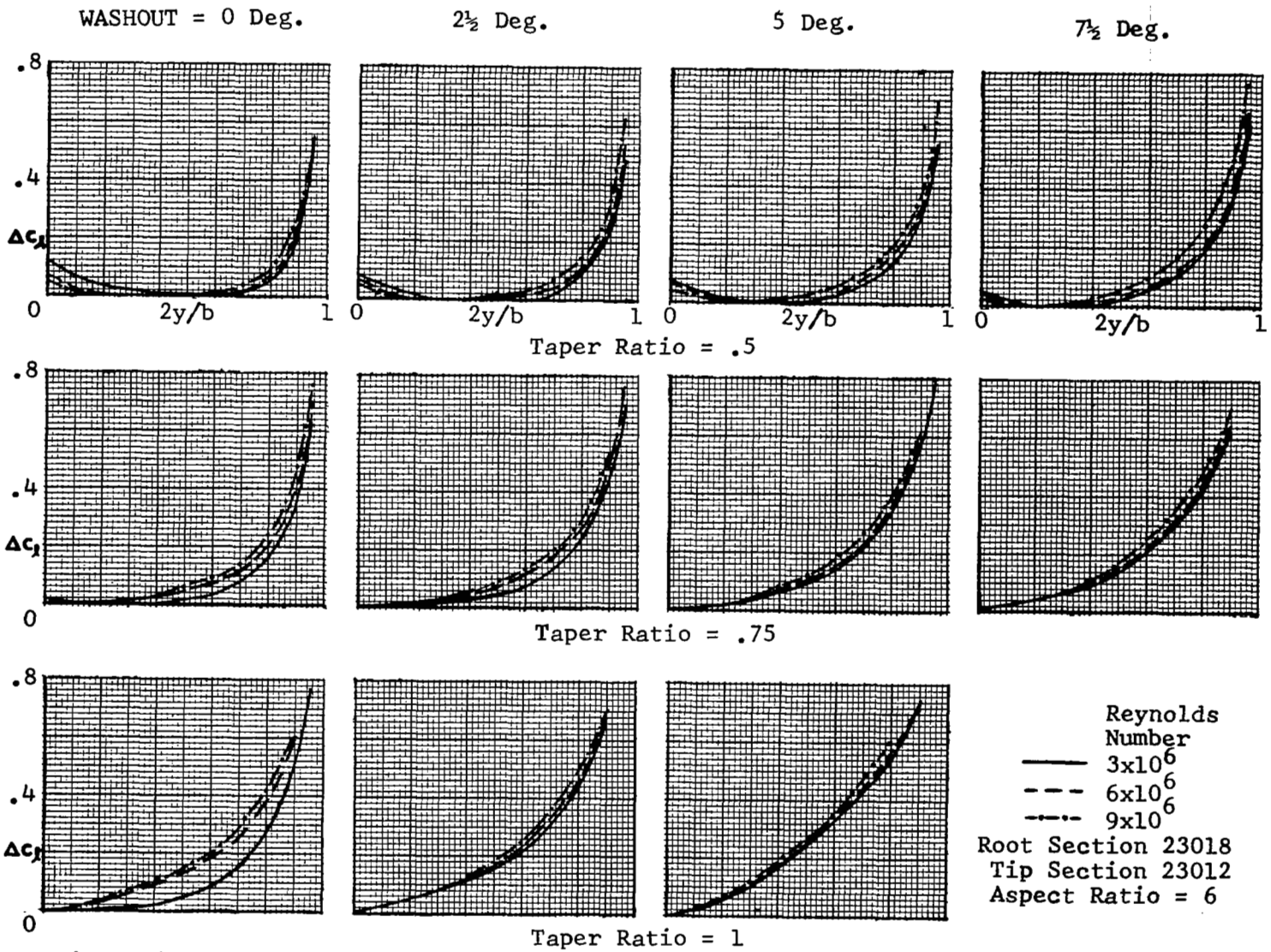

Figure 31. Effect of Reynolds Number on Stall Margin Distribution.

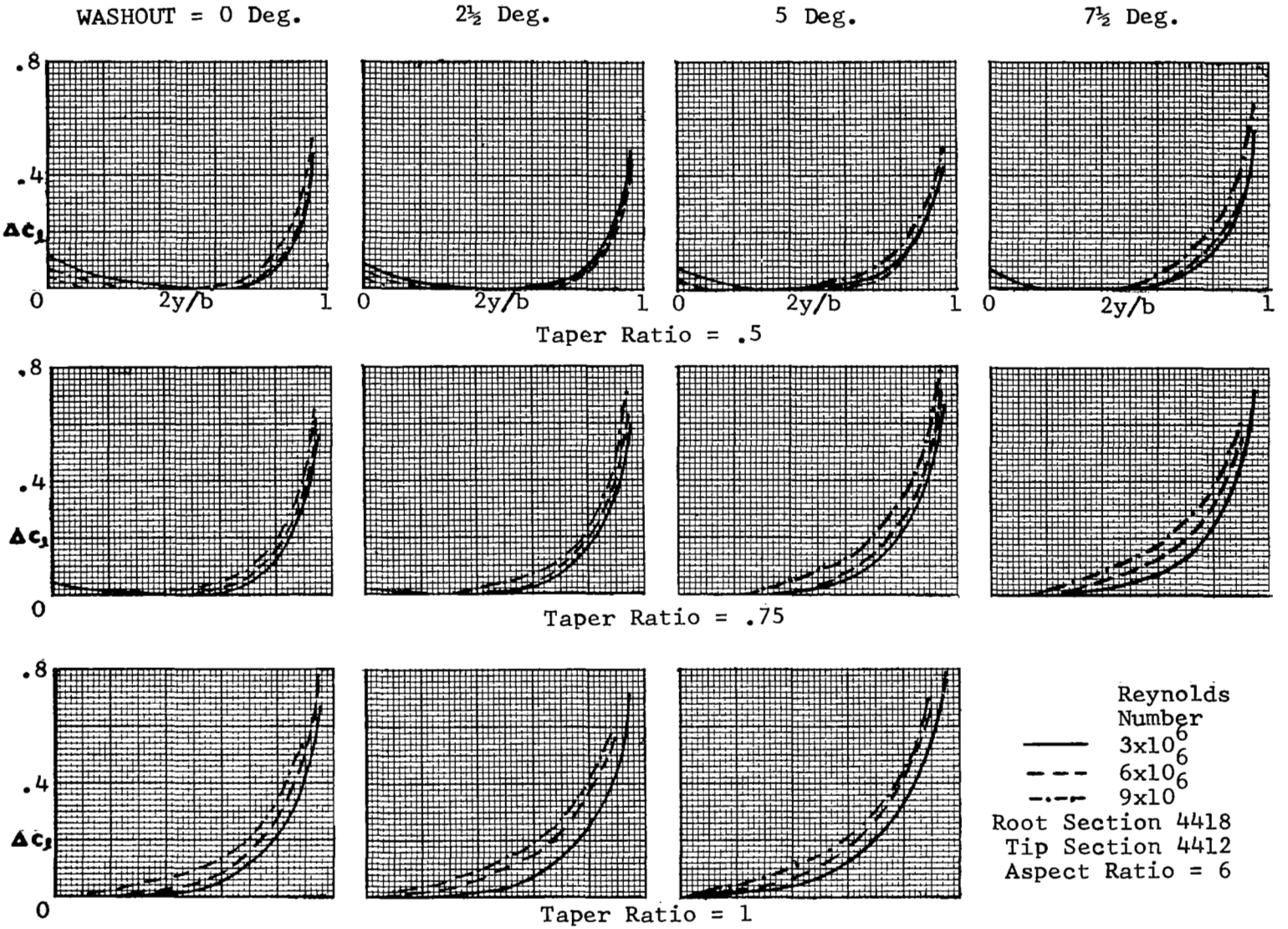

Figure 31. Continued

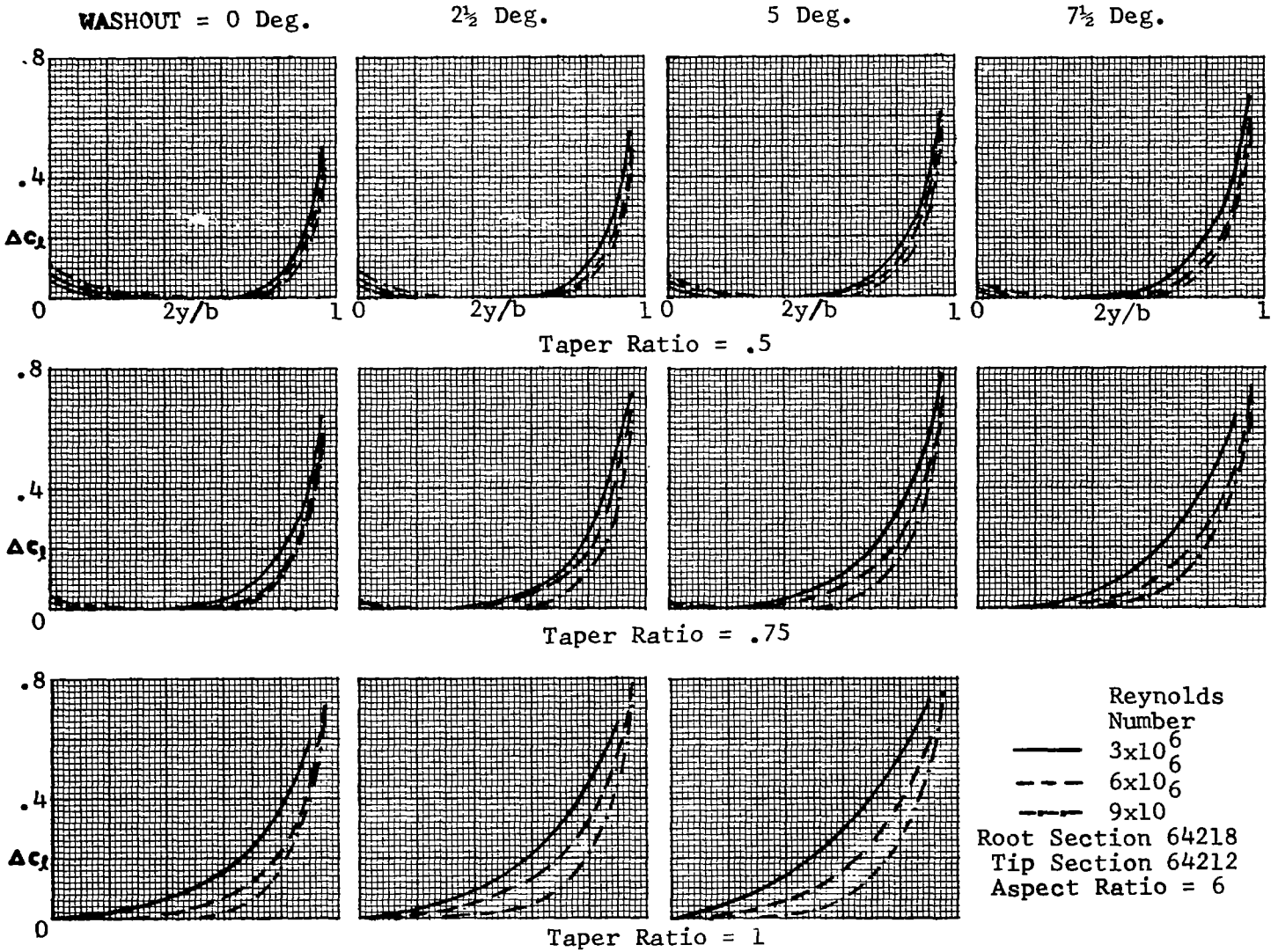

Figure 31. Concluded

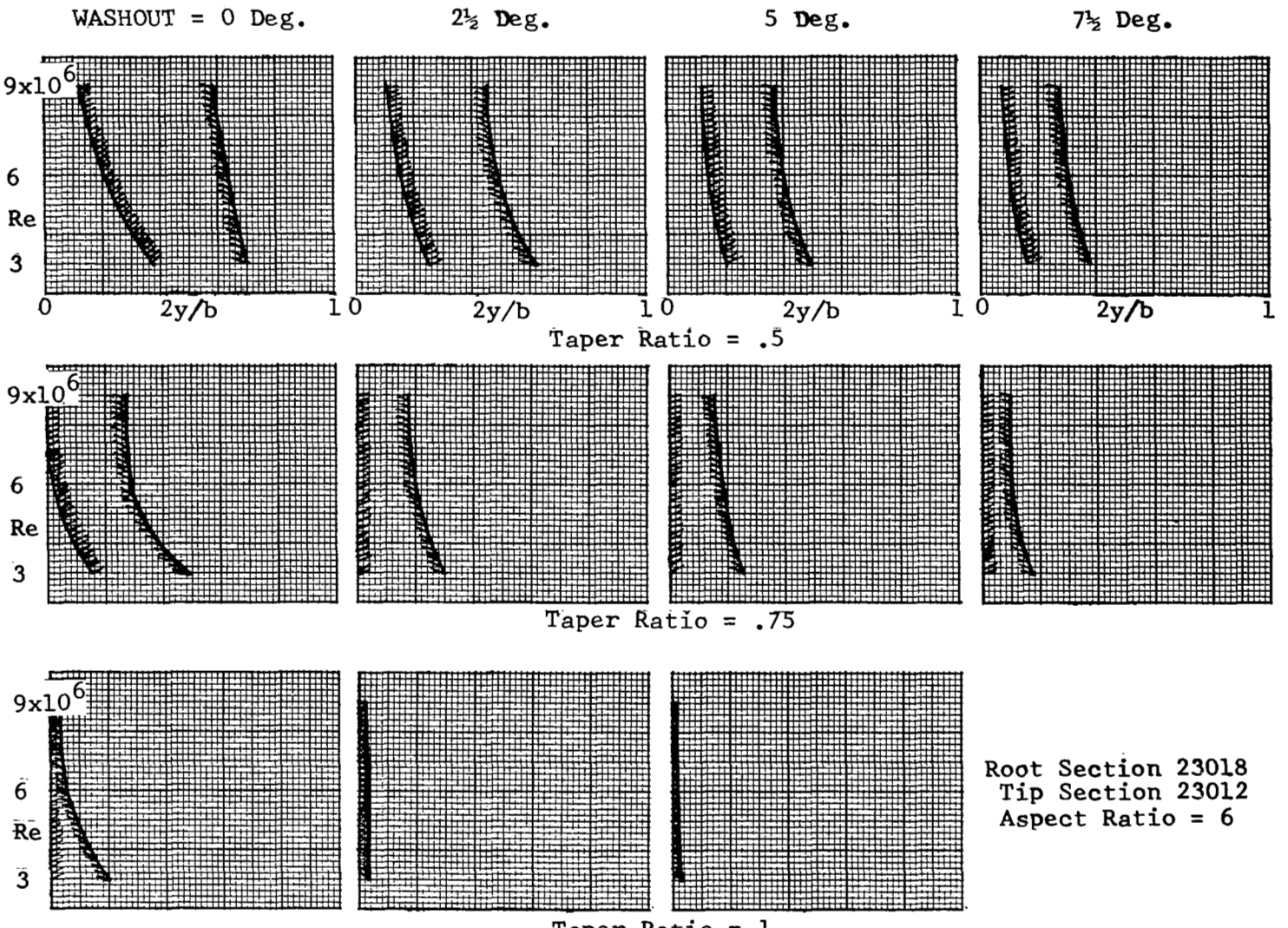

Figure 32. Effect of Reynolds Number on Wing Stall Pattern

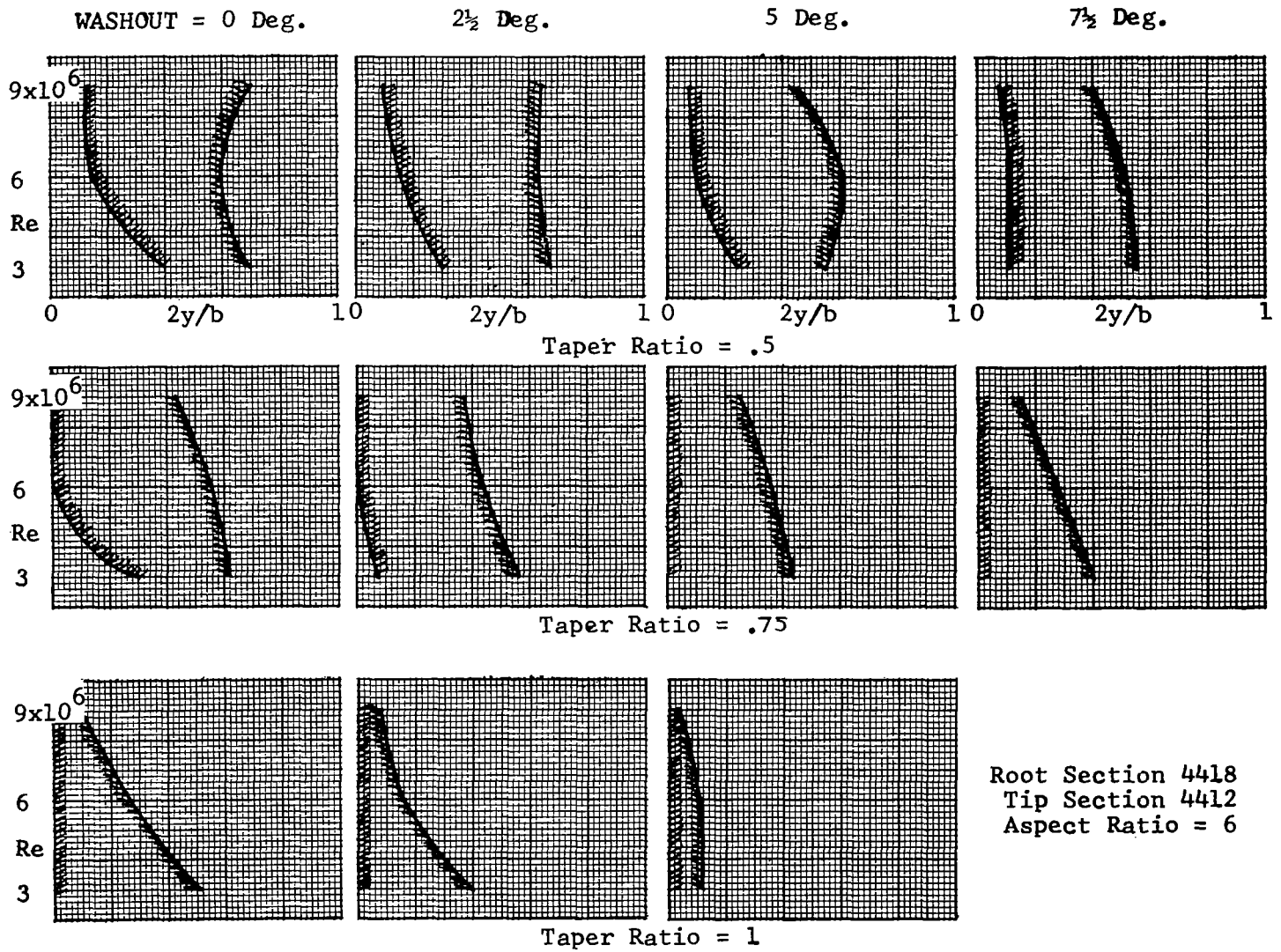

Figure 32. Continued

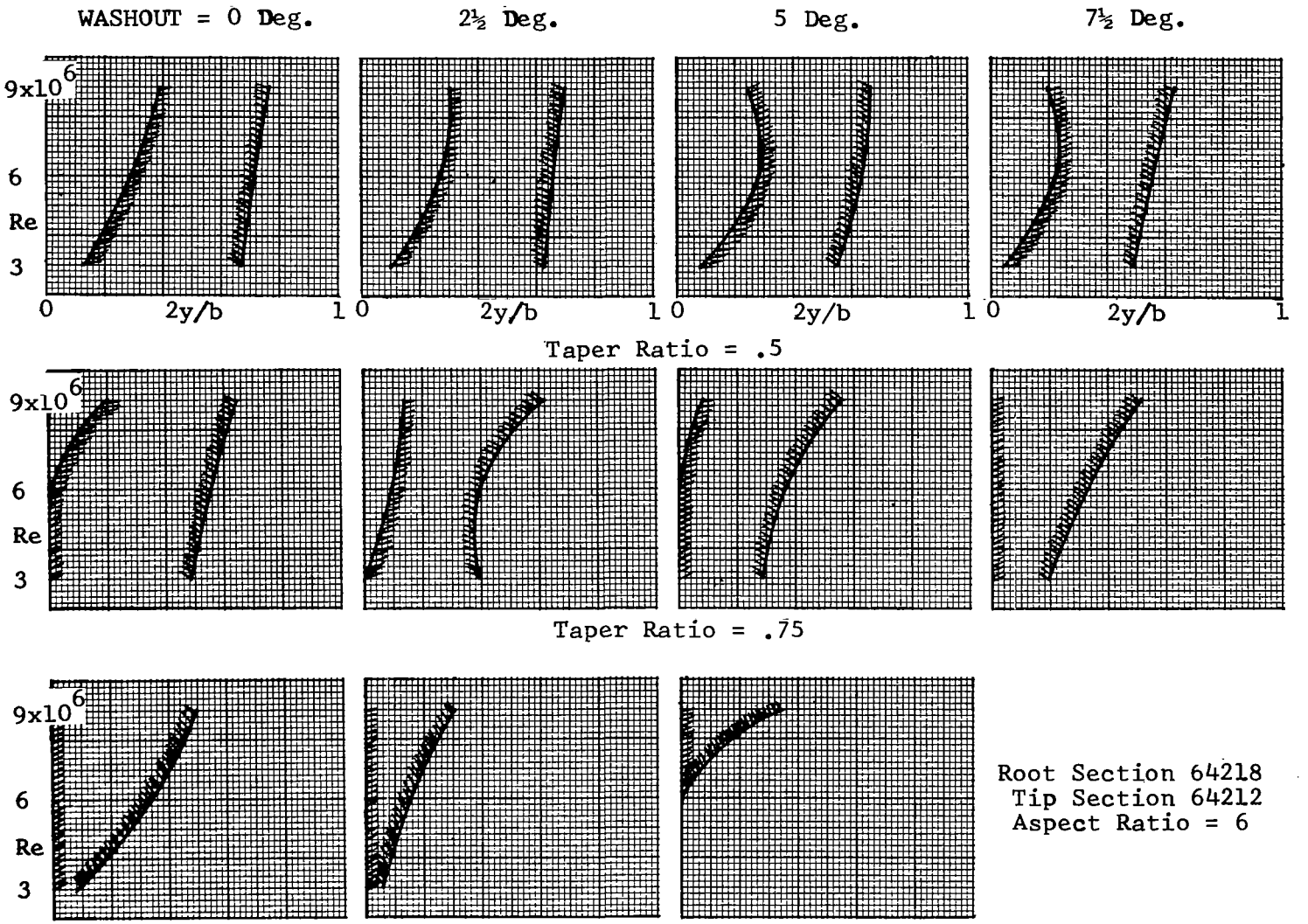

Figure 32. Concluded

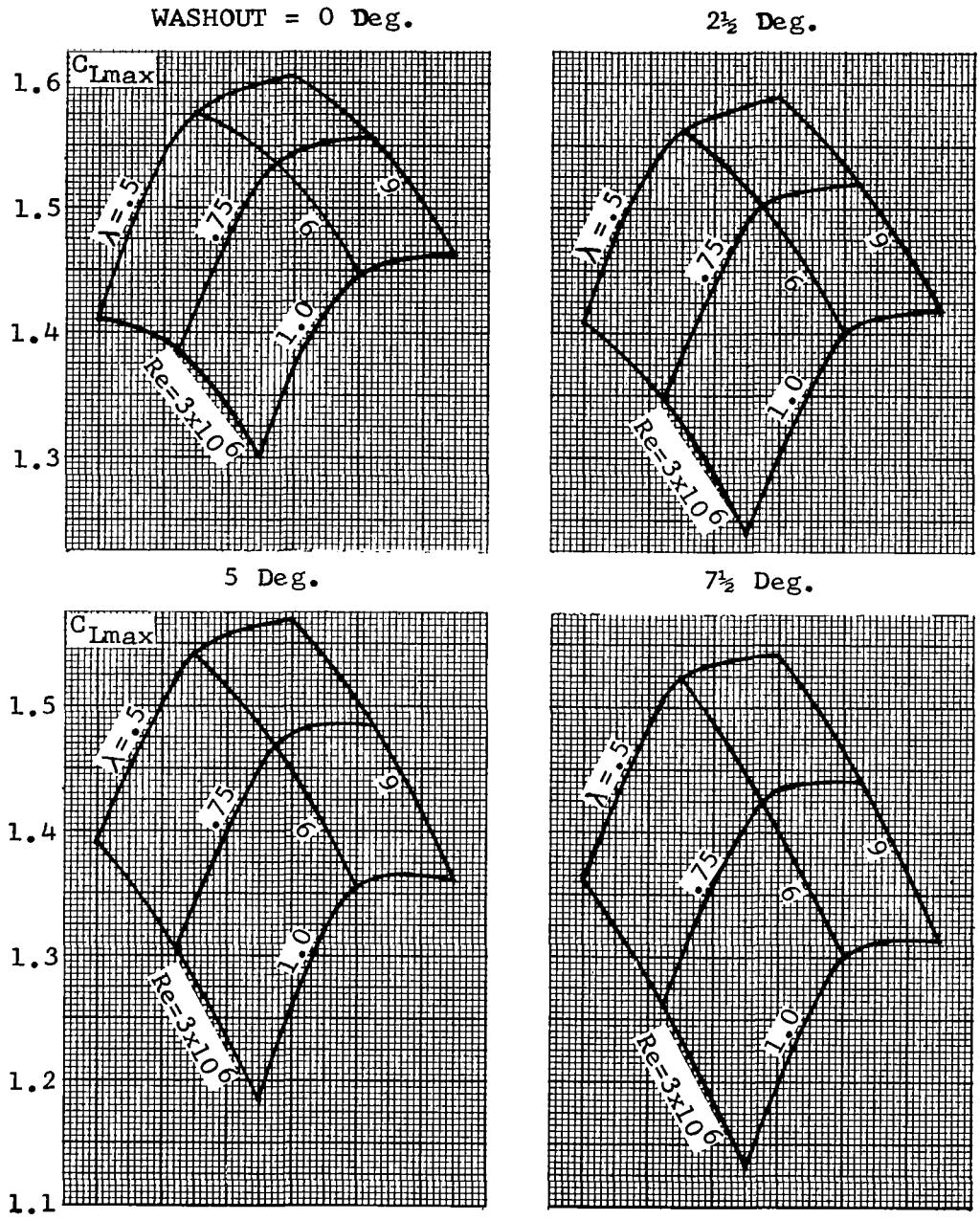

Root Section 23018 Tip Section 23012 Aspect Ratio = 6

Figure 33. Effect of Reynolds Number on C_{Lmax}

WASHOUT = 0 Deg.

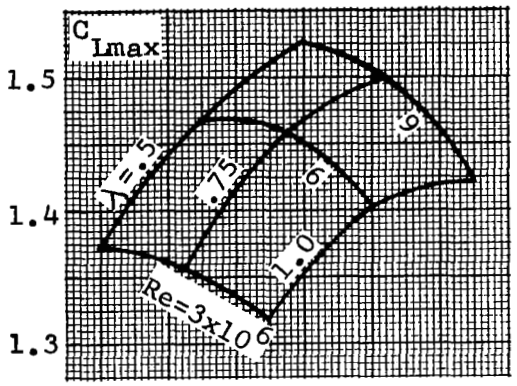

2½ Deg.

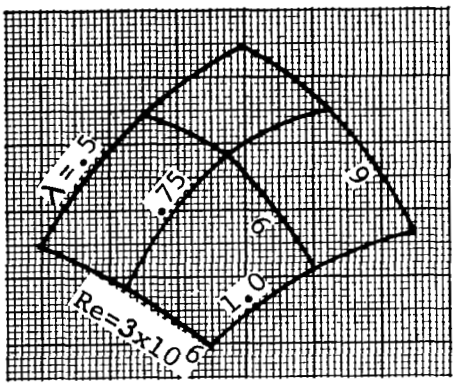

5 Deg.

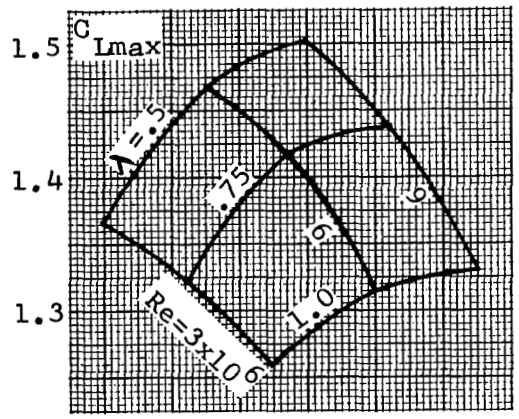

7½ Deg.

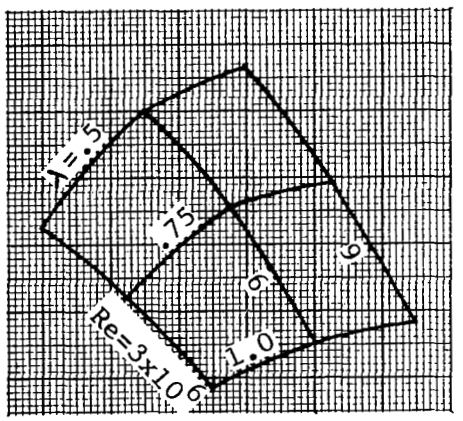

Root Section 4418 Tip Section 4412 Aspect Ratio = 6

Figure 33. Continued

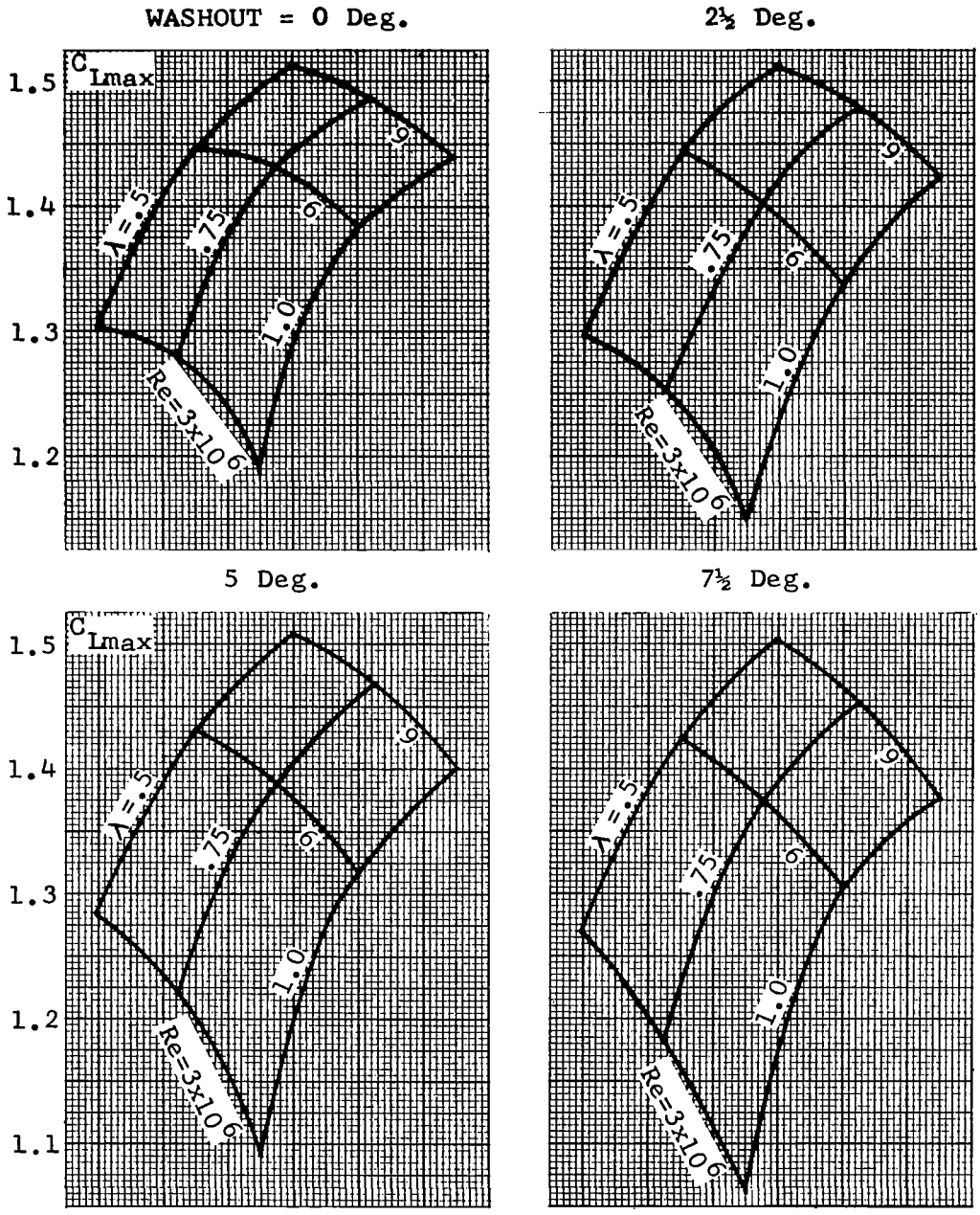

Root Section 64218 Tip Section 64212 Aspect Ratio = 6

Figure 33. Concluded

However, for the 642 series sections Figure 20 indicates the opposite effect, namely that the rate of increase of maximum section lift coefficient with Reynolds number is much larger for the inboard sections (t/c = 0.18) than that for the outboard sections (t/c = 0.12). This produces a spanwise variation of maximum lift coefficient which has an increasingly downward slope toward the wing tips and, since the value of local lift coefficient at any wing section increases with Reynolds number, the stall margins at the outboard sections will be reduced.

The effect of Reynolds number on wing maximum lift coefficient shows the expected increase with increasing Reynolds number. For the 230 series wing the maximum lift coefficient increases almost linearly with Reynolds number between 3 and 6 million, but with a further increase to 9 million the rate of increase is reduced. This trend is predictable from the section characteristics where it can be seen that the greatest changes in section maximum lift coefficient occurs below Reynolds number of 6×10^6. For the wing series 44 and 642 the variation of maximum wing lift coefficient with Reynolds number in the range of 6 to 9 million is more linear, again reflecting the trend of the airfoil section characteristics

5.3.7 Effect of Wing Camber

The effect of a linear root-to-tip increase in wing camber on the stall margins is shown in Figure 34 for three values of taper ratio, three Reynolds numbers and zero wing washout. The results are compared with those for a constant camber. The camber variation chosen was 64218 root section and 64412 tip section.

As can be seen from this figure the particular camber variation chosen is not very effective in changing the stall margins on the outboard sections of the wing. This ineffectiveness is attributed, in part, to the particular choice of a linear variation of camber. It is expected that a larger increase in stall margins would be obtained for a different combination of camber and wing airfoil sections.

5.3.8 Effect of Fuselage

Figure 35 presents the computer results for a wing alone and a high wing mounted on a fuselage of elliptical cross-section. The wing has an aspect ratio of 6 (based on the gross wing area) with zero washout, and root and tip thickness ratios of 0.18 and 0.12, respectively.

The computations were performed for taper ratios of 0.5, 0.75 and 1.0 and wing-fuselage settings of 0°, 2° and 4°. The spanwise distributions of lift coefficient at stall were found

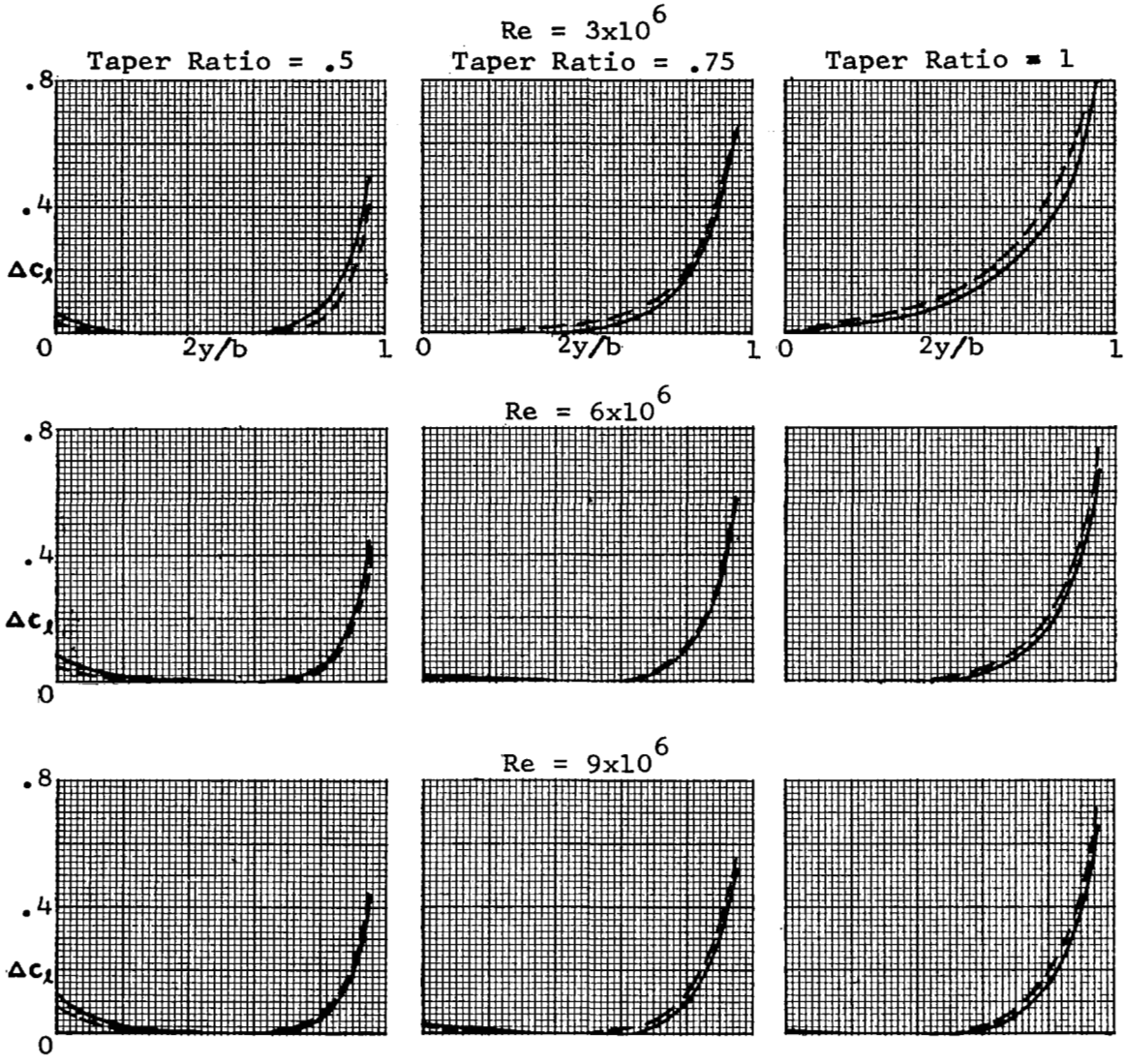

Figure 34. -Effect of Wing Camber on Stall Margin Distribution.

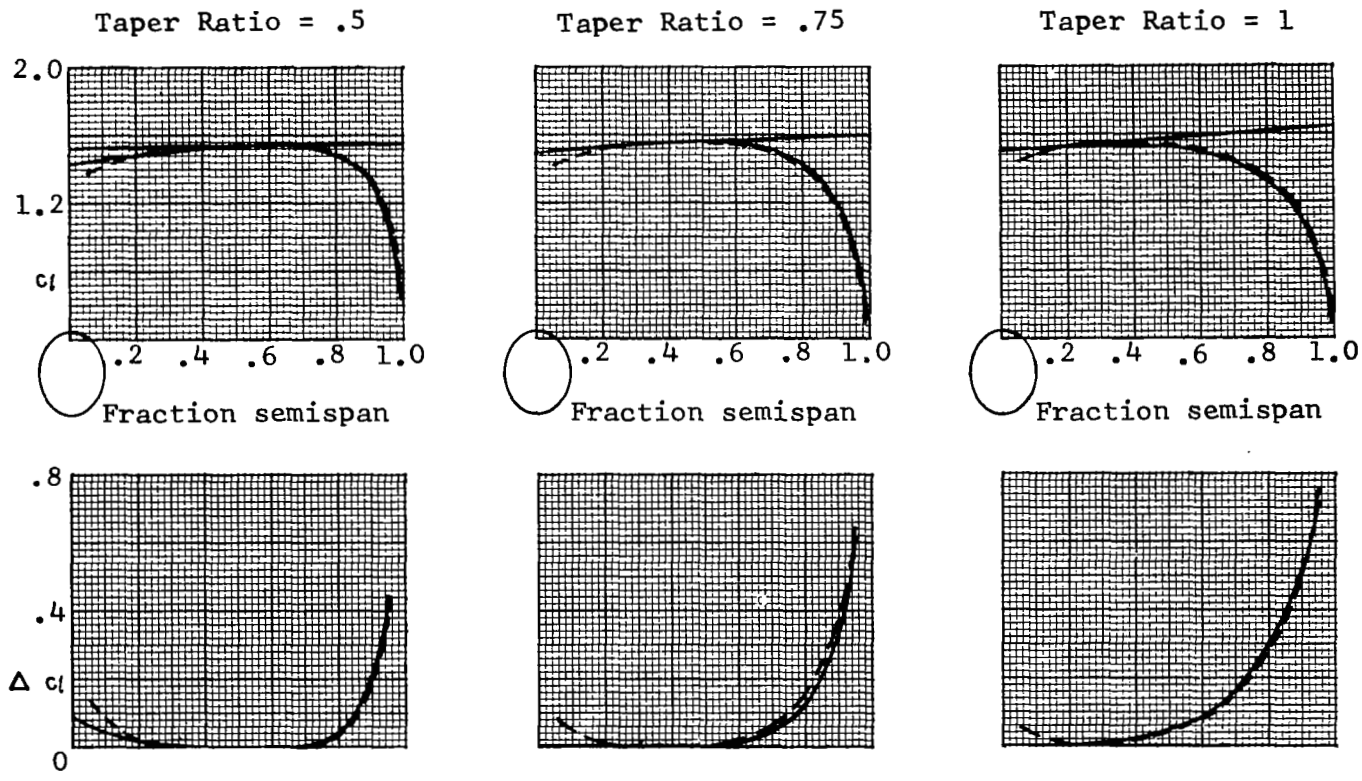

Figure 35. - Effect of Fuselage.

to be nearly identical for all the wing-fuselage settings considered, thus resulting in the value of maximum wing lift coefficient ($C_{L\,max}$) being unaffected by the wing-fuselage incidence. The effect of positive wing-fuselage setting is merely to reduce the body angle of attack at which the stall first occurs. This reduction is approximately equal to the wing-fuselage incidence.

Figure 35 indicates that for the high wing configuration shown, the effect of fuselage is to slightly reduce the wing loading specially in the region close to the fuselage. A similar reduction is indicated by the experimental results of Reference 50 where the lift distribution on a high wing circular fuselage combination is presented.

5.3.9 Effect of Partial Span Flap Deflection

Figure 36 shows the effects of flap deflection and flap span on the stalling characteristics of a rectangular wing with 64-series sections operating at a flight Reynolds number of 6 million. The results are presented for the wing having a 20% chord split flap, deflected 60° and extending over 45%, 60% and 70% of the wing span.

It can be noted from this figure that, the deflection of a part-span flap lowers the stall margins on the outboard portion of the wing and causes the wing to stall further outboard. Furthermore, for the range considered, increasing flap span moves the stall boundaries inboard and increases wing maximum lift coefficient. It should be noted that the stall point on a flapped wing does not always occur at the flap end as would be predicted by simpler analytical methods than the one used in this program.

A discussion of the above results and their influence on the design of an airplane for good stall characteristics is given in Section 7.

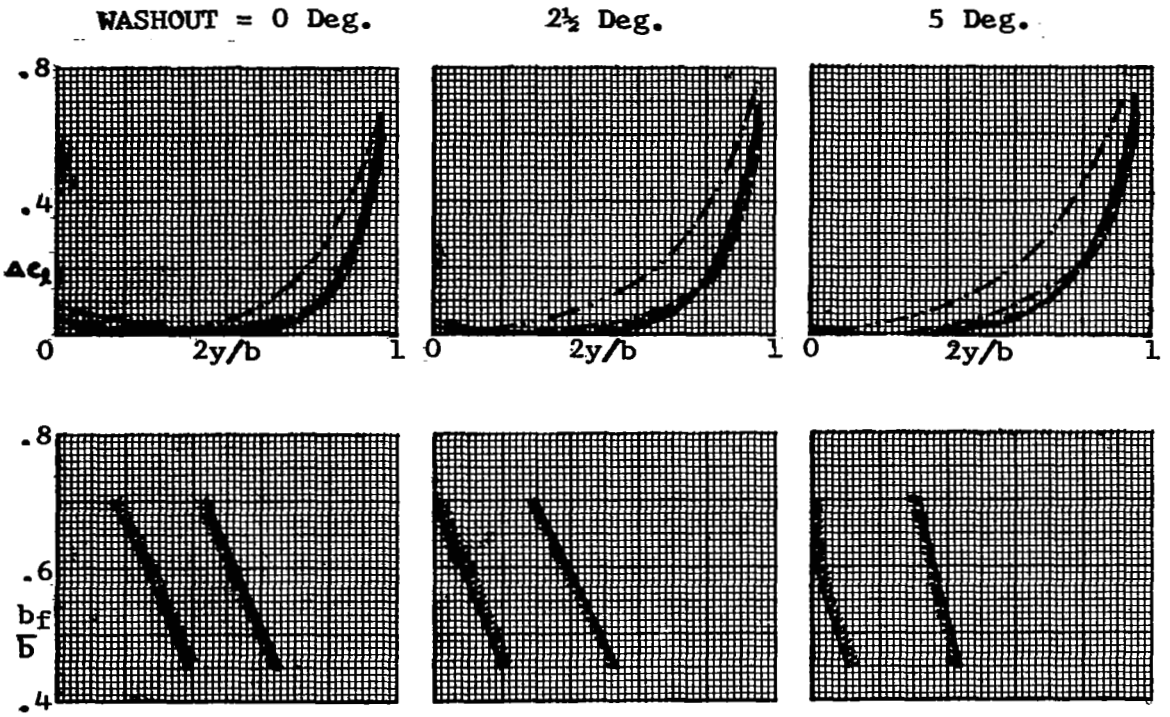

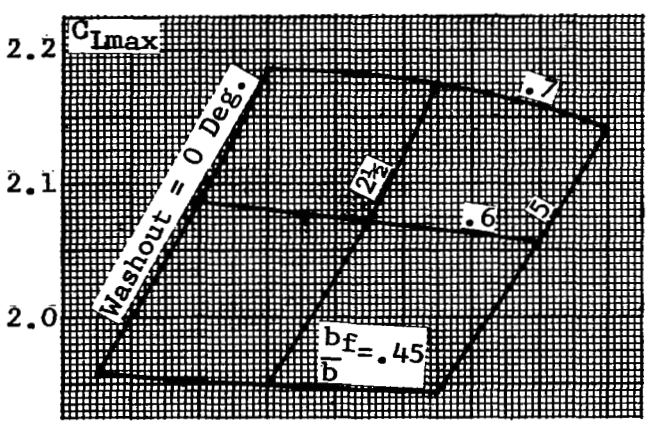

b_f/b
—·— 0
——— .45
– – – .60
—·—· .70

Root Section 64218
Tip Section 64212
Aspect Ratio = 6
Re = 6×10^6
Taper Ratio = 1
Flap Deflection = 60°

Figure 36. Effect of the Span of a 20% Chord Split Flap on the Wing Stalling Characteristics.

SECTION 6

SCALE MODEL WIND TUNNEL TESTING

It has previously been shown that the stalling characteristics of an isolated wing, with or without deflected flaps, can be adequately predicted through application of existing theoretical methods. In the case of a complete airplane, however, the interference of the fuselage, engine nacelles, propeller slipstream, etc., on the flow over the wing may be such as to drastically modify the wing stalling characteristics. The interference effects of the fuselage and nacelles are predictable with a fair degree of reliability as long as potential flow conditions prevail. Unfortunately, the body interference effects often precipitate flow separation and available theories are not capable of predicting such phenomena. At the present time no theory is available to adequately predict the effect of the propeller slipstream on wing stalling characteristics.

For these reasons, it is highly desirable to obtain experimental information concerning the complete airplane stalling characteristics before the airplane goes into production. In certain cases economic considerations may indicate the construction of a prototype model of the airplane with subsequent flight testing to obtain experimental information upon which to predicate the final design. In other cases, it may be more feasible to conduct a scale model wind tunnel investigation early in the airplane design stage in order to obtain the desired information.

During the period prior to World War II wind tunnel tests were ordinarily made of models without propellers and empirical methods were relied on to account for the effects of propelller operation on the observed characteristics. Such a procedure was shown to be inadequate when quantitative flight test data became available. In consequence it is now considered essential that wind tunnel model evaluation of airplane flying qualities, whether they be concerned with stalling or with stability and control, should involve the use of a powered model.

The following discussion will therefore consider some of the factors involved in powered model wind tunnel testing.

6.1 SCALE MODEL REQUIREMENTS

The selection of the model scale will be dependent on the size of the wind tunnel to be utilized in the investigation. As a rough rule of thumb the scale should be chosen such that the model wing span does not exceed approximately 75% of the width, or diameter, of the wind tunnel test section. Larger values of model size result in excessively large values of wind tunnel boundary corrections (Reference 23).

It is essential that the model be truly geometrically similar to the full scale airplane. In this regard, the leading-edge portion of the wing is particularly sensitive to deviations from contour. Caution must therefore be exercised to ensure that the airfoil shape over the forward 10 or 15 percent of the chord are true to the theoretical ordinates. Small deviations from true contour are not particularly critical over the aft portions of the airfoil. Wood, metal, plastic or combinations thereof may be satisfactorily utilized as material for model construction. However, it should be noted that composite wood and metal surfaces are not satisfactory because the wood shrinks and swells with change in atmospheric humidity conditions and thus gives rise to undesirable surface discontinuities. If wood construction is to be utilized, specially selected mahogany from the mainland of tropical America is suggested as being the most satisfactory. It has been found that mahogany from the islands of tropical America is not suitable for model construction because it shrinks and swells more and has a greater tendency to warp than mahogany from the mainland of tropical America. Similarly "Phillipine" mahogany is not suitable for model construction.

6.2 PROPELLER DRIVE SYSTEM

Specially constructed, compact squirrel cage induction motors have been utilized extensively as the propeller drive in powered models. Such motors are usually water cooled in order to increase their power output rating. In recent years some preference has been given to the use of compact pneumatic motors. The selection of motor type will depend to a large extent on availability of appropriate electric power supply or compressed air supply at the wind tunnel facilities being utilized.

Propeller rotational speed can be measured through the use of a high precision tachometer and the measurement of propeller torque may be accomplished using an appropriate strain gage balance system. If a squirrel-cage induction motor is utilized it is possible to obtain a straight line calibration of torque versus minimum current. The minimum current point is obtained by varying the voltage-frequency ratio of the electrical power supply until the minimum current point is arrived at.

The value of dynamic pressure at which power-on tests of an airplane model can be conducted is largely dictated by the torque rating of the propeller drive motor. For this reason it is advisable to at least make an approximate estimate of the critical simulation requirements before selecting the drive motor.

6.3 SIMULATION OF POWER CONDITIONS

In order to adequately simulate the effects of power in the wind-tunnel testing of models, it is essential that the axial and rotational velocity contributions of the propeller be in the

same ratio to the free stream velocity as that which prevails under the free flight conditions being simulated. This requires that the values of the propeller operating thrust and torque coefficients will change as the airplane flight speed or operating value of the lift coefficient is altered. It is usually most convenient to investigate the wind tunnel model through its operating range of lift coefficients at a fixed value of dynamic pressure, (constant velocity, fixed Reynolds number). To simulate the flight operating conditions during the constant velocity tests in the wind tunnel it is therefore necessary to provide a different operating condition of the propeller at each different value of lift coefficient or angle of attack investigated in the wind tunnel.

Various techniques have been developed for satisfying the conditions of power similitude in wind tunnel testing. It appears that each different wind tunnel staff has its own preference as to the particular technique to employ. It is suggested, however, that the power matching technique described in Reference 21. is most appropriate for use in wing stalling investigations because that technique ensures a nearly exact condition of power similitude at each test condition and hence no interpolation of observed results is required.

6.4 FLOW VISUALIZATION

Numerous methods of visualizing the flow over the airplane model in the wind tunnel have been utilized. The most familiar are probably the smoke flow technique, some variation of the lamp black and kerosene method and the use of tufts. Of the various techniques that have been developed, tufting is the least complex and is usually the most satisfactory. In utilizing this technique, numerous tufts are attached over the upper wing and fuselage surfaces by cellulose tape or by other means. The tufts should be of flexible material such as wool or nylon yarn. The length of the tufts is not critical. Usually a tuft length of approximately 3 or 4 percent of the wing chord will be found appropriate. Tufts should not be located forward of 20% chord.

The nature of the stall can be determined by noting the behavior of the tufts during the test conditions. Violent fluctuations and reversal of the flow direction as indicated by the tufts provides evidence of separation of the airflow from the surface under observation. The behavior of the tufts should of course be observed through a range of angle of attack from well below to well beyond the angle for maximum lift.

The flow condition as indicated by the tufts may be recorded photographically, using either a still camera or a movie camera, or it may be recorded manually on the basis of visual observation. Each method has its own particular advantages. Attention is drawn,

however, to the fact that still photographs of the tuft flow pattern can be misleading. This stems from the fact that in the case of some configurations the nature of the airflow as the stall is approached may be very unstable and erratic. At one point in time, the tuft pattern may indicate the flow to be attached to the surface, an instant later the tuft pattern may indicate large areas of separated flow. If a still picture were obtained at the instant of attached flow it could lead to an erroneous conclusion.

6.5 REYNOLDS NUMBER CONSIDERATIONS

Stalling behavior of an aircraft can not be reliably predicted using small scale models in the wind tunnel. This is primarily due to the fact that it is extremely difficult if not impossible to duplicate in the wind tunnel the values of flight Reynolds numbers unless recourse is made to a compressed air tunnel or to a tunnel utilizing a high density gas such as Freon as a test medium.

It has been well established that the maximum lift characteristics, including the wing stalling characteristics can be critically dependent on the value of the test Reynolds number. In consequence, judgment must be exercised in interpreting the wind tunnel stall test results in terms of the airplane flight Reynolds numbers condition.

As an aid in interpreting the wind tunnel stall observations, it is suggested that the theoretical analysis described earlier in this report be applied to predict the stall at a Reynolds number corresponding to the wind tunnel test condition and at a Reynolds number corresponding to the airplane flight condition. By taking account of the differences between theory and experiment at the test Reynolds number, an improved estimate of the stalling characteristics at the flight value of Reynolds number may be obtained. This approach should at least give an indication as to whether the free flight stall condition will be more or less severe than the stall condition observed in the wind tunnel tests.

6.6 MACH NUMBER CONSIDERATIONS

The effect of Mach number on the maximum lift characteristics of airfoils has not been isolated and studied as thoroughly as the effect of Reynolds number.

The results presented in Reference 51 indicate that at a given value of Reynolds number an increase in Mach number causes a moderate decrease in maximum lift coefficient under conditions such that the local velocities on the surface of the wing are somewhat below sonic speed. It has also been clearly demonstrated by the results of References 9, 51 and 52, that when the free

stream Mach number is increased to the point that sonic speed is reached, locally on the wing, a large reduction in maximum lift coefficient takes place. The same results show that critical local velocities can occur at values of the free stream Mach number as low as 0.20. There have been instances in the past where wind tunnel investigators have attempted to improve the test value of the Reynolds number by conducting the tests at high values of the wind tunnel airspeed. Such a procedure can lead to quite misleading test results, particularly if the free stream Mach number is sufficiently high to permit the attainment of critical local velocities over the wing surface.

SECTION 7

DESIGN PROCEDURES

The results presented in Section 5 are intended to serve as a guide in the preliminary design phase of an unswept wing aircraft to determine the effects of wing geometric and aerodynamic parameters on aircraft stalling behavior. While this data does not cover all the possible combinations of taper, twist, etc. which may be encountered, it should provide a basis for the assessment of the relative effectiveness of different wing designs in promoting acceptable airplane stalling characteristics.

In the early design stage of an airplane the values of wing aspect ratio, taper ratio, and root and tip thickness ratios are usually chosen from considerations of performance, structural strength, etc. rather than stalling characteristics. In regard to wing performance, the computer program described in this report can be of value in providing data on wing lift, drag, and pitching moment characteristics through the complete angle of attack range, as well as information on the span load distributions.

The stalling characteristics of the basic wing design can be assessed from the design charts presented in Section 5, and if poor stalling behavior is indicated, the effectiveness of various methods for improving the stall can then be investigated. When a wing design emerges which promises to fulfill the performance and stall requirements a final quantitative evaluation of its stalling characteristics can be made using the computer program which constitutes a part of this report.

7.1 APPLICATION OF THE RESULTS OF THE PARAMETRIC STUDY

The use of the design charts presented in Section 5 is best illustrated by a sample calculation described below.

Consider a light, single engined airplane having the following characteristics:

Wing aspect ratio	6
Wing taper ratio	0.5
Mean aerodynamic chord (m.a.c.)	5.4 ft.
Wing loading	17.2 lb/ft^2
Root airfoil section	23016.5
Tip airfoil section	23012

Cruise speed 154 m.p.h.

Cruise altitude 10,000 ft., (standard day)

A likely stalling speed for such an airplane, flaps up, is about 70 m.p.h. or a Reynolds number, based on the m.a.c. of 3.55×10^6. A good estimate of the stalling speed for the untwisted wing is obtained as follows:

(a) A number of speeds in the neighborhood of 70 m.p.h. is selected and the corresponding Reynolds numbers are calculated thus

V ft/sec.	=	90,	95,	100,	110,
V m.p.h.	=	61.35,	64.76,	68.17,	74.98,
Re	=	3.11,	3.28,	3.46,	3.80,

(b) Using Figure 33 for 0.5 taper ratio and a root thickness chord ratio of 0.18, the following values of $C_{L_{max}}$ are obtained corresponding to the Reynolds numbers calculated in step (a),

$C_{L_{max}}{}_{t/c=.18}$	=	1.42,	1.435,	1.45,	1.47,

(c) From Figure 28 the percentage change in $C_{L_{max}}$ due to changing root thickness-chord ratio from .18 to .165 is estimated to be 2%. Strictly, the data applies only to Re = 6×10^6, but the section characteristics, Figure 20, suggest that approximately the same changes can be expected at lower values of Reynolds number.

(d) The increments in $C_{L_{max}}$ obtained from step (c) are added to the $C_{L_{max}}$ values from step (b) yielding:

$C_{L_{max}}{}_{t/c=.165}$	=	1.45,	1.46,	1.48,	1.5

The results thus obtained are plotted versus stalling speed in Figure 37.

(e) A new series of values of $C_{L_{max}}$ based on the relationship $C_{L_{max}} = \frac{2 \times W/S}{\rho V^2}$ are calculated thus:

$$C_{L_{max}} = \frac{2\,W/S}{\rho V^2} = 1.78, \quad 1.60, \quad 1.445, \quad 1.19$$

These results are also plotted in Figure 37.

(f) The intersection of these curves yields the values of $C_{L_{max}}$ stall speed and Reynolds number as 1.475, 67.5 m.p.h. and 3.42×10^6, respectively, as shown in Figure 37.

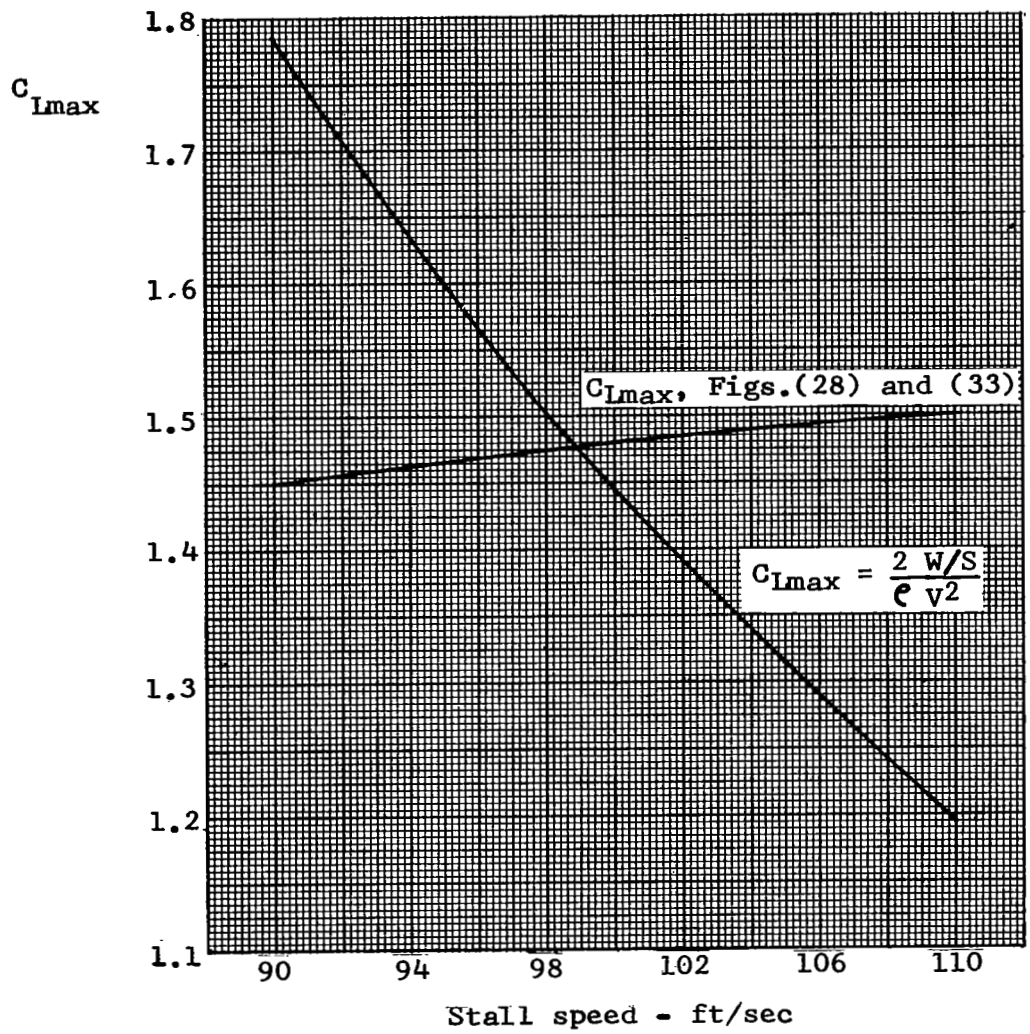

Figure 37. Variation of Wing Maximum Lift Coefficient with Stall Speed.

At this value of Reynolds number Figures 31 and 32 show that the stall margin at the 70% station is only 0.02 and that the stall begins inboard at about 35% semispan and extends to about 70% semispan. Obviously this is not acceptable and some means must be employed to move the stall inboard and increase the margin at the 70% semispan station.

An acceptable stall pattern would be the one in which the outer edge of the stalled area began, say, inboard of the 40% station and the stall margin at 70% of the semispan was at least 0.1. Figure 31 shows that, for the given taper ratio of 0.5, a stall margin of 0.1 at 70% semispan can be obtained with 7½ degrees of washout. For this case the corresponding stall boundaries lie between 15% and 37% semispan. Since the use of washout influences the value of $C_{L_{max}}$ and hence stalling speed, steps (b) through (f) are repeated using the data presented for 7½ washout. If these computations are performed the new values of $c_{L_{max}}$, stalling speed and Reynolds number are 1.4, 69 m.p.h. and 3.5 million respectively. Using the new value of Reynolds number and washout of 7½°, Figures 31 and 32 indicate that satisfactory stalling characteristics of the selected wing are attained with the safe stall margin of 0.1 at 70% semispan and inboard stall boundaries extending between 15% and 36% semispan.

If this amount of washout is used, a penalty may result in induced drag at the cruise speed. The magnitude of the increase in induced drag coefficient at the cruise lift coefficient of .38 and cruise Reynolds number of approximately 6 million is obtained from Figure 25 as $\Delta C_{D_i} = .0012$. The significance of this drag increase depends on the drag coefficient of the complete airplane. For an airplane having a drag coefficient equal to 0.02, an increase in induced drag coefficient of 0.0012 represents a 4 m.p.h. reduction in cruising speed at the cruise power setting.

An alternative to using a large amount of washout as high as 7½ degrees is to incorporate a tip section of higher camber than the root section with linear fairing in between, e.g. change the tip section from 23012 to 43012. On the basis of the results presented in Figure 34, for a wing employing linear camber increase from root to tip, it appears that increasing camber alone will not result in any significant improvement in the stalling characteristics. Combinations of linear camber increase with moderate amounts of washout may result in an effective compromise to yield satisfactory performance and acceptable stalling characteristics of the selected wing configurations. The parametric investigations of such effects can be easily performed utilizing the computer program presented in this report.

If an effective combination of camber increase and washout cannot be found the only remaining wing parameters which might influence stalling characteristics are aspect ratio, thickness distribution and taper ratio.

On the basis of the results shown in Figure 23, changing aspect ratio is ineffective. Increasing root thickness-chord ratio from .165 to say .18 is also of little value according to the results presented in Figure 27.

While an increase in wing taper ratio would represent a major change if the wing design were sufficiently far advanced, it might be less expensive, in the long run to make such a change than to try to solve bad wing stall problems by other means during the flight testing phase of development.

An illustration of the strong influence which is exerted by taper ratio on wing stalling characteristics is provided by repeating the above calculations for a taper ratio of 0.75 with $2\frac{1}{2}^{\circ}$ of washout. The increased taper ratio is achieved by reducing the root chord and increasing the tip chord by the same amount so as to maintain the same wing area as in the original design.

By interpolation between these results and results obtained for taper ratio of 0.5 it is found that an increase in taper ratio from 0.5 to 0.65 will produce a stall margin at 7/10th semispan equal to 0.1 with the stalled area extending between 10% and 40% semispan. The calculations also show that the change in taper ratio and the incorporation of $2\frac{1}{2}^{\circ}$ of washout does not alter the stalling speed to any significant degree. Furthermore, the induced drag penalty due to washout for this taper ratio is negligible.

If all of the above measures fail to indicate acceptable stalling characteristics then it must be left until the flight test phase to try to improve matters by the use of the various "fixes" discussed in Section 2. Even at this stage the computer program should prove valuable in assessing the relative merits of the post design modifications. For example, if the installation of sharp wedges over a portion of the leading edge is being considered, a precise evaluation of the effectiveness of such a device can be made by using the computer program if data is available pertaining to the aerodynamic characteristics of sharp nosed sections. Some data on the effect of sharp leading edges on section maximum lift coefficient can be found in References 53 and 54.

7.2 GENERAL CONSIDERATIONS

The design procedures discussed in this section together with the stall charts presented in Section 5 are considered

adequate for most practical cases in evaluating stalling characteristics of unswept wing aircraft. These procedures and charts should be specially valuable in the preliminary design phase in which numerous trade-off studies are required to obtain the best compromise in aircraft configurations. Once a given design has been frozen ensuring satisfactory aircraft performance, stalling characteristics, handling qualities, etc. it is recommended that the computer program presented as part of this report be utilized to more accurately predict the stalling behavior of the final aircraft configuration. As a by-product, the computer program will also yield valuable performance information such as distributions and integrated values of wing lift, drag and pitching moment coefficients, for cruise or any other aircraft operating condition.

SECTION 8

CONCLUSIONS AND RECOMMENDATIONS

Using the results presented in this report, the following conclusions and recommendations are made:

1. Based on good correlations obtained between the theoretical results and the available test data, it is concluded that the lifting line theory can be confidently used to predict stall characteristics of wings having aspect ratios of 6 and larger. This theory is expected to yield satisfactory predictions of overall load characteristics for wings of aspect ratios as low as 4.0.

2. From the results of the parametric study it can be concluded that taper ratio is one of the most effective design parameters influencing aircraft stall characteristics. Increase in taper ratio results in an increase of the stall margins on the outboard sections of the wing and in an inboard shift of stall boundaries. This, however, is accompanied by a reduction of maximum wing lift coefficient.

3. Washout may be used to improve stalling characteristics of moderate to high taper ratio wings. This improvement, however, may entail a performance penalty associated with a reduction of wing maximum lift coefficient and an increase in wing induced and profile drag.

4. An increase in root thickness-chord ratio and flight Reynolds number yields favorable effects on wing stalling characteristics associated with the 230 and 44 series airfoils. For the 642 series sections such increases result in unfavorable effects. Increasing tip thickness-chord ratio has an unfavorable effect for all three airfoil series. For all cases the values of wing maximum lift coefficient are reduced.

5. For the wing configurations investigated in this report, deflection of part-span flaps lowers the stall margins on the outboard portion of the wing and shifts the stall boundaries outboard. Increasing flap span moves the stall boundaries inboard and increases wing maximum lift coefficient.

6. The effects of aspect ratio, linear camber, and fuselage on wing stalling characteristics appear to be small and may be neglected for most present-day light aircraft.

7. The analysis and the design charts presented in this report apply strictly to unpowered flight, out of ground effect, as would be the case in aircraft approach to landing.

8. Based on the work accomplished in this program, it is recommended that the theoretical analysis be extended to include propeller slipstream and ground effects. Furthermore, additional flight test and wind tunnel test data should be obtained for the purpose of verifying the theory.

SECTION 9

REFERENCES

1. Sivells, James C., and Neely, Robert H.: Method of Calculating Wing Characteristics by Lifting-line Theory Using Nonlinear Section Lift Data. NACA Rep. 865, 1947.

2. Sivells, James C., and Westrick, Gertrude C.: Method for Calculating Lift Distributions for Unswept Wings With Flaps or Ailerons by use of Nonlinear Section Lift Data. NACA Rep. 1090, 1952.

3. Theodorsen, Theodore: Theory of Wing Sections of Arbitrary Shape. NACA Rep. 411, 1931.

4. Multhopp H.: Aerodynamics of the Fuselage. NACA TM 1036, 1942.

5. Abbott, Ira H., von Doenhoff, Albert E., and Stivers, Louis S.: Summary of Airfoil Data. NACA Rep. 824, 1945.

6. Loftin, Laurence K., Jr. and Smith, Hamilton A.: Aerodynamic Characteristics of 15 NACA Airfoil Sections at Seven Reynolds Numbers from 0.7×10^6 to 9.0×10^6. NACA TN 1945, 1949.

7. Bollech, Thomas V.: Experimental and Calculated Characteristics of Several High-Aspect-Ratio Tapered Wings Incorporating NACA 44-Series, 230 Series, and Low Drag 64-Series Airfoil Sections. NACA TN 1677, 1948.

8. Sweberg, Harold H. and Dingeldein, Richard C.: Summary of Measurements in Langley Full-Scale Tunnel of Maximum Lift Coefficients and Stalling Characteristics of Airplanes. NACA Rep. 829, 1945.

9. Fitzpatrick, James E. and Schneider, William C.: Effect of Mach Number Variation Between 0.07 and 0.34 and Reynolds Number Variation Between 0.97×10^6 and 8.10×10^6 on the Maximum Lift Coefficient of a Wing of NACA 64-210 Airfoil Series. NACA TN 2753, 1952.

10. Federal Aviation Agency: Airworthiness Standards: Normal, Utility and Aerobatic Category Aeroplanes. FAA Regulations, Part 23, Current.

11. Wimpenny, J. C.: Low Speed Stalling Characteristics. AGARD Rep. 356, 1961.

12. Zalovcik, John A.: Summary of Stall Warning Devices. NACA TN 2676, 1952.

13. McCullough, George B. and Gault, Donald E.: Examples of Three Representative Types of Airfoil-Section Stall at Low Speed. NACA TN 2502, 1951.

14. Gault, Donald E.: A Correlation of Low-Speed, Airfoil-Section Stalling Characteristics With Reynolds Number and Airfoil Geometry. NACA TN 3963, 1957.

15. Anderson, Raymond F.: Determination of the Characteristics of Tapered Wings. NACA Rep. 572, 1936.

16. Pearson, Henry A.: Span Load Distribution for Tapered Wings With Partial-Span Flaps. NACA Rep. 585, 1936.

17. Pearson, Henry A., and Anderson, Raymond F.: Calculation of the Aerodynamic Characteristics of Tapered Wings With Partial-Span Flaps. NACA Rep. 665, 1939.

18. Sivells, James C., and Spooner, Stanley H.: Investigation in the Langley 19-Foot Pressure Tunnel of Two Wings of NACA 65-210 and 64-210 Airfoil Sections With Various Type Flaps. NACA Rep. 942, 1949.

19. White, James A., and Hood, Manley J.: Wing Fuselage Interference, Tail Buffeting, and Airflow About the Tail of a Low-Wing Monoplane. NACA Rep. 482, 1934.

20. Weick, Fred E.: The Behavior of Conventional Airplanes in Situations Thought to Lead to Most Crashes. NACA TN 363, 1931.

21. Phillips, William H.: Appreciation and Prediction of Flying Qualities. NACA Rep. 927, 1949.

22. Prandtl, L.: Applications of Modern Hydrodynamics to Aeronautics. NACA Rep. 116, 1921.

23. Glanert, H.: The Elements of Aerofoil and Airscrew Theory. Cambridge University Press, Second Edition, 1959.

24. Sherman, Albert: A Simple Method of Obtaining Span Load Distributions. NACA TN 732, 1939.

25. Tani, Itiro: A Simple Method of Calcuating the Induced Velocity of a Monoplane Wing. Aeronautical Research Inst. Tokyo Imp. Univ. Rep. 111, Vol. IX, 1934, page 3.

26. Multhopp, H.: The Calculation of the Lift Distribution of Airfoils. Luftfahrforschung, Deutschland (R.T.P. Translation No. 2392), 1938.

27. Boshar, John: The Determination of Span Load Distribution at High Speeds by the Use of High-Speed Wind Tunnel Section Data. NACA ARC 4B22, 1944 (Wartime Rep. L-436).

28. Weissinger, J.: The Lift Distribution of Swept-Back Wings. NACA TM 1120, 1947.

29. Mutterperl, William: The Calculation of Span Load Distributions on Swept-Back Wings. NACA TN 834, 1941.

30. Schlichting, H., and Kahlert, W.: Calculation of Lift Distribution of Swept Wings. R.A.E. Rep. Aero. 2297, 1948.

31. Falkner, V.M.: The Calculation of the Aerodynamic Loading on Surfaces of any Shape. ARC R & M 1910, 1943.

32. Garner, H.C.: Methods of Approaching an Accurate Three-Dimensional Potential Solution for a Wing. R & M No. 2721, Brit. A.R.C., 1954.

33. Garner, H.C.: Theoretical Calculations of the Distribution of Aerodynamic Loading on a Delta Wing. R & M No. 2819, Brit. A.R.C., 1954.

34. Multhopp, H.: Methods of Calculating the Lift Distribution of Wings. (Subsonic Lifting Surface Theory). R & M No. 2884, Brit. A.R.C., 1955.

35. Schlichting, H.: Aerodynamics of the Mutual Influence of Aircraft Parts (Interference) Volkenrode R & T No. 171, Trans. 275, 1946.

36. Flax, A.H., and Lawrence, H.R.: The Aerodynamics of Low Aspect Ratio Wings and Wing-Body Combinations. Proc. Third Anglo-American Aeronautics Conference, Brighton, 1951, page 363.

37. Lennertz, J.: Influence of the Airplane Body on the Wings. Aerodynamic Theory; W.F. Durand, Editor, Vol. IV, Division K, Chapter III, page 152, Durand Reprinting Committee, 1943.

38. Pepper, P.A.: Minimum Induced Drag in Wing-Fuselage Interference. NACA TN 812, 1941.

39. Zlotnick, M., and Robinson, S.W., Jr.: A Simplified Mathematical Model for Calculating Aerodynamic Loading and Downwash for Wing-Fuselage Combinations With Wings of Arbitrary Plan Form. NACA TN 3057, 1954 (also NACA RN L52J27a, 1953).

40. Weber, J., Kirby, D.A., and Kettle, D.J.: An Extension of Multhopp's Method of Calculating the Spanwise Loading of Wing-Fuselage Combinations. R & M No. 2872, Brit. A.R.C., 1956.

41. Dynasciences Corporation: Effects of Propeller Slipstream on V/STOL Aircraft Performance and Stability. TRECOM TR 64-47, 1964.

42. George, M., and Kisielowski, E.: Investigation of Propeller Slipstream Effects on Wing Performance. USAAVLABS TR 67-67, 1967.

43. Laurence, H.R., and Flax, A.H.: Wing-Body Interference at Subsonic and Supersonic Speeds - Survey and New Developments. J. Ae.Sc., Vol. 21, No. 5, page 289, 1954.

44. Ribner, H.S., and Ellis, N.D.: Theory and Computer Study of a Wing in a Slipstream. AIAA Paper No. 66-466, 1966.

45. Ribner, H.S.: Theory of Wings in a Slipstream UTIAS Rep. 60, 1959.

46. Wieselsberger, C.: Contribution to the Mutual Interference of Wing and Propeller. NACA TM 754, 1934.

47. Yaggy, Paul F.: A Method for Predicting the Upwash Angles Induced at the Propeller Plane of a Combination of Bodies With an Unswept Wing. NACA TN 2528, 1951.

48. Jones, Robert T.: Correction of the Lifting-Line Theory for the Effect of the Chord. NACA TN 817, 1941.

49. Soulé, H.A., and Anderson, R.F.: Design Charts Relating to the Stalling of Tapered Wings. NACA Report 703, 1940.

50. Schlichting, H.: Report on the Special Field "Interference" to the Wind-Tunnel Committee in February 1945. NACA TM 1347, 1953.

51. Furlong, G. Chester and Fitzpatrick, James E.: Effects of Mach Number and Reynolds Number on the Maximum Lift Coefficient of a Wing of NACA 230-Series Airfoil Sections. NACA TN 1299, 1947.

52. Furlong, G. Chester and Fitzpatrick, James E.: Effects of Mach Number up to 0.34 and Reynolds Number up to 8×10^6 on the Maximum Lift Coefficient of a Wing of NACA 66-Series Airfoil Sections. NACA TN 2251, 1950.

53. Jacobs, Eastman N.: Characteristics of Two Sharp-Nosed Airfoils Having Reduced Spinning Tendencies. NACA TN 416, 1932.

54. Weick, Fred E. and Scudder, Nathan F.: The Effect of Lift, Drag, and Spinning Characteristics of Sharp Leading Edges on Airplane Wings. NACA TN 447, 1933.

APPENDIX A

INTERNAL LISTING OF THE COMPUTER PROGRAM

```
      OVERLAY(BLINDA,0,0)
      PROGRAM STALL(INPUT=201,OUTPUT=1001,TAPE8=INPUT,TAPE6=OUTPUT,TAPE1
     1=201,TAPE2=201,TAPE3=201,TAPE4=201,TAPE5=201,TAPE10=201,TAPE15=201
     2,TAPE20=201,TAPE44=201,TAPE7=1001,TAPE9=201)
C
C     PROGRAM STALL COMPUTES THE STALL CHARACTERISTICS OF STRAIGHT WING
C     AIRCRAFT
C
C     THIS PROGRAM WAS PREPARED FOR NASA LANGLEY RESEARCH CENTER UNDER
C     CONTRACT NAS1-8389 BY DYNASCIENCES CORPORATION, SCIENTIFIC SYSTEMS
C     DIVISION, BLUE BELL,PENNSYLVANIA
C
C     THE DYNASCIENCES PERSONNEL WHO CONDUCTED THE INVESTIGATION WERE
C     MESSRS. M. A. MCVEIGH, C. KISIELOWSKI, AND J. G. MCHUGH. AREA CODE
C     215-643-0250.
C
C     ANY ERRORS OR PROBLEMS ENCOUNTERED IN USING THE PROGRAM SHOULD BE
C     DIRECTED TO MR. CHARLES H. FOX, JR. AT NASA LANGLEY. AREA CODE 703
C     -827-3711.
C
C     A CARD DECK AND DOCUMENTATION FOR THE PROGRAM ARE AVAILABLE FROM
C     COSMIC, UNIVERSITY OF GEORGIA, ATHENS, GEORGIA, 30601.
C
C     THIS PROGRAM IS WRITTEN IN CDC FORTRAN IV, VERSION 2.3, TO RUN ON
C     CDC 6600 SERIES COMPUTERS WITH THE SCOPE 3.0 OPERATING SYSTEM AND
C     LIBRARY TAPE. THIS PROGRAM WAS WRITTEN TO PERMIT CONVENIENT
C     MODIFICATION FOR USE ON OTHER COMPUTERS.
C
      DIMENSION ARRAY(5,25,12),C(19),EPS(19),TRANS(19),REY(19),ETA(19),
     1HOPP(19),CLMAX(19),ZHERE(2,6),WHERE(2,6),Y(19),TAU(19),BETA(19,19)
     2,TRIX(19,19),MAZZ(6),MZCOL(6),MAXX(6),MXCOL(6),XHERE(2,6),MWCOL(6)
     3,MAWW(6),CM(19),CBG(19),CVAL(19),ALPC(19),CBC(19),ALPHU(19),ALPH(
     419),ALPHZ(19),ALPHE(19),DELTA(19),CL(19),ALPHV(20),YHERE(2,6),MYCO
     5L(6),MAYY(6),CLADD(19),CLDEL(19),CLAD2(19),CLAD1(19),F(19),ALPC(19
     6),TONY(19)
      COMMON INNOW,ISWIT(3),ALPHA,RLYN,CLL,REYON,XMAX,ALMAX(19),CLMAX,C,
     1EPS,TRANS,REY,ETA,HOPP,ZHERE,WHERE,ARRAY,Y,BETA,TFAC,TRIX,TAU,MAXX
     2,MAZZ,MXCOL,MZCOL,ASPEC,TAPER,BF,REYND,DISCR,PIER,CRB,Q,TSTAX,EDGE
     3,SIG,ALPHR,NFLAP,NLVL,NP,IY,IZ,IR,IP,ISIS,ISTAR,A,B,H,TAUT,TAUR,
     4TWIST,R,BWX,YHERE,MYCOL,MAYY,FLAP,TONY,TWISA,X,Z,CM,ACC,XHERE,MWCO
     5L,MAWW,CAMB(19),CAMBR,CAMBT,DUMY1,DUMY2,NAME(25),AHERE(2,6),MAAA(6
     6),MACC(6),BHERE(2,6),MABB(6),MBCOL(6),CHERE(2,6),MACC(6),MCCOL(6)
     7,DHERE(2,6),MADD(6),MDCOL(6),ALPHE,ALPHV,CLAUD,CLDEL,CLAD2,CLAD1,
     8F,ERI,FF,LOCER,IPRAB,IKT,IQT,IAGN,ITR,IS,DUM(100)
      BLINDA=6HBLINDA
      RECALL=6HRECALL
   10 CALL OVERLAY(BLINDA,1,0,RECALL)
      IF(NFLAP) 20,20,30
   20 CALL OVERLAY(BLINDA,2,0,RECALL)
      GO TO 10
   30 CALL OVERLAY(BLINDA,3,0,RECALL)
      GO TO 10
      END
      SUBROUTINE MINV(A,N,D,L,M)
C
C                                MATRIX INVERSION SUBROUTINE
C
      DIMENSION A(1),L(1),M(1)
C
C                                SEARCH FOR LARGEST ELEMENT
C
      D=1.0
      NK=-N
      DO 180 K=1,N
      NK=NK+N
      L(K)=K
      M(K)=K
      KK=NK+K
      BIGA=A(KK)
```

```
      DO 20 J=K,N
      IZ=N*(J-1)
      DO 20 I=K,N
      IJ=IZ+I
      IF(ABS(BIGA)-ABS(A(IJ))) 10,20,20
   10 BIGA=A(IJ)
      L(K)=I
      M(K)=J
   20 CONTINUE
C
CC                                    INTERCHANGE ROWS
C
      J=L(K)
      IF(J-K) 50,50,30
   30 KI=K-N
      DO 40 I=1,N
      KI=KI+N
      HOLD=-A(KI)
      JI=KI-K+J
      A(KI)=A(JI)
   40 A(JI)=HOLD
C
CC                                    INTERCHANGE COLUMNS
C
   50 I=M(K)
      IF(I-K) 80,80,60
   60 JP=N*(I-1)
      DO 70 J=1,N
      JK=NK+J
      JI=JP+J
      HOLD=-A(JK)
      A(JK)=A(JI)
   70 A(JI)=HOLD
C
CC                                    DIVIDE COLUMN BY MINUS PIVOT (VALUE OF
CC                                    PIVOT ELEMENT IS CONTAINED IN BIGA)
C
   80 IF(ABS(BIGA)-1.E-20) 90,90,100
   90 D=0.0
      RETURN
  100 DO 120 I=1,N
      IF(I-K) 110,120,110
  110 IK=NK+I
      A(IK)=A(IK)/(-BIGA)
  120 CONTINUE
C
CC                                    REDUCE MATRIX
C
      DO 150 I=1,N
      IK=NK+I
      HOLD=A(IK)
      IJ=I-N
      DO 150 J=1,N
      IJ=IJ+N
      IF(I-K) 130,150,130
  130 IF(J-K) 140,150,140
  140 KJ=IJ-I+K
      A(IJ)=HOLD*A(KJ)+A(IJ)
  150 CONTINUE
C
CC                                    DIVIDE ROW BY PIVOT
C
      KJ=K-N
      DO 170 J=1,N
      KJ=KJ+N
      IF(J-K) 160,170,160
  160 A(KJ)=A(KJ)/BIGA
  170 CONTINUE
C
```

```
C                                   PRODUCT OF PIVOTS
CC
      D=D*BIGA
C
CC                                  REPLACE PIVOT BY RECIPROCAL
CC
      A(KK)=1.0/BIGA
  180 CONTINUE
C
CC                                  FINAL ROW AND COLUMN INTERCHANGE
CC
      K=N
  190 K=K-1
      IF(K) 260,260,200
  200 I=L(K)
      IF(I-K) 230,230,210
  210 JQ=N*(K-1)
      JR=N*(I-1)
      DO 220 J=1,N
      JK=JQ+J
      HOLD=A(JK)
      JI=JR+J
      A(JK)=-A(JI)
  220 A(JI)=HOLD
  230 J=M(K)
      IF(J-K) 190,190,240
  240 KI=K-N
      DO 250 I=1,N
      KI=KI+N
      HOLD=A(KI)
      JI=KI-K+J
      A(KI)=-A(JI)
  250 A(JI)=HOLD
      GO TO 190
  260 RETURN
      END
      SUBROUTINE DACET(ARRAY,IFILE,II)
C
CC                                  SUBROUTINE TO GET TABLE FROM DISK AND PUT
CC                                  IT INTO CORE
C
      DIMENSION ARRAY(5,25,12),DRRAY(5,25,12)
      COMMON INNOW,ISWII(3),ALPHA,REYN,CLL,REYON,XMAX,ALMAX(19),CLMAX(19
     1),C(19),EPS(19),TRANS(19),REY(19),ETA(19),HOPP(19),ZHERE(2,6),
     2WHERE(2,6),DRRAY,Y(19),BETA(19,19),TFAC,TRIX(19,19),TAU(19),MAXX(6
     3),MAZZ(6),MXCOL(6),MZCOL(6),ASPEC,TAPER,BF,REYND,DISCR,PIER,CRB,Q,
     4ISTAX,EDGE,SIG,ALPHR,NFLAP,NLVL,NP,IY,IZ,IR,IP,ISIS,ISTAR,A,B,H,
     5TAUT,TAUR,TWIST,R,BRX,YHERE(2,6),MYCOL(6),MAYY(6),FLAP,TONY(19),
     6TWISA,X,Z,CM(19),ACC,XHERE(2,6),MWCOL(6),MAWW(6),CAMB(19),CAMBR,
     7CAMBT,DUMY1,DUMY2,NAME(25),AHERE(2,6),MAAA(6),MACOL(6)
C
CC                                  TABLE PRESENTLY IN CORE IS INNOW
CC
CC                                  IF TABLE IS ALREADY IN CORE THEN RETURN
CC                                  IF NOT THEN GET TABLE FROM DISK
C
      IF(IFILE-INNOW) 10,90,10
   10 II=1
      REWIND IFILE
      READ(IFILE) ARRAY
      REWIND IFILE
C
CC                                  RESET TABLE PRESENTLY IN CORE INDICATOR
C
      INNOW=IFILE
      IF(NFLAP) 90,20,90
   20 IF(IFILE-5) 50,30,90
   30 DO 40 JFOX=1,NLVL
      KROW=MAAA(JFOX)-2
```

```
      KCOL=MACOL(JFOX)
      DO 40 KBOB=2,KCOL
   40 ARRAY(JFOX,KROW,KBOB)=0.
      GO TO 90
   50 IF(IFILE-1) 90,60,90
   60 DO 80 JFOX=1,NLVL
      KROW=MAXX(JFOX)-2
      KCOL=MXCOL(JFOX)
      DO 70 KBOB=2,KCOL
   70 ARRAY(JFOX,KROW,KBOB)=0.
   80 CONTINUE
   90 RETURN
      END
      SUBROUTINE AAA(CLIST,NV)
C
CC                                    SUBROUTINE TO OUTPUT A ONE DIMENSIONAL
CC                                    ARRAY
C
      DIMENSION CLIST(1)
      IP=6
      WRITE(IP,10) (J,CLIST(J),J=1,NV)
      WRITE(IP,20)
      RETURN
C
   10 FORMAT(5(1X,1H(,I2,2H) ,E16.8))
   20 FORMAT(2(1H ))
      END
      SUBROUTINE ZZZ(VALUE)
C
CC                                    SUBROUTINE TO OUTPUT A SINGLE VALUE
CC
CC                                    OUTPUT VALUE IN BOTH F AND E FORMAT
C
      IP=6
      WRITE(IP,10) VALUE,VALUE
      RETURN
C
   10 FORMAT(1X,F15.8,E16.8/1X)
      END
      SUBROUTINE SSS(A,NP)
C
CC                                    SUBROUTINE TO OUTPUT A SQUARE TWO
CC                                    DIMENSIONAL ARRAY
C
      DIMENSION A(19,19)
      IP=6
      WRITE(IP,10) ((J,K,A(J,K),K=1,NP),J=1,NP)
      WRITE(IP,20)
      RETURN
C
   10 FORMAT(5(1X,1H(,I2,1H,I2,2H) ,E16.8))
   20 FORMAT(3(1H0/))
      END
      FUNCTION TERP(R1,R2,R3,C1,C3)
C
CC                                    INTERPOLATION FUNCTION
C
      IF(R1-R3) 20,10,20
   10 TERP=C1
      RETURN
   20 TERP=C1+((C3-C1)*((R2-R1)/(R3-R1)))
      RETURN
      END
      SUBROUTINE SETSW
C
CC                                    SUBROUTINE CHECKS SWITCH SETTINGS ON DATA
CC                                    CARD AND LISTS OPTIONS SELECTED
C
      COMMON INNOW,ISWI(3)
```

```
      K=0
      IP=6
      WRITE(IP,90)
      IF(ISWIT(1)) 20,20,10
   10 K=K+1
      WRITE(IP,100)
   20 IF(ISWIT(2)) 40,40,30
   30 K=K+1
      WRITE(IP,110)
   40 IF(ISWIT(3)) 60,60,50
   50 K=K+1
      WRITE(IP,120)
   60 IF(K) 80,70,80
   70 WRITE(IP,130)
   80 RETURN
C
   90 FORMAT(1H1/1HO/1HO,50X,29HSPECIAL FEATURES FOR THIS RUN/1HO)
  100 FORMAT(51X,14HREAD IN VALUES/1HO)
  110 FORMAT(51X,34HTRACE (OUTPUT OF KEY CALCULATIONS)/1HO)
  120 FORMAT(51X,26HPRINT MATRICES BETA AND TRIX/1HO)
  130 FORMAT(51X,31HNO SWITCH SETTINGS  REGULAR RUN)
      END
      SUBROUTINE DATSW(N,ICOND)
C
CCC                              SUBROUTINE MAKES DECISION BASED ON THE
CCC                              SETTING OF THE SWITCH  SET=1,NOT SET=0
CCC                              ICOND=1 IF SWITCH IS SET
CCC                              ICOND=2 IF SWITCH IS NOT SET
C
      COMMON INNOW,ISWIT(3)
      IF(N-3) 10,20,30
   10 IF(ISWIT(1)) 40,40,50
   20 IF(ISWIT(2)) 40,40,50
   30 IF(ISWIT(3)) 40,40,50
   40 ICOND=2
      RETURN
   50 ICOND=1
      RETURN
      END
      SUBROUTINE AERDA(ARRAY,NLVL,WHERE,MXCOL,MAXX,IFILE,II)
C
CCC                              SUBROUTINE TO READ AERODYNAMIC TABLES FROM
CCC                              CARDS AND PUT TABLES ON DISK
C
      DIMENSION NAME(40),MAXX(6),MXCOL(6),WHERE(2,6),ARRAY(5,25,12)
      COMMON INNOW
C
CCC                              MAXX(6) CONTAINS NUMBER OF ROWS IN A TABLE
CCC                              WHERE(2,6) CONTAINS TABLE NUMBER AND TAU
CCC                              VALUE
CCC                              INNOW IS THE TABLE PRESENTLY IN CORE
C
      IR=6
      IP=6
C
CCC                              INITIALIZE LEVELS IN WHERE
C
      DO 10 J=1,NLVL
   10 WHERE(1,J)=J
C
CCC                              LOOP TO READ IN LEVELS OF A SET OF EITHER
CCC                              LIFT, DRAG, OR PITCHING MOMENT
C
      DO 40 LVL=1,NLVL
C
CCC                              READ AND PRINT NUMBER OF ROWS, COLUMNS, TAU
CCC                              VALUES FOR A GIVEN LEVEL
C
      READ(IR,50) NC,NCOL,WHERE(2,LVL)
```

```
      WRITE(IP,60) NC,NCOL,WHERE(2,LVL)
C
CC                                    STORE NUMBER OF COLUMNS
C
      MXCOL(LVL)=NCOL
C
CC                                    STORE NUMBER OF ROWS
C
      MAXX(LVL)=NC
C
CC                                    READ AND WRITE TITLE OF TABLE
C
      READ(IR,70) NAME
      WRITE(IP,80) NAME,LVL
C
CC                                    READ VALUES FOR TABLE
C
      DO 20 I=1,NC
   20 READ(IR,90) (ARRAY(LVL,I,J),J=1,12)
      DO 30 JJ=1,NC
   30 WRITE(IP,100) (ARRAY(LVL,JJ,II),II=1,NCOL)
   40 CONTINUE
      II=1
C
CC                                    WRITE COMPLETE TABLE ON DISK
C
      WRITE(IFILE) ARRAY
      RETURN
C
  100 FORMAT(12F10.5)
   50 FORMAT(2I2,F10.0)
   60 FORMAT(1X,2I2,F5.2)
   70 FORMAT(40A2)
   80 FORMAT(11X,40A2,2X,I2)
   90 FORMAT(F7.3,9F8.3)
      END
      SUBROUTINE BRIDG(CCZ1,NS,NP,LDM,IZXY,IE,EY,AU,AMB,XX,IS,IP,YY)
C
CC                                    SUBROUTINE TO INTERPOLATE BETWEEN TABLES
C
      DIMENSION XX(1),EY(1),AU(1),CCZ1(1),CCZ2(19),CCLR1(19),CALR1(19),
     1CCLR2(19),CALR2(19),AIMP(19),REY(19),TAU(19),ARRAY(5,25,12),C(19),
     2EPS(19),TRANS(19),ETA(19),HOPP(19),CLMAX(19),ZHERE(2,6),WHERE(2,6)
     3,Y(19),BETA(19,19),IRIX(19,19),MAZZ(6),MZCOL(6),MAXX(6),MXCOL(6),
     4YHERE(2,6),MYCOL(6),MAYY(6),CM(19),XHERE(2,6),MAWW(6),MWCOL(6)
      COMMON INNOW,ISWIT(3),ALPHA,RLYN,CLL,REYCN,XMAX,ALMAX(19),CLMAX,C,
     1EPS,TRANS,REY,ETA,HOPP,ZHERE,WHERE,ARRAY,Y,BLTA,TFAC,TRIX,TAU,MAXX
     2,MAZZ,MXCOL,MZCOL,ASPEC,TAPER,BF,REYND,DISCR,PIER,CRB,Q,TSTAX,EDGE
     3,SIG,ALPER,NFLAP,NLVL,NQ,IY,IZ,IR,IO,IT,ISTAR,A,B,H,TAUT,TAUR,
     4TWIST,R,BWX,YHERE,MYCOL,MAYY,FLAP,TONY(19),TWISA,X,Z,CM,ACC,XHERE,
     5MWCOL,MAWW,CAMB(19),CAMBR,CAMBI,DUMY1,DUMY2,NAME(25),AHERE(2,6),
     6MAAA(6),MACOL(6),BHERE(2,6),MABB(6),MBCOL(6),CHERE(2,6),MACC(6),
     7MCCOL(6),DHERE(2,6),MADD(6),MDCOL(6)
C
CC                                    INITIALIZATION
CC                                    IF REYON=999 THEN SPECIAL CASE
C
      DUMY2=0.0
      DUMY1=0.0
      IF(RLYON-999.) 20,10,20
   10 KEY=1
      GO TO 30
   20 KEY=2
C
CC                                    STORE C VALUE
C
   30 CLT=CLL
C
C                                     NEW IS THE FILE NUMBER OF THE OTHER CUBE
```

```
C                                  PRIMARY CUBES ARE NUMBERED 1,2,3,4
C                                  SECONDARY CUBES ARE NUMBERED 5,10,15,20
C
      NEW=LDM*5
C
C                                  STORE XMAX
C
      XMX=XMAX
C
C                                  DETERMINE IF SINGLE VALUE IS TO BE USED OR
C                                  LIST OF VALUES IS TO BE USED IN LOOK UP
C
      IF(IS-IP) 50,40,50
   40 KGO=1
C
C                                  SET UP FOR CONSTANT VALUE OF X
C
      ATMP(1)=XX(1)
      GO TO 70
C
C                                  SET UP FOR VARIABLE VALUE OF X
C
   50 KGO=2
      DO 60 J=NS,NP
   60 ATMP(J)=XX(J)
C
C                                  PUT PROPER TABLE IN CORE
C
   70 CALL DAGET(ARRAY,NEW,IZXY)
C
C                                  SET UP ALPHA EITHER VARIABLE OR CONSTANT
C
      DO 190 K=NS,NP
      GO TO (80,90), KGO
   80 ALPHA=ATMP(IS)
      GO TO 100
   90 ALPHA=ATMP(K)
C
C                                  GET TAU VALUE FROM ARRAY
C
  100 TAUX=TAU(K)
      GO TO (120,110), KEY
C
C                                  GET PROPER REYNOLDS NUMBER EITHER REGULAR
C                                  OR MAX NUMBER
C
  110 REYDN=REY(K)
      REYN=999.
      GO TO 130
  120 REYN=REY(K)
  130 CLL=CLT
      XMAX=XMX
C
C                                  PERFORM LOOK FOR LIFT, DRAG, PITCHING
C                                  MOMENT OR FLAP CASE
C
      GO TO (140,150,160,170), LDM
  140 CALL ARC(ARRAY,TAUX,MAAA,MACOL,IE,AHERE,NLVL)
      GO TO 180
  150 CALL ARC(ARRAY,TAUX,MABB,MBCOL,IE,BHERE,NLVL)
      GO TO 180
  160 CALL ARC(ARRAY,TAUX,MACC,MCCOL,IE,CHERE,NLVL)
      GO TO 180
  170 CALL ARC(ARRAY,TAUX,MADD,MDCOL,IE,DHERE,NLVL)
C
C                                  STORE VALUES FOUND IN LOOK UP
C
  180 CCZZ(K)=YY
      CCLR2(K)=DUMY1
```

```
      CALR2(K)=DUMY2
C
CCC                                   REPEAT FOR NUMBER OF VALUES TO BE FOUND
C
  190 CONTINUE
C
CCC                                   GET NEXT TABLE IN CORE
C
      CALL DAGET(ARRAY,LDM,IY)
C
CCC                                   SET UP ALPHA VALUE
C
      DO 310 K=NS,NP
      GO TO (200,210), KGO
  200 ALPHA=ATMP(IS)
      GO TO 220
  210 ALPHA=ATMP(K)
C
CCC                                   SET UP REYNOLDS NUMBER
C
  220 GO TO (240,230), KEY
  230 REYON=REY(K)
      REYN=999.
      GO TO 250
  240 REYN=REY(K)
C
CCC                                   SET UP CVAL, TAU, AND XMAX VALUE
C
  250 CLL=CLT
      TAUX=TAU(K)
      XMAX=XMX
C
CCCC                                  LOOK UP FOR SECOND LIFT, DRAG, PITCHING
                                      MOMENT, OR FLAP CASE
C
      GO TO (260,270,280,290), LDM
  260 CALL ARC(ARRAY,TAUX,MAXX,MXCOL,IE,WHERE,NLVL)
      GO TO 300
  270 CALL ARC(ARRAY,TAUX,MAZZ,MZCOL,IE,ZHERE,NLVL)
      GO TO 300
  280 CALL ARC(ARRAY,TAUX,MAYY,MYCOL,IE,YHERE,NLVL)
      GO TO 300
  290 CALL ARC(ARRAY,TAUX,MAWW,MWCOL,IE,XHERE,NLVL)
C
CCC                                   STORE VALUES FOUND IN LOOK UP
C
  300 CCZ1(K)=YY
      CCLR1(K)=DUMY1
      CALR1(K)=DUMY2
  310 CONTINUE
C
CCC                                   SPECIAL CASE FOR LIFT LOOK UP
C
      GO TO (320,400,400,400), LDM
C
CCC                                   REPEAT FOR ALL VALUES OF TAU
C
  320 DO 390 K=NS,NP
      ALPHA=ATMP(K)
      CCLR=TERP(CAMBR,CAMB(K),CAMBT,CCLR1(K),CCLR2(K))
      CALR=TERP(CAMBR,CAMB(K),CAMBT,CALR1(K),CALR2(K))
      IF((ALPHA-CALR1(K))*(ALPHA-CALR2(K))) 340,330,330
  330 CCZ1(K)=TERP(CAMBR,CAMB(K),CAMBT,CCZ1(K),CCZ2(K))
      GO TO 390
  340 IF(CALR2(K)-CALR1(K)) 350,350,360
  350 IF(ALPHA-CALR) 370,370,380
  360 IF(ALPHA-CALR) 380,380,370
  370 CLA=TERP(CALR1(K),CALR2(K),ALPHA,CCLR1(K),CCZ1(K))
      CLC=TERP(CAMBR,CAMB(K),CAMBT,CLA,CCLR2(K))
```

```
      CCZ1(K)=TERP(CALR2(K),ALPHA,CALR,CLC,CCLR)
      GO TO 390
  380 CLB=TERP(CALR2(K),CALR1(K),ALPHA,CCLR2(K),CCZ2(K))
      CLC=TERP(CAMBR,CAMB(K),CAMBT,CCLR1(K),CLB)
      CCZ1(K)=TERP(CALR1(K),ALPHA,CALR,CLC,CCLR)
  390 CONTINUE
      RETURN
C
C                                     REGULAR INTERPOLATION BETWEEN TABLES
C
  400 DO 410 K=NS,NP
  410 CCZ1(K)=TERP(CAMBR,CAMB(K),CAMBT,CCZ1(K),CCZ2(K))
      RETURN
      END
      SUBROUTINE ARC(ARRAY,TAU,NROWS,NCOLS,IE,WHERE,NLVLS)
C
C                                     SUBROUTINE TO INTERPOLATE BETWEEN LEVELS OF
C                                     A GIVEN TABLE
C
      DIMENSION ARRAY(5,25,12),NROWS(6),NCOLS(6),CLR(2),ALR(2),TONY(19),
     1WHERE(2,6),YHERE(2,6),MYCOL(6),MAYY(6),CM(19),XHERE(2,6),MAWW(6),
     2MWCOL(6),C(19),EPS(19),TRANS(19),REY(19),ETA(19),HOPP(19),CLMAX(19
     3),ZHERE(2,6),HERE(2,6),Y(19),UAU(19),BETA(19,19),TRIX(19,19),MAZZ(
     46),MZCOL(6),MAXX(6),MXCOL(6)
      COMMON INNOW,ISWIT(3),ALPHA,REYN,CVAL,REYON,XMAX,ALMAX(19),CLMAX,C
     1,EPS,TRANS,REY,ETA,HOPP,ZHERE,HERE,ARRAY,Y,BETA,TFAC,TRIX,UAU,MAXX
     2,MAZZ,MXCOL,MZCOL,ASPEC,TAPER,BF,REYND,DISCR,PIER,CRB,Q,TSTAX,EDGE
     3,SIG,ALPHR,NFLAP,NLVL,NP,IY,IZ,IR,IP,IV,ISTAR,A,B,H,TAUT,TAUR,
     41WIST,R,BMX,YHERE,MYCOL,MAYY,FLAP,TONY,TWISA,X,Z,CM,ACC,XHERE,
     5MWCOL,MAWW,CAMB(19),CAMBR,CAMBT,DUMY1,DUMY2,NAME(25),AHERE(2,6),
     6MAAA(6),MACOL(6),BHERE(2,6),MABB(6),MBCOL(6),CHERE(2,6),MACC(6),
     7MCCOL(6),DHERE(2,6),MADD(6),MDCOL(6)
      IL=6
      XTRAL=0.
      XTRAU=0.
C
C                                     IS TAU LESS THAN OR EQUAL TO LOWEST LEVEL
C                                     TAU VALUE
C
      IF(TAU-WHERE(2,1)) 10,20,20
   10 J=2
      XTRAL=1.
      GO TO 80
   20 IF(TAU-WHERE(2,NLVLS)) 40,30,30
C
C                                     YES, SET J EQUAL TO MAX LEVEL
C
   30 J=NLVLS
      XTRAU=1.
      GO TO 80
C
C                                     NO, SEARCH LIST OF LEVELS (TAU VALUES)
C                                     UNTIL ONE GIVEN IS GREATER THAN ONE TO BE
C                                     FOUND
C
   40 DO 50 J=2,NLVLS
      IF(TAU-WHERE(2,J)) 90,90,50
   50 CONTINUE
C
C                                     ERROR IF NONE CAN BE FOUND
C
      IE=6
      IF(IE) 70,70,60
   60 WRITE(IP,540) IE,INNOW,CVAL,ALPHA,REYN,REYON,XMAX
   70 RETURN
   80 CONTINUE
   90 LVL=WHERE(1,J)
      MAXR=NROWS(J)
      MAXC=NCOLS(J)
```

```
      IF(ALPHA-999.) 100,130,100
  100 IF(REYN-999.) 110,120,110
  110 IF(CVAL-999.) 260,250,260
  120 IF(CVAL-999.) 240,260,240
  130 IF(CVAL-999.) 140,150,140
  140 IF(REYN-999.) 230,260,230
  150 IF(REYN-999.) 260,160,260
  160 IF(REYON-999.) 180,170,180
  170 IF(XMAX) 220,260,220
  180 IF(XMAX) 200,190,200
  190 IFLP=1
      GO TO 210
  200 IFLP=2
  210 IS=5
      GO TO 270
  220 IS=4
      GO TO 270
  230 IS=1
      GO TO 270
  240 IS=2
      GO TO 270
  250 IS=3
      GO TO 270
  260 IE=6
      RETURN
  270 CALL LOOK(ARRAY,LVL,MAXR,MAXC,IE)
      CLR(2)=DUMY2
      ALR(2)=DUMY1
      GO TO (280,290,300,310,320), IS
  280 FIND=ALPHA
      ALPHA=999.
      GO TO 350
  290 FIND=REYN
      REYN=999.
      GO TO 350
  300 FIND=CVAL
      CVAL=999.
      GO TO 350
  310 FIND=REYON
      REYON=999.
      GO TO 350
  320 FIND=XMAX
      GO TO (330,340), IFLP
  330 XMAX=0.
      GO TO 350
  340 XMAX=100.
  350 LVL=WHERE(1,J-1)
      MAXR=NROWS(J-1)
      MAXC=NCOLS(J-1)
C
C                                   SPECIAL PROCEDURE FOR INTERPOLATION IN THE
C                                   NEIGHBORHOOD OF CL MAX
C
      CALL LOOK(ARRAY,LVL,MAXR,MAXC,IE)
      CLR(1)=DUMY2
      ALR(1)=DUMY1
      IF(IE) 360,360,60
  360 R1=WHERE(2,J-1)
      R2=TAU
      R3=WHERE(2,J)
      C3=FIND
      GO TO (490,500,370,520,530), IS
  370 IF(INNOW-1) 380,390,380
  380 IF(INNOW-5) 510,390,510
  390 DUMY1=TERP(R1,R2,R3,CLR(1),CLR(2))
      DUMY2=TERP(R1,R2,R3,ALR(1),ALR(2))
      IF((ALPHA-ALR(1))*(ALPHA-ALR(2))) 400,510,510
  400 IF(XTRAL-1.) 410,420,410
  410 IF(XTRAU-1.) 440,430,440
```

```
  420 CVAL=DUMY1-CLR(1)+TERP(ALPHA,DUMY2,ALR(1),CLR(1),CVAL)
      RETURN
  430 CVAL=DUMY1-CLR(2)+TERP(ALPHA,DUMY2,ALR(2),CLR(2),C3)
      RETURN
  440 IF(ALR(2)-ALR(1)) 450,450,460
  450 IF(ALPHA-DUMY2) 470,470,480
  460 IF(ALPHA-DUMY2) 480,480,470
  470 CLA=TERP(ALR(1),ALR(2),ALPHA,CLR(1),CVAL)
      CLC=TERP(R1,R2,R3,CLA,CLR(2))
      CVAL=TERP(ALR(2),ALPHA,DUMY2,CLC,DUMY1)
      RETURN
  480 CLB=TERP(ALR(2),ALR(1),ALPHA,CLR(2),C3)
      CLC=TERP(R1,R2,R3,CLR(1),CLB)
      CVAL=TERP(ALR(1),ALPHA,DUMY2,CLC,DUMY1)
      RETURN
  490 C1=ALPHA
      ALPHA=TERP(R1,R2,R3,C1,C3)
      RETURN
  500 C1=REYN
      REYN=TERP(R1,R2,R3,C1,C3)
      RETURN
  510 C1=CVAL
      CVAL=TERP(R1,R2,R3,C1,C3)
      RETURN
  520 C1=REYON
      REYON=TERP(R1,R2,R3,C1,C3)
      RETURN
  530 C1=XMAX
      XMAX=TERP(R1,R2,R3,C1,C3)
      RETURN
C
  540 FORMAT(20X,12HERROR CODE (,I2,42H ) IF 1 CVAL GREATER THAN MAX VAL
     1UE LISTED/37X,34HIF 2 CVAL GREATER THAN TABLE VALUE/37X,41HIF 3 AL
     2PHA VALUE GREATER THAN TABLE VALUE/37X,29HIF 6 TAU VALUE CANNOT BE
     3FOUND/37X,13HTABLE NUMBER ,I2,8H IN CORE/10X,8HC-VALUE=,F10.2,5X,
     46HALPHA=,F10.2,5X,13HREYNOLDS NO.=,F10.2,5X,6HREYON=,F10.2,5X,5HXM
     5AX=,F10.2/120(1H/))
      END
      SUBROUTINE LOOK(AR,LVL,MAXR,MAXC,IE)
C
C                                     SUBROUTINE FOR TWO DIMENSIONAL TABLE LOOKUP
C
      DIMENSION A(5,25,12),TONY(19),YHERE(2,6),MYCOL(6),MAYY(6),CM(19),
     1XHERE(2,6),MAWW(6),MWCOL(6),C(19),EPS(19),TRANS(19),REY(19),ETA(19
     2),HOPP(19),CLMAX(19),ZHERE(2,6),HERE(2,6),Y(19),UAU(19),BETA(19,19
     3),TRIX(19,19),MAZZ(6),MZCOL(6),MAXX(6),MXCOL(6)
      COMMON INNOW,ISWIT(3),ALPHA,REYN,CVAL,REYON,XMAX,ALMAX(19),CLMAX,C
     1,EPS,TRANS,REY,ETA,HOPP,ZHERE,HERE,A,Y,BETA,TFAC,TRIX,UAU,MAXX,
     2MAZZ,MXCOL,MZCOL,ASPEC,TAPER,BF,REYND,DISCR,PIER,CRB,Q,TSTAX,EDGE,
     3SIG,ALPHR,NFLAP,NLVL,NP,IY,IZ,IR,IP,IS,ISTAR,AA,B,H,TAUT,TAUR,
     4TWIST,R,BMX,YHERE,MYCOL,MAYY,FLAP,TONY,TWISA,X,Z,CM,ACC,XHERE,
     5MWCOL,MAWW,CAMB(19),CAMBR,CAMBT,DUMY1,DUMY2
C
C                                     SECTION TO LOCATE REYNOLDS NUMBER IN TABLE
C
      XTRAL=0.
      XTRAU=0.
C
C                                     LROW IS THE LAST ROW CONTAINING INFORMATION
C                                     IN ANY TABLE. THE LAST TWO ROWS OF ANY
C                                     TABLE CONTAIN MAX DATA.
C
      LROW=MAXR-2
      IS=1
C
C                                     IS REYON EQUAL TO 999.
C                                     IF YES THEN NORMAL AND WE WILL ALREADY HAVE
C                                     SET THE SWITCH IS TO 1 AND WE WILL USE THE
C                                     VALUE OF REYN
```

```
C                                       IF NO THEN SET REYN TO REYON AND SET SWITCH
CC                                      IS TO 2
C
      IF(REYON-999.) 10,20,10
   10 REYN=REYON
      IS=2
C
CC                                      IS THE REYNOLDS NUMBER WE ARE LOOKING FOR
CC                                      GREATER THAN OR EQUAL TO THE REYNOLDS
CC                                      NUMBER GIVEN ALONG THE FIRST ROW OF THE
CC                                      TABLE
C
   20 IF(REYN-A(LVL,1,MAXC)) 40,30,30
   30 LOCR=MAXC
      XTRAU=1.
      GO TO 70
C
CC                                      NORMAL CASE. IF REYNOLDS NUMBER IS LESS
CC                                      THAN MAX REYN NUMBER IN TABLE THEN WE
CC                                      CHECK TO SEE IF IT IS GREATER THAN THE
CC                                      MINIMUM REYNOLDS NUMBER LISTED IN THE TABLE
C
   40 IF(REYN-A(LVL,1,2)) 50,60,60
C
CC                                      IF LESS THAN MINIMUM WE WANT TO USE THE
CC                                      MINIMUM VALUE IN THE TABLE
C
   50 LOCR=3
      XTRAL=1.
      GO TO 70
C
CC                                      IF LESS THAN MAXIMUM AND GREATER THAN
CC                                      MINIMUM WE WANT TO SEARCH TABLE UNTIL WE
CC                                      FIND A REYNOLDS NUMBER GREATER THAN THE
CC                                      GIVEN REYNOLDS NUMBER
CC                                      IF REYN LESS THAN KEEP LOOKING
CC                                      IF REYN GREATER THAN SET UP R1,R3 FOR
CC                                      INTERPOLATION
C
   60 DO 610 LOCR=3,MAXC
      IF(REYN-A(LVL,1,LOCR)) 70,70,610
   70 R1=A(LVL,1,LOCR-1)
      R3=A(LVL,1,LOCR)
      GO TO (80,150), IS
C
CC                                      SECTION FOR NORMAL LOOK UP OF ALPHA AND
CC                                      CVAL. A VALUE OF 999 SPECIFIES THAT THIS
CC                                      VARIABLE IS THE ONE WHOSE VALUE IS TO BE
CC                                      FOUND IN THE TABLE.
C
   80 IF(ALPHA-999.) 90,110,90
   90 IF(REYN-999.) 100,600,100
  100 IF(CVAL-999.) 600,190,600
  110 IF(CVAL-999.) 120,130,120
  120 IF(REYN-999.) 160,600,160
  130 IF(REYN-999.) 600,140,600
  140 IF(REYON-999.) 150,600,150
C
CC                                      SECTION FOR LOOKING UP MAX VALUES
C
  150 IF(XMAX) 580,590,580
C
CC                                      SECTION TO LOOK UP ALPHA FOR GIVEN CVAL BY
CC                                      INTERPOLATING BETWEEN COLUMNS WHERE
CC                                      REYNOLDS NUMBERS BRACKET GIVEN REYN
C
  160 DO 170 J=3,LROW
      CCC=TERP(R1,REYN,R3,A(LVL,J,LOCR-1),A(LVL,J,LOCR))
      IF(CVAL-CCC) 180,180,170
```

```
  170 CONTINUE
      IE=2
      GO TO 600
  180 CC2=TERP(R1,REYN,R3,A(LVL,J-1,LOCR-1),A(LVL,J-1,LOCR))
      ALPHA=TERP(CC2,CVAL,CCC,A(LVL,J-1,1),A(LVL,J,1))
      GO TO 600
C
C                                 LOOK UP CVAL FOR GIVEN ALPHA. CHECK TO SEE
C                                 IF WE HAVE A LIFT OR DRAG TABLE IN AT THIS
C                                 TIME. DRAG TABLES HAVE ZERO VALUES FOR ALL
C                                 MAXIMUM VALUES (LAST TWO ROWS).
C
  190 IF(A(LVL,MAXR,LOCR-1)) 210,200,210
  200 IF(A(LVL,MAXR,LOCR)) 210,550,210
C
C                                 FOR LIFT TABLE, DUMY1 AND DUMY2 ARE THE
C                                 MAXIMUM INTERPOLATED VALUES FOR GIVEN
C                                 REYNOLDS NUMBERS OF ALPHA MAX AND CVAL MAX
C
  210 CONTINUE
      DUMY1=TERP(R1,REYN,R3,A(LVL,MAXR,LOCR-1),A(LVL,MAXR,LOCR))
      DUMY2=TERP(R1,REYN,R3,A(LVL,MAXR-1,LOCR-1),A(LVL,MAXR-1,LOCR))
      IF(XTRAL-1.) 220,240,220
  220 IF(XTRAU-1.) 230,240,230
  230 CONTINUE
      IF((ALPHA-A(LVL,MAXR,LOCR-1))*(ALPHA-A(LVL,MAXR,LOCR)))240,250,250
  240 IF(A(LVL,MAXR,LOCR)-A(LVL,MAXR,LOCR-1)) 270,260,260
  250 GO TO 550
  260 ALPH1=A(LVL,MAXR,LOCR-1)
      ALPH2=A(LVL,MAXR,LOCR)
      GO TO 280
  270 ALPH1=A(LVL,MAXR,LOCR)
      ALPH2=A(LVL,MAXR,LOCR-1)
  280 IF(XTRAL-1.) 290,300,290
  290 IF(XTRAU-1.) 480,390,480
  300 IF(ALPH2-DUMY1) 350,550,310
  310 IF((ALPHA-DUMY1)*(ALPHA-ALPH2)) 320,550,550
  320 DO 330 J=3,LROW
      IF(ALPH2-A(LVL,J,1)) 340,340,330
  330 CONTINUE
      IE=3
      GO TO 600
  340 C1=A(LVL,J,LOCR-1)
      CVAL=DUMY2+(A(LVL,MAXR-1,LOCR-1)-C1)/(ALPH1-ALPH2)*(ALPHA-DUMY1)
      GO TO 600
  350 IF((ALPHA-DUMY1)*(ALPHA-ALPH1)) 360,550,550
  360 DO  370 J=3,LROW
      IF(ALPH1-A(LVL,J,1)) 380,380,370
  370 CONTINUE
      IE=3
      GO TO 600
  380 C1=A(LVL,J,LOCR-1)
      CVAL=DUMY2+(A(LVL,MAXR-1,LOCR-1)-C1)/(ALPH2-ALPH1)*(ALPHA-DUMY1)
      GO TO 600
  390 IF(ALPH2-DUMY1) 400,550,440
  400 IF((ALPHA-DUMY1)*(ALPHA-ALPH1)) 410,550,550
  410 DO 420 J=3,LROW
      IF(ALPH1-A(LVL,J,1)) 430,430,420
  420 CONTINUE
      IE=3
      GO TO 600
  430 C1=A(LVL,J,LOCR)
      CVAL=DUMY2+(A(LVL,MAXR-1,LOCR)-C1)/(ALPH2-ALPH1)*(ALPHA-DUMY1)
      GO TO 600
  440 IF((ALPHA-DUMY1)*(ALPHA-ALPH2)) 450,550,550
  450 DO 460 J=3,LROW
      IF(ALPH2-A(LVL,J,1)) 470,470,460
  460 CONTINUE
      IE=3
```

```
      GO TO 600
  470 C1=A(LVL,J,LOCR)
      CVAL=DUMY2+(A(LVL,MAXR-1,LOCR)-C1)/(ALPH2-ALPH1)*(ALPHA-DUMY1)
      GO TO 600
  480 IF(ALPHA-DUMY1) 490,490,520
  490 DO 500 J=3,LROW
      IF(ALPH1-A(LVL,J,1)) 510,510,500
  500 CONTINUE
      IE=3
      GO TO 600
  510 C1=A(LVL,J,LOCR-1)
      C3=A(LVL,J,LOCR)
      C1=TERP(R1,REYN,R3,C1,C3)
      CVAL=TERP(ALPH1,ALPHA,DUMY1,C1,DUMY2)
      GO TO 600
  520 DO 530 J=3,LROW
      IF(ALPH2-A(LVL,J,1)) 540,540,530
  530 CONTINUE
      IE=3
      GO TO 600
  540 C1=A(LVL,J,LOCR-1)
      C3=A(LVL,J,LOCR)
      C3=TERP(R1,REYN,R3,C1,C3)
      CVAL=TERP(DUMY1,ALPHA,ALPH2,DUMY2,C3)
      GO TO 600
  550 DO 560 J=3,LROW
C
C                                 SEARCH FOR ALPHA
C
      IF(ALPHA-A(LVL,J,1)) 570,570,560
  560 CONTINUE
      IE=3
      GO TO 600
  570 CCC=TERP(R1,REYN,R3,A(LVL,J-1,LOCR-1),A(LVL,J-1,LOCR))
      CC2=TERP(R1,REYN,R3,A(LVL,J,LOCR-1),A(LVL,J,LOCR))
      CVAL=TERP(A(LVL,J-1,1),ALPHA,A(LVL,J,1),CCC,CC2)
      GO TO 600
  580 XMAX=TERP(R1,REYN,R3,A(LVL,MAXR,LOCR-1),A(LVL,MAXR,LOCR))
      GO TO (600,620), IS
  590 XMAX=TERP(R1,REYN,R3,A(LVL,MAXR-1,LOCR-1),A(LVL,MAXR-1,LOCR))
      GO TO (600,620), IS
  600 RETURN
  610 CONTINUE
      IE=1
      GO TO 600
  620 REYN=999.
      GO TO 600
      END
      OVERLAY(BLINDA,1,0)
      PROGRAM ONE
      CALL MAIN
      RETURN
      END
      SUBROUTINE MAIN
C
C                                 SUBROUTINE MAIN IS THE MAIN PROGRAM FOR
C                                 AERODYNAMIC ANALYSIS OF STRAIGHT WING
C                                 AIRCRAFT. THIS IS THE FIRST OF A SERIES OF
C                                 OF MAIN SUBROUTINES.
C                                 THE SEQUENCE IS
C                                                 MAIN
C                                                 MAIN1
C                                      (FLAP)                  (NON FLAP)
C                                      MAIN3                   MAIN2
C                                      MAIN5                   MAIN4
C                                             (END OF PROGRAM)
C
C
C                                 LIFT1        WHERE  MXCUL  MAXX
```

```
C                                DRAG1        ZHERE   MZCOL   MAZZ
C                                PM1          YHERE   MYCOL   MAYY
C                                PMM(FLAP)    XHERE   MWCOL   MAWW
C                                LIFT2        AHERE   MACOL   MAAA
C                                DRAG2        BHERE   MBCOL   MABB
C                                PM2          CHERE   MCCOL   MACC
C                                PMM2(FLAP)   DHERE   MDCOL   MADD
C
      DIMENSION C(19),EPS(19),TRANS(19),REY(19),ETA(19),HOPP(19),CLMAX(1
     19),ZHERE(2,6),WHERE(2,6),ARRAY(5,25,12),Y(19),TAU(19),BETA(19,19),
     2MAZZ(6),MZCOL(6),MAXX(6),MXCOL(6),YHERE(2,6),MYCOL(6),MAYY(6),TRIX
     3(19,19),CM(19),DIST(19),YDA(19),YDAX(19),YX(19),TONY(19),ALPG(19),
     4ALPHZ(19),XHERE(2,6),MWCOL(6),MAWW(6)
      COMMON INNOW,ISWIT(3),ALPHA,REYN,CLL,REYON,XMAX,ALMAX(19),CLMAX,C,
     1EPS,TRANS,REY,ETA,HOPP,ZHERE,WHERE,ARRAY,Y,BETA,TFAC,TRIX,TAU,MAXX
     2,MAZZ,MXCOL,MZCOL,ASPEC,TAPER,BF,REYND,DISCR,PIER,CRB,Q,TSTAX,EDGE
     3,SIG,ALPHR,NFLAP,NLVL,NP,IY,IZ,IR,IP,IS,ISTAR,A,B,H,TAUT,TAUR,
     4TWIST,R,BWX,YHERE,MYCOL,MAYY,FLAP,TONY,TWISA,X,Z,CM,ACC,XHERE,
     5MWCOL,MAWW,CAMB(19),CAMBR,CAMBT,DUMY1,DUMY2,NAME(25),AHERE(2,6),
     6MAAA(6),MACOL(6),BHERE(2,6),MABB(6),MBCOL(6),CHERE(2,6),MACC(6),
     7MCCOL(6),DHERE(2,6),MADD(6),MDCOL(6)
C
C                                READER (IR) AND PRINTER (IP) LOGICAL UNIT
C                                NUMBERS
C
      IR=8
      IP=6
      REWIND 1
      REWIND 2
      REWIND 3
      REWIND 4
      REWIND 5
      REWIND 10
      REWIND 15
      REWIND 20
      REWIND 7
C
C                                INPUT DATA SECTION
C
      IS=1
      READ(IR,650) ASPEC,TAUT,TAUR,TAPER,TWIST,R,BF,REYND,DISCR,A,B,H,
     1ALPHR,NFLAP,FLAP,X,Z,TWISA,CAMBT,CAMBR
      IF(ASPEC-99.) 20,10,10
   10 CALL EXIT
   20 CONTINUE
C
C                                LAYOUT OF FOURTH DATA CARD
C
C                                FIELD 1   I1   NUMBER OF TAU VALUES PER TABLE
C
C                                FIELD 2   I1   1 FOR READ IN OF TAU, REY,ETC.
C                                               0 FOR NO READ IN
C
C                                FIELD 3   I1   1 FOR DUMP OF COMPUTED ARRAYS
C                                               0 FOR NO DUMP
C
C                                FIELD 4   I1   1 FOR DUMP OF BETA ARRAY
C                                               0 FOR NO DUMP
C
C                                FIELD 5   I1   1 READ CUBE 1 FROM TAPE, LOAD
C                                                 TO DISK, COPY CUBE 1 TO CUBE
C                                                 2 ON DISK.
C                                               2 READ CUBE 1 FROM TAPE, LOAD
C                                                 TO DISK, READ CUBE 2 FROM
C                                                 TAPE,LOAD TO DISK.
C                                               3 READ CUBE 1 FROM CARDS, LOAD
C                                                 TO TAPE, LOAD TO DISK, COPY
C                                                 CUBE 1 TO CUBE 2 ON DISK
C                                               4 READ CUBE 1 FROM CARDS, LOAD
```

```
C                                                  TO TAPE, LOAD TO DISK, READ
C                                                  CUBE 2 FROM CARDS, LOAD TO
C                                                  TAPE, LOAD TO DISK
C
C                                 FIELD 6   25A2   FIFTY COLUMNS OF IDENTIFING
C                                                  INFORMATION. THIS IS PRINTED
C                                                  AT THE TOP OF EACH PAGE OF
C                                                  OUTPUT
C
      READ (IR,660) NLVL,ISWIT,IG,NAME
C
C                                 SWITCH ZERO ON WILL READ IN VALUES FROM
C                                 CARDS FOR TAU, REY, C, EPS, EDGE, CRB, AND
C                                 ACC. FORMAT IS 16F5.0. ARRAYS ARE READ IN
C                                 ROWWISE
C
      CALL SETSW
      DO 30 J=1,6
      WHERE(1,J)=0.
      WHERE(2,J)=0.
      MAWW(J)=0
   30 MACOL(J)=0
      IY=0
      IF(IG-3) 80,40,40
   40 DO 50 J=1,4
      CALL AERDA(ARRAY,NLVL,WHERE,MACOL,MAWW,7,IY)
   50 WRITE(7) WHERE,MACOL,MAWW
      IF(IG-4) 80,60,80
   60 DO 70 J=1,4
      CALL AERDA(ARRAY,NLVL,WHERE,MACOL,MAWW,7,IY)
   70 WRITE(7) WHERE,MACOL,MAWW
   80 IK=1
      REWIND 7
      READ(7) ARRAY
      READ(7) WHERE,MXCOL,MAXX
      WRITE(IK) ARRAY
      IK=IK+1
      READ(7) ARRAY
      READ(7) ZHERE,MZCOL,MAZZ
      WRITE(IK) ARRAY
      IK=IK+1
      READ(7) ARRAY
      READ(7) YHERE,MYCOL,MAYY
      WRITE(IK) ARRAY
      IK=IK+1
      READ(7) ARRAY
      READ(7) XHERE,MWCOL,MAWW
      WRITE(IK) ARRAY
      REWIND 1
      REWIND 2
      REWIND 3
      REWIND 4
      IF(IG-1) 100,100,90
   90 IF(IG-3) 130,100,130
  100 IK=1
      DO 110 J=1,4
      READ(IK) ARRAY
      KK=IK*5
      IK=IK+1
  110 WRITE(KK) ARRAY
      DO 120 J=1,6
      AHERE(1,J)=WHERE(1,J)
      AHERE(2,J)=WHERE(2,J)
      BHERE(1,J)=ZHERE(1,J)
      BHERE(2,J)=ZHERE(2,J)
      CHERE(1,J)=YHERE(1,J)
      CHERE(2,J)=YHERE(2,J)
      DHERE(1,J)=XHERE(1,J)
      DHERE(2,J)=XHERE(2,J)
```

```
      MACOL(J)=MXCOL(J)
      MBCOL(J)=MZCOL(J)
      MCCOL(J)=MYCOL(J)
      MDCOL(J)=MWCOL(J)
      MAAA(J)=MAXX(J)
      MABB(J)=MAZZ(J)
      MACC(J)=MAYY(J)
  120 MADD(J)=MAWW(J)
      GO TO 140
  130 IK=5
      READ(7) ARRAY
      READ(7) AHERE,MACOL,MAAA
      WRITE(IK) ARRAY
      IK=IK+5
      READ(7) ARRAY
      READ(7) BHERE,MBCOL,MABB
      WRITE(IK) ARRAY
      IK=IK+5
      READ(7) ARRAY
      READ(7) CHERE,MCCOL,MACC
      WRITE(IK) ARRAY
      IK=IK+5
      READ(7) ARRAY
      READ(7) DHERE,MDCOL,MADD
      WRITE(IK) ARRAY
  140 REWIND 5
      REWIND 10
      REWIND 15
      REWIND 20
      REWIND 1
      REWIND 2
      REWIND 3
      REWIND 4
      ALPG(1)=0.
      NP=R-1.
      JP=R/2.
      PIER=3.14159/R
      CALL DATSW(0,I)
      GO TO (150,160), I
  150 READ(IR,670) (TAU(I),I=1,NP)
      READ(IR,670) (REY(I),I=1,NP)
      READ(IR,670) (C(I),I=1,NP)
      READ(IR,670) (EPS(I),I=1,NP)
      READ(IR,670) EDGE
      READ(IR,670) CRB
      READ(IR,670) ACC
  160 CONTINUE
C
CC                                    IF NO FUSE (FUSELAGE)
C
      IF(A) 410,410,170
  170 YO=B*SQRT(1.-H**2/A**2)
      ECC=SQRT(A**2-B**2)
      CALL DATSW(0,I)
      GO TO (190,180), I
  180 CRB=2.*(1.-YO)/(ASPEC*(1.+TAPER-2.*YO*TAPER))
  190 TFAC=1.-(YO*TAUR*CRB/(3.14159*A*B))**4.
      JPP=JP+1
C
CC                                    Y PRIME (I)
C
      DO 200 I=1,JPP
      XII=I-1
  200 YDA(I)=YO+(1.-YO)*COS(XII*PIER)
C
CC                                    CHECK IF FUSE ELLIPTICAL OR CIRCULAR
C
      IF(A-B) 230,230,210
C
```

```
C                                   ELLIPTICAL FUSE
C
  210 CONTINUE
      DISTX=0.5*(SQRT(1.+(H-ECC)**2)+SQRT(1.+(H+ECC)**2))
      BWX=1./(A-B)*(A-B*DISTX/SQRT(DISTX**2-ECC**2))
      DO 220 I=1,JPP
      DIST(I)=0.5*(SQRT(YDA(I)**2+(H-ECC)**2)+SQRT(YDA(I)**2+(H+ECC)**2
     1))
C
CC                                  Y BAR PRIME (I)
C
  220 YDAX(I)=(YDA(I)/(A-B)*(A-B*DIST(I)/SQRT(DIST(I)**2-ECC**2)))/BWX
      GO TO 250
C
CC                                  Y BAR PRIME (I) FOR CIRCULAR FUSE
C
  230 DO 240 I=1,JPP
  240 YDAX(I)=YDA(I)*(1.-A**2/(YDA(I)**2+H**2))
      BWX=1.-A**2/(1.+H**2)
C
CC                                  COMMON TO ELLIPTIC AND CIRCULAR FUSE
C
  250 DO 260 I=1,JPP
C
CC                                  Y BAR (I)
C
      AI=I-1
  260 YX(I)=COS(AI*PIER)
C
CC                                  Y (I)
C
      DO 270 I=2,JPP
  270 Y(I)=TERP(YDAX(I-1),YX(I),YDAX(I),YDA(I-1),YDA(I))
      DO 280 I=1,JP
      Y(I)=Y(I+1)
  280 YX(I)=YX(I+1)
      M=JP-1
      DO 290 I=1,M
      IRI=R
      IRI=IRI-I
      YX(IRI)=-YX(I)
  290 Y(IRI)=-Y(I)
      IF(A-B) 360,360,300
C
CC                                  FUSE IS ELLIPTICAL
C
  300 DO 310 I=1,JP
      DIST(I)=0.5*(SQRT(Y(I)**2+(H-ECC)**2)+SQRT(Y(I)**2+(H+ECC)**2))
      Q=DIST(I)/SQRT(DIST(I)**2-ECC**2)
      S=1.+(ECC*Y(I)/(DIST(I)**2-ECC**2))**2
      TRANS(I)=1./(A-B)*(A-B*Q/S)
      IRI=R
      IRI=IRI-I
  310 TRANS(IRI)=TRANS(I)
C
CC                                  WING ON TOP OR BOTTOM OF FUSELAGE
C
      IF(A-H) 320,320,350
  320 TRANS(JP)=1.
  330 IF(NFLAP) 520,520,340
  340 IF(BF-1.) 350,520,520
  350 DISF=0.5*(SQRT(BF**2+(H-ECC)**2)+SQRT(BF**2+(H+ECC)**2))
      BFX=(BF/(A-B)*(A-B*DISF/SQRT(DISF**2-ECC**2)))/BWX
      GO TO 460
  360 DO 370 I=1,JP
      TRANS(I)=1.+A**2*(Y(I)**2-H**2)/((Y(I)**2+H**2)**2)
      IRI=R
      IRI=IRI-I
  370 TRANS(IRI)=TRANS(I)
```

```
      IF(A-H) 380,380,390
  380 TRANS(JP)=1.0
  390 IF(BF-1.) 400,520,520
  400 BFX=(BF*(1.-A**2/(BF**2+H**2)))/BWX
      GO TO 460
  410 DO 420 I=1,NP
      AI=I
      Y(I)=COS(AI*PIER)
      YX(I)=Y(I)
  420 TRANS(I)=1.
      YO=0.
C
C                                 SPECIAL CASE IF VALUES HAVE BEEN READ IN
C                                 DO NOT WANT TO COMPUTE CRB.
C                                 WILL NOT COMPUTE VALUES ALREADY READ IN
C
      CALL DATSW(0,I)
      GO TO (440,430), I
  430 CRB=2.*(1.-YO)/(ASPEC*(1.+TAPER-2.*YO*TAPER))
  440 TFAC=1.
      BWX=1.
      IF(BF-1.) 450,520,520
  450 BFX=BF
  460 TSTAX=ACOS(BFX/BWX)
      DO 510 I=1,JP
      AI=I
      C3=AI*PIER
      TSTX=TSTAX
      IF(C3-TSTX) 510,470,480
  470 TSTAX=C3
      ISTAR=I
      GO TO 520
  480 AM=C3-TSTAX
      C1=(AI-1.)*PIER
      AK=TSTAX-C1
      IF(AM-AK) 490,490,500
  490 ISTAR=I
      TSTAX=C3
      GO TO 520
  500 ISTAR=I-1
      TSTAX=C1
      GO TO 520
  510 CONTINUE
  520 CALL DATSW(0,I)
      GO TO (550,530), I
  530 EDGE=SQRT(1.+4./(ASPEC**2))
      DO 540 I=1,NP
      C(I)=1.-(1.-TAPER)*(ABS(Y(I))-YO)/(1.-YO)
      TAU(I)=TAUR/C(I)*(1.-(1.-TAPLR*TAUT/TAUR)*(ABS(Y(I))-YO)/(1.-YO))
      CAMB(I)=CAMBR+(CAMBT-CAMBR)*(ABS(Y(I))-YO)/(1.-YO)
      ACC=0.6666*(1.+TAPER*(1.+TAPER))/(1.+TAPER)
  540 REY(I)=REYND*C(I)/ACC
  550 LOCFR=3
      ALPHA=999.
      CLL=0.
      REYON=999.
      XMAX=0.
C
C                                 LOOK UP ZERO LIFT ANGLE FOR TIP SECTION
C
      CALL BRIDG(ALPHZ,1,1,1,IY,IE,REY,TAU,CAMB,ALPHA,1,1,ALPHA)
      IF(IE) 560,560,640
C
C                                 LOOK UP ZERO LIFT ANGLE FOR ROOT SECTION
C
  560 ALPHA=999.
      CALL BRIDG(ALPHZ,JP,JP,1,IY,IE,REY,TAU,CAMB,ALPHA,1,1,ALPHA)
      IF(IE) 570,570,640
C
```

```
C                                   CALCULATE AERODYNAMIC AND GEOMETRIC TWIST
C
  570 IF(TWISA-100.) 580,590,590
  580 TWIST=TWISA-(ALPHZ(JP)-ALPHZ(1))
      GO TO 600
  590 TWISA=TWIST+(ALPHZ(JP)-ALPHZ(1))
  600 CALL DATSW(0,I)
      GO TO (630,610), I
  610 DO 620 I=1,NP
  620 EPS(I)=TWIST*TAPER*(ABS(Y(I))-YO)/(C(I)*(1.-YO))
  630 LOCER=1
      CLL=999.
      ALPHA=999.
      REYN=999.
      REYCN=0.
C
CC                                  FOR XMAX=100. ARC WILL LOOK UP ALPHA MAX
CC                                  FOR XMAX=0. ARC WILL LOOK UP CL MAX
C
      XMAX=100.
      CALL BRIDG(ALMAX,1,NP,1,IY,IE,REY,TAU,CAMB,ALPHA,1,1,XMAX)
      CALL MAIN1
      RETURN
  640 WRITE(IP,680) IF,LOCER
      CALL EXIT
C
  650 FORMAT(8F10.0/5F10.0,I10,4F5.0/2F10.0)
  660 FORMAT(9I1,25A2)
  670 FORMAT(16F5.0)
  680 FORMAT(1X,11HERROR CODE ,I2,13H -IN SECTION ,I3,9H  ABORTED)
      END
      SUBROUTINE MAIN1
C
CC                                  CONTINUATION OF SUBROUTINE MAIN
C
      DIMENSION C(19),EPS(19),TRANS(19),REY(19),ETA(19),HOPP(19),CLMAX(
     119),ZHERE(2,6),WHERE(2,6),ARRAY(5,25,12),Y(19),TAU(19),BETA(19,19)
     2,MAZZ(6),MZCOL(6),MAXX(6),MXCOL(6),YHERE(2,6),MYCOL(6),MAYY(6),
     3TRIX(19,19),THE(19),TONY(19),GENE(19),SIGMA(19),LL(19),MM(19),CM(
     419),XHERE(2,6),MWCOL(6),MAWW(6)
      COMMON INNOW,ISWIT(3),ALPHA,REYN,CLL,REYCN,XMAX,ALMAX(19),CLMAX,C,
     1EPS,TRANS,REY,ETA,HOPP,ZHERE,WHERE,ARRAY,Y,BETA,TFAC,TRIX,TAU,MAXX
     2,MAZZ,MXCOL,MZCOL,ASPEC,TAPER,BF,REYND,DISCR,PIER,CRB,Q,TSTAX,EDGE
     3,SIG,ALPHR,NFLAP,NLVL,NP,IY,IZ,IR,IP,IS,ISTAR,A,B,H,TAUT,TAUR,
     4TWIST,R,BWX,YHERE,MYCOL,MAYY,FLAP,TONY,TWISA,X,Z,CM,ACC,XHERE,
     5MWCOL,MAWW,CAMB(19),CAMBR,CAMBT,DUMY1,DUMY2,NAME(25),AHERE(2,6),
     6MAAA(6),MACOL(6),BHERE(2,6),MABB(6),MBCOL(6),CHERE(2,6),MACC(6),
     7MCCOL(6),DHERE(2,6),MADD(6),MDCOL(6)
C
CC                                  COMPUTATION OF BETA
C
      DO 80 M=1,NP
      DO 80 K=1,NP
      AK=K
      AM=M
      IF(K-M) 20,10,20
   10 BETA(M,K)=180.*R/(8.*3.14159*SIN(AK*PIER))
      GO TO 50
   20 KK=IABS(K-M)-2*((IABS(K-M))/2)
      IF(KK-1) 40,30,40
   30 BETA(M,K)=180./(4.*3.14159*R*SIN(AK*PIER))*(1./(1.-COS((AK+AM)*
     13.14159/R))-1./(1.-COS((AK-AM)*3.14159/R)))
      GO TO 50
   40 BETA(M,K)=0.
   50 IF(M-K) 70,60,70
   60 TRIX(M,K)=1.+0.1*C(K)*CRB/BWX*BETA(M,K)*TRANS(K)
      GO TO 80
   70 TRIX(M,K)=0.1*C(K)*CRB/BWX*BETA(M,K)*TRANS(K)
   80 CALL DATSW(4,I)
```

```
      GO TO (90,100), I
   90 WRITE(IP,430)
      CALL SSS(BETA,NP)
  100 DO 110 I=1,NP
      AI=I
  110 ETA(I)=0.523598/R*(3.-(-1.)**I)*SIN(AI*PIER)
C
CC                                    CHECK IF FLAP CASE
C
      IF(NFLAP) 310,310,120
C
CC                                    IS THERE A PART-SPAN FLAP
C
  120 IF(BF-1.) 130,310,310
  130 DO 170 I=1,NP
      AI=I
      THE(I)=AI*PIER
      IF(THE(I)-TSTAX) 150,140,150
  140 TONY(I)=1./45.*TSTAX*SIN(THE(I))
      GO TO 160
  150 TONY(I)=1./90.*((COS(THE(I))-COS(TSTAX))*(ALOG(1.-COS(THE(I)+TSTAX
     1))-ALOG(1.-COS(THE(I)-TSTAX)))+2.*TSTAX*SIN(THE(I)))
  160 GENE(I)=1./90.*((COS(THE(I))+COS(TSTAX))*(ALOG(1.+COS(THE(I)-TSTAX
     1))-ALOG(1.+COS(THE(I)+TSTAX)))+2.*(3.14159-TSTAX)*SIN(THE(I)))
  170 CONTINUE
C
CC                                    CHECK FOR DUMP
C
      CALL DATSW(3,I)
      GO TO (180,190), I
  180 WRITE(IP,440)
      CALL AAA(GENE,NP)
      WRITE(IP,450)
      CALL AAA(TONY,NP)
  190 DO 230 K=1,NP
      SUM=0.
      DO 200 M=1,NP
  200 SUM=TONY(M)*BETA(M,K)+SUM
      IF(K-ISTAR) 210,210,220
  210 HOPP(K)=1.-SUM
      GO TO 230
  220 HOPP(K)=-SUM
  230 CONTINUE
      DO 270 K=1,NP
      SUM=0.
      DO 240 M=1,NP
  240 SUM=GENE(M)*BETA(M,K)+SUM
      IRI=K
      IF(K-IRI+ISTAR) 250,260,260
  250 SIGMA(K)=1.-SUM
      GO TO 270
  260 SIGMA(K)=-SUM
  270 CONTINUE
      DO 280 K=1,NP
      HOPP(K)=SIGMA(K)-HOPP(K)
  280 TONY(K)=GENE(K)-TONY(K)
C
CC                                    CHECK FOR DUMP
C
      CALL DATSW(3,I)
      GO TO (290,300), I
  290 WRITE(IP,460)
      CALL AAA(HOPP,NP)
      WRITE(IP,470)
      CALL AAA(SIGMA,NP)
      WRITE(IP,440)
      CALL AAA(GENE,NP)
      WRITE(IP,450)
      CALL AAA(TONY,NP)
```

```
  300 CONTINUE
  310 IBTA=1
C
CC                                    STORE BETA TEMPORARILY ON DISK SO WE CAN
CC                                    COMPUTE THE TRANSPOSE OF TRIX
C
      REWIND 44
      WRITE(44) BETA
      REWIND 44
C
CC                                    STORE TRIX IN BETA
C
      DO 320 M=1,NP
      DO 320 K=1,NP
  320 BETA(M,K)=TRIX(M,K)
C
CC                                    NOW TRANSPOSE BETA (OLD TRIX)
C
      DO 330 M=1,NP
      DO 330 K=1,NP
  330 TRIX(M,K)=BETA(K,M)
      IBTA=1
C
CC                                    RESTORE BETA
C
      READ(44) BETA
C
CC                                    INVERT TRIX
C
      CALL MINV(TRIX,NP,AK,LL,MM)
      CALL DATSW(4,I)
      GO TO (340,350), I
  340 WRITE(IP,480)
      CALL SSS(TRIX,NP)
  350 IF(NFLAP-1) 360,370,370
  360 WRITE(IP,490) NAME
      WRITE(IP,500)
      CALL AAA(Y,NP)
      WRITE(IP,510)
      CALL AAA(CLMAX,NP)
C
CC                                    SET UP FOR CL MAX LOOK UP
C
      IY=1
      REYON=0.
      ALPHA=999.
      CLL=999.
      REYN=999.
C
CC                                    LOOK UP CL MAX VALUES
C
      XMAX=0.
      CALL BRIDG(CLMAX,1,NP,1,IY,IE,REY,TAU,CAMB,ALPHA,1,1,XMAX)
      WRITE(IP,520)
      CALL AAA(CLMAX,NP)
  370 IF(NFLAP) 380,380,390
  380 WRITE(IP,530)
      CALL AAA(TAU,NP)
      WRITE(IP,540)
      CALL AAA(REY,NP)
      WRITE(IP,550)
      CALL AAA(C,NP)
      WRITE(IP,560)
      CALL AAA(EPS,NP)
      WRITE(IP,570)
      CALL AAA(CAMB,NP)
      IF(NFLAP-1) 420,390,390
C
C                                     CHECK FOR DUMP
```

```
C
  390 CALL DATSW(3,I)
      GO TO (400,420), I
  400 CALL DATSW(3,I)
      GO TO (420,410), I
  410 WRITE(IP,580)
      STAR=ISTAR
      CALL ZZZ(STAR)
      WRITE(IP,450)
      CALL AAA(TONY,NP)
      WRITE(IP,440)
      CALL AAA(GENE,NP)
      WRITE(IP,460)
      CALL AAA(HOPP,NP)
  420 RETURN
C
  430 FORMAT(10X,11HMATRIX BETA)
  440 FORMAT(10X,4HGENE)
  450 FORMAT(10X,4HTONY)
  460 FORMAT(10X,4HHOPP)
  470 FORMAT(10X,5HSIGMA)
  480 FORMAT(10X,11HMATRIX TRIX)
  490 FORMAT(1H1/1HO/35X,25A2/1X)
  500 FORMAT(1X/10X,17HSPANWISE STATIONS)
  510 FORMAT(10X,9HALPHA MAX)
  520 FORMAT(10X,7H CL MAX)
  530 FORMAT(10X,30HTHICKNESS / CHORD DISTRIBUTION)
  540 FORMAT(10X,24HSECTION REYNOLDS NUMBERS)
  550 FORMAT(10X,18HCHORD DISTRIBUTION)
  560 FORMAT(10X,16HTWIST DISTRIBUTION)
  570 FORMAT(10X,19HCAMBER DISTRIBUTION)
  580 FORMAT(10X,5HISTAR)
      END
      OVERLAY(BLINDA,2,0)
      PROGRAM TWO
      DIMENSION ARRAY(5,25,12),C(19),EPS(19),TRANS(19),REY(19),ETA(19),
     1HOPP(19),CLMAX(19),ZHERE(2,6),WHERE(2,6),Y(19),TAU(19),BETA(19,19)
     2,TRIX(19,19),MAZZ(6),MZCOL(6),MAXX(6),MXCOL(6),CBG(19),CVAL(19),
     3ALPG(19),CBC(19),ALPHU(19),ALPH(19),ALPHZ(19),ALPHE(19),DELTA(19),
     4ALPHV(20),YHERE(2,6),MYCOL(6),MAYY(6),CM(19),XHERE(2,6),MAWW(6),
     5MWCOL(6)
      COMMON INNOW,ISWIT(3),ALPHA,REYN,CLL,REYON,XMAX,ALMAX(19),CLMAX,C,
     1EPS,TRANS,REY,ETA,HOPP,ZHERE,WHERE,ARRAY,Y,BETA,TFAC,TRIX,TAU,MAXX
     2,MAZZ,MXCOL,MZCOL,ASPEC,TAPER,BF,REYND,DISCR,PIER,CRB,Q,TSTAX,EDGE
     3,SIG,ALPHR,NFLAP,NLVL,NP,IY,IZ,IR,IP,IG,ISTAR,A,B,H,TAUT,TAUR,
     4TWIST,R,BWX,YHERE,MYCOL,MAYY,FLAP,TONY(19),TWISA,X,Z,CM,ACC,XHERE,
     5MWCOL,MAWW,CAMB(19),CAMBR,CAMBT,DUMY1,DUMY2,NAME(25),AHERE(2,6),
     6MAAA(6),MACOL(6),BHERE(2,6),MABB(6),MBCOL(6),CHERE(2,6),MACC(6),
     7MCCOL(6),DHERE(2,6),MADD(6),MDCOL(6),CVAL,ALPHU,CBC,CBG,DELTA,
     8ALPHZ,ALPH,ALPHV,ALPHE,ALPHB,IPRAB,ISS,IQT,DIR,IAGN
   10 CALL MAIN2
      CALL MAIN4
      IF(IQT-2) 10,20,20
   20 RETURN
      END
      SUBROUTINE MAIN2
C
C                                  SUBROUTINE FOR THE CASE WITHOUT A FLAP
C
      DIMENSION ARRAY(5,25,12),C(19),EPS(19),TRANS(19),REY(19),ETA(19),
     1HOPP(19),CLMAX(19),ZHERE(2,6),WHERE(2,6),Y(19),TAU(19),BETA(19,19)
     2,TRIX(19,19),MAZZ(6),MZCOL(6),MAXX(6),MXCOL(6),CBG(19),CVAL(19),
     3ALPG(19),CBC(19),ALPHU(19),ALPH(19),ALPHZ(19),ALPHE(19),DELTA(19),
     4ALPHV(20),YHERE(2,6),MYCOL(6),MAYY(6),CM(19),XHERE(2,6),MAWW(6),
     5MWCOL(6)
      COMMON INNOW,ISWIT(3),ALPHA,REYN,CLL,REYON,XMAX,ALMAX(19),CLMAX,C,
     1EPS,TRANS,REY,ETA,HOPP,ZHERE,WHERE,ARRAY,Y,BETA,TFAC,TRIX,TAU,MAXX
     2,MAZZ,MXCOL,MZCOL,ASPEC,TAPER,BF,REYND,DISCR,PIER,CRB,Q,TSTAX,EDGE
     3,SIG,ALPHR,NFLAP,NLVL,NP,IY,IZ,IR,IP,IG,ISTAR,A,B,H,TAUT,TAUR,
```

```
     4TWIST,R,BWX,YHERE,MYCOL,MAYY,FLAP,TONY(19),TWISA,X,Z,CM,ACC,XHERE,
     5MWCOL,MAWW,CAMB(19),CAMBR,CAMBT,DUMY1,DUMY2,NAME(25),AHERE(2,6),
     6MAAA(6),MACOL(6),BHERE(2,6),MABB(6),MBCOL(6),CHERE(2,6),MACC(6),
     7MCCOL(6),DHERE(2,6),MADD(6),MDCOL(6),CVAL,ALPHU,CBC,CBG,DELTA,
     8ALPHZ,ALPH,ALPHV,ALPHE,ALPHB,IPRAB,ISS,IQT,DIR,IAGN
C
C                                    LOOPING PARAMETER. IF IR (THE LOGICAL UNIT
C                                    NUMBER OF THE READER) IS SET PROPERLY AT
C                                    THIS TIME THEN THIS IS THE FIRST ENTRY INTO
C                                    THIS SUBROUTINE. IF IR IS 100 THEN WE WISH
C                                    TO ITERATE AGAIN TO FIND CONVERGENCE.
C
      IF(IR-8) 20,10,60
   10 IW=1
      IPRAB=1
      IS=1
      ISS=IS
C
C                                    INPUT OF ALPHA VALUES TO BE USED FOR THIS
C                                    RUN. A LIST OF ALPHA VALUES MAY BE
C                                    TERMINATED IN TWO WAYS. (1) INCLUDE ALPHA
C                                    VALUES LARGE ENOUGH TO CAUSE A STALL. (2)
C                                    END LIST OF VALUES WITH A 99.
C
      READ(IR,320) ALPHV
      IR=100
      GO TO 30
C
C                                    IF IR IS ZERO THEN WE WISH TO TAKE THE NEXT
C                                    ALPHA VALUE
C
   20 IS=ISS
      IPRAB=IPRAB+1
   30 DIR=0.
      IQT=1
      ALPHB=ALPHV(IPRAB)
C
C                                    TEST FOR END OF ALPHA VALUES
C
      IF(ALPHB-99.) 50,40,50
   40 CALL EXIT
   50 WRITE(IP,330) NAME
      WRITE(IP,340) ALPHB,DISCR,A,B,ASPEC,H,ALPHR,TAUT
      WRITE(IP,350) TAUR,TWIST,R,TWISA,BF,TAPER,FLAP,REYND,X,Z
      WRITE(IP,360)
      IAGN=0
   60 ITR=0
      IS=ISS
      IY=1
      LOCLR=2
      DO 70 K=1,NP
   70 ALPG(K)=ALPHB+ALPHR+EPS(K)+ALPHB*TFAC*(TRANS(K)-1.)
C
C                                    SWITCH NUMBER 3 IS USED FOR AN INTERNAL
C                                    DUMP OF ARRAYS COMPUTED DURING  ITERATION
C                                    PROCESS
C
      CALL LATSW(3,JUNK)
      GO TO (80,90), JUNK
   80 WRITE(IP,370)
      CALL AAA(ALPG,NP)
C
C                                    FIND CL(K)
C
   90 CLL=999.
      REYON=999.
      XMAX=0.
      CALL BRIDG(CVAL,1,NP,1,IY,IE,REY,TAU,CAMB,ALPG,1,NP,CLL)
      IF(IE) 100,100,310
```

```
  100 DO 110 K=1,NP
      AK=K
  110 CBG(K)=CVAL(K)*(ASPEC/(ASPEC+1.8))*C(K)*CRB*(0.5+(1.+TAPER)*SIN(AK
     1*PIER)/(3.14159*C(K)))
C
C                                     CHECK FOR DUMP
C
      CALL DATSW(3,JUNK)
      GO TO (120,130), JUNK
  120 WRITE(IP,380)
      CALL AAA(CVAL,NP)
C
C                                     LOOK UP ALPHA VALUE FOR ZERO LIFT
C
  130 LOCER=3
      ALPHA=999.
      CLL=.0001
      REYON=999.
      XMAX=0.
      CALL BRIDG(ALPHZ,1,NP,1,IY,IE,REY,TAU,CAMB,ALPHA,1,1,ALPHA)
      IF(IE) 140,140,310
  140 DO 160 K=1,NP
      SIG=0.
      DO 150 M=1,NP
  150 SIG=CBG(M)*BETA(M,K)+SIG
      ALPHU(K)=SIG*(1.+TFAC*(TRANS(K)-1.))
      ALPH(K)=ALPG(K)-ALPHU(K)
  160 ALPHE(K)=(ALPH(K)-ALPHZ(K)*(1.-EDGE))/EDGE
C
C                                     LOOK UP CL VALUES FOR A LIST OF ALPHA
C                                     VALUES
C
      LOCER=4
      CLL=999.
      REYON=999.
      XMAX=0.
      CALL BRIDG(CVAL,1,NP,1,IY,IE,REY,TAU,CAMB,ALPHE,1,NP,CLL)
      IF(IE) 170,170,310
  170 DO 180 K=1,NP
      CBC(K)=CVAL(K)*C(K)*CRB/BWX
  180 DELTA(K)=CBC(K)-CBG(K)
C
C                                     CHECK FOR DUMP
C
      CALL DATSW(3,JUNK)
      GO TO (190,200), JUNK
  190 WRITE(IP,390)
      CALL AAA(CBG,NP)
      WRITE(IP,410)
      CALL AAA(ALPHU,NP)
      WRITE(IP,420)
      CALL AAA(ALPHE,NP)
      WRITE(IP,380)
      CALL AAA(CVAL,NP)
      WRITE(IP,420)
      CALL AAA(CBC,NP)
      WRITE(IP,430)
      CALL AAA(DELTA,NP)
C
C                                     CHECK TOLERANCE
C
  200 DO 220 K=1,NP
      IF(ABS(DELTA(K))-DISCR) 210,210,230
  210 IF(K-NP) 220,300,300
  220 CONTINUE
  230 DO 250 I=1,NP
      SUM=0.
      DO 240 J=1,NP
  240 SUM=TRIX(I,J)*DELTA(J)+SUM
```

```
  250 CBG(I)=CBG(I)+SUM
C
C                                   CHECK FOR DUMP
C
      CALL DATSW(3,JUNK)
      GO TO (260,270), JUNK
  260 WRITE(IP,390)
      CALL AAA(CBG,NP)
C
C                                   REPEAT CYCLE
C
  270 ITR=ITR+1
      IF(ITR-30) 130,130,280
C
C                                   IF UNABLE TO CONVERGE AFTER 30 ITERATIONS
C                                   DUMP DELTA VALUES, C VALUES, AND TABLE
C                                   PRESENTLY IN CORE BEING USED FOR LOOK UP
C
  280 WRITE(IP,440)
      WRITE(IP,430)
      CALL AAA(DELTA,NP)
      WRITE(IP,380)
      CALL AAA(CVAL,NP)
      DO 290 J=1,NLVL
      NR=MAXX(J)
      NC=MXCOL(J)
      TAUX=WHERE(2,J)
      WRITE(IP,450) J,J,NR,NC,TAUX
      DO 290 K=1,NR
  290 WRITE(IP,460) (ARRAY(J,K,L),L=1,NC)
      CALL EXIT
  300 WRITE(IP,470) ITR,ALPHB
      ISS=IS
      RETURN
  310 WRITE(IP,480) IE,LOCER
      CALL EXIT
C
  320 FORMAT(10F8.0)
  330 FORMAT(1H1/1H0/35X,25A2/1X)
  340 FORMAT(1X,40(3H./.)/1H0/15X,30HBODY ANGLE OF ATTACK, DEG. . =,F10.
     12,10X,30HVALUE OF DISCRIMINANT. . . . =,F10.6/15X,30HBODY HEIGHT /
     2 SPAN . . . . . =,F10.2,10X,30HBODY WIDTH / SPAN. . . . . =,F10.
     32/15X,30HASPECT RATIO . . . . . =,F10.2,10X,30HWING HEIGHT /
     4 SPAN . . . . . =,F10.2/15X,30HWING BODY INCIDENCE, DEG . . =,F10.
     52,10X,30HTIP THICKNESS CHORD. . . . . =,F10.2)
  350 FORMAT(15X,30HROOT THICKNESS CHORD . . . . =,F10.2,10X,30HGEOMETRI
     1C TWIST, DEG . . . . =,F10.2/15X,30HNUMBER OF SPANWISE STATIONS.
     2,F10.2,10X,30HAERODYNAMIC TWIST, DEG . . . =,F10.2/15X,30HFLAP SPA
     3N / WING SPAN. . . . =,F10.2,10X,30HTAPER RATIO. . . . . =
     4,F10.2/15X,30HFLAP SETTING, DEG. . . . . =,F10.2,10X,30HREYNOLDS
     5 NUMBER. . . . . =,F10.2/15X,37HCOORDINATES OF MOMENT REFERENC
     6E POINT,14X,2HX=,F10.2,9X,2HZ=,F10.2)
  360 FORMAT(1H0/1X,40(3H./.)/1X)
  370 FORMAT(10X,4HALPG)
  380 FORMAT(10X,4HCVAL)
  390 FORMAT(10X,3HCBG)
  400 FORMAT(10X,5HALPHU)
  410 FORMAT(10X,5HALPHE)
  420 FORMAT(10X,3HCBC)
  430 FORMAT(10X,5HDELTA)
  440 FORMAT(1X,48HUNABLE TO CONVERGE AFTER 30 ITERATIONS   ABURTED)
  450 FORMAT(1H0/1H0,7H ARRAY(,I2,11H 1, 1) TO (,I2,1H,,I2,1H,,I2,1H),F1
     10.5/1H0)
  460 FORMAT(12F10.4)
  470 FORMAT(10X,I2,63H  ITERATIONS REQUIRED TO CONVERGE FOR ANGLE OF AT
     1TACK EQUAL TO ,F8.1/1X)
  480 FORMAT(1X,10HERROR CODE,I2,1X,10HAT SECTION,I3,1X,32HIN PROGRAM, E
     1XECUTION TERMINATED)
      END
```

```
      SUBROUTINE MAIN4
C
CC                                    CONTINUATION OF SUBROUTINE MAIN2
C
      DIMENSION ARRAY(5,25,12),C(19),EPS(19),TRANS(19),REY(19),ETA(19),
     1HOPP(19),CLMAX(19),ZHERE(2,6),WHERE(2,6),Y(19),TAU(19),BETA(19,19)
     2,TRIX(19,19),MAZZ(6),MZCOL(6),MAXX(6),MXCOL(6),ALPG(19),ALPHE(19),
     3CL(19),CDO(19),CDOC(19),ALPHU(19),CBG(19),CBG(19),DELTA(19),ALPHZ(
     419),ALPH(19),ALPHV(20),CVAL(19),YHERE(2,6),MYCOL(6),MAYY(6),CM(19)
     5,XHERE(2,6),MAWW(6),MWCOL(6)
      COMMON INNOW,ISWIT(3),ALPHA,REYN,CLL,REYON,XMAX,ALMAX(19),CLMAX,C,
     1EPS,TRANS,REY,ETA,HOPP,ZHERE,WHERE,ARRAY,Y,BETA,TFAC,TRIX,TAU,MAXX
     2,MAZZ,MXCOL,MZCOL,ASPEC,TAPER,BF,REYND,DISCR,PIER,CRB,Q,TSTAX,EDGE
     3,SIG,ALPHR,NFLAP,NLVL,NP,IY,IZ,IR,IP,IG,ISTAR,A,B,H,TAUT,TAUR,
     4TWIST,R,BWX,YHERE,MYCOL,MAYY,FLAP,TONY(19),TWISA,X,Z,CM,ACC,XHERE,
     5MWCOL,MAWW,CAMB(19),CAMBR,CAMBT,DUMY1,DUMY2,NAME(25),AHERE(2,6),
     6MAAA(6),MACOL(6),BHERE(2,6),MABB(6),MBCOL(6),CHERE(2,6),MACC(6),
     7MCCOL(6),DHERE(2,6),MADD(6),MDCOL(6),CVAL,ALPHU,CBC,CBG,DELTA,
     8ALPHZ,ALPH,ALPHV,ALPHE,ALPHB,IPRAB,ISS,IQT,DIR,IAGN
      IS=ISS
      IKT=2
      DO 10 K=1,NP
   10 CL(K)=CVAL(K)
      IZ=1
      LOCER=5
C
CC                                    COMPUTE PROFILE DRAG COEFFICIENTS
C
      CLL=999.
      REYON=999.
      XMAX=0.
      CALL BRIDG(CDO,1,NP,2,IZ,IE,REY,TAU,CAMB,CL,1,NP,CLL)
      DO 20 K=1,NP
   20 CL(K)=CVAL(K)
C
CC                                    COMPUTE QUARTER CHORD PITCHING MOMENT
CC                                    COEFFICIENTS
C
      CLL=999.
      REYON=999.
      XMAX=0.
      CALL BRIDG(CM,1,NP,3,IW,IE,REY,TAU,CAMB,CL,1,NP,CLL)
      DO 50 K=1,NP
C
CC                                    CHECK IF SECTION STALLED
C
      IF(ALPHE(K)-ALMAX(K)) 40,30,30
   30 WRITE(IP,260) K,ALPHE(K),ALMAX(K)
      IS=2
      ISS=IS
      IKT=1
C
CC                                    COMPUTE SECTION PITCHING MOMENT
C
   40 SUM1=COS(3.14159/180.*(ALPHB-ALPHU(K)))
      SUM2=SIN(3.14159/180.*(ALPHB-ALPHU(K)))
      CM(K)=CM(K)-X/C(K)*(CL(K)*SUM1+CDO(K)*SUM2)-Z/C(K)*(CL(K)*SUM2-CDO
     1(K)*SUM1)
   50 CDOC(K)=CDO(K)*C(K)*CRB/BWX
      WRITE(IP,270)
      CALL AAA(CM,NP)
C
CC                                    CHECK FOR DUMP
C
      CALL DATSW(3,JUNK)
      GO TO (60,70), JUNK
   60 WRITE(IP,280)
      CALL AAA(CLMAX,NP)
      WRITE(IP,290)
```

```
      CALL AAA(CDOC,NP)
   70 WRITE(IP,300)
      CALL AAA(ALPHE,NP)
      WRITE(IP,310)
      CALL AAA(CDO,NP)
      DO 80 K=1,NP
   80 ALPG(K)=ALPHU(K)*CL(K)*3.14159/180.
      WRITE(IP,320)
      CALL AAA(ALPG,NP)
      WRITE(IP,330)
      CALL AAA(CL,NP)
C
CC                                  COMPUTE OVERALL LIFT, DRAG, AND PITCHING
CC                                  MOMENT COEFFICIENTS
C
      SUM1=0.
      SUM2=0.
      SUM3=0.
      SUM4=0.
      DO 90 I=1,NP
      SUM1=CBC(I)*ETA(I)+SUM1
      SUM2=CBC(I)*ALPHU(I)*ETA(I)+SUM2
      SUM3=CDOC(I)*ETA(I)+SUM3
   90 SUM4=CM(I)*C(I)**2*ETA(I)+SUM4
      Q=ASPEC*BWX**2
      COLIFT=Q*SUM1
      CDI=0.017453*Q*SUM2
      CDP=Q*SUM3
      CD=CDI+CDP
      ZM=ASPEC*BWX*CRB/ACC*SUM4
      WRITE(IP,340) ALPHB,CDI,COLIFT,CDP,ZM,CD
      GO TO (250,100), IS
C
CC                                  DEFINE EXACT STALL ANGLE OF ATTACK
C
  100 IAGN=IAGN+1
      IF(IAGN-2) 120,120,110
  110 IF(DIR) 130,120,140
  120 GO TO (160,180), IKT
  130 GO TO (160,150), IKT
  140 GO TO (150,180), IKT
  150 IQT=2
  160 IY=1
      DO 170 K=1,NP
  170 TONY(K)=CLMAX(K)-CL(K)
      WRITE(IP,350)
      CALL AAA(TONY,NP)
      GO TO (180,240),  IQT
  180 GO TO (190,210,210,210,240), IAGN
  190 IPRAB=IPRAB-1
      IF(IPRAB-1) 200,210,200
  200 ALPHB=ALPHB-((ALPHV(IPRAB)-ALPHV(IPRAB-1))/2.)
      ALPHB=ALPHB+0.001
      GO TO 220
  210 ALPHB=(ALPHB+(-1.)**IKT*0.2)
      ALPHB=ALPHB+0.001
      DIR=(-1.)**IKT
  220 WRITE(IP,370) NAME
      WRITE(IP,360) ALPHB
      IPRAB=IPRAB+1
      IR=100
  230 RETURN
  240 IQT=2
      RETURN
  250 IR=0
      RETURN
C
  260 FORMAT(10X,11HSTALLED AT ,I3,32H POINT SECTION ANGLE OF ATTACK =,
     1F10.3,10X,30HMAX. SECTION ANGLE OF ATTACK =,F10.3)
```

```
  270 FORMAT(10X,35HSECTION PITCHING MOMENT COEFFICIENT)
  280 FORMAT(10X,5HCLMAX)
  290 FORMAT(10X,4HCDUC)
  300 FORMAT(1X/10X,33HEFFECTIVE SECTION ANGLE OF ATTACK)
  310 FORMAT(10X,32HSECTION PROFILE DRAG COEFFICIENT)
  320 FORMAT(10X,32HSECTION INDUCED DRAG COEFFICIENT)
  330 FORMAT(10X,40HDISTRIBUTION OF SECTION LIFT COEFFICIENT)
  340 FORMAT(1X,120(1H.)/1HO/15X,30HBODY ANGLE OF ATTACK, DEG. . . =,F10.2
     1,10X,30HINDUCED DRAG COEFFICIENT . . =,F10.6/15X,30HLIFT COEFFICIE
     2NT . . . . . =,F10.6,10X,30HPROFILE DRAG COEFFICIENT . . =,F10.6
     3/15X,30HPITCHING MOMENT COEFFICIENT. =,F10.6,10X,30HTOTAL DRAG COE
     4FFICIENT . . . =,F10.6/1HO/1X,120(1H.))
  350 FORMAT(10X,25HSTALL MARGIN DISTRIBUTION/1X)
  360 FORMAT(1X,40(3H./.)/1X/10X,28HADJUSTED ANGLE OF ATTACK TO,F8.2,32H
     1,SEARCHING FOR EXACT STALL POINT,/1X/1X,40(3H./.)/1X)
  370 FORMAT(1H1/1HO/35X,25A2/1X)
      END
      OVERLAY(BLINDA,3,0)
      PROGRAM THREE
      CALL MAIN3
      RETURN
      END
      SUBROUTINE MAIN3
C
C                                  SUBROUTINE FOR THE CASE WITH FLAPS
C
      DIMENSION ARRAY(5,25,12),C(19),EPS(19),TRANS(19),REY(19),ETA(19),
     1HOPP(19),CLMAX(19),ZHERE(2,6),WHERE(2,6),Y(19),TAU(19),BETA(19,19)
     2,TRIX(19,19),MAZZ(6),MZCOL(6),MAXX(6),MXCOL(6),XHERE(2,6),MWCOL(6)
     3,MAWW(6),CM(19),CBG(19),CVAL(19),ALPG(19),CBC(19),ALPHU(19),ALPH(1
     49),ALPHZ(19),ALPHE(19),DELTA(19),CL(19),ALPHV(20),YHERE(2,6),MYCOL
     5(6),MAYY(6),CLADD(19),CLDEL(19),CLAD2(19),CLAD1(19),F(19),ALPC(19)
     6,TONY(19)
      COMMON INNOW,ISWIT(3),ALPHA,REYN,CLL,REYON,XMAX,ALMAX(19),CLMAX,C,
     1EPS,TRANS,REY,ETA,HOPP,ZHERE,WHERE,ARRAY,Y,BETA,TFAC,TRIX,TAU,MAXX
     2,MAZZ,MXCOL,MZCOL,ASPEC,TAPER,BF,REYND,DISCR,PIER,CRB,Q,TSTAX,EDGE
     3,SIG,ALPHR,NFLAP,NLVL,NP,IY,IZ,IR,IP,ISIS,ISTAR,A,B,H,TAUT,TAUR,
     4TWIST,R,BWX,YHERE,MYCOL,MAYY,FLAP,TONY,TWISA,X,Z,CM,ACC,XHERE,
     5MWCOL,MAWW,CAMB(19),CAMBR,CAMBT,DUMY1,DUMY2,NAME(25),AHERE(2,6),
     6MAAA(6),MACOL(6),BHERE(2,6),MABB(6),MBCOL(6),CHERE(2,6),MACC(6),
     7MCCOL(6),DHERE(2,6),MADD(6),MDCOL(6),ALPHE,ALPHV,CLADD,CLDEL,CLAD2
     8,CLAD1,F,IRI,FF,LOCER,IPRAB,IKT,IQT,IAGN,ITR,IS
      ALPHB=0.
      CL(1)=0.
      JP=R/2.
      IPRAB=0
      IRI=R
      IS=1
C
C                                  INPUT ALPHA VALUES
C
      READ(IR,700) ALPHV
      IPRAB=IPRAB+1
      DIR=0.
      IQT=1
      IAGN=0
      ITR=0
      IY=1
C
C                                  PUT CUBE 1 IN CORE
C
      CALL DAGET(ARRAY,1,IY)
      LOCER=2
      DO 10 K=1,NP
   10 ALPG(K)=3.
      CALL DATSW(3,JUNK)
      GO TO (20,30), JUNK
   20 WRITE(IP,710)
      CALL AAA(ALPG,NP)
```

```
C
C                                   LOOK UP CL VALUES
C
   30 DO 60 K=1,NP
      CLL=999.
      ALPHA=ALPG(K)
      REYN=REY(K)
      TAUX=TAU(K)
      REYON=999.
      XMAX=0.
      CALL ARC(ARRAY,TAUX,MAXX,MXCOL,IE,WHERE,NLVL)
C
C                                   CHECK FOR ERROR STOP
C
      IF(IE) 50,50,40
   40 WRITE(IP,720) IE,LOCER
      CALL EXIT
   50 CVAL(K)=CLL
      AK=K
   60 CBG(K)=CVAL(K)*(ASPEC/(ASPEC+1.6))*C(K)*CRB*(0.5+(1.+TAPER)*SIN(AK
     1*PIER)/(3.14159*C(K)))
      CALL DATSW(3,JUNK)
      GO TO (70,80), JUNK
   70 WRITE(IP,730)
      CALL AAA(CVAL,NP)
   80 DO 120 K=1,NP
      SIG=0.
      DO 90 M=1,NP
   90 SIG=CBG(M)*BETA(M,K)+SIG
      ALPHU(K)=SIG*(1.+TFAC*(TRANS(K)-1.))
      ALPH(K)=ALPG(K)-ALPHU(K)
C
C                                   LOOK UP ALPHA FOR ZERO LIFT
C
      LOCER=3
      ALPHA=999.
      CLL=0.0001
      REYN=REY(K)
      TAUX=TAU(K)
      REYON=999.
      XMAX=0.
      CALL ARC(ARRAY,TAUX,MAXX,MXCOL,IE,WHERE,NLVL)
      IF(IE) 100,100,40
  100 ALPHZ(K)=ALPHA
      ALPHE(K)=(ALPH(K)-ALPHZ(K)*(1.-EDGE))/EDGE
C
C                                   LOOK UP CL VALUES
C
      LOCER=4
      CLL=999.
      ALPHA=ALPHE(K)
      REYN=REY(K)
      TAUX=TAU(K)
      REYON=999.
      XMAX=0.
      CALL ARC(ARRAY,TAUX,MAXX,MXCOL,IE,WHERE,NLVL)
      IF(IE) 110,110,40
  110 CVAL(K)=CLL
      CBC(K)=CVAL(K)*C(K)*CRB/BWX
  120 DELTA(K)=CBC(K)-CBG(K)
      CALL DATSW(3,JUNK)
      GO TO (130,140), JUNK
  130 WRITE(IP,740)
      CALL AAA(CBC,NP)
      WRITE(IP,750)
      CALL AAA(ALPHU,NP)
      WRITE(IP,760)
      CALL AAA(ALPHE,NP)
      WRITE(IP,730)
```

```
      CALL AAA(CVAL,NP)
      WRITE(IP,770)
      CALL AAA(CBC,NP)
      WRITE(IP,750)
      CALL AAA(DELTA,NP)
  140 DO 160 K=1,NP
      IF(ABS(DELTA(K))-DISCR) 150,150,170
  150 IF(K-NP) 160,240,240
  160 CONTINUE
  170 DO 190 I=1,NP
      SUM=0.
      DO 180 J=1,NP
  180 SUM=IRIX(I,J)*DELTA(J)+SUM
  190 CBG(I)=CBG(I)+SUM
      CALL DATSW(3,JUNK)
      GO TO (200,210), JUNK
  200 WRITE(IP,740)
      CALL AAA(CBG,NP)
  210 ITR=ITR+1
C
CCC                                   ITERATION CONTROL
C
      IF(ITR-30) 80,80,220
C
CCC                                   IF UNABLE TO CONVERGE, DUMP ALL
C
  220 WRITE(IP,790)
      WRITE(IP,780)
      CALL AAA(DELTA,NP)
      WRITE(IP,730)
      CALL AAA(CVAL,NP)
      DO 230 J=1,NLVL
      NR=MAXX(J)
      NC=MXCOL(J)
      TAUX=WHERE(2,J)
      WRITE(IP,800) J,J,NR,NC,TAUX
      DO 230 K=1,NR
  230 WRITE(IP,810) (ARRAY(J,K,L),L=1,NC)
      CALL EXIT
C
CCC                                   CONVERGENCE
C
  240 WRITE(IP,820) NAME
      WRITE(IP,830) ITR,ALPHB
      IKT=2
      SUM=0.
      DO 250 I=1,NP
  250 SUM=CBC(I)*ETA(I)+SUM
      Q=ASPEC*BWX**2
C
CCC                                   LIFT COEFFICIENT
C
      COLIFT=Q*SUM
      DO 260 K=1,NP
  260 CLADD(K)=CVAL(K)/COLIFT
      CLL=0.
      ALPHA=999.
      REYN=REY(ISTAR)
      TAUX=TAU(ISTAR)
      REYCN=999.
      CALL ARC(ARRAY,TAUX,MAXX,MXCOL,IE,WHERE,NLVL)
      A1=ALPHA
      ALPHA=999.
      CALL DAGET(ARRAY,4,IW)
      CALL ARC(ARRAY,TAUX,MAYY,MYCOL,IE,YHERE,NLVL)
      A2=ALPHA
      SLELT=A1-A2
      ALPG(JP)=0.
      ALPHA=ALPG(JP)
```

```
      CLL=999.
      REYN=REY(JP)
      TAUX=TAU(JP)
C
CC                                  LOOK UP FLAP LIFT (4)
C
      REYON=999.
      CALL DAGET(ARRAY,4,IW)
      CALL ARC(ARRAY,TAUX,MAWW,MWCOL,IE,XHERE,NLVL)
      CVAL(JP)=CLL
      DO 290 K=1,JP
      AK=K
      STAR=ISTAR
      IF(K-ISTAR) 280,280,270
  270 CBG(K)=0.5*CVAL(JP)*C(K)*CRB/BWX*(1.+SQRT(1.-(COS(AK*PIER)/COS(
     1STAR*PIER))**2))
      GO TO 290
  280 CBG(K)=0.5*CVAL(JP)*C(K)*CRB/BWX*(1.-SQRT(1.-((1.-COS(AK*PIER))/
     1(1.-COS(STAR*PIER)))**2))
  290 CONTINUE
      DO 300 K=1,JP
      IRI=R
      IRI=IRI-K
  300 CBG(IRI)=CBG(K)
      IRI=R
      DO 310 K=1,NP
  310 ALPG(K)=0.
      CALL DATSW(3,I)
      GO TO (320,330), I
  320 WRITE(IP,840)
      CALL AAA(CLADD,NP)
      WRITE(IP,850)
      CALL ZZZ(CLL)
      WRITE(IP,860)
      CALL AAA(CBG,NP)
  330 ITR=0
  340 DO 400 K=1,NP
      SIG=0.
      DO 350 M=1,NP
  350 SIG=CBG(M)*BETA(M,K)+SIG
      ALPHU(K)=SIG*(1.+TFAC*(TRANS(K)-1.))
      ALPH(K)=ALPG(K)-ALPHU(K)
      ALPC(K)=SDELT*HOPP(K)
      ALPH(K)=ALPH(K)-ALPC(K)
      CLL=0.
      ALPHA=999.
      REYN=REY(K)
      REYON=999.
      TAUX=TAU(K)
      IF(K-ISTAR) 380,380,360
  360 IF(K-IRI+ISTAR) 370,380,380
  370 CALL DAGET(ARRAY,4,IW)
      CALL ARC(ARRAY,TAUX,MAWW,MWCOL,IE,XHERE,NLVL)
      ALPHZ(K)=ALPHA
      ALPHA=(ALPH(K)-ALPHZ(K)*(1.-EDGE))/EDGE
      CLL=999.
      CALL DAGET(ARRAY,4,IW)
      CALL ARC(ARRAY,TAUX,MAWW,MWCOL,IE,XHERE,NLVL)
      CVAL(K)=CLL
      GO TO 390
  380 CALL DAGET(ARRAY,1,IY)
      CALL ARC(ARRAY,TAUX,MAXX,MXCOL,IE,WHERE,NLVL)
      ALPHZ(K)=ALPHA
      ALPHA=(ALPH(K)-ALPHZ(K)*(1.-EDGE))/EDGE
      CLL=999.
      CALL DAGET(ARRAY,1,IY)
      CALL ARC(ARRAY,TAUX,MAXX,MXCOL,IE,WHERE,NLVL)
      CVAL(K)=CLL
  390 CBG(K)=CVAL(K)*C(K)*CRB/BWX
```

```
400 DELTA(K)=CBC(K)-CBG(K)
    CALL DATSW(3,JUNK)
    GO TO (410,420), JUNK
410 WRITE(IP,870)
    CALL AAA(ALPHU,NP)
    WRITE(IP,880)
    CALL AAA(ALPC,NP)
    WRITE(IP,890)
    CALL AAA(ALPH,NP)
    WRITE(IP,900)
    CALL AAA(ALPHZ,NP)
    WRITE(IP,910)
    CALL AAA(CVAL,NP)
    WRITE(IP,920)
    CALL AAA(CBC,NP)
    WRITE(IP,930)
    CALL AAA(DELTA,NP)
420 DO  440 K=1,NP
    IF(ABS(DELTA(K))-DISCR) 430,430,450
430 IF(K-NP) 440,500,500
440 CONTINUE
450 DO 470 I=1,NP
    SUM=0.
    DO 460 J=1,NP
460 SUM=TRIX(I,J)*DELTA(J)+SUM
470 CBG(I)=CBG(I)+SUM
    CALL DATSW(3,JUNK)
    GO TO (480,490), JUNK
480 WRITE(IP,940)
    CALL AAA(CBG,NP)
490 ITR=ITR+1
    IF(ITR-30) 340,340,220
500 DO 510 K=1,NP
510 CLDEL(K)=CVAL(K)
    F1=CLDEL(JP)/CLADD(JP)
    F2=CLDEL(1)/CLADD(1)
    DO 520 K=1,ISTAR
520 CLAD2(K)=F2*CLADD(K)
    DO 530 K=ISTAR,JP
530 CLAD1(K)=F1*CLADD(K)
    BDELT=CLAD1(ISTAR)-CLAD2(ISTAR)
    DO 540 K=1,ISTAR
540 F(K)=(CLDEL(K)-CLAD2(K))/BDELT
    FF=(CLDEL(ISTAR)-CLAD1(ISTAR))/BDELT
    IST=ISTAR+1
    DO 550 K=IST,JP
550 F(K)=(CLDEL(K)-CLAD1(K))/BDELT
    DO 560 K=1,JP
    IRI=R
    IRI=IRI-K
560 F(IRI)=F(K)
    CALL DATSW(3,JUNK)
    GO TO (570,580), JUNK
570 WRITE(IP,950)
    CALL AAA(CLADD,NP)
    WRITE(IP,960)
    CALL AAA(CLDEL,NP)
    WRITE(IP,970)
    CALL ZZZ (F1)
    WRITE(IP,980)
    CALL ZZZ (F2)
    WRITE(IP,990)
    CALL AAA(CLAD2,NP)
    WRITE(IP,1000)
    CALL AAA(CLAD1,NP)
    WRITE(IP,1010)
    CALL AAA(F,NP)
    WRITE(IP,1020)
    CALL ZZZ(FF)
```

```
C
C                                   LOOK UP CL MAX CUBE 1
C
  580 CALL DAGET(ARRAY,1,IY)
      REYN=999.
      XMAX=0.
      CLL=999.
      ALPHA=999.
      REYON=REY(ISTAR)
      TAUX=TAU(ISTAR)
      CALL ARC(ARRAY,TAUX,MAXX,MXCOL,IE,WHERE,NLVL)
      CLMNF=XMAX
      XMAX=0.
C
C                                   LOOK UP CL MAX CUBE 4 (FLAP)
C
      CALL DAGET(ARRAY,4,IW)
      CALL ARC(ARRAY,TAUX,MAWW,MWCOL,IE,XHERE,NLVL)
      CLMF=XMAX
      DCLMA=CLMF-CLMNF
      CLL=999.
      ALPHA=999.
      REYN=999.
      XMAX=0.
      DO 630 K=1,NP
      IRI=R
      IF(K-ISTAR) 600,600,590
  590 IF(K-IRI+ISTAR) 610,600,600
  600 XMAX=0.
      REYON=REY(K)
      TAUX=TAU(K)
C
C                                   LOOK UP ALPHA MAX CUBE 1
C
      CALL DAGET(ARRAY,1,IY)
      CALL ARC(ARRAY,TAUX,MAXX,MXCOL,IE,WHERE,NLVL)
      GO TO 620
  610 XMAX=0.
      REYON=REY(K)
      TAUX=TAU(K)
C
C                                   LOOK UP ALPHA MAX CUBE 4 (FLAP)
C
      CALL DAGET(ARRAY,4,IW)
      CALL ARC(ARRAY,TAUX,MAWW,MWCOL,IE,XHERE,NLVL)
  620 F(K)=1.+F(K)*DCLMA/XMAX
  630 CLMAX(K)=F(K)*XMAX
      FF=1.+FF*DCLMA/CLMF
      DO 670 K=1,NP
      IF(K-ISTAR) 650,650,640
  640 IF(K-IRI+ISTAR) 660,650,650
C
C                                   LOOK UP ALPHA MAX CUBE 1
C
  650 CALL DAGET(ARRAY,1,IY)
      ALPHA=999.
      REYN=999.
      CLL=999.
      REYON=REY(K)
      TAUX=TAU(K)
      XMAX=100.
      CALL ARC(ARRAY,TAUX,MAXX,MXCOL,IE,WHERE,NLVL)
      GO TO 670
C
C                                   LOOK UP ALPHA MAX CUBE 4 (FLAP)
C
  660 CALL DAGET(ARRAY,4,IW)
      XMAX=100.
      REYON=REY(K)
```

```
      TAUX=TAU(K)
      REYN=999.
      ALPHA=999.
      CLL=999.
      CALL ARC(ARRAY,TAUX,MAWW,MWCOL,IE,XHERE,NLVL)
  670 ALMAX(K)=ALPHZ(K)+(XMAX-ALPHZ(K))*EDGE*F(K)
      WRITE(IP,820) NAME
      WRITE(IP,1030)
      CALL AAA(Y,NP)
      WRITE(IP,1040)
      CALL AAA(ALMAX,NP)
      WRITE(IP,1050)
      CALL AAA(CLMAX,NP)
      WRITE(IP,1060)
      CALL AAA(TAU,NP)
      WRITE(IP,1070)
      CALL AAA(REY,NP)
      WRITE(IP,1080)
      CALL AAA(C,NP)
      WRITE(IP,1090)
      CALL AAA(EPS,NP)
      CALL DATSW(3,JUNK)
      GO TO (680,690), JUNK
  680 WRITE(IP,1100)
      CALL ZZZ(DCLMA)
      WRITE(IP,1010)
      CALL AAA(F,NP)
      WRITE(IP,1020)
      CALL ZZZ(FF)
  690 CALL MAIN5
      RETURN
C
  700 FORMAT(10F8.0)
  710 FORMAT(10X,4HALPG)
  720 FORMAT(1X,10HERROR CODE,I2,1X,10HAT SECTION,I3,1X,32HIN PROGRAM, E
     1XECUTION TERMINATED)
  730 FORMAT(10X,4HCVAL)
  740 FORMAT(10X,3HCBG)
  750 FORMAT(10X,5HALPHU)
  760 FORMAT(10X,5HALPHF)
  770 FORMAT(10X,3HCBC)
  780 FORMAT(10X,5HDELTA)
  790 FORMAT(2X,48HUNABLE TO CONVERGE AFTER 30 ITERATIONS   ABORTED)
  800 FORMAT(1HO/1HO,7H ARRAY(,I1,1H 1, 1) TO (,I1,1H,,I2,1H,,I2,1H),F
     110.5/1HO)
  810 FORMAT(12F10.4)
  820 FORMAT(1H1/1HO/35X,25A2/1X)
  830 FORMAT(1X,33H ITERATIONS REQUIRED TO CONVERGE ,I2,19H FOR ALPHB EQ
     1VAL TO,F10.1/1HO)
  840 FORMAT(10X,5HCLADD)
  850 FORMAT(10X,2HCL)
  860 FORMAT(10X,3HCBG)
  870 FORMAT(10X,5HALPHU)
  880 FORMAT(10X,4HALPC)
  890 FORMAT(10X,4HALPH)
  900 FORMAT(10X,5HALPHZ)
  910 FORMAT(10X,4HCVAL)
  920 FORMAT(10X,3HCBC)
  930 FORMAT(10X,5HDELTA)
  940 FORMAT(10X,3HCBG)
  950 FORMAT(10X,5HCLADD)
  960 FORMAT(10X,5HCLCEL)
  970 FORMAT(10X,2HF1)
  980 FORMAT(10X,2HF2)
  990 FORMAT(10X,5HCLAD2)
 1000 FORMAT(10X,5HCLAD1)
 1010 FORMAT(10X,1HF)
 1020 FORMAT(10X,2HFF)
 1030 FORMAT(1X/10X,17HSPANWISE STATIONS)
```

```
 1040 FORMAT(10X,10H ALPHA MAX)
 1050 FORMAT(10X,7H CL MAX)
 1060 FORMAT(10X,31H THICKNESS / CHORD DISTRIBUTION)
 1070 FORMAT(10X,24H SECTION REYNOLDS NUMBER)
 1080 FORMAT(10X,19H CHORD DISTRIBUTION)
 1090 FORMAT(10X,16H GEOMETRIC TWIST)
 1100 FORMAT(10X,6HDDCLMA)
      END
      SUBROUTINE MAIN5
C
C                                  CONTINUATION OF SUBROUTINE MAIN3
C
      DIMENSION ARRAY(5,25,12),C(19),EPS(19),TRANS(19),REY(19),ETA(19),
     1HOPP(19),CLMAX(19),ZHERE(2,6),WHERE(2,6),Y(19),TAU(19),BETA(19,19)
     2,TRIX(19,19),MAZZ(6),MZCOL(6),MAXX(6),MXCOL(6),CBC(19),CVAL(19),
     3ALPC(19),CBC(19),ALPHU(19),ALPH(19),ALPHZ(19),ALPHE(19),DELTA(19),
     4CL(19),ALPHV(20),XHERE(2,6),MWCOL(6),MAWW(6),CM(19),YHERE(2,6),
     5MYCOL(6),MAYY(6),CLADD(19),CLDEL(19),CLAD2(19),CLAD1(19),F(19),
     6ALPC(19),TONY(19)
      COMMON INNOW,ISWIT(3),ALPHA,REYN,CLL,REYON,XMAX,ALMAX(19),CLMAX,C,
     1EPS,TRANS,REY,ETA,HOPP,ZHERE,WHERE,ARRAY,Y,BETA,TFAC,TRIX,TAU,MAXX
     2,MAZZ,MXCOL,MZCOL,ASPEC,TAPER,BF,REYND,DISCR,PIER,CRB,Q,TSTAX,EDGE
     3,SIG,ALPHR,NFLAP,NLVL,NP,IY,IZ,IR,IP,ISIS,ISTAR,A,B,H,TAUT,TAUR,
     4TWIST,R,BWX,YHERE,MYCOL,MAYY,FLAP,TONY,TWISA,X,Z,CM,ACC,XHERE,
     5MWCOL,MAWW,CAMB(19),CAMBR,CAMBT,DUMY1,DUMY2,NAME(25),AHERE(2,6),
     6MAAA(6),MACOL(6),BHERE(2,6),MABB(6),MBCOL(6),CHERE(2,6),MACC(6),
     7MCCOL(6),DHERE(2,6),MADD(6),MDCOL(6),ALPHE,ALPHV,CLADD,CLDFL,CLAD2
     8,CLAD1,F,IRI,FF,LOCER,IPRAB,IKT,IQT,IAGN,ITR,IS
  10 ALPHB=ALPHV(IPRAB)
     IF(ALPHV(IPRAB).EQ.99.) CALL EXIT
     IPRAB=IPRAB+1
     WRITE(IP,560) NAME
     WRITE(IP,570) ALPHB,DISCR,A,B,ASPEC,H,ALPHR,TAUT
     WRITE(IP,580) TAUR,TWIST,R,TWISA,BF,TAPER,FLAP,REYND,X,Z
     WRITE(IP,590)
  20 IKT=2
     DO 60 K=1,NP
     AK=K
     ALPG(K)=ALPHB+ALPHR+EPS(K)+ALPHB*TFAC*(TRANS(K)-1.)
     IF(K-ISTAR) 40,40,30
  30 IF(K-IRI+ISTAR) 50,40,40
C
C                                  LOOK UP CVAL CUBE 1
C
  40 ALPHA=ALPG(K)
     CLL=999.
     REYN=REY(K)
     TAUX=TAU(K)
     REYON=999.
     CALL DAGET(ARRAY,1,IY)
     CALL ARC(ARRAY,TAUX,MAXX,MXCOL,IE,WHERE,NLVL)
     CVAL(K)=CLL
     GO TO 60
C
C                                  LOOK UP CVAL CUBE 4 (FLAP)
C
  50 ALPHA=ALPG(K)
     CLL=999.
     REYN=REY(K)
     TAUX=TAU(K)
     REYON=999.
     CALL DAGET(ARRAY,4,IW)
     CALL ARC(ARRAY,TAUX,MAWW,MWCOL,IE,XHERE,NLVL)
     CVAL(K)=CLL
  60 CBC(K)=CVAL(K)*(ASPEC/(ASPEC+1.8))*C(K)*CRB*(0.5+(1.+TAPER)*SIN(AK
    1*PIER)/(3.14159*C(K)))
C
C                                  CHECK FOR DUMP
C
```

```
      CALL DATSW(3,JUNK)
      GO TO (70,80), JUNK
   70 WRITE(IP,610)
      CALL AAA(TRANS,NP)
      WRITE(IP,600)
      CALL ZZZ(TFAC)
      WRITE(IP,620)
      CALL AAA(ALPG,NP)
      WRITE(IP,630)
      CALL AAA(CBG,NP)
   80 CLSTA=CBG(ISTAR)*BWX/(C(ISTAR)*CRB)
C
CCC                                   CHECK FOR DUMP
C
      CALL DATSW(3,JUNK)
      GO TO (90,100), JUNK
   90 WRITE(IP,640)
      CALL ZZZ(CLSTA)
C
CCC                                   LOOK UP ALPHA CUBE 4 (FLAP)
C
  100 CALL DAGET(ARRAY,4,IW)
      ALPHA=999.
      CLL=0.
      REYN=REY(ISTAR)
      TAUX=TAU(ISTAR)
      REYON=999.
      CALL ARC(ARRAY,TAUX,MAWW,MWCOL,IE,XHERE,NLVL)
      A3=ALPHA
      CALL DATSW(3,JUNK)
      GO TO (110,120), JUNK
  110 WRITE(IP,650)
      CALL ZZZ(A3)
C
CCC                                   LOOK UP ALPHA CUBE 1
C
  120 CALL DAGET(ARRAY,1,IY)
      CLL=0.
      ALPHA=999.
      CALL ARC(ARRAY,TAUX,MAXX,MXCOL,IE,WHERE,NLVL)
      A4=ALPHA
      CLSTU=CLSTA/FF
      CALL DATSW(3,JUNK)
      GO TO (130,140), JUNK
  130 WRITE(IP,660)
      CALL ZZZ(CLSTU)
      WRITE(IP,670)
      CALL ZZZ(A4)
  140 CALL DAGET(ARRAY,4,IW)
      ALPHA=999.
      CLL=CLSTU
      REYN=REY(ISTAR)
      TAUX=TAU(ISTAR)
      REYON=999.
      CALL ARC(ARRAY,TAUX,MAWW,MWCOL,IE,XHERE,NLVL)
      ALPHX=ALPHA
      A1=EDGE*FF*(ALPHX-A3)+A3
      CALL DATSW(3,JUNK)
      GO TO (150,160), JUNK
  150 WRITE(IP,680)
      CALL ZZZ(A1)
  160 CLSTU=CLSTA/F(ISTAR)
C
CCC                                   LOOK UP ALPHA CUBE 1
C
      CALL DAGET(ARRAY,1,IY)
      ALPHA=999.
      CLL=CLSTU
      REYN=REY(ISTAR)
```

```
      TAUX=TAU(ISTAR)
      REYON=999.
      CALL ARC(ARRAY,TAUX,MAXX,MXCOL,IE,WHERE,NLVL)
      ALPHX=ALPHA
      A2=EDGE*F(ISTAR)*(ALPHX-A4)+A4
      CALL DATSW(3,JUNK)
      GO TO(170,180), JUNK
  170 WRITE(IP,690)
      CALL ZZZ(A2)
  180 SDELT=A2-A1
      ITR=0
      DO 240 K=1,NP
      SIG=0.
      DO 190 M=1,NP
  190 SIG=CBG(M)*BETA(M,K)+SIG
      ALPHU(K)=SIG*(1.+TFAC*(TRANS(K)-1.))
      ALPH(K)=ALPG(K)-ALPHU(K)
      ALPC(K)=SDELT*HOPP(K)
      ALPH(K)=ALPH(K)-ALPC(K)
      CLL=0.
      ALPHA=999.
      REYN=REY(K)
      TAUX=TAU(K)
      REYON=999.
      IF(K-ISTAR) 220,220,200
  200 IF(K-IRI+ISTAR) 210,220,220
  210 CALL DAGET(ARRAY,4,IZ)
      CALL ARC(ARRAY,TAUX,MAWW,MWCOL,IE,XHERE,NLVL)
      ALPHZ(K)=ALPHA
      ALPN=(ALPH(K)-ALPHZ(K)*(1.-F(K)*EDGE))/(EDGE*F(K))
      CLL=999.
      ALPHA=ALPN
      CALL ARC(ARRAY,TAUX,MAWW,MWCOL,IE,XHERE,NLVL)
      CVAL(K)=CLL*F(K)
      GO TO 230
  220 CALL DAGET(ARRAY,1,IY)
      CALL ARC(ARRAY,TAUX,MAXX,MXCOL,IE,WHERE,NLVL)
      ALPHZ(K)=ALPHA
      ALPN=(ALPH(K)-ALPHZ(K)*(1.-F(K)*EDGE))/(EDGE*F(K))
      ALPHA=ALPN
      CLL=999.
      CALL DAGET(ARRAY,1,IY)
      CALL ARC(ARRAY,TAUX,MAXX,MXCOL,IE,WHERE,NLVL)
      CVAL(K)=CLL*F(K)
  230 CBC(K)=CVAL(K)*C(K)*CRB/BWX
  240 DELTA(K)=CBC(K)-CBG(K)
      CALL DATSW(3,JUNK)
      GO TO (250,260), JUNK
  250 WRITE(IP,720)
      CALL AAA(ALPHU,NP)
      WRITE(IP,700)
      CALL AAA(ALPH,NP)
      WRITE(IP,710)
      CALL AAA(ALPC,NP)
      WRITE(IP,730)
      CALL AAA(CVAL,NP)
      WRITE(IP,740)
      CALL AAA(DELTA,NP)
  260 DO 280 K=1,NP
      IF(ABS(DELTA(K))-DISCR) 270,270,290
  270 IF(K-NP) 280,360,360
  280 CONTINUE
  290 DO 310 I=1,NP
      SUM=0.
      DO 300 J=1,NP
  300 SUM=TRIX(I,J)*DELTA(J)+SUM
  310 CBG(I)=CBG(I)+SUM
      CALL DATSW(3,JUNK)
      GO TO (320,330), JUNK
```

```
  320 WRITE(IP,630)
      CALL AAA(CBG,NP)
  330 ITR=ITR+1
      IF(ITR-30) 80,80,340
C
CC                                NON CONVERGENCE DUMP
C
  340 WRITE(IP,750)
      WRITE(IP,740)
      CALL AAA(DELTA,NP)
      WRITE(IP,730)
      CALL AAA(CVAL,NP)
      DO 350 J=1,NLVL
      NR=MAXX(J)
      NC=MXCOL(J)
      TAUX=WHERE(2,J)
      WRITE(IP,760) J,J,NR,NC,TAUX
      DO 350 K=1,NR
  350 WRITE(IP,770) (ARRAY(J,K,L),L=1,NC)
      CALL EXIT
  360 DO 360 K=1,NP
      IF(ALPH(K)-ALMAX(K)) 380,370,370
  370 WRITE(IP,780) K,ALPH(K),ALMAX(K)
      IS=2
      IKT=1
  380 CONTINUE
      CALL DATSW(3,JUNK)
      GO TO (390,400), JUNK
  390 WRITE(IP,790)
      CALL AAA(CLMAX,NP)
  400 WRITE(IP,800)
      CALL AAA(CVAL,NP)
      DO 410 K=1,NP
  410 CL(K)=CLMAX(K)-CVAL(K)
      WRITE(IP,810)
      CALL AAA(CL,NP)
      SUM1=0.
      DO 420 I=1,NP
  420 SUM1=CBC(I)*ETA(I)+SUM1
      Q=ASPEC*BWX**2
      COLIFT=Q*SUM1
      WRITE(IP,820) ALPHB,COLIFT
      GO TO (10,430), IS
  430 IAGN=IAGN+1
      IF(IAGN-2) 450,450,440
  440 IF(DIR) 460,450,470
  450 GO TO (490,500), IKT
  460 GO TO (490,480), IKT
  470 GO TO (480,500), IKT
  480 IQT=2
  490 IY=1
      GO TO (500,550), IQT
  500 GO TO (510,530,530,530,550), IAGN
  510 IPRAB=IPRAB-1
      IF(IPRAB-1) 520,530,520
  520 ALPHB=ALPHB-((ALPHV(IPRAB)-ALPHV(IPRAB-1))/2.)
      GO TO 540
  530 ALPHB=(ALPHB+(-1.)**IKT*0.2)
      ALPHB=ALPHB+0.001
      DIR=(-1.)**IKT
  540 WRITE(IP,560) NAME
      WRITE(IP,830) ALPHB
      IPRAB=IPRAB+1
      GO TO 20
  550 RETURN
C
CC                                . . . . . DID IT STALL . . . .
CC                                :                           :
C                                 :                           :
```

```
C                                NO                              YES
C                                .                               .
C                                .                               .
C                                GET                             BACK OFF 1/2 THE DISTANCE
C                                ANOTHER                         BETWEEN LAST ALPHA VALUE
C                                ALPHA                           AND PRESENT ALPHA IF THIS
C                                                                WAS THE FIRST STALL
C                                                                OTHERWISE INCREASE OR
C                                                                DECREASE THE ANGLE OF
C                                                                ATTACK BY 0.2 DEGREES
C                                                                DEPENDING ON.
C                                                                        .
C                                                                        .
C                                                                IS IT STALLED AT 1/2 POINT
C                                                                .                       .
C                                                                .                       .
C                                                                NO                      YES
C                                                                .                       .
C                                                                SUBTRACT 0.2            ADD 0.2
C
C                                                                IF THIS IS THE FIRST ANGLE
C                                                                OF ATTACK THEN DECREASE BY
C                                                                0.2 DEGREES UNTIL UNSTALL
      560 FORMAT(1H1/1H0/35X,25A2/1X)
      570 FORMAT(1X,40(3H./.)/1H0/15X,30HBODY ANGLE OF ATTACK, DEG. . =,F10.
         12,10X,30HVALUE OF DISCRIMINANT. . . . =,F10.6/15X,30HBODY HEIGHT /
         2SPAN. . . . . =,F10.2,10X,30HBODY WIDTH / SPAN. . . . . =,F10.
         32/15X,30HASPECT RATIO . . . . . =,F10.2,10X,30HWING HEIGHT /
         4SPAN. . . . . =,F10.2/15X,30HWING BODY INCIDENCE, DEG . . =,F10
         5.2,10X,30HTIP THICKNESS CHORD. . . . . =,F10.2)
      580 FORMAT(15X,30HROOT THICKNESS CHORD . . . . =,F10.2,10X,30HGEOMETRI
         1C TWIST, DEG . . . . =,F10.2/15X,30HNUMBER OF SPANWISE STATIONS. =
         2,F10.2,10X,30HAERODYNAMIC TWIST, DEG . . . =,F10.2/15X,30HFLAP SPA
         3N / WING SPAN. . . . =,F10.2,10X,30HTAPER RATIO. . . . . =
         4,F10.2/15X,30HFLAP SETTING, DEG. . . . . =,F10.2,10X,30HREYNOLDS
         5 NUMBER. . . . . =,F10.2/15X,37HCOORDINATES OF MOMENT REFERENC
         6E POINT,14X,2HX=,F10.2,9X,2HZ=,F10.2)
      590 FORMAT(1H0/1X,40(3H./.)/1X)
      600 FORMAT(10X,16HTHICKNESS FACTOR)
      610 FORMAT(10X,13HR OU BAR / OU)
      620 FORMAT(10X,4HALPG)
      630 FORMAT(10X,3HCBG)
      640 FORMAT(10X,5HCLSTA)
      650 FORMAT(10X,2HA3)
      660 FORMAT(10X,5HCLSTU)
      670 FORMAT(10X,2HA4)
      680 FORMAT(10X,2HA1)
      690 FORMAT(10X,2HA2)
      700 FORMAT(10X,4HALPH)
      710 FORMAT(10X,4HALPC)
      720 FORMAT(10X,5HALPHO)
      730 FORMAT(10X,4HCVAL)
      740 FORMAT(10X,5HDELTA)
      750 FORMAT(1X,48HUNABLE TO CONVERGE AFTER 30 ITERATIONS   ABORTED)
      760 FORMAT(1H0/1H0,7H ARRAY(,I1,1H, 1) TO (,I1,1H,,I2,1H,,I2,1H),F
         110.5/1H0)
      770 FORMAT(12I10.4)
      780 FORMAT(1X,11HSTALLED AT ,I3,32H POINT SECTION ANGLE OF ATTACK =,F
         110.3,29HMAX. SECTION ANGLE OF ATTACK=,F10.3)
      790 FORMAT(10X,5HCLMAX)
      800 FORMAT(10X,40HDISTRIBUTION OF SECTION LIFT COEFFICIENT)
      810 FORMAT(10X,25HSTALL MARGIN DISTRIBUTION)
      820 FORMAT(1X,120(1H.)/1H0/15X,30HBODY ANGLE OF ATTACK, DEG. . =,F 10.
         12,10X,30HLIFT COEFFICIENT . . . . . =,F10.6/1X,120(1H.))
      830 FORMAT(1X,40(3H./.)/1X/10X,28HADJUSTED ANGLE OF ATTACK TO ,F10.2,
         131HSEARCHING FOR EXACT STALL POINT,/1X/1X,40(3H./.)/1X)
          END
```

APPENDIX B

AVAILABILITY OF THE COMPUTER PROGRAM

The computer program developed for the CDC 6400 and 6600 series computers has been stored in the COSMIC Computer Center and is available for public use. All inquiries pertaining to availability and use of the program should be directed to:

COSMIC
Computer Center
Barrow Hall
University of Georgia
Athens, Georgia 30601

Telephone: (404) 542-3265

BIBLIOGRAPHY

Presented herein is a compilation of a total of 243 technical reports related to the state of the art of wing, and wing-body aerodynamics. For convenience, the following papers are arranged in an alphabetical order by authors within the subgroups of each of the three main groups; Theoretical Methods, Wind-Tunnel Tests, and Aircraft Flight Tests.

1. THEORETICAL METHODS

   (a) Wing Theory

   1. Allen, H. Julian: Calculation of the Chordwise Load Distribution over Airfoil Sections with Plain, Split or Serially-hinged Trailing Edge Flaps. NACA Rep. 634, 1938.

   2. Allen, H. Julian: A Simplified Method for the Calculation of Airfoil Pressure Distribution. NACA TN 708, 1939.

   3. Allen, H. Julian: General Theory of Airfoil Sections Having Arbitrary Shape or Pressure Distribution. NACA ACR 3G29, 1943.

   4. Allen, H. Julian: Notes on the Effect of Surface Distortion on the Drag and Critical Mach Number of Airfoils. NACA ACR 3129, 1943.

   5. Anderson, Raymond F: Determination of the Characteristics of Tapered Wings. NACA Rep. 572, 1936.

   6. Anderson, Raymond F.: A Comparison of Several Tapered Wings Designed to Avoid Tip Stalling. NACA TN 713, 1939.

   7. Boshar, John: The Determination of Span Load Distribution at High Speeds by the Use of High-speed Wing Tunnel Section Data. NACA ACR 4B22, 1944 (Wartime Rep. L-436).

   8. Weissinger, J.,: The Lift Distribution of Sweptback Wings, NACA TM 1120, 1947.

   9. Crabtree, L.F., Kuchemann, D., and Maskell, E.C.: A Survey of Some Research on the Stalling of Wings of Contemporary Design in Progress at the R.A.E. R.A.E. TN Aero 2331, 1954.

10. De Young, John: Theoretical Symmetric Span Loading Due to Flap Deflection for Wings of Arbitrary Plan Form at Subsonic Speeds. NACA Rep. 1071, 1952.

11. De Young, John & Harper, Charles W.: Theoretical Symmetric Span Loading at Subsonic Speeds for Wings Having Arbitrary Plan Form. NACA Rep. 921, 1948.

12. Diederich, Franklin W. & Zlotnick, Martin: Calculated Spanwise Lift Distributions, Influence Functions, and Influence Coefficients for Unswept Wings in Subsonic Flow. NACA Rep. 1228, 1955.

13. Furlong, Chester G. & McHugh, James G.: A Summary and Analysis of the Low-Speed Longitudinal Characteristics of Swept Wings at High Reynolds Number. NACA Rep. 1339, 1957.

14. Glauert, H.: Theoretical Relationships for an Aerofoil with Hinged Flap. R & M No. 1095, British ARC, 1927.

15. Glauert, H.: The Effect of Compressibility on the Lift of an Aerofoil. R & M No. 1135, British ARC, 1927.

16. Glauert, H. & Gates, S.B.: The Characteristics of a Tapered and Twisted Wing With Sweep-Back. ARC R & M 1226, 1928.

17. Goldstein, Sidney: Low-drag and Suction Airfoils, Eleventh Wright Brothers Lecture, J. Inst. Aeronaut Sci., Vol. 15, No. 4, 1948, pages 189-214.

18. Harper, Charles W. & Maki, Ralph L.: A Review of the Stall Characteristics of Swept Wings. NASA TN D-2373, 1964.

19. Jacobs, Eastman N.: Preliminary Report on Laminar Flow Airfoils and New Methods Adopted for Airfoil and Boundary-layer Investigations. NACA ACR, June, 1939, (Wartime Rep. L-345).

20. Jones, Robert T.: Correction of the Lifting-Line Theory for the Effect of the Chord. NACA TN 817, 1941.

21. Kus, Yung-Huai: On the Stability of Two-Dimensional Smooth Transonic Flows. J. Ae. S., Vol. 18, No. 1, (1951), page 1.

22. Lippisch, A.: Method for the Determination of the Spanwise Lift Distribution. NACA TM 778.

23. Martina, Albert P.: Method for Calculating the Rolling and Yawing Moments Due to Rolling for Unswept Wings With or Without Flaps or Ailerons by Use of Nonlinear Lift Data. NACA Rep. 1167, 1954.

24. Muggia, Aldo: Remark on the Theory of Lifting Surfaces. NACA TM 1386, 1956.

25. Multhopp, H.: The Calculation of the Lift Distribution of Airfoils. Luftfahrforschung, Deutschland (RTP Translation No. 2392), 1938.

26. Multhopp, H.: Methods for Calculating the Lift-Distribution of Wings (Subsonic Lifting Surface Theory). R.A.E. Rep. No. Aero 2353, 1950.

27. Munk, Max. M.: The Determination of the Angles of Attack of Zero Lift and Zero Moment, Based on Munk's Integrals. NACA TN 122, 1923.

28. Munk, Max. M.: Elements of the Wing Section Theory and of the Wing Theory. NACA Rep. 191, 1924.

29. Munk, Max M.: Calculation of Span Lift Distribution (Part 2), Aero Digest, Vol. 48, No. 3, 1945, page 84.

30. Naiman, Irven: Numerical Evaluation of the ϵ -Integral Occurring in the Theodorsen Arbitrary Airfoil Potential Theory. NACA ARR L4D27a, 1944 (Wartime Rep. L-136).

31. Naiman, Irven: Numerical Evaluation by Harmonic Analysis of the ϵ -Function of the Theodorsen Arbitrary Potential Theory. NACA ARR L5H18, 1945 (Wartime Rep. L-153).

32. Nitzberg, Gerald E.: A Concise Theoretical Method for Profile-drag Calculation. NACA ACR 4B05, 1944.

33. Pankhurst, R.C.: A Method for the Rapid Evaluation of Glauert's Expressions for the Angle of Zero Lift and the Moment at Zero Lift. R & M No. 1914 British ARC, 1944.

34. Pearson, Henry A.: Span Load Distribution for Tapered Wings with Partial-Span Flaps. NACA Rep. 585, 1936.

35. Pearson, Henry A. and Jones, Robert T.: Theoretical Stability and Control Characteristics of Wings with Various Amounts of Taper and Twist. NACA Rep. 635, 1938.

36. Pearson, Henry A. and Anderson, Raymond F.: Calculation of the Aerodynamic Characteristics of Tapered Wings With Partial-Span Flaps. NACA Rep. 665, 1939.

37. Reissner, E.: Note on the Theory of Lifting Surfaces, Proceedings of the National Academy of Sciences, Vol. 35, No. 4, 1949, pages 208-215.

38. Roshko, A.: Computation of the Increment of Maximum Lift Due to Flaps. Douglas Aircraft Rep. SM-23626, 1959.

39. Sherman, Albert: A Simple Method of Obtaining Span Load Distributions. NACA TN 732, 1939.

40. Sivells, James C.: An Improved Approximate Method for Calculating Lift Distributions Due to Twist. NACA TN 2282, 1951.

41. Sivells, James C., and Neely, Robert H.: Method of Calculating Wing Characteristics by Lifting-Line Theory Using Nonlinear Section Lift Data. NACA TN 1269, 1947, Also NACA Rep. 865, 1947.

42. Sivells, James C. and Westrick, Gertrude C.: Method for Calculating Lift Distributions for Unswept Wings With Flaps or Ailerons by Use of Nonlinear Section Lift Data. NACA Rep. 1090, 1952.

43. Soule, Hartley A. and Gough, V., Melvin N.: Some Aspects of the Stalling of Modern Low-Wing Monoplanes. NACA TN 645, 1938.

44. Squire, H. B. and Young, A.D.: The Calculation of the Profile Drag of Aero foils. R & M No. 1838, British ARC, 1938.

45. Tani, Itiro: A Simple Method of Calculating the Induced Velocity of a Monoplane Wing. Aeronaut. Research Inst. Tokyo Imp. Univ. Rep. 111, Vol. IX, page 3, August 1934.

46. Tetervin, Neal: A Method for the Rapid Estimation of Turbulent Boundary-layer Thickness for Calculating Profile Drag. NACA ACR L4G14, 1944 (Wartime Rep. L-16).

47. Theodorsen, Theodore: On the Theory of Wing Sections with Particular Reference to the Lift Distribution. NACA Rep. 383, 1931.

48. Theodorsen, Theodore: Theory of Wing Sections of Arbitrary Shape. NACA Rep. 411, 1931.

49. Theodorsen, Theodore: Airfoil Contour Modification Based on ϵ-Curve Method of Calculating Pressure Distribution. NACA ARR L4G05, 1944 (Wartime Rep. L-135).

50. Theodorsen, Theodore, and Garrick, I. E.: General Potential Theory of Arbitrary Wing Sections. NACA Rep. 452, 1933.

51. von Doenhoff, Albert E.: A Method of Rapidly Estimating the Laminar Separation Point. NACA TN 671, 1938.

52. von Karman, T.: Turbulence and Skin Friction, J. Aeronaut. Sci., Vol. 1, No. 1, 1934, pages 1-20.

53. von Karman, T.: Compressibility Effects in Aerodynamics, J. Aeronaut. Sci., Vol. 8, No. 9, 1941, pages 337-356.

54. Walz, A.: Theoretical Calculation of the Maximum Lift Coefficient of Wings With and Without Lift-Flaps. ZWB Research Report No. 1769, 1943 (Translated by Frank, Richard and Fahle, John, Cornell Aeronautical Laboratory, Inc., 1951).

55. Weich, Fred E., Flanagan, L.E., Jr., and Cherry, H.H.: An Analytical Investigation of Effect of High-Lift Flaps on Take-Off of Light Airplanes. NACA TN 2404, 1951.

56. Weich, Fred E. and Abramson, H. Norman: Investigation of Lateral Control Near the Stall. Analysis for Required Longitudinal Trim Characteristics and Discussion of Design Variables. NACA TN 3677, 1956.

57. Wimpenny, J.C.: Low-Speed Stalling Characteristics. AGARD Rep. 356, 1961.

(b) Interference Methods

1. Chester, D. H.: The Lift of a Propeller-Wing Combination Due to the Slip-Stream. Israel Journal of Technology, Vol. 3, No. 1, 1965, page 102.

2. Dynasciences Corporation: Effects of Propeller Slipstream on V/STOL Aircraft Performance and Stability, TRECOM TR 64-47, 1964.

3. Ellis, N.D.: A Computer Study of a Wing in a Slipstream. UTIAS TN 101, 1965.

4. Flax, A.H. and Treanor, C.E.: A Variational Calculation of Subsonic Wing-Body Interference According to Lifting-Line Theory. Cornell Aeronautical Laboratory. (To be published.)

5. Franke, A. and Weinig F.: The Effect of the Slipstream on an Airplane Wing. NACA TM 920, 1939.

6. George, M. and Kisielowski, E.: Investigation of Propeller Slipstream Effects on Wing Performance. USAAVLABS TR 67-67, 1967.

7. Lawrence, H.R. and Flax A.H.: Wing-Body Interference at Subsonic and Supersonic Speeds - Survey and New Developments. J. Ae. Sc., Vol. 21, No. 5, Page 289, 1954.

8. Lennertz, J.: Influence of the Airplane Body on the Wings, Aerodynamic Theory; W. F. Durand, Editor, Vol. IV, Division K, Chapter III, Durand Reprinting Committee, 1943.

9. Low, L., and Stone, H. N.: The Subsonic Aerodynamic Characteristics of Wings in Combination with Slender Bodies of Revolution, Cornell Aeronautical Laboratory, Bumblebee Report No. CAL/CM-679, 1951.

10. Matthews, Clarence W.: A Comparison of the Experimental Subsonic Pressure Distributions About Several Bodies of Revolution with Pressure Distributions Computed by Means of the Linearized Theory. NACA Rep. 1155, 1953.

11. Multhopp, H.: Aerodynamics of the Fuselage, NACA TM 1036, 1942.

12. Munk, Max M.: The Aerodynamic Forces on Airship Hulls, NACA TR 184, 1924.

13. Pepper, P.A., Minimum Induced Drag in Wing-Fuselage Interference, NACA TN 812, 1941.

14. Pitts, William C., Nielsen, Jack N., and Kaattari, George E.: Lift and Center of Pressure of Wing-Body-Tail Combinations at Subsonic, Transonic, and Supersonic Speeds. NACA Rep. 1307, 1957.

15. Ribner, H. S. and Ellis, N.D.: Theory and Computer Study of a Wing in a Slipstream. AIAA Paper No. 66-466, 1966.

16. Ribner, H.S.: Theory of Wings in a Slipstream. UTIAS Rep. 60, 1959.

17. Schlichting, H., Monograph on the Aerodynamics of Mutual Interference Between the Components of the Airplane, National Research Council of Canada, Technical Translation No. TT-92, 1949.

18. White, Richard P., Jr.: VTOL Periodic Aerodynamic Loadings. The Problems-What is Being Done and What Needs to be Done. Paper presented at the Symposium on the Noise and Loading Actions on Helicopter V/STOL Aircraft and Ground Effect Machines, at University of Southampton, Hampshire, England, Aug. 30 to Sept. 3, 1965.

19. Wieselsberger, C.: Contribution to the Mutual Interference of Wing and Propeller. NACA TM 754, 1934.

20. Yaggy, Paul F.: A Method for Predicting the Upwash Angles Induced at the Propeller Plane of a Combination of Bodies with an Unswept Wing. NACA TN 2528, 1951.

21. Young, A.D.: Note on the Effect of Slipstream on Boundary Layer Flow. Rep. B.A. 1404, British RAE, 1937.

22. Young, A. D.: Further Note on the Effect of Slipstream on Boundary Layer Flow. Rep. No. B.A. 1404a, British RAE, 1938.

23. Young, A.D., and Morris D.E.: Further Note on the Effect of Slipstream on Boundary Layer Flow. Rep. No. B.A. 1404b, British RAE, 1939.

24. Zlotnick M., and Robinson, S.W., Jr.: A Simplified Mathematical Model for Calculating Aerodynamic Leading and Downwash for Midwing Wing-Fuselage Combinations with Wings of Arbitrary Planform, NACA RN L52J27a, 1953.

25. Zlotnick, Martin and Robinson, Samuel W., Jr.: A Simplified Mathematical Model for Calculating Aerodynamic Loading and Downwash for Wing-Fuselage Combinations With Wings of Arbitrary Plan Form. NACA TN 3057, 1954.

(c) Total Aircraft Analysis

1. Goranson, R. Fabian: A Method for Predicting the Elevator Deflection Required to Land. NACA WR L-95 (Originally issued as ARR L4116), 1944.

2. Graham, Ernest W. & Luskin, Harold: The Determination of the Stalling Speed and the Maximum Lift Coefficient in Flight. J.A.S., page 95, Feb., 1946.

3. Howe, John T.: Some Fluid Mechanical Problems Related to Subsonic and Supersonic Aircraft. NASA SP-183, 1968.

4. Lovell, J. Calvin & Lipson, Stanley: An Analysis of the Effect of Lift-Drag Ratio and Stalling Speed on Landing-Flare Characteristics. NACA TN 1930, 1949.

5. Pinsker, W.J.G.: "Zero Rate of Climb Speed" as a Low Speed Limitation for the Stall-Free Aircraft. ARC C.P. 931, 1966.

6. Priestley, E.: A General Treatment of Static Longitudinal Stability With Propellers, With Application to Single-Engined Aircraft. ARC R & M 2732, 1953.

7. Staff of Langley Research Center: A Preliminary Study of V/STOL Transport Aircraft and Bibliography of NASA Research in the VTOL-STOL Field. NASA TN D-624, 1961.

8. Zalovcik, John A.: Summary of Stall Warning Devices. NACA TN 2676, 1952.

2. WIND TUNNEL TESTS

(a) Section Characteristics

1. Abbott, Frank T., Jr., and Turner, Harold R., Jr.: The Effects of Roughness at High Reynolds Numbers on the Lift and Drag Characteristics of Three Thick Airfoils, NACA ACR No. L4H21, 1944 (Wartime Rep. L-46).

2. Abbott, Ira H., and Greenberg, Harry: Tests in the Variable-Density Wind Tunnel of the NACA 23012 Airfoil With Plain and Split Flaps. NACA Rep. 661, 1939.

3. Abbott, Ira H., von Doenhoff, Albert E., and Stivers, Louis S.: Summary of Airfoil Data. NACA Rep. 824, 1945.

4. Abbott, Ira H. & Sherman, Albert: Flow Observations With Tufts and Lampblack of the Stalling of Four Typical Airfoil Sections in the N.A.C.A. Variable-Density Tunnel. NACA TN 672, 1938.

5. Aeronautics Laboratory, Cambridge: An Experimental Study of the Stalling of Wings. ARC R & M 1588, 1933.

6. Bullwant, W. Kenneth: Tests of the NACA 0025 and 0035 Airfoils in the Full-Scale Wind Tunnel. NACA Rep. 708, 1941.

7. Cahill, Jones F.: Summary of Section Data on Trailing-Edge High-lift Devices. NACA RM No. L8D09, 1948 (Also NACA Rep. 938, 1949).

8. Cahill, Jones F.: Two-dimensional Wind-tunnel Investigation of Four Types of High-lift Flap on an NACA 65-210 Airfoil Section. NACA TN 1191, 1947.

9. Cahill, Jones F., and Racisz, Stanley: Wind-tunnel Development of Optimum Double-slotted-flap Configurations for Seven Thin NACA Airfoil Sections. NACA RM No. L7B17, 1947, also TN 1545.

10. Clay, William C.: Characteristics of the N.A.C.A. 23012 Airfoil From Tests in the Full-Scale and Variable-Density Tunnels. NACA Rep. 530, 1935.

11. Fischel, Jack, and Riebe, John M.: Wind-tunnel Investigation of a NACA 23021 Airfoil with a 0.32-airfoil-chord Double Slotted Flap. NACA ARR No. L4J05, 1944 (Wartime Rep. L-7).

12. Fitzpatrick, James E. & Schneider, William C.: Effect of Mach Number Variation Between 0.07 and 0.34 and Reynolds Number Variation Between 0.97 x 10^6 and 8.10 x 10^6 on the Maximum Lift Coefficient of a Wing of NACA 64-210 Airfoil Series. NACA TN 2753, 1952.

13. Fullmer, Felicien F., Jr.: Wind-Tunnel Investigation of NACA 66(215)-216, 66, 1-212, and 65,-212 Airfoils With 0.20-Airfoil-Chord Split Flaps. NACA WR L-140 (Originally Issued as CB L4G10), 1944.

14. Fullmer, Felicien F., Jr.: Two-dimensional Wind-tunnel Investigation of the NACA 64_1-012 Airfoil Equipped With Two Types of Leading-edge Flap. NACA TN 1277, 1947.

15. Furlong, G. Chester & Fitzpatrick, James E.: Effects of Mach Number and Reynolds Number on the Maximum Lift Coefficient of a Wing of NACA 230-Series Airfoil Sections. NACA TN 1299, 1947 (Originally issued as MR L6F04, 1946).

16. Gault, Donald E.: Boundary-Layer and Stalling Characteristics of the NACA 63-009 Airfoil Section. NACA TN 1894, 1949.

17. Goett, Harry J. & Bullivant, W. Kenneth: Tests of N.A.A.A. 0009, 0012, and 0018 Airfoils in the Full-Scale Tunnel. NACA Rep. 647, 1939.

18. Graham, Donald J.: The Development of Cambered Airfoil Sections Having Favorable Lift Characteristics at Supercritical Mach Numbers. NACA Rep. 947, 1949.

19. Harris, Thomas A.: Wind-tunnel Investigation of an NACA Airfoil With Two Arrangements of a Wide-chord Slotted Flap. NACA TN 715, 1939.

20. Harris, Thomas A., and Recant, Isidore G.: Wind-tunnel Investigation of NACA 23012, 23021, and 23030 Airfoils Equipped with 40-percent-chord Double Slotted Flaps. NACA Rep. 723, 1941.

21. Harris, Thomas A., and Lowry, John G.: Pressure Distribution Over an NACA 23012 Airfoil with a Fixed Slot and a Slotted Flap. NACA Rep. 732, 1942.

22. Hood, Manley J., and Gaydos, M. Edward: Effects of Propellers and of Vibration on the Extent of Laminar Flow on the NACA 27-212 Airfoil. NACA ACR, October 1939, (Wartime Rep. L-784).

23. Jacobs, Eastman N., and Abbott, Ira H.: Airfoil Section Data Obtained in the NACA Variable-density Tunnel as Affected by Support Interference and Other Corrections. NACA Rep. 669, 1939.

24. Jacobs, Eastman N., and Pinkerton, Robert M.: Tests in the Variable-density Wind Tunnel of Related Airfoils Having the Maximum Camber Unusually Far Forward. NACA Rep. 537, 1935.

25. Jacobs, Eastman N., and Pinkerton, Robert M.: Pressure, Distribution Over a Symmetrical Airfoil Section With Trailing Edge Flap. NACA Rep. 360, 1930.

26. Jacobs, Eastman N., Pinkerton, Robert M., and Greenberg, Harry: Tests of Related Forward-camber Airfoils in the Variable-density Wind Tunnel. NACA Rep. 610, 1937.

27. Jacobs, Eastman N., Ward, Kenneth E., and Pinkerton, Robert M.: The Characteristics of 78 Related Airfoil Sections from Tests in the Variable-density Wind Tunnel. NACA Rep. 460, 1932.

28. Kelly, John A. & Hayter, Nora-Lee F.: Lift and Pitching Moment at Low Speeds of the NACA 64A010 Airfoil Section Equipped With Various Combinations of a Leading-Edge Stat, Leading-Edge Flap, Split Flap, and Double-Slotted Flap. NACA TN 3007, 1953.

29. Kruger, W.: Wind-tunnel Investigation on a Changed Mustang Profile With Nose Flap. Force and Pressure Distribution Measurements. NACA TM 1177, 1947.

30. Loftin, Laurence K., Jr.: Theoretical and Experimental Data for a Number of NACA 6A-Series Airfoil Sections. NACA Rep. 903, 1947.

31. Loftin, Laurence K., Jr.: Airfoil Section Characteristics at High Angles of Attack. NACA TN 3241, 1954.

32. Loftin, Lawrence K., Jr.: Aerodynamic Characteristics of the NACA 64-010 and 0010-1.10 40/1.051 Airfoil Sections at Mach Numbers from 0.30 to 0.85 and Reynolds Numbers from 4.0×10^6 to 8.0×10^6. NACA TN 3244, 1954.

33. Loftin, Laurence K., Jr.: Effects of Specific Types of Surface Roughness on Boundary-Layer Transition. NACA ACR L5J29a, 1945 (Wartime Rep. L-48).

34. Loftin, Laurence K., Jr. & Bursnall, William J.: The Effects of Variations in Reynolds Number Between 3.0×10^6 and 25.0×10^6 Upon the Aerodynamic Characteristics of a Number of NACA 6-Series Airfoil Sections. NACA Rep. 964, 1950.

35. Loftin, Laurence K., Jr. and Cohen, Kenneth S.: Aerodynamic Characteristics of a Number of Modified NACA Four-digit-series Airfoil Sections. NACA RM L7122, 1947.

36. Loftin, Laurence K., Jr. & Smith, Hamilton, A.: Aerodynamic Characteristics of 15 NACA Airfoil Sections at Seven Reynolds Numbers From 0.7×10^6 to 9.0×10^6. NACA TN 1945, 1949.

37. Loftin, Laurence K., Jr. & Smith, Hamilton A.: Two-dimensional Aerodynamic Characteristics of 34 Miscellaneous Airfoil Sections. NACA RM L8L08, 1949.

38. Lowry, John G.: Wind-tunnel Investigation of an NACA 23012 Airfoil with Several Arrangements of Slotted Flap With Extended Lips. NACA TN 808, 1941.

39. Maki, Ralph L. & Hunton, Lynn W.: An Investigation at Subsonic Speeds of Several Modifications to the Leading-Edge Region of the NACA 64A010 Airfoil Section Designed to Increase Maximum Lift. NACA TN 3871, 1956.

40. McCullough, George B. & Gault, Donald E.: Boundary-Layer and Stalling Characteristics of the NACA 64A 006 Airfoil Section. NACA TN 1923, 1949.

41. McCullough, George B. & Gault, Donald E.: Examples of Three Representative Types of Airfoil-Section Stall at Low Speed. NACA TN 2502, 1951.

42. Peterson, Robert F.: The Boundary-Layer and Stalling Characteristics of the NACA 64A 010 Airfoil Section. NACA TN 2235, 1950.

43. Pinkerton, Robert M.: Calculated and Measured Pressure Distribution Over the Midspan Section of the NACA Rep. 563, 1936.

44. Platt, Robert C., and Abbott, Ira H.: Aerodynamic Characteristics of NACA 23012 and 23021 Airfoils with 20-percent-chord External-airfoil Flaps of NACA 23012 Section. NACA Rep. 573, 1936.

45. Purser, Paul E. Fischel, Jack, and Riebe, John M.: Wind-tunnel Investigation of an NACA 23012 Airfoil With a 0.30-airfoil-chord Double Slotted Flap. NACA ARR No. 3L10, 1943 (Wartime Rep. No. L-469).

46. Purser, Paul E., and Johnson, Harold S.: Effects of Trailing-edge Modifications on Pitching-moment Characteristics of Airfoils. NACA CB L4130, 1944 (Wartime Rep. L-664).

47. Quinn, John H., Jr.: Summary of Drag Characteristics of Practical-Construction Wing Sections. NACA Rep. 910, 1948.

48. Recant, I.G.: Wind-tunnel Investigation of an NACA 23030 Airfoil With Various Arrangements of Slotted Flap. NACA TN 755, 1940.

49. Schuldenfrei, Marvin J.: Wind-tunnel Investigation of an NACA 23012 Airfoil With a Handley Page Slot and Two Flap Arrangements. NACA ARR, February, 1942 (Wartime Rep. L-261).

50. Sherman, Albert, and Harris, T.A.: The Effects of Equal Pressure Fixed Slots on the Characteristics of a Clark-Y Airfoil. NACA TN 507, 1934.

51. Stack, John, and von Doenhoff, Albert E.: Tests of 16 Related Airfoils at High Speeds. NACA Rep. 492, 1934.

52. University of Southampton: Determination of the Forces Moments on an Airfoil Oscillating Through the Stall. A.A.S.U. 252, 1964.

53. von Doenhoff, Albert E., and Abbott, Frank T., Jr.: The Langley Two-dimensional Low-turbulence Pressure Tunnel. NACA TN 1283, 1947.

54. von Doenhoff, Albert E., and Tetervin, Neal: Investigation of the Variation of Lift Coefficient With Reynolds Number at a Moderate Angle of Attack on a Low-drag Airfoil. NACA CB, 1942 (Wartime Rep. L-661).

55. Weick, Fred E., and Shortal, Joseph A.: The Effect of Multiple Fixed Slots and a Trailing-edge Flap on the Lift and Drag of a Clark Y Airfoil. NACA Rep. 427, 1932.

56. Wenzinger, Carl J.: Wind-tunnel Investigation of Ordinary and Split Flaps on Airfoils of Different Profile. NACA Rep. 554, 1936.

57. Wenzinger, Carl J.: Pressure Distribution Over an Airfoil Section With a Flap and Tab. NACA Rep. 574, 1936.

58. Wenzinger, Carl J.: Pressure Distribution Over an NACA 23012 Airfoil With an NACA 23012 External-airfoil Flap. NACA Rep. 614, 1938.

59. Wenzinger, Carl J., and Delano, James B.: Pressure Distribution Over an NACA 23012 Airfoil With a Slotted and a Plain Flap. NACA Rep. 633, 1938.

60. Wenzinger, Carl J. & Gauvain, William E.: Wind-Tunnel Investigation of an N.A.C.A. 23012 Airfoil With a Slotted Flap and Three Types of Auxiliary Flap. NACA Rep. 679, 1939.

61. Wenzinger, Carl J., and Harris, Thomas A.: Wind-tunnel Investigation of an NACA 23012 Airfoil With Various Arrangements of Slotted Flaps. NACA Rep. 664, 1939.

62. Wenzinger, Carl J., and Harris, Thomas A.: Wind-tunnel Investigation of NACA 23012, 23021, and 23030 Airfoils With Various Sizes of Split Flap. NACA Rep. 668, 1939.

63. Wenzinger, Carl J., and Harris, Thomas A.: Wind-tunnel Investigation of an NACA 23021 Airfoil With Various Arrangements of Slotted Flaps. NACA Rep. 677, 1939.

64. Wenzinger, Carl J., and Rogallo, Francis M.: Resume of Airload Data on Slats and Flaps. NACA TN 690, 1939.

65. Wilson, Homer B., Jr. & Horton, Elmer A.: Aerodynamic Characteristics at High and Low Subsonic Mach Numbers of Four NACA 6-Series Airfoil Sections at Angles of Attack From -2° to 31°. NACA RM L53C20, 1953.

66. Young, A.D.: A Review of Some Stalling Research. ARC R & M 2609, 1942.

(b) Wing Alone Tests

1. Bollech, Thomas V.: Experimental and Calculated Characteristics of Several High-Aspect-Ratio Tapered Wings Incorporating NACA 44-Series, 230 Series, and Low Drag 64-Series Airfoil Sections. NACA TN 1677, 1948.

2. Cahill, Jones F.: Aerodynamic Data for a Wing Section of the Republic XF-12 Airplane Equipped With a Double Slotted Flap. NACA MR No. L6A08a, 1946 (Wartime Rep. L-544).

3. Greenberg, Harry: Characteristics of NACA 4400R Series Rectangular and Tapered Airfoils, Including the Effect of Split Flaps. NACA WR L-493, 1941.

4. Hamilton, William T. & Nelson, Warren H.: Summary Report on the High-Speed Characteristics of Six Model Wings Having NACA 65-Series Sections. NACA Rep. 877, 1947.

5. Hood, Manley J.: The Effects of Some Common Surface Irregularities on Wing Drag. NACA TN 695, 1939.

6. Jessen, Henry, Jr.: A Summary Report on the Effects of Mach Number on the Span Load Distribution on Wings of Several Models. NACA RM A7C28, 1947.

7. Neely, Robert H. Bollech, Thomas V., Westrick, Gertrude C., and Graham, Robert R.: Experimental and Calculated Characteristics of Several NACA 44-Series Wings with Aspect Ratios of 8, 10, and 12, and Taper Ratios of 2.5 and 3.5. NACA TN 1270, 1947.

8. Nonweiler, T.: A Resume of Maximum Lift Data for Symmetrical Wings With Various High-Lift Aids. College of Aeronautics, Cranfield CoA Note No. 5, 1954.

9. Noyes, Richard W.: Wind-tunnel Tests of a Wing with a Trailing-edge Auxiliary Airfoil Used as a Flap. NACA TN 524, 1935.

10. Palme, H.O.: Summary of Stalling Characteristics and Maximum Lift of Wings at Low Speeds. SAAB Aircraft Company, Sweden, TN 15, 1953.

11. Pearson, E.O., Jr., Evans, A.J., and West, F.E.: Effects of Compressibility on the Maximum Lift Characteristics, and Spanwise Load Distribution of a 12-foot-span Fighter-type Wing of NACA 230-series Airfoil Sections. NACA ACR L5G10, 1945 (Wartime Rep. L-51).

12. Platt, Robert C.: Aerodynamic Characteristics of a Wing With Fowler Flaps, Including Flap Loads Down-wash, and Calculated Effect on Take-Off. NACA Rep. 534, 1935.

13. Platt, Robert C.: Aerodynamic Characteristics of Wings with Cambered External-airfoil Flaps, Including Lateral Control With a Full-span Flap. NACA Rep. 541, 1935.

14. Platt, Robert C., and Shortal, Joseph A.: Wind-tunnel Investigation of Wings With Ordinary Ailerons and Full-span External Airfoil Flaps. NACA Rep. 603, 1937.

15. Sherman, Albert: The Aerodynamic Effects of Wing Cut-Outs. NACA Rep. 480, 1934.

16. Sivells, James C.: Experimental and Calculated Characteristics of Three Wings of NACA 64-210 and 65-210 Airfoil Sections With and Without 2° Washout. NACA TN 1422, 1947.

17. Soule, H. A. & Anderson, R.F.: Design Charts Relating to the Stalling of Tapered Wings. NACA Rep. 703, 1940.

18. Stack, John & Lindsey, W.F.: Characteristics of Low-Aspect-Ratio Wings at Supercritical Mach Numbers. NACA Rep. 922, 1949.

19. Sweberg, Harold H. & Lange, Roy H.: Summary of Available Data Relating to Reynolds Number Effects on the Maximum Lift Coefficients of Swept Back Wings. NACA RM L6L202, 1947.

20. Wallace, Rudolf: Investigation of Full-Scale Split Trailing-Edge Wing Flaps With Various Chords and Hinge Locations. NACA Rep. 539, 1935.

21. Weick, Fred E., and Harris, Thomas A.: The Aerodynamic Characteristics of a Model Wing Having a Split Flap Deflected Downward and Moved to the Rear. NACA TN 422, 1932.

22. Weick, Fred E., and Platt, Robert C.: Wind-tunnel Tests on a Model Wing With Fowler Flap and Specially Developed Leading-edge Slot. NACA TN 459, 1933.

23. Weick, Fred E., and Sanders, Robert: Wind-tunnel Tests of a Wing with Fixed Auxiliary Airfoils Having Various Chords and Profiles. NACA Rep. 472, 1933.

24. Wenzing, Carl J.: Wind-tunnel Tests of a Clark Y Wing Having Split Flaps With Gaps. NACA TN 650, 1938.

25. Wenzinger, Carl J. & Harris, Thomas A.: Pressure Distribution Over a Rectangular Airfoil With a Partial-Span Split Flap. NACA Rep. 571, 1936.

26. Woodward, D.S.: On the Errors Induced at Tunnel Reference Pressure Tappings by High Lift Models. R.A.E. Technical Report No. 66049, 1966.

(c) Complete Model Tests

1. Brewer, Gerald W., & May, Ralph W., Jr.: Investigation of a 1/7 Scale Powered Model of a Twin Boom Airplane and a Comparison of its Stability, Control, and Performance with Those of a Similar All-Wing Airplane. NACA TN 1649, 1948.

2. Goodman, A.: Effects of Wing Position and Horizontal-Tail Position on Static Stability Characteristics of Models With Unswept and 45° Sweptback Surfaces with Some Reference to Mutual Interference. NACA TN 2502, 1951.

3. Hagerman, John R.: Wind-tunnel Investigation of the Effect of Power and Flaps on the Static Longitudinal Stability and Control Characteristics of a Single-Engine High-wing Airplane Model. NACA TN 1339, 1947.

4. Harper, Paul W. & Flanigan, Roy E.: Investigation of the Variation of Maximum Lift for a Pitching Airplane Model and Comparison With Flight Results. NACA TN 1734, 1948.

5. Harper, Paul W. & Flanigan, Ray E.: The Effect of Rate of Change of Angle of Attack on the Maximum Lift of a Small Model. NACA TN 2061, 1950.

6. Hartshorn, A.S., Hirst, D.M., & Midwood, G.F.: Tests on Model of "Wapiti" Including Effect of Slipstream. ARC R & M 1419, 1932.

7. Hopkins, Edward J. & Carel, Hubert C.: Experimental and Theoretical Study of the Effects of Body Size on the Aerodynamic Characteristics of an Aspect Ratio 3.0 Wing-Body Combination. NACA RM A51G24, 1951.

8. Hopkins, Edward J. & Carel, Hubert C.: Experimental and Theoretical Study of the Interference at Low Speed Between Slender Bodies and Triangular Wings. NACA RM A53A14, 1953.

9. House, Refus O. & Wallace, Arthur R.: Wind-Tunnel Investigation of Effect of Interference on Lateral-Stability Characteristics of Four NACA 23012 Wings, An Elliptical and a Circular Fuselage, and Vertical Fins. NACA Rep. 705, 1941.

10. Jacobs, Eastman N. & Ward, Kenneth E.: Interference of Wing & Fuselage from Tests of 209 Combinations in the N.A.C.A. Variable-Density Tunnel. NACA Rep. 540, 1935.

11. Johnson, Harold S.: Wind-tunnel Investigation of Effects of Tail Length on the Longitudinal and Lateral Stability Characteristics of a Single-Propeller Airplane Model. NACA TN 1766, 1948.

12. Jordan, Gareth H. & Cole, Richard I.: The Effect of a Simulated Propeller Slipstream on the Aerodynamic Characteristics of an Unswept Wing Panel With and Without Nacelles at Mach Numbers from 0.30 to 0.86. NACA TN 2776, 1952.

13. Letko, William & Williams, James L.: Experimental Investigation at Low Speed of Effects of Fuselage Cross Section on Static Longitudinal and Lateral Stability Characteristics of Models Having 0^{o} and 45^{o} Sweptback Surfaces. NACA TN 3551, 1955.

14. Letko, William: Experimental Investigation at Low Speed of the Effects of Wing Position on the Static Stability of Models Having Fuselages of Various Cross Section and Unswept and 45^{o} Sweptback Surfaces. NACA TN 3857, 1956.

15. Martina, Albert P.: The Interference Effects of a Body on the Spanwise Load Distributions of two 45^{o} Sweptback Wings of Aspect Ratio 8.02 From Low-speed Tests. NACA TN 3730, 1956.

16. Muttray, H.: Investigation of the Effect of the Fuselage on the Wing of a Low-Wing Monoplane. NACA TM 517, 1929.

17. Pitkin, Marvin: Free-Flight-Tunnel Investigation of the Effect of Mode of Propeller Rotation Upon the Lateral-Stability Characteristics of a Twin-Engine Airplane Model With Single Vertical Tails of Different Size. NACA WR L-354. (Originally Issued as ARR 3J18), 1943.

18. Prandtl, L.: Effects of Varying the Relative Vertical Position of Wing and Fuselage. NACA TN 75, 1921.

19. Ribner, Herbert S. & Mac Lachlan, Robert: Effect of Slipstream Rotation in Producing Asymmetric Forces on a Fuselage. NACA TN 1210, 1947.

20. Robinson, Russell G. & Herrnstein, William H., Jr.: Wing-Nacelle-Propeller Interference for Wings of Various Spans. Force and Pressure-Distribution Tests. NACA Rep. 569, 1936.

21. Sandahl, Carl A. & Vollo, Samuel D.: Wind-Tunnel Investigation of the Air Load Distribution on Two Combinations of Lifting Surfaces and Fuselage. NACA TN 1295, 1947.

22. Schlichting, H.: Report on the Special Field "Interference" to the Wind-Tunnel Committee in February 1945. NACA TM 1347, 1953.

23. Sherman, Albert: Interference of Wing and Fuselage from Tests of 28 Combinations in the N.A.C.A. Variable-Density Tunnel. NACA Rep. 575, 1936.

24. Sherman, Albert: Interference of Tail Surfaces and Wing and Fuselage From Tests of 17 Combinations in the N.A.C.A. Variable Density Tunnel. NACA Rep. 678, 1939.

25. Sivells, James C., and Spooner, Stanley H.: Investigation in the Langley 19-Foot Pressure Tunnel of Two Wings of NACA 65-210 Airfoil Sections With Various Type Flaps. NACA Rep. 942, 1949.

26. Sleeman, William C., Jr. & Lindsley, Edward L.: Low-speed Wind-Tunnel Investigation of the Effects of Propeller Operation at High Thrust on the Longitudinal Stability and Trim of a Twin-Engine Airplane Configuration. NACA RM L52D04, 1952.

27. Stuper, J.: Effect of Propeller Slipstream on Wing and Tail. NACA TM 874, 1938.

28. Teplitz, Jerome: Effects of Small Angles of Sweep and Amounts of Dihedral on Stalling and Lateral Characteristics of a Wing-Fuselage Combination Equipped With Partial-and Full-Span Double Slotted Flaps. NACA Rep. 800, 1944.

29. Wallace, Arthur R., Rossi, Peter F., and Wells, Evelyn G.: Wind-tunnel Investigation of the Effect of Power and Flaps on the Static Longitudinal Stability Characteristics of a Single-Engine Low-Wing Airplane Model. NACA TN 1239, 1947.

30. Weil, Joseph & Sleeman, William C., Jr.: Prediction of the Effects of Propeller Operation on the Static Longitudinal Stability of Single-Engine Tractor Monoplanes With Flaps Retracted. NACA TN 1722, 1948.

31. Windler, Ray: Tests of a Wing-Nacelle-Propeller Combination at Several Pitch Settings Up to 42°. NACA Rep. 564, 1936.

(d) Full-Scale Wind-Tunnel Tests

1. Davis, Don D., Jr., and Sweberg, Harold H.: Investigation of Some Factors Affecting Comparisons of Wind-Tunnel and Flight Measurements of Maximum Lift Coefficients for a Fighter-Type Airplane. NACA TN 1639, 1948.

2. Fink, Marvin P. & Freeman, Delma C., Jr.: Full-Scale Wind-Tunnel Investigation of Static Longitudinal and Lateral Characteristics of a Light Twin-Engine Airplane. NASA TN D-4983, 1969.

3. Kayten, Gerald G.: Analysis of Wind-Tunnel Stability and Control Tests in Terms of Flying Qualities of Full-Scale Airplanes. NACA Rep. 825, 1945.

4. Roberts, John C. & Yaggy, Paul F.: A Survey of the Flow at the Plane of the Propeller of a Twin-Engine Airplane. NACA TN 2192, 1950.

5. Sweberg, Harold H. and Dingeldein, Richard C.: Summary of Measurements in Langley Full-Scale Tunnel of Maximum Lift Coefficients and Stalling Characteristics of Airplanes. NACA Rep. 829, 1945.

6. White, James A. & Hodd, Manley J.: Wing-Fuselage Interference, Tail Buffeting, and Air Flow About the Tail of a Low-Wing Monoplane. NACA Rep. 482, 1934.

3. AIRCRAFT FLIGHT TESTS

1. Anderson, Seth B.: Correlation of Flight and Wind-Tunnel Measurements of Roll-Off in Low-Speed Stalls on a 35° Swept-Wing Aircraft. NACA RM A53G22, 1953.

2. Barnes, F. W. & Newman, B.G.: The Effect of Leading-Edge Wedges on the Stalling Behavior of the Wirraway. R.A.A.F. Aircraft Research and Development Unit TN Aero/8, 1951.

3. Bicknell, Joseph: Determination of the Profile Drag of an Airplane Wing in Flight at High Reynolds Numbers. NACA Rep. 667, 1939.

4. Donely, Philip & Pearson, Henry A.: Flight and Wind-Tunnel Tests of an XBM-1 Dive Bomber. NACA TN-644, 1938.

5. Gadeberg, Bernett, L.: The Effect of Rate of Change of Angle of Attack on the Maximum Lift Coefficient of a Pursuit Airplane. NACA TN 2525, 1951.

6. Gray, William E., Jr.: NASA Flight Research Center Handling-Qualities Program on General-Aviation Aircraft, NASA TM X-56004, 1964.

7. Hunter, Paul A.: Flight Measurements of the Flying Qualities of Five Light Airplanes. NACA TN 1573, 1948.

8. Hunter, P.A. & Vensel, J.R.: A Flight Investigation to Increase the Safety of a Light Airplane. NACA TN 1203, 1947.

9. Huston, Wilber B. & Skopinski, T.H.: Measurement and Analysis of Wing and Tail Buffeting Loads on a Fighter Airplane. NACA Rep. 1219, 1955.

10. Kayten, Gerald G. & Koven, William: Comparison of Wind-Tunnel and Flight Measurements of Stability and Control Characteristics of a Douglas A-26 Airplane. NACA Rep. 816, 1945.

11. La Plant II, Porter & Johnson, Albinus P.: Evaluation of the Giannini Dual Stall Warning System and Stall Margin Indicators Installed in a C-133B. FTC TR-67-5, 1967.

12. Nissen, James M. & Gadeberg, Burnett L.: Effect of Mach & Reynolds Numbers on the Power-Off Maximum Lift Coefficient Obtainable on a P-39N-1 Airplane as Determined in Flight. NACA ACR 4F28, 1944.

13. Nissen, James M., Gadeberg, Burnett L. & Hamilton, William T.: Correlation of the Drag Characteristics of a Typical Pursuit Airplane Obtained from High-Speed Wind-Tunnel and Flight Tests. NACA Rep. 916, 1948.

14. Phillips, W. H. & Nissen, J.M.: Flight Tests of Various Tail Modifications on the Brewster XSBA-1 Airplane. I-Measurements of Flying Qualities With Original Tail Surfaces. NACA WR L-412 (Originally Issued as ARR 3F07), 1943.

15. Rhode, Richard V.: The Influence of Tip Shape on the Wing-Load Distribution as Determined by Flight Tests. NACA Rep. 500, 1934.

16. Silverstein, Abe, Katzoff, Samuel, and Hootman, James: Comparative Flight and Full-scale Wind-tunnel Measurements of the Maximum Lift of an Airplane. NACA Rep. 618, 1938.

17. Sjoberg, S.A., Crane, H.L., & Hoover, H.H.: Measurement of Flying Qualities of a Douglas A-26 B Airplane. Part III-Stalling Characteristics. NACA WR L-607 (Originally issued as MR No. L5A04a), 1945.

18. Soule, Hartley A. & Wetmore, J.W.: The Effects of Slots and Flaps on Lateral Control of a Low-Wing Monoplane as Determined in Flight. NACA TN 478, 1933.

19. Spreiter, John R. & Steffen, Paul J.: Effect of Mach and Reynolds Numbers on Maximum Lift Coefficients. NACA TN 1044, 1946.

20. Stokke, Allen R. & Aiken, William S., Jr.: Flight Measurements of Buffeting Tail Loads. NACA TN 1719, 1948.

21. Weick, Fred E.: The Behavior of Conventional Airplanes in Situations Thought to Lead to Most Crashes. NACA TN 363, 1931.

22. Weick, Fred E. & Abramson, H. Norman: Investigation of Lateral Control Near the Stall. Flight Tests With High-Wing and Low-Wing Monoplanes of Various Configurations. NACA TN 3676, 1956.

23. White, M.D. & Reeder, J.P.: Effect of Wing-Tip Slots on the Stalling and Aileron Control Characteristics of a Curtiss SB2C-1 Airplane. NACA MR L4K13, 1944.

24. Zalovick, John A.: Profile Drag Coefficients of Conventional and Low-drag Airfoils as Obtained in Flight. NACA ACR No. L4E31, 1944 (Wartime Rep. L-139).

NASA-Langley, 1971 — 1 CR-1646